De Bank, Paul A. (2001) Synthesis and biological evaluation of novel compounds as potential modulators of cannabinoid signalling pathways. PhD thesis, University of Nottingham.

Synthesis and Biological Evaluation of Novel Compounds as Potential Modulators of Cannabinoid Signalling Pathways

Paul A. De Bank

Thesis submitted to the University of Nottingham for the degree of Doctor of Philosophy, October 2000.

Preface

The work described in this thesis was undertaken within the School of Pharmaceutical Sciences and the School of Biomedical Sciences at the University of Nottingham between October 1996 and October 1999. It is original except where otherwise stated and includes nothing which is the outcome of work in collaboration or which has been submitted for any other qualification at this or any other university.

Acknowledgements

On the academic side of things, I would first and foremost like to thank Professor Dave Kendall and Dr Steve Alexander. Their constant support, advice and light-hearted approach was a huge help, especially when things weren't going according to plan. Secondly, I would like to thank my former supervisor, Dr Andy Boyd, for his continued help and enthusiasm despite his hectic jet-set schedule. I would also like to thank all members of Chem Corner past and present, especially Dr Vince Loh for his guidance with the phosphorus chemistry, and the members of technical staff in both the School of Pharmaceutical Sciences and the School of Biomedical Sciences, particularly Dr Cath Ortori for running mass spectra. Finally, I would like to thank the University of Nottingham for funding my research.

Many thanks to all of my friends for their support throughout my PhD, especially my old housemates Mark Hurst and Al Maynard who were in the same boat and knew what I was going through. The biggest thank you, however, goes to my family for their continued support and encouragement and, above all, to Christine for her love and understanding throughout.

Abstract

Most of the biological effects of cannabis are due to the activation of specific cannabinoid receptors. To date, two such receptors have been discovered and are found predominantly in the central nervous system (the CB1 receptor) or the immune system (the CB2 receptor). Endogenous cannabinoid receptor ligands, the endocannabinoids, have also been isolated and the mechanisms of their synthesis and degradation postulated. By modulating the activation of cannabinoid receptors and endocannabinoid metabolism, synthetic cannabimimetic compounds have enormous therapeutic potential for the treatment of such diverse symptoms and diseases as pain, inflammation, cancer, hypertension, schizophrenia and multiple sclerosis. This thesis describes the design, synthesis and subsequent biological evaluation of three classes of novel, potentially cannabimimetic drugs, namely aryl ethanolamides, phenylphosphinic acids and alkylphosphinic acids. In order to assess cannabimimetic activity, the ability of these compounds to bind to the cannabinoid receptors and to inhibit endocannabinoid uptake and enzymatic hydrolysis was examined.

Affinity for the CB1 receptor was assessed using radioligand binding assays in rat brain membranes. Although none of the compounds proved to be high-affinity CB1 receptor ligands, two aryl ethanolamide compounds exhibited some affinity for this receptor, suggesting that this general class of compound may have cannabimimetic potential.

In order to ascertain whether the test compounds had affinity for the CB2 receptor, a radioligand binding assay was developed using porcine spleen membranes. To date, only the human, murine and rat CB2 receptors have been cloned and there has been no detailed examination of the cannabinoid binding profile of the porcine CB2 receptor. The K_d of the radiolabelled cannabinoid [^{3}H]-CP-55,940 was determined in porcine spleen membranes and the B_{max} subsequently calculated. The K_i values of a number of cannabinoid receptor ligands were then determined. These values were shown to be similar to the corresponding values obtained using cloned CB2 receptors. However, when the test compounds were assessed in this assay system, no affinity for the CB2 receptor was observed.

To determine the effect, if any, of the test compounds on the endocannabinoid uptake system, accumulation of the radiolabelled endocannabinoid [^{3}H]-anandamide into N18TG2 mouse neuroblastoma cells was examined. [^{3}H]-Anandamide accumulation had previously been reported in this cell line but, until now, this mechanism had not been characterized. This accumulation was shown to be time-, temperature- and concentration-dependent and was inhibited by AM404 and bromocresol green, known inhibitors of the endocannabinoid carrier system. [^{3}H]-Anandamide accumulation exhibited a K_m value similar to those previously described for rat astrocytes and neurones and the time taken to achieve half maximal rate was shown to be considerably greater than in these rat cells. None of the test compounds significantly inhibited [^{3}H]-anandamide uptake by N18TG2 cells although one phenylphosphinic acid compound, with structural similarities to AM404, appeared to be inhibitory at high concentrations.

The final biological target examined was fatty acid amide hydrolase (FAAH), the enzyme that catalyses the hydrolysis of endocannabinoids. For FAAH studies, a novel, inexpensive and rapid spectrophotometric assay was developed as an alternative to the traditional radiochemical- and chromatography-based assays. Using this novel assay system, the K_m and V_{max} values of rat liver FAAH were determined and shown to be similar to those published in the literature. Known FAAH inhibitors were shown to inhibit FAAH in a concentration-dependent manner with IC_{50} values comparable to previously published data. In addition, this assay was used to demonstrate differences in FAAH activity between soluble and insoluble membrane preparations from rat liver and brain, possibly indicating the presence of, as yet, unknown FAAH enzymes. Attempts were also made to adapt this assay for use on a microtiter plate, where it was possible to detect FAAH inhibitors. Therefore, this spectrophotometric assay may prove to be of use in the high-throughput screening of chemical libraries for drugs that cause cannabimimetic effects *via* FAAH inhibition. None of the test compounds synthesized inhibited FAAH activity and this, combined with their lack of biological activity at the other targets tested, showed that they exerted no cannabimimetic effects.

The most exciting phrase to hear in science, the one that heralds new discoveries, is not Eureka! (I found it!) but rather, "hmm.... that's funny..."

Isaac Asimov

Abbreviations and Chemical Names

AAI	aminoalkylindole
ADP	adenosine diphosphate
AE	aryl ethanolamide
2-AG	2-arachidonylglycerol
AM251	N-(piperidin-1-yl)-5-(4-iodophenyl)-1-(2,4-dichlorophenyl)-4-methyl-1H-pyrazole-3-carboxamide
AM281	N-(piperidin-1-yl)-1-((2,4-dichlorophenyl)-5-(4-iodophenyl)-4-methyl-1H-pyrazole-3-carboxamide
AM404	N-(4-hydroxyphenyl)arachidonylamide
AM630	6-iodopravadoline
Anandamide	arachidonylethanolamide
ANOVA	analysis of variance
APA	alkylphosphinic acid
ATP	adenosine triphosphate
B_0	specific radioligand binding
B_{max}	receptor number
Bromocresol green	3',3'',5',5''-tetrabromo-m-cresolsulphone phthalein
BSA	bovine serum albumin
BTSP	bis(trimethylsilyl)phosphonite
BTSPP	bis(trimethylsilyl)phenylphosphonite
cAMP	cyclic adenosine monophosphate
β-CD	β-cyclodextrin
cDNA	complementary DNA
CHAPS	3-[(3-cholamidopropyl)dimethylammonio]-1-propane sulphonate
CHO	Chinese hamster ovary
Ci	Curie
CMK	megakaryoblastic cells
CNS	central nervous system
COX	cyclooxygenase

CP-47,497	(*Z*)-3-[4-(1,1-dimethylheptyl)-2-hydroxyphenyl] cyclohexanol
CP-55,940	(1*R*,3*R*,4*R*)-3-[2-hydroxy-4-(1,1-dimethylheptyl)phenyl]-*trans*-4-(3-hydroxypropyl)cyclohexan-1-ol
CPF	crude particulate fraction
CREAE	chronic relapsing experimental allergic encephalomyelitis
CT-3	1',1'-dimethylheptyl-Δ^8-tetrahydrocannabinol-11-oic acid
DAUDA	11-(5-dimethylamino naphthalenesulphonyl)-undecanoic acid
DCM	dichloromethane
DIPEA	diisopropylethylamine
DMAP	4-dimethylaminopyridine
DMEM	Dulbecco's modified Eagle medium
DMF	*N,N*-dimethylformamide
DMSO	dimethyl sulphoxide
dpm	disintegrations per minute
EC_{50}	concentration of drug required for 50 % of maximum response
ED_{50}	dose of drug required for 50 % of maximum response
EDC	1-(3-dimethylaminopropyl)-3-ethycarbodiimide hydrochloride
EDHF	endothelium-derived hyperpolarizing factor
EDRF	endothelium-derived relaxant factor
EDTA	ethylenediamine tetraacetic acid
ERK	extracellular signal-regulated kinase
FAAH	fatty acid amide hydrolase
FABP	fatty acid binding protein
FBS	foetal bovine serum
GABA	γ-aminobutyric acid
GDH	L-glutamate dehydrogenase
GDP	guanosine diphosphate
GI	gastrointestinal
Glu	L-glutamate

GPCR	G protein-coupled receptor
GTP	guanosine triphosphate
GTP-γ-S	guanosine 5'-*O*-thiotriphosphate
HBCC	human breast cancer cells
HEPES	*N*-(2-hydroxyethyl)piperazine-*N'*-(2-ethanesulphonic acid)
HHC	9-nor-9β-hydroxyhexahydrocannabinol
HMDS	hexamethyldisilazane
HOBt	1-hydroxybenzotriazole
HPLC	high-performance liquid chromatography
5-HT	5-hydroxytryptamine
HTS	high-throughput screening
HU-210	3-(1,1-dimethylheptyl)-(-)-11-hydroxy-Δ^8-tetrahydro cannabinol
HU-211	3-(1,1-dimethylheptyl)-(+)-11-hydroxy-Δ^8-tetrahydro cannabinol
HU-243	11-hydroxy-3-(1,1'-dimethylheptyl)hexahydrocannabinol
HU-308	4-[4-(1,1-dimethylheptyl)-2,6-dimethoxyphenyl]-6,6-dimethyl-(1*R*,4*R*,5*R*)-(+)-bicyclo[3.1.1]hept-2-ene-2-methanol
i.p.	intra-peritoneal
i.v.	intra-venous
IC_{50}	concentration required to produce 50 % of the maximum possible inhibition
IL	interleukin
iNOS	inducible nitric oxide synthase
JWH-015	1-propyl-2-methyl-3-(1-naphthoyl)indole
JWH-051	1-deoxy-11-hydroxy-Δ^8-tetrahydrocannabinol-dimethylheptyl
K_d	dissociation constant
K_i	inhibitory constant
K_m	Michaelis constant
α-KG	α-ketoglutaric acid
kDa	kilo Daltons

kU	kilo units
L759633	(6a*R*,10a*R*)-3-(1,1-dimethyl-heptyl)-1-methoxy-6,6,9-trimethyl-6a,7,10,10a-tetrahydro-6*H*-benzo[*c*]chromene
L759656	(6a*R*,10a*R*)-3-(1,1-dimethyl-heptyl)-1-methoxy-6,6-dimethyl-9-methylene-6a,7,8,9,10,10a-hexahydro-6*H*-benzo[*c*]chromene
L-759,787	2-methyl-3-(4-morpholinylmethyl)-1-(1-naphthalenyl carbonyl)-1*H*-indole
L-768,242	1-(2,3-dichlorobenzoyl)-5-methoxy-2-methyl-3-[2-(4-morpholinyl)ethyl]-1*H*-indole
LPS	lipopolysaccharide
LY320135	[6-methoxy-2-(4-methoxyphenyl)benzo[*b*]thien-3-yl][4-cyanophenyl]methanone
M	moles/dm^3
m.p.	melting point
MAFP	methylarachidonyl fluorophosphonate
MAPK	mitogen-activated protein kinase
MCP-1	monocyte chemotactic protein-1
MHz	megahertz
mRNA	messenger RNA
MS	multiple sclerosis
NAD$^+$	nicotinamide adenine dinucleotide
NADH	nicotinamide adenine dinucleotide (reduced form)
NF	nuclear factor
NGF	nerve growth factor
NMR	nuclear magnetic resonance
NSAID	non-steroidal anti-inflammatory drug
Oleamide	*cis*-9,10-octadecenamide
PAA	*N*-propyl arachidonyl amide
PAG	periaqueductal gray
PBS	phosphate buffered saline
PDMAA	*N*-propyl-α,α-dimethylarachidonyl amide
PEI	polyethylenimine

PMAA	*N*-propyl-α-methylarachidonyl amide
PMSF	phenylmethylsulphonyl fluoride
PPA	phenylphosphinic acid
ppm	parts per million
Pravadoline	(4-methoxyphenyl)[2-methyl-1-[2-(4-morpholinyl)-ethyl]-1*H*-indol-3-yl]methanone
PRLr	prolactin receptor
RP-HPLC	reverse-phase high-performance liquid chromatography
RT-PCR	reverse transcriptase polymerase chain reaction
SEM	standard error of mean
SPECT	single photon emission computed topography
SR141716A	*N*-(piperidin-1-yl)-5-(4-chlorophenyl)-1-(2,4-dichlorophenyl)-4-methyl-1*H*-pyrazole-3-carboxamide hydrochloride
SR144528	*N*-[(1*S*)-endo-1,3,3-trimethyl bicyclo [2.2.1] heptan-2-yl]-5-(4-chloro-3-methylphenyl)-1-(4-methylbenzyl)-pyrazole-3-carboxamide
THC	tetrahydrocannabinol
TLC	thin layer chromatography
TMEV	Theiler's murine encephalomyelitis virus
TMSCl	trimethylsilyl chloride
TNFα	tumour necrosis factor α
Tris	tris(hydroxymethyl)aminomethane
TX-100	*t*-octylphenoxypolyethoxy ethanol
V_{max}	maximum rate
WIN 55-212,2	(*R*)-(+)-[2,3-dihydro-5-methyl-3-[(4-morpholinly) methyl]pyrrolo[1,2,3-*de*-]-1,4-benzoxazin-6-yl](1-naphthalenyl) methanone

Materials

All chemicals used in this research were of the highest grade possible and obtained from the following commercial sources:

Affiniti Research Products Ltd., Exeter, U.K. - MAFP

Aldrich, Poole, U.K. – alkyl iodides, bromocresol green, 3-bromopropan-1-ol, carboxylic acids, DIPEA, DMAP, ethanolamine, HMDS, HOBt, hypophosphorus acid, $KHSO_4$, oxalyl chloride, phenylphosphinic acid, TMSCl and triethylamine

Amersham Pharmacia Biotech, Amersham U.K. – [^{35}S]-GTP-γ-S and [^{3}H]-SR141716A

Avocado Research Chemicals Ltd., Heysham, U.K. - EDC

BDH Laboratory Supplies, Poole, U.K. – EDTA, ethanol, D-(+)-glucose, NaCl, $NaHCO_3$, NaOH and Tris

Calbiochem, Nottingham, U.K. – GDH, α-KG and NADH.

Fisher Scientific Ltd., Loughborough, U.K. - cyclohexane, dichloromethane, ethyl acetate, HCl, hexane, methanol, $MgSO_4$ and sucrose

Fisons Scientific Equipment, Loughborough, U.K. - $CaCl_2$, chloroform, DMSO, KCl, methanol and orthophosphoric acid

ICN Biomedicals Inc., Basingstoke, U.K. - GDP

NEN Life Science Products Inc., Hounslow, UK - [^{3}H]-anandamide and [^{3}H]-CP-55,940

Sigma, Poole, U.K.- ADP, ammonium acetate, BSA, CHAPS, coomassie Brilliant Blue G, DMEM, Dulbecco's PBS, FBS, glycerol, HEPES, PMSF, polyethylenimine, theophylline, triethanolamine, trypsin and TX-100

Tocris Cookson Ltd., Avonmouth, U.K. - AM404 and HU210

Research Biochemicals International, Dorset, U.K. - β-CD

Life Technologies Ltd., Paisley, U.K. - L-glutamine

SR141716A and SR 144528 were a generous gift from Dr F. Barth, Sanofi-Synthelabo, Paris. CP-55,940 was a kind gift from Pfizer Central Research, Groton, CT, U.S.A.

Anandamide and oleamide were synthesized as described in **appendix A**.

Contents

Chapter 1:

Introduction

1.1 Cannabis

The plant *cannabis sativa* has been extensively utilized by mankind throughout history. It has been used as a source of textiles and food, but it is most widely known as a psychoactive drug of abuse. The earliest recorded use of cannabis is from China nearly four thousand years ago where it was used as a sedative and all-purpose medicine, although there is no evidence of widespread use for its psychoactive properties. From China, the use of cannabis spread through Asia to the Middle East and Europe. There are many references to its use in religious ceremonies where it was thought, like many psychoactive drugs, to promote union with God, but its medicinal properties superseded its religious use. Medicinally, cannabis was used in many cultures to treat diverse complaints including sickness, pain, convulsions, inflammation, urinary infections, asthma and lack of appetite. The drug preparation was usually taken orally but, in India, the practice of smoking cannabis became established. As smoking cannabis leads to a more rapid onset of its effects compared to oral delivery, this practice soon spread globally.

Although preparations of *cannabis sativa* were known to contain numerous "cannabinoid" compounds, it was not known whether the effects of cannabis were due to a single compound, a number of compounds or metabolites of the cannabinoids. The only cannabinoid to be isolated in a pure form by the middle of the twentieth century was cannabinol, which is not psychoactive. However, in 1964, the major active constituent of cannabis was isolated and characterized as (-)-Δ^9-tetrahydrocannabinol (Δ^9-THC), an oily, viscous liquid (Gaoni & Mechoulam, 1964). When used in pharmacological tests, purified Δ^9-THC demonstrated the same effects as cannabis preparations. Subsequent research demonstrated the existence of a number of structurally related cannabinoids in *cannabis sativa*, with Δ^8-THC, an isomer of Δ^9-THC, also being psychoactive but found in lower levels than Δ^9-THC. Other naturally occurring cannabinoids include the tetrahydrocannabinolic acids, cannabidiol and cannabidiolic acid, all of which are non-psychoactive (**figure 1.1**).

2

R=H: Cannabinol
R=CO$_2$H: Cannabinolic acid

R=H: Cannabidiol
R=CO$_2$H: Cannabidiolic acid

R = H: Δ^9-THC
R = CO$_2$H: Δ^9-Tetrahydrocannabinolic acid
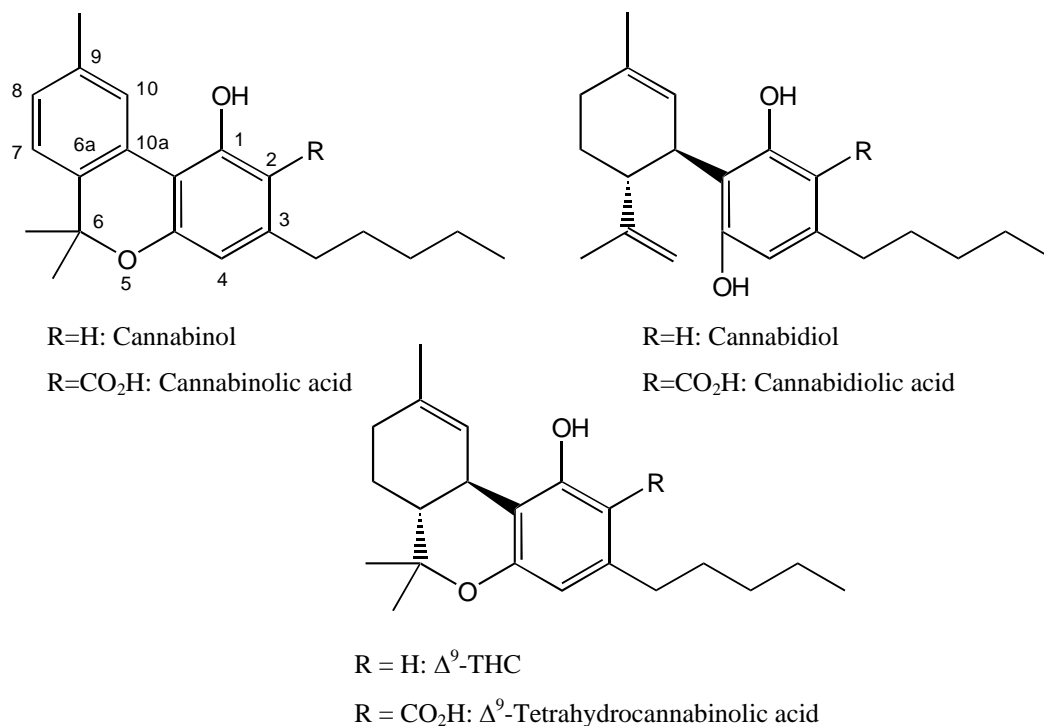
Figure 1.1: The structures of some of the cannabinoids found in *cannabis sativa*, showing the widely accepted dibenzopyran numbering system.

Although cannabis has well established medicinal effects, its widespread abuse for the psychotropic "high" it produces means that it remains an illegal substance. Yet today, many thousands of people continue to risk arrest and imprisonment by using cannabis to relieve chronic symptoms that are not helped by prescription medicines. One of the most publicized illnesses in which cannabis is particularly effective at relieving symptoms is multiple sclerosis (MS). Indeed, research has recently confirmed that Δ^9-THC is effective at reducing spasticity and tremor in a mouse model of MS (Baker *et al.*, 2000). Understandably, the medicinal use of cannabis is an extremely controversial and widely debated issue, particularly in recent years. Even if cannabis were to be decriminalized for medicinal use, smoking preparations of the plant is an undesirable route of administration. Although smoking enables a rapid onset of the effects of cannabis and enables effective self-administration of a suitable dose by the user, there is a major disadvantage. Like cigarettes, smoking cannabis is extremely damaging to the lungs. Recently, this was highlighted by a study which showed that smoking three

to four cannabis cigarettes per day produces histological effects on the lungs comparable to smoking 20 tobacco cigarettes (Johnson *et al*., 2000). In order to deliver the medicinal effects of cannabis safely, research in to the delivery of this drug is now concentrating on pure Δ^9-THC. Currently, studies are being performed to investigate its delivery by nasal inhalers and dermal patches similar to those used in nicotine and hormone replacement therapies. Indeed, a recent publication using aerosolized cannabinoids has demonstrated the feasibility of this route of administration (Lichtman *et al*., 2000). If effective delivery can be demonstrated by these routes, Δ^9-THC may well become a licensed drug in the future.

During the last decade, research in to cannabis has greatly accelerated. The discovery of specific cannabinoid receptors in the body and an entire endogenous cannabinoid system has led to the development of numerous synthetic cannabimimetic drugs and a greater understanding of their effects at the cellular level. The rest of this chapter describes the cannabinoid receptors, their endogenous ligands and the potential therapeutic uses of modulators of this endogenous cannabinoid system.

1.2 Cannabinoid Receptors

The pharmacological potencies of cannabinoids both *in vitro* and *in vivo* are dependent on their stereochemistry, with (-)-enantiomers usually being considerably more potent than (+)-enantiomers. For example, the synthetic cannabinoid 3-(1,1-dimethylheptyl)-(-)-11-hydroxy-Δ^8-tetrahydrocannabinol was shown to be highly psychotropic in mice, rats and pigeons while its (+)-enantiomer was inactive at doses up to several thousand times higher (Mechoulam *et al*., 1988). The psychotropic potencies of cannabinoids are also on a par with those of drugs that are known to act *via* receptors, and much greater than those of drugs, such as ethanol, that do not. This evidence indicated that the actions of cannabinoids may be receptor mediated. Further evidence suggested that cannabinoids exert their effects *via* a G protein-coupled receptor (GPCR). Many

GPCRs use cyclic AMP (cAMP) as a second messenger and influence its enzymatic synthesis by adenylate cyclase. In its inactive state, the G protein component of GPCRs exists as a trimer of G_α, G_β and G_γ subunits with a molecule of GDP bound to G_α. On ligand binding, a conformational change in G_α reduces its affinity for GDP and results in its displacement by GTP. This, in turn, causes G_α to dissociate from $G_{\beta\gamma}$ and, if the GPCR is coupled to adenylate cyclase, G_α binds to the enzyme (see **figure 1.2**) either stimulating or inhibiting it, depending on whether the α subunit is stimulatory ($G_{s\alpha}$) or inhibitory ($G_{i\alpha}$). This effect is terminated when the GTP bound to G_α is hydrolysed to GDP by GTPase, causing inactivation of the receptor. Cannabinoids were shown to exert a concentration-dependent inhibition of both basal and forskolin-stimulated cAMP production in N18TG2 neuroblastoma cell membranes (Howlett, 1984; Howlett, 1985). A further study showed that when N18TG2 cells were pre-treated with pertussis toxin, a substance which inhibits $G_{i/o}$ proteins, the cannabinoid-induced inhibition of cAMP accumulation was abolished (Howlett *et al*., 1986). This further supported the idea that the effect of cannabinoids on cAMP production is GPCR-mediated and not a result of a direct interaction with adenylate cyclase.
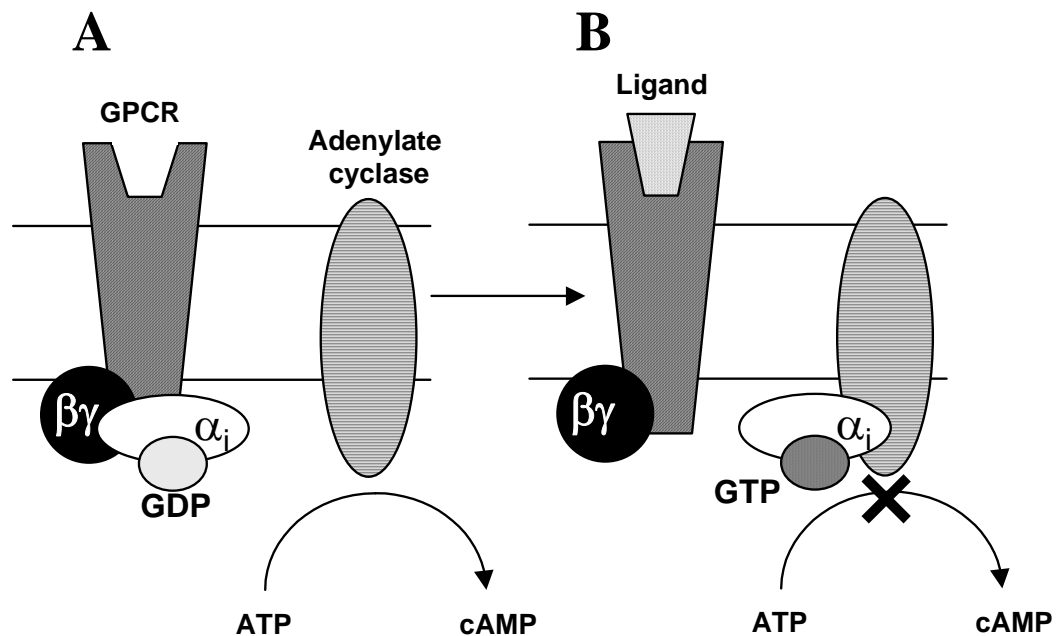
Figure 1.2: The inactive (**A**) and active (**B**) states of an adenylate cyclase-linked inhibitory G protein-coupled receptor.

1.2.1 The CB1 Cannabinoid Receptor

The search for cannabinoid receptors was initially impeded by the high lipophilicity of Δ^9-THC and its synthetic analogues. This made them unsuitable candidates for radioligands to probe for the existence of cannabinoid receptors, as their tendency to randomly partition in to biological membranes would mask any specific binding sites. However, experiments using the ^{3}H analogue of the synthetic compound CP-55,940, a more polar molecule than previous cannabinoids, demonstrated a single population of specific cannabinoid binding sites in rat brain P_2 membranes (Devane *et al*., 1988). This first cannabinoid receptor, now termed the CB1 receptor, was subsequently cloned from a rat cerebral cortex complementary DNA (cDNA) library (Matsuda *et al*., 1990) and shown to be a protein of 473 amino acid residues. When this receptor was functionally expressed in Chinese hamster ovary (CHO) cells, it was shown that both Δ^9-THC and CP-55,940 inhibited forskolin-sensitive cAMP accumulation in a concentration-dependent manner, with the (-) enantiomers being considerably more potent than the (+) enantiomers. This inhibition of cAMP production was abolished by pre-treatment with pertussis toxin, indicating that the response was $G_{i/o}$ protein-mediated. In addition, neither Δ^9-THC nor CP-55,940 affected cAMP accumulation in CHO cells that were not transfected with the putative cannabinoid receptor cDNA. Analysis of the amino acid sequence of the rat CB1 receptor (rCB1) confirmed that it belonged to the GPCR superfamily, possessing seven hydrophobic transmembrane domains, a cytosolic *C*-terminus and an extracellular *N*-terminus containing three possible glycosylation sites (Song & Howlett, 1995).

Mammalian CB1 receptors were subsequently cloned from human (Gerard *et al*., 1991) and mouse brain (Chakrabarti *et al*., 1995) and shown to be proteins of 472 and 473 amino acids, respectively. Sequence analysis of these peptides demonstrated extensive homologies between them and the rCB1 receptor. The human receptor (hCB1) had 97.3 % amino acid identity with rCB1, while the murine CB1 receptor (mCB1) exhibited 99 % and 97 % identity with rCB1 and hCB1, respectively, suggesting that the CB1 receptor is a pharmacologically important molecule, at least in mammals.

Alternate splicing of CB1 receptor messenger RNA (mRNA) has also been demonstrated in both human and rat, resulting in an isoform of the receptor named CB1A. This receptor is functionally similar to CB1 but is 61 amino acids shorter at its *N*-terminus, resulting in the absence of two of the three possible glycosylation sites. In addition, the first 28 amino acids of the peptide are totally different to CB1, being more hydrophobic. A study of the relative distribution of mRNA for the two isoforms using RT-PCR showed that CB1A is present at levels up to a maximum of 20 % of those for CB1, depending on the tissue (Shire *et al*., 1995). Studies to compare cannabinoid binding to the two CB1 receptor isoforms showed that [^{3}H]-CP-55,940 binds to both receptors in a highly specific and saturable manner. Of the cannabinoids compounds tested, the order of affinity for both CB1 and CB1A was CP-55,940 > Δ^9-THC > WIN 55-212,2, although the affinity of these compounds for CB1A was approximately three times less than for the CB1 receptor (Rinaldi-Carmona *et al*., 1996).

In addition to the mammalian CB1 receptors cloned to date, CB1 receptors have also been cloned from two other vertebrate species. The nCB1 receptor from the roughskin newt *Taricha granulosa* (Soderstrom *et al*., 2000) and the FCB1A and FCB1B receptor isoforms from the puffer fish *Fugu rubripes* (Yamaguchi *et al*., 1996) have been shown to exhibit 84.2, 72.2 and 59.0 % amino acid homology with hCB1, respectively. There is also functional evidence of the CB1 receptor in a number of other non-mammalian species including chicken, turtle, frog and trout (Howlett *et al*., 1990) and a possible CB1-like receptor in the leech central nervous system (CNS) with 49.3 % amino acid homology compared to hCB1. This receptor appears to be a chimeric cannabinoid/melanocortin receptor that may be a "living fossil" of the CB1 and melanocortin receptors found today in higher organisms (Elphick, 1998; Stefano *et al*., 1997). The conservation of CB1 amino acid sequence in species that are evolutionary distant suggests that the evolution of the CB1 receptor itself was an ancient event and that this receptor plays a key physiological role.

CB1 Receptor Tissue Distribution

The CB1 receptor is predominantly expressed within the CNS and its distribution appears to be consistent with the known psychoactive effects of cannabinoids. A detailed, quantitative autoradiographic study of CB1 receptor distribution in human brain using [^{3}H]-CP-55,940 has demonstrated that the expression of CB1 is heterogeneous (Glass *et al*., 1997). Furthermore, the CB1 receptor distribution revealed in this study is consistent with the effects cannabinoids have on behaviour and locomotion. Specific binding of [^{3}H]-CP-55,940 was observed in all areas of the brain and spinal cord, with the highest levels of CB1 receptor expression in the areas responsible for memory, movement, higher cognitive functions and control of the autonomic nervous system.

The CB1 receptor has also been shown to be present in a number of peripheral tissues. Both functional studies and isolation of CB1 receptor mRNA have shown the receptor to be present in testis (Gerard *et al*., 1991), lung (Rice *et al*., 1997), heart, kidney, colon, pancreas, spleen, placenta and liver (Shire *et al*., 1995). However, evidence from the ileum (Croci *et al*., 1998), urinary bladder (Pertwee & Fernando, 1996), vas deferens, whole gut and myenteric plexus longitudinal muscle (Griffin *et al*., 1997), suggests that the presence of CB1 in these tissues may be confined to peripheral nerve terminals. The CB1 receptor has also recently been found in the retinas of rhesus monkey, rat, mouse, chick, salamander and goldfish using a subtype-specific monoclonal antibody (Straiker *et al*., 1999).

In the immune system, the CB1 receptor has been described in a number of primary cells and cell lines. Northern blotting has shown CB1 to be present in mouse spleen, but not in the thymus (Schatz *et al*., 1997), suggesting that the receptor is predominantly expressed in B cells. In the same study, quantitative RT-PCR showed CB1 receptor mRNA to be present in mouse spleen at 1.96×10^2 molecules/100 ng RNA compared to 2.8×10^5 molecules/10 ng RNA in the brain. A more detailed study of CB1 mRNA expression within the human immune system demonstrated the presence of the receptor in tonsils, spleen and leukocytes, although at levels much lower than CB1 mRNA expression in the CNS (Bouaboula *et al*., 1993). The rank order of CB1 receptor mRNA expression in immune cells was B cells > natural killer cells $\geq$ polymorphonuclear neutrophils $\geq$ T8 cells > monocytes > T4 cells.

1.2.2 The CB2 Cannabinoid Receptor

Consistent with the anti-inflammatory and immunosuppressive effects of cannabis, a second cannabinoid receptor, CB2, was reported in the human macrophage-derived cell line HL60 (Munro *et al.*, 1993). When the human CB2 (hCB2) cDNA was transfected into COS cells, which do not usually express any receptors for cannabinoids, a saturable number of high affinity binding sites for the synthetic cannabinoids WIN 55-212,2 and CP-55,940 were observed with dissociation constants (K_d) of 3.7 and 1.6 nM, respectively, for the two compounds. In the same expression system, it was also shown that, like CB1, the CB2 receptor is negatively coupled to adenylate cyclase *via* the $G_{i/o}$ GTP binding protein (Bayewitch *et al.*, 1995; Shire *et al.*, 1996). Analysis of the hCB2 receptor amino acid sequence indicated that it also belongs to the GPCR superfamily with the characteristic seven transmembrane domains, an intracellular *C*-terminal domain and an extracellular *N*-terminus. However, the homology between the hCB1 and hCB2 receptors was relatively low, with an overall amino acid identity of only 44 %, rising to 68 % in the transmembrane domains. Despite this structural difference, many cannabinoid compounds display nearly equal affinity for the two receptors (see **section 1.7.1**).

Mouse and rat CB2 receptors (mCB2 and rCB2) were subsequently cloned and, although the amino acid sequences are highly conserved between the species, they are more divergent than the CB1 receptor. The mCB2 receptor is 13 amino acids shorter at the *C*-terminus than the hCB2 receptor and shares 82 % amino acid identity (Shire *et al.*, 1996), whereas the rCB2 receptor is the same length as hCB2, with 93 % homology (Griffin *et al.*, 2000). In addition to the human, murine and rat CB2 receptors, there is also evidence for the existence of CB2 receptors in a number of other species.

CB2 Receptor Tissue Distribution

In contrast to the high levels of CB1 receptor expression within the CNS, the CB2 receptor is found predominantly in the immune system. There is little evidence of any CB2 receptor expression in the CNS except one report of CB2 mRNA in mouse cerebellar granule cells, although the level of CB2 expression was not

determined (Skaper *et al*., 1996). In addition, there is evidence of the CB2 receptor being present in the peripheral nervous system. Functional studies and RT-PCR have demonstrated the presence of the CB2 receptor on peripheral nerve terminals in mouse vas deferens (Griffin *et al*., 1997).

In the immune system, as well as the HL60 macrophage cell line that the receptor was originally cloned from, CB2 has been reported in a number of different cells from various species. These include primary rat peritoneal mast cells and the leaukaemic basophil cell line RBL-2H3 (Facci *et al*., 1995), primary mouse splenocytic T-cells (Schatz *et al*., 1997), the macrophage cell line RAW264.7 (Jeon *et al*., 1996), the murine T-cell line EL4.IL-2 (Condie *et al*., 1996) and primary murine natural killer cells (Massi *et al*., 2000). Quantitative RT-PCR has demonstrated the presence of CB2 receptor mRNA in mouse spleen and thymus at 3.69×10^3 and 3.6×10^2 molecules/100 ng RNA, respectively (Schatz *et al*., 1997). A more in-depth study of CB2 receptor mRNA expression within the immune system revealed that in spleen and tonsils, CB2 mRNA levels are equivalent to those of CB1 mRNA in the CNS (Galiègue *et al*., 1995). The rank order of CB2 mRNA expression in immune cells was determined as B cells > natural killer cells >> monocytes > polymorphonuclear neutrophils > T8 cells > T4 cells, similar to the rank order for CB1 mRNA expression. However, CB2 receptor mRNA expression was found to be between 10 and 100 times greater than that of the CB1 receptor.

1.2.3 Cannabinoid Receptor Signal Transduction

As described earlier in this section, both CB1 and CB2 receptors are negatively coupled to adenylate cyclase, their activation causing a decrease in intracellular cAMP levels. This inhibition of cAMP synthesis results in a number of downstream events, which will be dealt with later in this chapter. However, the coupling of cannabinoid receptors to adenylate cyclase may not be as simple as originally thought. There is evidence in the literature that in the striatum, where CB1 receptors are localized on the same neurones as $G_{i/o}$-coupled dopamine D2 receptors, cannabinoid agonists can cause an accumulation of cAMP through the stimulatory G protein, G_s (Glass & Felder, 1997). This effect was also seen in CHO cells transfected with the CB1 receptor, but was not observed in cells

transfected with CB2. Although the effect of cannabinoid receptors on adenylate cyclase is a major route of cannabinoid signal transduction, other mechanisms are known. Soon after the discovery of the CB1 receptor, it was demonstrated that its activation caused an inhibition of N-type Ca^{2+} channels in the NG108-15 neuroblastoma-glioma cell line (Mackie & Hille, 1992; Caulfield & Brown, 1992). Since this discovery, it has also been shown that activation of the CB1 receptor inhibits P/Q-type Ca^{2+} channels and activates inwardly rectifying K^+ currents within the CNS (Mackie *et al*., 1995; Felder *et al*., 1995; Twitchell *et al*., 1997). This cannabinoid-induced modulation of intracellular Ca^{2+} and K^+ ion levels affects the electrochemical properties of neurones and, ultimately, results in the well-documented neuromodulatory effects of cannabinoid compounds. These effects, however, are exclusively CB1 receptor-mediated and there is no evidence to date of CB2 receptor coupling to ion channels.

A signal transduction mechanism common to both CB1 and CB2 receptors is the $G_{i/o}$-dependent activation of mitogen-activated protein kinase (MAPK) (Bouaboula *et al*., 1997; Bouaboula *et al*., 1999). This enzyme phosphorylates other proteins downstream of it, modulating their activities and subsequently affecting cellular processes.

1.3 Endogenous Cannabinoid Receptor Ligands

With the discovery of cannabinoid receptors came an effort to isolate and characterize putative endogenous cannabinoid receptor ligands, the "endocannabinoids", and the first of these compounds was isolated from porcine brain by Devane *et al.* (1992). Organic solvent extracts of brain were partially purified by chromatography and assayed for their ability to displace a radiolabelled cannabinoid, [^{3}H]-HU-243, from rat synaptosomal membranes. Further purification of the fractions that displaced [^{3}H]-HU-243 yielded a single compound that was spectroscopically characterized as *N*-arachidonylethanolamide, an arachidonic acid derivative, subsequently named anandamide ("ananda" meaning bliss in Sanskrit). Anandamide was shown to inhibit the specific binding of [^{3}H]-HU-243 to synaptosomal membranes with an

inhibition constant (K_i) of 52 nM, compared to 46 nM for Δ^9-THC using the same assay system. Anandamide is also a ligand for the CB2 cannabinoid receptor. When CB2 was originally discovered, anandamide was shown to inhibit [^{3}H]-WIN 55-212,2 binding to CB2 expressed in COS cells with a K_i of 1.6 μM, compared to 320 nM for Δ^9-THC. In addition, anandamide, like known psychotropic cannabinoids, was shown to inhibit the twitch response of isolated murine vas deferens in a concentration-dependent manner (Devane *et al.*, 1992a). In the tetrad of pharmacological tests commonly used to define cannabimimetic activity, anandamide reduced spontaneous activity, caused antinociception and catalepsy and reduced core body temperature in a similar manner to Δ^9-THC, although it was between 1.3 and 18 times less potent (Smith *et al.*, 1994).

Soon after the discovery of anandamide, a slightly different approach resulted in the discovery of two more endocannabinoids. Rather than isolating the compounds directly from brain preparations, long chain, unsaturated fatty acid ethanolamides related to anandamide were synthesized and their presence, or lack of, was examined in porcine brain by thin layer chromatography. The two compounds that were found to exist in this tissue, homo-γ-linolenyl ethanolamide and docosatetraenyl ethanolamide, displaced [^{3}H]-HU-243 from rat synaptosomal membranes with K_i values of 53.4 and 34.4 nM, respectively (Hanus *et al.*, 1993).

More recently, a fourth endocannabinoid was isolated from canine small intestine (Mechoulam *et al.*, 1995) and was characterized as 2-arachidonyl glycerol (2-AG). Like anandamide, 2-AG is a derivative of arachidonic acid but differs from the other endocannabinoids by being a monoglyceride rather than an ethanolamide. Initial binding studies demonstrated that 2-AG displaced [^{3}H]-HU-243 from membranes of COS-7 cells transfected with CB1 or CB2 receptors with K_i values of 472 and 1400 nM, respectively. These values are much higher than those determined for anandamide, although later work by the same group showed that 2-AG exhibited K_i values for the CB1 and CB2 receptors of 58.3 and 145 nM, respectively, using the same assay system (Ben-Shabat *et al.*, 1998). When assayed with cells that were not transfected with either cannabinoid receptor, no 2-AG binding was observed. In addition to binding to both cannabinoid receptors, 2-AG inhibited electrically evoked contractions of isolated mouse vas deferens, although it was less potent than Δ^9-THC. In the tetrad of pharmacological tests, 2-

AG reduced spontaneous activity, induced antinociception and catalepsy and reduced rectal temperature after intra-venous (i.v.) administration to mice (Mechoulam *et al*., 1995). Although 2-AG was approximately equipotent with anandamide, it was less potent than Δ^9-THC and was lethal within two minutes of injection at 60 mg/kg. The mechanism of this effect was not determined. The structures of the endocannabinoids are shown in **figure 1.3**.

Anandamide

Homo-γ-linolenyl ethanolamide

Docosatetraenyl ethanolamide

2-Arachidonyl glycerol
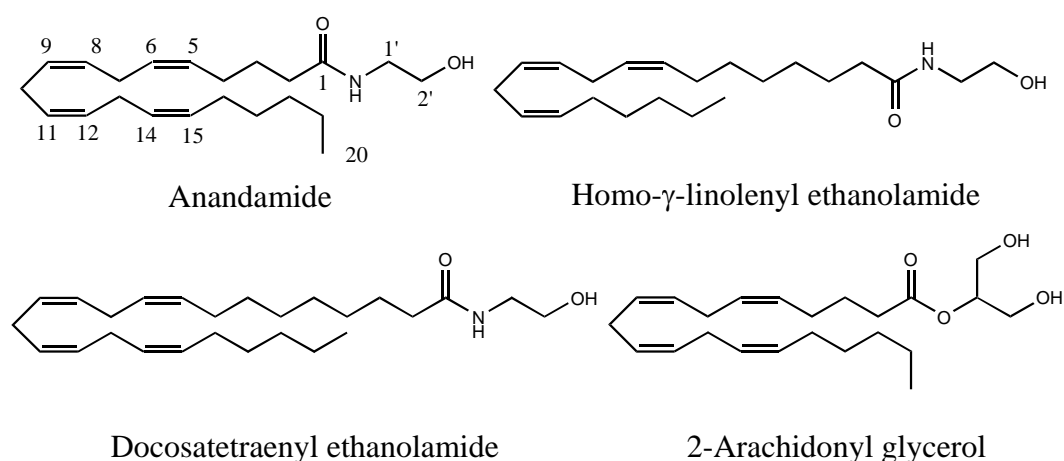
Figure 1.3: The endogenous cannabinoids, showing the numbering system for the carbon chain.

1.3.1 Other Endocannabinoid Candidates

There are two particular endogenous fatty acid amides that are candidate endocannabinoids, although there are varying reports of their abilities to bind to the cannabinoid receptors. The first of these, palmitoylethanolamide (**figure 1.4**), was originally described as an endogenous CB2 receptor ligand, binding to and activating this receptor with a higher affinity than anandamide (Facci *et al*., 1995). However, subsequent binding studies have indicated that palmitoylethanolamide and its analogues have little or no affinity for either the CB1 or CB2 receptors (Showalter *et al*., 1996; Sheskin *et al*., 1997; Lambert *et al*., 1999). Despite this apparent lack of cannabinoid receptor affinity, palmitoylethanolamide has been shown to be orally active in down-regulating mast cell activity in rodent models of inflammation (Mazzari *et al*., 1996) and has also been shown to be involved in the

control of pain initiation in mice. This effect will be described in more detail in **section 1.8**.
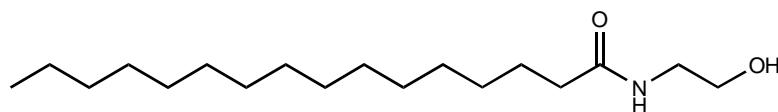
Figure 1.4: The structure of palmitoylethanolamide, a putative endocannabinoid.

The other endocannabinoid candidate is oleamide (*cis*-9,10-octadecenamide) (**figure 1.5**), a sleep-inducing lipid originally isolated from the cerebrospinal fluid of sleep deprived cats (Cravatt *et al*., 1995). This compound has been shown to allosterically modulate ligand binding to 5-hydroxytryptamine (5-HT) and GABA receptors (Huidobro-Toro & Harris, 1996; Lees *et al*., 1998). Although there is conflicting evidence concerning the affinity of oleamide for cannabinoid receptors, recent evidence suggests that it does have some affinity, albeit low, for the CB1 receptor (Cheer *et al*., 1999). The same group also demonstrated that the CB1 receptor is involved in the allosteric regulation of 5-HT receptors by oleamide, possibly due to a direct interaction between the two receptors.
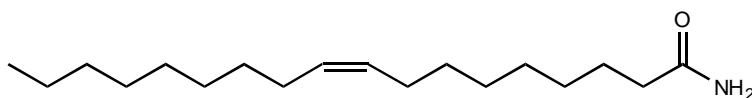
Figure 1.5: The structure of oleamide, an endogenous sleep-inducing ligand and possible modulator of endocannabinoid signalling.

1.3.2 Tissue Distribution of Anandamide and 2-AG

Quantification of anandamide in rat brain showed that it is present at levels ranging from 20 pmol/g of tissue in the thalamus to 29 pmol/g in the hippocampus. In human brain, anandamide was found in all of the five regions tested, with levels ranging from 25 pmol/g of tissue in the cerebellum to 148 pmol/g in the hippocampus (Felder *et al*., 1996). However, 2-arachidonyl glycerol has been shown to be present at much higher levels than anandamide. In the rat brain, 2-AG was shown to be present at up to 4 nmol/g of tissue, over 100 times more concentrated than anandamide, suggesting that 2-AG may be the

predominant endocannabinoid (Sugiura *et al*., 1995; Stella *et al*., 1997). Both anandamide and 2-AG have been found in peripheral tissues, albeit at lower levels than in the brain. So far, both compounds have been found in the spleen (Felder *et al*., 1996; Ben-Shabat *et al*., 1998) and kidney (Deutsch *et al*., 1997a; Kondo *et al*., 1998), while anandamide has been found in the uterus (Schmid *et al*., 1997) and heart (Felder *et al*., 1996) with 2-AG found in the gut (Mechoulam *et al*., 1995), liver, lung and plasma (Kondo *et al*., 1998). There is also evidence that, like the CB1 cannabinoid receptor, endocannabinoids are present in invertebrate species. To date, anandamide has been isolated from five species of bivalve mollusc (Sepe *et al*., 1998) and the ovaries of sea urchins (Bisogno *et al*., 1997b). Interestingly, anandamide levels have been shown to increase in post-mortem brain, possibly due to activation of the biosynthetic pathways implicated in anandamide formation (Felder *et al*., 1996). It remains to be seen whether this effect has any effect on cannabinoid assays using brain preparations.

1.3.3 Endocannabinoid Signalling

On binding to the CB1 or CB2 cannabinoid receptors, anandamide and 2-AG activate the signalling mechanisms described in **section 1.2.3**, namely inhibition of N- and P/Q-type Ca^{2+} channels, activation of inwardly rectifying K^+ currents, inhibition of adenylate cyclase and activation of MAPK *via* the CB1 and CB2 receptors. However, it is apparent that anandamide is only a partial agonist at the CB1 receptor, binding to the receptor but not fully activating it. When CB1 receptor activation was measured in mouse brain membranes, the synthetic cannabinoids CP-55,940 and HU-210 were full agonists, while both anandamide and Δ^9-THC elicited only a partial response (Burkey *et al*., 1997). In fact, anandamide exhibited greater efficacy than Δ^9-THC, despite having a lower affinity for the receptor. Although 2-AG has a lower affinity for the cannabinoid receptors than anandamide it is fully efficacious, suggesting that 2-AG may be the primary endocannabinoid.

1.3.4 Metabolism of the Endogenous Cannabinoids

There are three key mechanisms involved in the metabolism of the endocannabinoid compounds, namely their synthesis and release from the cell, transport from the extracellular space back in to the cytoplasm and hydrolytic degradation by an intracellular enzyme, inactivating them. As the research presented in this thesis aims to develop compounds that may inhibit the transport mechanism or the hydrolytic enzyme, these mechanisms will be described in the subsequent sections. Reviews of endocannabinoid synthesis may be found elsewhere (Hillard & Campbell, 1997; Piomelli *et al*., 1998).

1.4 Anandamide Uptake

In order for the termination of endogenous cannabinoid signalling to be achieved, the compounds must be removed from the extracellular space and in to the cytoplasm for enzymatic degradation. This may occur by simple diffusion across a concentration gradient or by a facilitated transport mechanism. The latter route is described below.

The first reported evidence of a cellular uptake mechanism for endogenous cannabinoids was obtained using rat glioma C6 and mouse neuroblastoma N18TG2 cells. When these cells were incubated with [^{3}H]-anandamide, there was a time-dependent decrease in its levels in the medium (Deutsch & Chin, 1993). A more detailed examination of anandamide uptake was carried out in primary rat neural cells and astrocytes (Di Marzo *et al*., 1994). In these cells, a rapid, saturable and temperature-dependent accumulation of [^{3}H]-anandamide was observed. Moreover, this accumulation appeared to be specific for anandamide, as other *N*-acylethanolamines did not compete for [^{3}H]-anandamide uptake. Subsequently, these characteristics for anandamide accumulation were also demonstrated in cerebellar granule cells (Hillard *et al*., 1997) and in the immune system using RBL-2H3 cells, a human leukocyte cell line (Bisogno *et al*., 1997a). In addition, a time-, temperature- and concentration-dependent anandamide uptake mechanism has been demonstrated in rat neurones and astrocytes (Beltramo *et al*., 1997). Research has also shown that in both the CNS and immune system, cellular

16

accumulation of anandamide is independent of ATP and ion gradients and is significantly inhibited by phloretin, a non-specific inhibitor of carrier-mediated uptake systems (Hillard *et al*., 1997; Rakhshan *et al*., 2000). This evidence suggests that anandamide uptake is carrier-mediated and is a passive process, dependent on the anandamide concentration gradient across the cell membrane. Evidence also suggests that anandamide accumulation is independent of the CB1 receptor. The potent CB1 receptor ligands WIN 55,212-2 and SR141716A failed to inhibit anandamide uptake at a concentration of 10 µM. However, the more lipophilic ligands Δ^9-THC and HU-210 both inhibited this accumulation at the same concentration. This suggests that these lipophilic compounds affect anandamide uptake by non-specific effects on the cell membrane. Although it is widely accepted that anandamide is removed from the extracellular space by this mechanism, the transport of 2-AG is less clear. It was originally thought that 2-AG crossed the membrane by diffusion (Di Marzo *et al*., 1998), but more recent evidence suggests that it is also a substrate of the anandamide transporter. Inhibition studies demonstrated that 2-AG inhibited the transport of anandamide in to astrocytoma cells with an IC_{50} (the concentration required to inhibit 50 % of anandamide uptake) of 18.5 µM. In addition, it was shown that [^{3}H]-2-AG was accumulated by astrocytoma cells with comparable kinetics to anandamide accumulation (Piomelli *et al*., 1999).

1.4.1 Substrate Specificity of the Anandamide Transporter

Uptake and inhibition studies have revealed particular structural requirements for optimal translocation by the anandamide transporter (Piomelli *et al*., 1999). Perhaps the most important requirement is at least one *cis* double bond, indicating that it may be necessary for substrates to adopt a U-shaped configuration for transport. Of the anandamide analogues tested, most head groups were tolerated by the transporter with a *para*-phenolic substitution particularly favourable. Notable exceptions were benzyl analogues with *para*-methyl, methyl ester, cyano or chlorine groups. These alterations effectively abolished recognition by the transport mechanism.

1.5 Fatty Acid Amide Hydrolase

With the discovery of anandamide, it was soon apparent that, as an amide, it was susceptible to hydrolytic inactivation. This was demonstrated using the non-specific serine protease inhibitor phenylmethylsulphonyl fluoride (PMSF). This compound was shown to increase the potency of anandamide as an inhibitor of electrically evoked contractions of guinea pig myenteric plexus preparations (Pertwee *et al*., 1995a). The increase in potency was proportional to the concentration of PMSF, suggesting that it was inhibiting the hydrolysis of anandamide by a serine protease enzyme. However, even before the discovery of the endogenous cannabinoids, evidence existed in the literature for an amidohydrolase enzyme in rat liver and dog brain that catalysed the hydrolysis of *N*-acylethanolamines, a family of compounds of which anandamide is a member (Natarajan *et al*., 1984; Schmid *et al*., 1985). The first direct evidence of an enzyme activity that could hydrolyse anandamide was obtained using soluble or membrane fractions from mouse neuroblastoma N18TG2 and rat glioma C6 cells. The enzyme activity that hydrolysed anandamide was mainly localized in the membrane fractions and this activity was totally inhibited by PMSF at concentration of 1.5 mM. Furthermore, this enzyme activity was also present in homogenates of rat liver, brain, lung and kidney (Deutsch & Chin, 1993). Following this discovery, an amidohydrolase activity that hydrolysed anandamide was identified and partially characterized in rat brain microsomes. This "anandamide amidohydrolase" was highly selective for anandamide and other polyunsaturated *N*-acylethanolamines and demonstrated maximal activity at pH 6 and 8 (Desarnaud *et al*., 1995).

A similar enzyme activity was also described using oleamide. When incubated with rat brain membrane fractions, oleamide was rapidly hydrolysed to oleic acid and this enzymatic activity was also inhibited by 1 mM PMSF. Only a small amide hydrolysis activity was present in soluble rat brain fractions and no activity was present in rat pancreatic microsomes (Cravatt *et al*., 1995). This "oleamide hydrolase" was subsequently studied in rat liver plasma membranes and shown to be pH-dependent with a maximal rate at pH 10 (Patterson *et al*., 1996). In addition to this, a partially purified anandamide amidohydrolase activity from N18TG2

membrane fractions was shown to catalyse the hydrolysis of both anandamide and oleamide with identical pH and temperature profiles, suggesting both compounds were substrates of the same enzyme (Maurelli *et al*., 1995).

Using detergent-solubilized rat liver plasma membranes, this enzyme was subsequently purified and cloned (Cravatt *et al*., 1996). The deduced amino acid sequence showed the enzyme to be a protein of 579 amino acids that exhibits extensive homology with members of the family of "amidase signature" enzymes. These enzymes exist in a diverse range of species, although this was the first (and, to date, only) mammalian member of the family. When the cloned enzyme was expressed in COS-7 cells, there was a high level of activity compared to untransfected cells. Using this expression system, anandamide and oleamide were both rapidly hydrolysed to their parent fatty acids with rates of 333 and 242 nmol/min/mg protein, respectively (with both substrates at 100 μM). The enzyme was also shown to hydrolyse several other fatty acid amides in addition to anandamide and oleamide and, therefore, was named fatty acid amide hydrolase (FAAH). FAAH has since been cloned from both human and mouse liver (Giang & Cravatt, 1997) and pig brain (Goparaju *et al*., 1999a). All of these enzymes are 579 amino acids in length with well conserved sequences and homologies ranging from 81 to 91 % (see **table 1.1**), suggesting an important physiological role.

Enzyme	Size (kDa)	Amino Acid Homology (%)			
		Rat FAAH	Mouse FAAH	Human FAAH	Pig FAAH
Rat FAAH	63.3				
Mouse FAAH	63.4	91			
Human FAAH	63.0	82	84		
Pig FAAH	62.9	81	80	85	

Table 1.1: The sizes and cross-species homologies of cloned fatty acid amide hydrolase enzymes.

1.5.1 Substrate Specificity of FAAH

Biochemically, the four cloned FAAH enzymes have been shown to have similar, but subtly different, substrate specificities. FAAH hydrolyses all fatty acid amides to some extent, but there are structural features that define the recognition of substrates by the enzyme (Lang *et al*., 1999). For example, a primary amide is more rapidly hydrolysed by FAAH than a secondary or tertiary amide. Arachidonyl amide (100 μM) was shown to be hydrolysed by rat brain microsomal FAAH at a rate of 2.85 nmol/min/mg protein compared to 1.30 nmol/min/mg protein for anandamide at the same concentration. The saturation of the carbon chain is also important, with increasing unsaturation resulting in a higher rate of hydrolysis. Thus, anandamide and other arachidonic acid derivatives are hydrolysed more rapidly than more saturated fatty acid amides. An important and unusual feature of FAAH is that, although classed as an amidase, it also catalyses the hydrolysis of esters, including 2-AG (Di Marzo *et al*., 1998). In fact, the rate of 2-AG hydrolysis by FAAH has been shown to be considerably greater than that of anandamide. When recombinant porcine FAAH was overexpressed in COS-7 cells, 100 μM anandamide was hydrolysed at a rate of 207 nmol/min/mg protein, whereas 2-AG was hydrolysed at 733 nmol/min/mg protein at the same concentration (Goparaju *et al*., 1999a). The difference in rate was even more pronounced using recombinant rat FAAH.

1.5.2 Tissue Distribution of FAAH

Northern blot analysis of rat tissues with a probe for FAAH revealed it to be most abundant in the brain and liver with lesser amounts in the lung, kidney, testes and spleen. The enzyme was not detectable in heart or skeletal muscle (Cravatt *et al*., 1996). Subsequent work has demonstrated that low levels of FAAH are also detectable in the stomach, small intestine and colon while confirming the absence of the enzyme in heart and skeletal muscle (Katayama *et al*., 1997). More detailed analysis of FAAH in the rat brain has shown it to be heterogeneously distributed and predominantly localized on large principal neurones (Tsou *et al*., 1998; Egertova *et al*., 1998). This correlates well with the distribution of the CB1 receptor, suggesting that anandamide and 2-AG are hydrolysed at their site of action. Discrepancies between FAAH and CB1 receptor co-localization may

indicate that FAAH is also important in inactivating other neuromodulatory fatty acid amides such as oleamide.

1.5.3 Structural and Catalytic Features of FAAH

As described above, the initial evidence for an enzymatic activity that hydrolysed anandamide suggested it was membrane-bound. When FAAH was initially purified and cloned, analysis of its amino acid sequence confirmed the presence of a transmembrane domain at the extreme *N*-terminus (Cravatt *et al*., 1996), FAAH being the only member of the "amidase signature" family with such a domain. Studies using a mutant of FAAH in which the transmembrane domain was deleted showed that this deletion did not prevent its tight association with the plasma membrane. In addition, when incubated with oleamide, the kinetic profiles of the mutant and wild type FAAH enzymes were nearly identical (Patricelli *et al*., 1998). The only characteristic of the enzyme that appeared to be altered by this deletion was its ability to form oligomers. Both enzymes could achieve this, but the mutant could not form complexes as large as the wild type, suggesting a role for the transmembrane domain in self-association.

Before the cloning and molecular characterization of FAAH, its inhibition by PMSF suggested that it was a serine protease and research using FAAH mutants has confirmed this. Replacing each of the three serine residues that are conserved in all amidase signature enzymes (serine-217, serine-218 and serine-241) with alanine residues severely compromized FAAH's catalytic activity (Patricelli *et al*., 1999). In addition, mutation of the conserved histidine residues did not affect activity, showing that FAAH does not contain the serine-histidine-aspartic acid catalytic unit commonly found in other mammalian serine proteases. More unusual is the ability of FAAH to catalyse the hydrolysis of both amides and esters. Further work with FAAH mutants demonstrated that the lysine-142 residue is essential for this catalysis and added to the evidence that FAAH may act *via* a novel catalytic mechanism (Patricelli & Cravatt, 1999).

1.5.4 Evidence for Other Enzymes That Hydrolyse Endogenous Cannabinoids

Although FAAH is the only cloned enzyme that is known to hydrolyse endogenous cannabinoids, there is evidence in the literature that other such enzymes exist. Work comparing the ability of porcine brain preparations to hydrolyse anandamide and 2-AG demonstrated that the optimum pH for 2-AG hydrolysis was around 7.0, compared to a pH of around 9.0 for anandamide. In both the cytosol and particulate fraction, the 2-AG hydrolysing activity at pH 7.0 was much greater than the corresponding anandamide hydrolysing activity at pH 9.0, being 800- and 30-fold greater, respectively. When the 2-AG hydrolysing activity was partially purified from both cytosol and particulate fraction, it catalysed the hydrolysis of 2-AG at pH 7.0 with rates of 3480 and 4970 nmol/min/mg protein, respectively. Anandamide hydrolysis by the partially purified enzymes was not detectable under the described assay conditions, suggesting that porcine brain has at least two enzymes capable of hydrolysing 2-AG (Goparaju *et al*., 1999b).

Evidence for the existence of another enzyme that catalyses anandamide hydrolysis has also been reported. Using a human megakaryoblastic cell line (CMK), this enzyme was solubilized by freeze-thawing the 12000*g* pellet of cell homogenate. The pH optimum of the enzyme was around 5.0, compared to around 9.0 for FAAH. Activity was almost absent at alkaline pH, suggesting that this enzyme may be present in the acidic environment of lysozymes. Furthermore, the enzyme was less sensitive to PMSF than FAAH and effectively hydrolysed palmitoylethanolamide, a relatively poor substrate for FAAH (Ueda *et al*., 1999).

1.6 Reinforcement of Endocannabinoid Signalling

As described in the previous sections, endocannabinoid signalling is terminated by transport across the plasma membrane and subsequent enzymatic hydrolysis. This leads to a relatively short duration of endocannabinoid signalling, but naturally occurring mechanisms or the action of synthetic drugs may regulate this degradation.

1.6.1 The Entourage Effect

As the endocannabinoids and their naturally occurring analogues are substrates for the anandamide uptake mechanism and/or FAAH, they compete with one another for uptake and hydrolysis. Thus, the duration of action of the endocannabinoids is lengthened by this competition. This "entourage effect" was first described for 2-AG. In the brain, spleen and gut, two major 2-acyl glycerol esters, 2-linoleoyl glycerol and 2-palmitoyl glycerol, are present in addition to 2-AG. Neither of these esters binds to or activates the CB1 or CB2 receptors but, when incubated with 2-AG, they potentiated its binding to the receptors and its ability to inhibit adenylate cyclase (Ben-Shabat *et al*., 1998). In addition, these esters increased the potency of 2-AG in the tetrad of pharmacological assays in mice and, although 2-palmitoyl glycerol was ineffective, 2-linoleoyl glycerol significantly inhibited the degradation of 2-AG by intact neuronal and basophilic cells. A similar effect has also been demonstrated using 2-AG and anandamide. As 2-AG is found at much higher levels *in vivo* than anandamide, when 50 μM of 2-AG and 4 μM of radiolabelled anandamide were incubated together with intact RBL-2H3 cells, the hydrolysis of anandamide was significantly reduced (Di Marzo *et al*., 1998). However, in this study, anandamide uptake was not affected by the presence of 2-AG conflicting with the evidence that 2-AG is a substrate of the anandamide transporter. Although there are conflicting reports in the literature, the data described above indicate that, *in vivo*, the action of endocannabinoids may be reinforced by other endocannabinoids and related compounds by the inhibition of FAAH, uptake and, possibly, other mechanisms such as allosteric activation of cannabinoid receptors.

1.6.2 Artificial Reinforcement

There is great therapeutic potential in the artificial reinforcement of endocannabinoid signalling by synthetic drugs with the two main therapeutic targets being the anandamide transporter and FAAH. Inhibition of either, or both, of these targets would lead to a net increase in the amount of endocannabinoids available to bind to cannabinoid receptors or prolong their duration of action. An alternative strategy would be endocannabinoid analogues that activate cannabinoid receptors but are poor substrates for the anandamide transporter or

FAAH. In addition, drugs that inhibit uptake and/or FAAH and also activate cannabinoid receptors would have an additional mechanism of cannabimimetic activity. Synthetic compounds that artificially reinforce endocannabinoid signalling will be described in **sections 1.7.2** and **1.7.3**.

1.7 Synthetic Cannabimimetic Compounds

Even before the discovery of the endogenous cannabinoid system, there was a great deal of interest in the synthesis of cannabinoid compounds to mimic the therapeutic actions of Δ^9-THC. The discovery of the CB1 and CB2 cannabinoid receptors, the anandamide transporter and FAAH, however, has led to a renewed effort to synthesize cannabimimetic drugs that bind to and modulate the activity of these targets. These compounds are described below.

1.7.1 Cannabinoid Receptor Ligands

There are three different types of cannabinoid receptor ligand, namely agonists, antagonists and inverse agonists. An agonist of a receptor is a compound that causes activation of that receptor upon binding, inducing the appropriate downstream events. For example, a CB1 receptor agonist will inhibit N-type calcium channels in neuroblastoma cells upon binding to the receptor. As described earlier, anandamide and Δ^9-THC are only partial CB1 agonists, binding to but not fully activating the receptor. An antagonist of a receptor is a compound that occupies a receptor, yet fails to produce receptor activation and signalling. For example, a competitive cannabinoid receptor antagonist will decrease the level of adenylate cyclase inhibition caused by a cannabinoid receptor agonist by competing for a common binding site.

It is now thought that many receptors, especially GPCRs, exist in an auto-activated state thereby causing a basal level of signalling in the absence of a receptor ligand. Inverse agonists are thought to attenuate this basal activity by causing a conformational change in the receptor that inhibits its interaction with effector proteins. Both the CB1 and CB2 receptors have been shown to possess some tonic activity. This can be demonstrated by the fact that when either receptor

is stably transfected in to a cell line that does not normally express it, a basal level of signalling can be detected. Specific examples include the MAPK activity of Chinese hamster ovary cells. When wild type cells were compared to cells expressing hCB1, it was shown that the transfected cells showed an enhanced level of MAPK activity (Bouaboula *et al*., 1997). An inverse agonist reduces this basal receptor signalling in addition to antagonizing the effect of an agonist.

The synthesis of high-affinity cannabinoid receptor ligands has been invaluable in the discovery of the cannabinoid receptors and the elucidation of their pharmacology. Perhaps the most important synthetic cannabinoids are the cannabinoid receptor antagonists/inverse agonists, which have been vital tools for demonstrating the receptor-mediated effects of cannabinoids. In addition, the design and synthesis of receptor-specific cannabinoid ligands has led to compounds with high affinities for one cannabinoid receptor over the other, therefore paving the way for cannabinoid drugs that target either the CNS or immune system. This section summarizes some of the compounds in the main structural classes of cannabinoid compounds.

Classical Cannabinoid Receptor Agonists

Before the discovery of the cannabinoid receptors, synthetic cannabinoids were almost exclusively based on the dibenzopyran ring system that characterizes Δ^9-THC and the other naturally occurring "classical" cannabinoids. However, of the numerous synthetic classical cannabinoids, the only one that is licensed for use in the U.K. is nabilone (**figure 1.6**), which is prescribed as an anti-emetic and to prevent weight loss in AIDS patients by stimulating appetite. There are many classical cannabinoid compounds that are more potent and selective than nabilone and, to date, all are cannabinoid receptor agonists.

The classical cannabinoid that is perhaps most widely used in cannabinoid research, apart from Δ^9-THC itself, is HU-210. This compound is an analogue of Δ^8-THC, with a dimethylheptyl side chain replacing the pentyl side chain of the naturally occurring cannabinoids. In mice, rats and pigeons, HU-210 was shown to be psychotropic and approximately 90 times more potent than Δ^9-THC (Mechoulam *et al*., 1988).
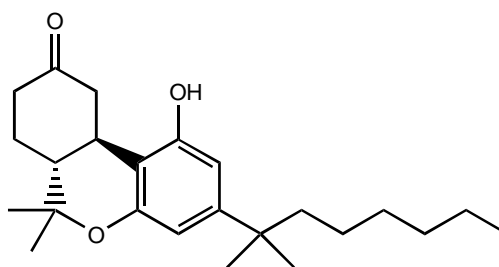
Figure 1.6: The structure of nabilone, the only cannabinoid drug licensed for use in the U.K.

HU-210 and its saturated analogue HU-243 (Devane *et al*., 1992b) are among the most potent cannabinoids synthesized to date, although they do not exhibit selectivity for either the CB1 or CB2 cannabinoid receptors. Of the classical cannabinoids that are selective for one cannabinoid receptor over the other, three compounds are particularly noteworthy being selective agonists for the CB2 receptor. JWH-051, the 1-deoxy analogue of HU-210, shows very high affinity for CB2 with a K_i of 0.032 nM, although the CB1/CB2 ratio is only 37.5. L759633 and L759656, on the other hand, are less potent than JWH-051 but exhibit CB1/CB2 ratios of 163 and 414, respectively (Ross *et al*., 1999). The structures of these compounds and their K_i values at both cannabinoid receptors are summarized in **figure 1.7** and **table 1.2**.

Non-Classical Cannabinoid Receptor Agonists

In an attempt to minimize the structural features necessary in order for cannabinoid compounds to produce analgesia, CP-47,497, an analogue of the potent analgesic compound HHC, was synthesized (see **figure 1.8**). This new compound was bicyclic, lacking the pyran ring of HHC and, like the most potent classical cannabinoids, possessed a dimethylheptyl rather than a pentyl side chain. In five animal models of pain, CP-47,497 was as potent an analgesic as morphine, demonstrating that the pyran ring of HHC is not necessary for analgesia (Melvin *et al*., 1984).
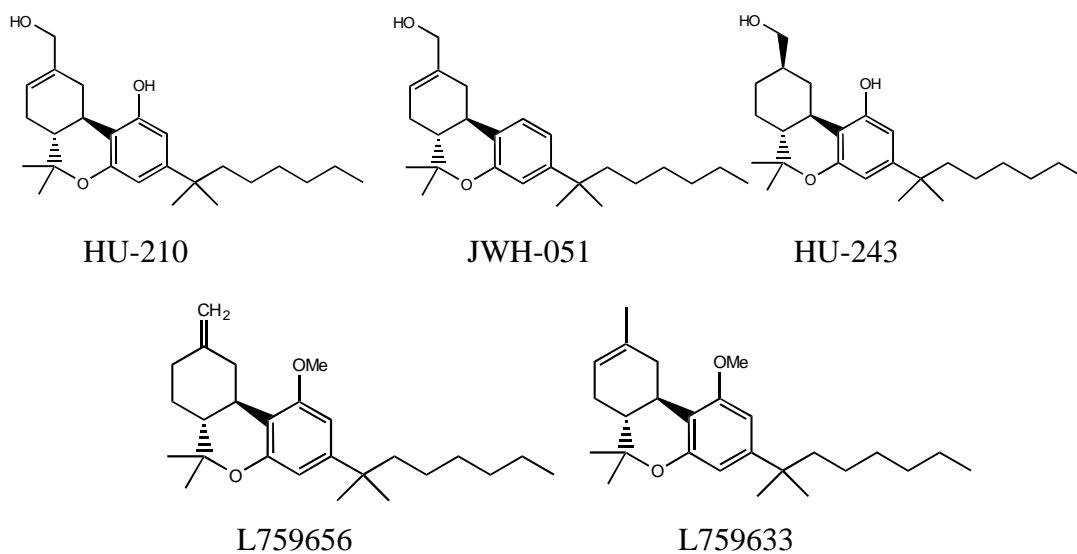
Figure 1.7: The structures of some of the most significant synthetic classical cannabinoid receptor agonists.

Compound	CB1 K_i (nM)	CB2 K_i (nM)	CB1/CB2 Ratio	Reference
Δ^9-THC	53.3	75.3	0.71	Felder *et al.*, 1998
	40.7	36.4	1.12	Showalter *et al.*, 1996
HU-210	0.0608	0.524	0.12	Felder *et al.*, 1998
	0.73	0.22	3.32	Showalter *et al.*, 1996
HU-243	2.3	2.3	1.00	Drake *et al.*, 1998
JWH-051	1.2	0.032	37.5	Huffman *et al.*, 1996
L759656	1043	6.4	163.0	Ross *et al.*, 1999
L759633	4888	11.8	414.2	Ross *et al.*, 1999

Table 1.2: The K_i values at the CB1 and CB2 receptors of some of the most significant classical cannabinoid receptor agonists.
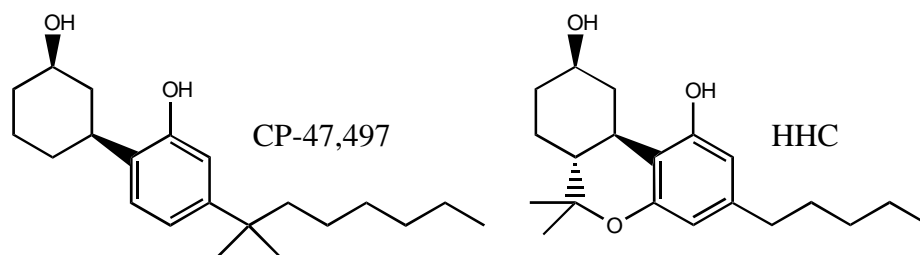
Figure 1.8: Structures of the prototypical non-classical cannabinoid CP-47,497 and the potent classical cannabinoid analgesic HHC.

Hence, CP-47,497 became the prototype of the "non-classical" cannabinoid family of compounds which, like the classical cannabinoids, are all cannabinoid receptor agonists. Today, the most widely known and used non-classical cannabinoid is CP-55,940, which exhibits K_i values in the low nanomolar range at both cannabinoid receptors but does not show any specificity. As mentioned in **section 1.2.1**, the development of [³H]-CP-55,940, being less lipophilic than Δ^9-THC, resulted in the discovery of the CB1 receptor and [³H]-CP-55,940 is still probably the most widely used radiolabelled cannabinoid. Recently, HU-308, an extremely selective non-classical cannabinoid was described in the literature. This compound exhibits very high affinity for CB2 with a K_i of 22.7 nM compared to > 10 µM at the CB1 receptor, resulting in a CB1/CB2 ratio of > 441. HU-308 has also been shown to be effective at reducing blood pressure, blocking defecation, and inducing anti-inflammatory and analgesic effects (Hanus *et al.*, 1999). The structures and K_i values of CP-55,940 and HU-308 are shown in **figure 1.9** and **table 1.3**.
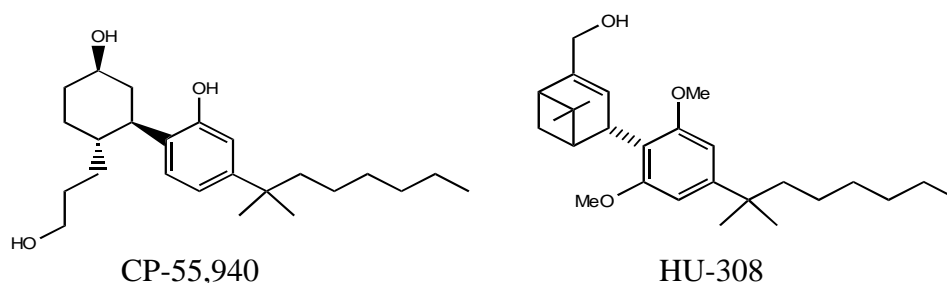
Figure 1.9: The Structures of the potent non-classical cannabinoid receptor agonists CP-55,940 and HU-308.

28

Compound	CB1 K_i (nM)	CB2 K_i (nM)	CB1/CB2 Ratio	Reference
CP-55,940	3.72	2.55	1.46	Felder *et al*., 1998
	0.58	0.69	0.84	Showalter *et al*., 1996
	5.0	1.8	2.78	Ross *et al*., 1999
HU-308	> 10 μM	22.7	> 441	Hanus *et al*., 1999

Table 1.3: The K_i values at the CB1 and CB2 receptors of the non-classical cannabinoid receptor agonists CP-55,940 and HU-308.

Aminoalkylindoles and Their Derivatives

In an attempt to develop non-steroidal anti-inflammatory drugs (NSAIDs) with less ulcerogenicity than existing compounds of this class, Bell *et al.* (1991) synthesized the aminoalkylindole (AAI) derivative pravadoline (**figure 1.10**). This compound inhibited prostaglandin synthesis as it was designed to but, in addition, it exhibited antinociceptive activity in several animal assays.
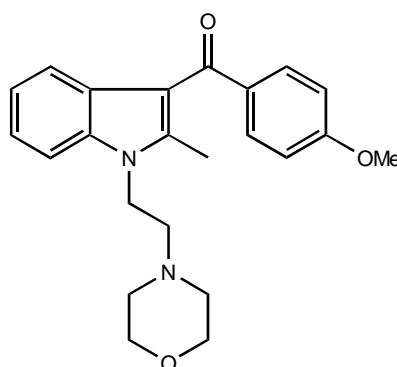
Figure 1.10: The structure of pravadoline, the prototypical aminoalkylindole cannabinoid receptor ligand.

Further structural development of pravadoline culminated in the synthesis of WIN 55-212,2, one of the most potent and widely used cannabinoid receptor agonists (Dambra *et al*., 1992). WIN 55-212,2 has K_i values in the low nanomolar range at both the CB1 and CB2 cannabinoid receptors, showing some selectivity for the CB2 receptor. A more selective, though less potent, member of this family of

compounds is JWH-015 which, again, is selective for the CB2 receptor. Other aminoalkylindole cannabinoid receptor agonists exhibit much higher selectivity. The compounds L-759,787 and L-768,242 are AAIs where the substitution at the 1 and 3 positions is inverted compared to the classical AAI structure, resulting in CB1/CB2 K_i ratios of 160 and 103, respectively (Gallant *et al.*, 1996). In addition to cannabinoid receptor agonists, aminoalkylindole cannabinoid receptor antagonists have been developed. AM630 is an iodinated analogue of pravadoline (Pertwee *et al.*, 1995b) and, although originally described as a cannabinoid receptor antagonist in the brain, it is now known to act as a CB2 receptor-selective inverse agonist and a weak partial agonist at the CB1 receptor (Ross *et al.*, 1999). A final noteworthy compound related to the AAIs is LY320135, a substituted benzofuran compound. This substance has been shown to be an extremely selective antagonist of the CB1 receptor with over one hundred times greater affinity for CB1 than CB2 (Felder *et al.*, 1998).

WIN 55-212,2   JWH-015   L-759,787

L-768,242   AM630   LY320135
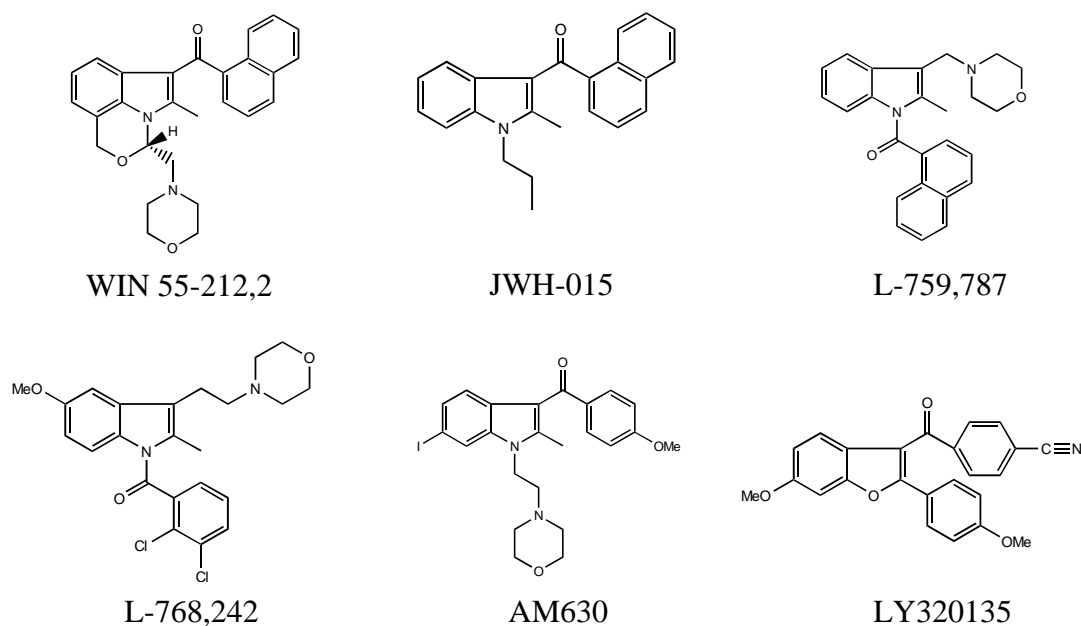
Figure 1.11: The structures of some of the most significant aminoalkylindole
cannabinoid receptor ligands and the related compound LY320135.

Interestingly, there is evidence in the literature that the interaction of WIN 55-212,2 and, presumably other members of the AAI family, with the CB1 receptor may be *via* a different mechanism than for other receptor agonists. A mutant CB1 receptor in which the lysine-192 amino acid residue was replaced with alanine

was stably transfected in to HEK-293 cells. WIN 55-212,2 bound to and activated this mutant receptor, while HU-210, CP-55,940 and anandamide did not (Song & Bonner, 1996). The structures and K_i values of these AAI compounds are shown in **figure 1.11** and **table 1.4**.

Compound	CB1 K_i (nM)	CB2 K_i (nM)	CB1/CB2 Ratio	Reference
WIN 55-212,2	62.3	3.3	18.88	Felder *et al*., 1998
	1.89	0.28	6.75	Showalter *et al*., 1996
JWH-015	383	13.8	27.75	Showalter *et al*., 1996
L-759,787	1917	12.0	159.8	Gallant *et al*., 1996
L-768,242	877	8.5	103.2	Gallant *et al*., 1996
AM-630	5152	31.2	165.1	Ross *et al*., 1999
LY320135	141	14900	9.5×10^{-3}	Felder *et al*., 1998

Table 1.4: The K_i values at the CB1 and CB2 receptors of some of the aminoalkylindole cannabinoid receptor ligands.

Diarylpyrazoles

The diarylpyrazole cannabinoid receptor ligands were developed by Sanofi Recherche and have proved to be invaluable tools in elucidating the receptor-mediated effects of cannabinoids. SR141716A and SR144528 were the first potent and selective antagonists of the CB1 and CB2 receptors, respectively (Rinaldi-Carmona *et al*., 1994; Rinaldi-Carmona *et al*., 1998). Subsequent reports, however, suggest that these drugs both act as inverse agonists (Bouaboula *et al*., 1997; Portier *et al*., 1999). SR141716A may also prove to be useful in characterizing CB1 cannabinoid receptor binding *in vivo*. Its iodinated analogue AM281 is a candidate for SPECT (single photon emission computed topography) imaging of living brain (Lan *et al*., 1999). The structures and K_i values of SR141716A and SR144528 are shown in **figure 1.12** and **table 1.5**.

SR141716A   SR144528
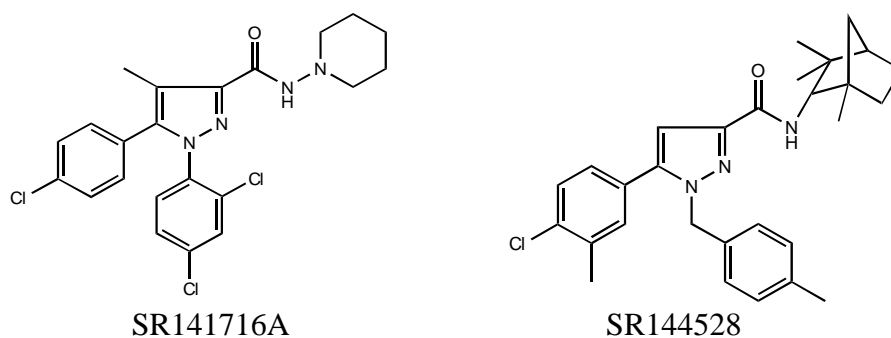
Figure 1.12: The structures of the CB1 and CB2 cannabinoid receptor-selective antagonists/inverse agonists SR141716A and SR144528.

Compound	CB1 K_i (nM)	CB2 K_i (nM)	CB1/CB2 Ratio	Reference
SR141716A	11.8	13200	8.9×10^{-4}	Felder *et al*., 1998
	12.3	702	0.018	Showalter *et al*., 1996
SR144528	> 10 μM	5.6	>1786	Ross *et al*., 1999
	437	0.6	728.3	Rinaldi-Carmona *et al*., 1998

Table1.5: The K_i values at the CB1 and CB2 receptors of the diarylpyrazole cannabinoid receptor antagonists/inverse agonists SR141716A and SR144528.

Endocannabinoid Derivatives

Since the discovery of endogenous cannabinoids, numerous analogues have been synthesized although few are as potent as the leading compounds from the other classes of cannabinoids described above. Endocannabinoid analogues can be divided in to two main classes: those that are head group analogues of anandamide or 2-AG (i.e. where the ethanolamide/glycerol substituent is altered) and those that have variations in the fatty carbon chain. The first endocannabinoid analogues were head group analogues and perhaps the best known is (*R*)-methanandamide (Abadji *et al*., 1994). This compound is identical to anandamide except for a methyl group at the 1' carbon, that increases its potency approximately four-fold compared to its parent compound and confers a considerable degree of resistance to enzymatic hydrolysis. (*R*)-Methanandamide, like anandamide, also proved to be

selective for the CB1 receptor with a CB1/CB2 K_i ratio of 0.02 (Khanolkar *et al.*, 1996). Other notable head group analogues include fluoroanandamide (Showalter *et al.*, 1996), chloroanandamide (Lin *et al.*, 1998), *N*-propyl-α,α-dimethylarachidonyl amide (PDMAA), *N*-propyl arachidonyl amide (PAA) and *N*-propyl-α-methylarachidonyl amide (PMAA) (Sheskin *et al.*, 1997). The K_i values of these compounds demonstrate that the hydroxyl on the ethanolamide group of anandamide is not required for cannabinoid receptor affinity and, without it, these compounds are more potent than anandamide.

The endocannabinoid analogues with an altered carbon chain are also more potent than the parent endocannabinoids. Dimethylheptyl anandamide, where the last five carbons of the carbon chain are replaced with a dimethylheptyl group (as is present in the most potent classical and non-classical cannabinoids) has an affinity for the CB1 receptor than is an order of magnitude higher than anandamide. This is also evident in the isolated mouse vas deferens assay and the mouse tetrad of *in vivo* assays where the EC_{50} and ED_{50} values (the effective concentration and dose required to achieve 50 % of the maximal response) are also reduced compared to anandamide (Ryan *et al.*, 1997; Seltzman *et al.*, 1997). The structures and K_i values of endocannabinoid analogues are summarized in **figure 1.13** and **table 1.6**.
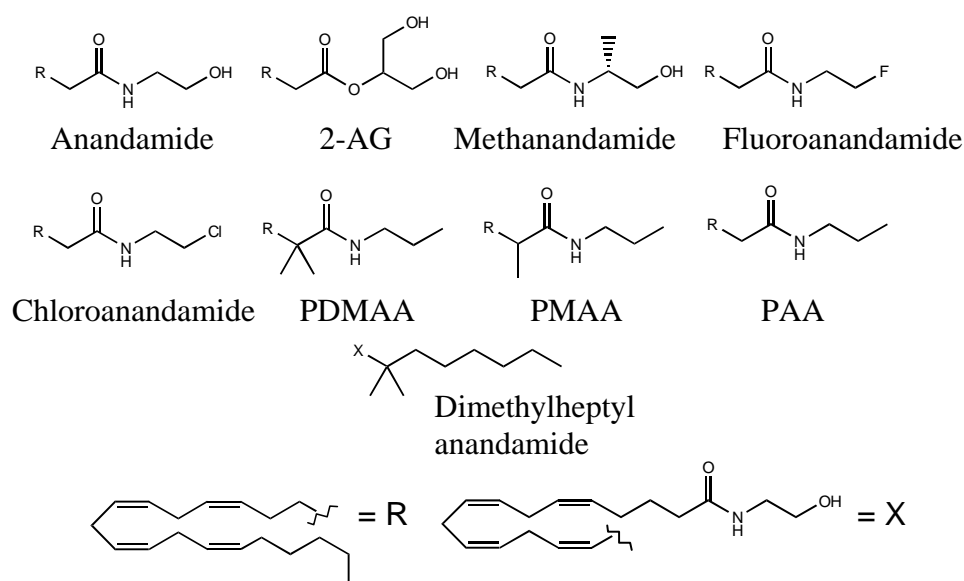
Figure 1.13: The structures of anandamide, 2-AG and some of the most significant synthetic endogenous cannabinoid analogues.

33

Compound	CB1 K_i (nM) No PMSF	PMSF	CB2 K_i (nM)[b]	CB1/CB2 Ratio	Reference
Anandamide	N.D.	89	371	0.24	Showalter *et al.*, 1996
	N.D.	78	1926	0.04	Khanolkar *et al.*, 1996
	5810	61.0	1930	0.03	Lin *et al.*, 1998
2-AG	N.D.	58.3	145	0.40	Ben-Shabat *et al.*, 1998
(*R*)-Meth-anandamide	N.D.	20	815	0.02	Khanolkar *et al.*, 1996
	28.3	17.9	868	0.02	Lin *et al.*, 1998
Fluoroanandamide	N.D.	8.6	324	0.03	Showalter *et al.*, 1996
	4640	26.7	908	0.03	Lin *et al.*, 1998
Chloroanandamide	3400	5.29	195	0.03	Lin *et al.*, 1998
PDMAA	6.9[a]	N.D.	N.D.	-	Sheskin *et al.*, 1997
PMAA	7.4[a]	N.D.	N.D.	-	Sheskin *et al.*, 1997
PAA	11.7[a]	N.D.	N.D.	-	Sheskin *et al.*, 1997
Dimethylheptyl anandamide	7.0	N.D.	N.D.	-	Ryan *et al.*, 1997
	N.D.	1.9	N.D.	-	Seltzman *et al.*, 1997

Table 1.6: The K_i values at the CB1 and CB2 receptors of some of the endocannabinoid analogues. a. The centrifugation binding assay used to obtain these values is not affected by PMSF. b. PMSF not required as CB2 K_i values are obtained using transfected cells or spleen membranes where FAAH is not present. N.D. Not determined.

1.7.2 Synthetic Inhibitors of Anandamide Uptake

To date, the only selective inhibitor of cellular anandamide uptake is the synthetic fatty acid amide, AM404 (**figure 1.14**). This compound competitively inhibits anandamide uptake in rat cortical neurones and astrocytes with IC_{50} values of 1 and 5 μM, respectively. AM404's specificity for the anandamide transporter was

demonstrated by its low affinity for the CB1 receptor and failure to inhibit anandamide hydrolysis (Beltramo *et al*., 1997). The competitive nature of the AM404 inhibition of anandamide uptake suggested that this compound is a substrate of the transporter and this was confirmed using [^{3}H]-AM404 (Piomelli *et al*., 1999).
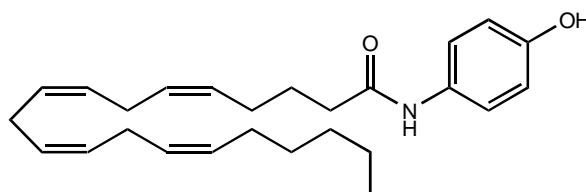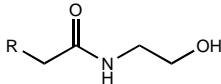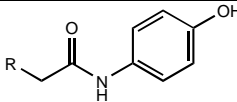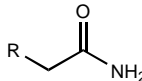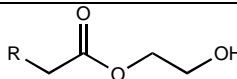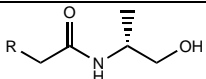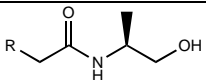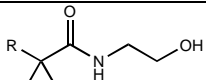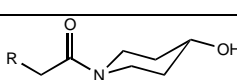
Figure 1.14: The structure of AM404, a selective inhibitor of the anandamide transporter.

Since most anandamide analogues are substrates for the anandamide transporter, the endocannabinoid analogues described in the previous section are substrates for the transport mechanism and compete with anandamide, reducing its rate of uptake. This means that these compounds, including the endocannabinoids themselves, have a dual cannabimimetic action, binding to the cannabinoid receptors and increasing extracellular endocannabinoid levels by inhibiting uptake. The structures and IC$_{50}$ values of some of the endocannabinoid analogues are shown in **table 1.7**.

1.7.3 Synthetic FAAH Inhibitors

As described in **section 1.5**, FAAH is a potential therapeutic target as its inhibition results in an increased level of endocannabinoids as well as other biologically important molecules such as oleamide. A number of potent FAAH inhibitors have been developed and, like the uptake inhibitors, some bind to the cannabinoid receptors giving them dual cannabimimetic activity. In addition, as substrates of FAAH, endocannabinoids and their related fatty acid amides and esters compete at FAAH resulting in the "entourage effect" described earlier. Perhaps the most widely used FAAH inhibitor is methyl arachidonyl fluorophosphonate (MAFP), a potent, irreversible inhibitor with an IC$_{50}$ in the low nanomolar range (Deutsch *et al*., 1997c).
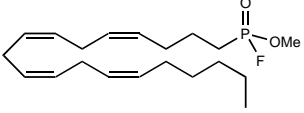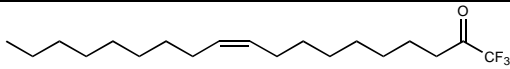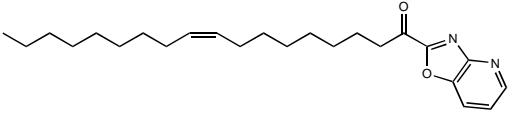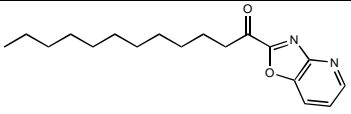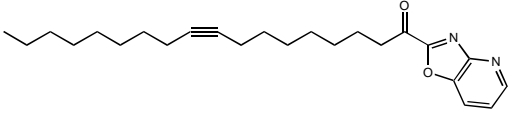
Compound	IC_{50} (μM)
R ⎯ C(=O)NH ⎯ OH Anandamide	15.1
R ⎯ C(=O)NH ⎯ OH AM404	2.2
R ⎯ C(=O)NH₂ Arachidonyl amide	9.0
R ⎯ C(=O)O ⎯ OH	6.7
R ⎯ C(=O)NH ⎯ OH (R)-Methanandamide	37.7
R ⎯ C(=O)NH ⎯ OH (S)-Methanandamide	10.4
R ⎯ C(=O)NH ⎯ OH	7.6
R ⎯ C(=O)N ⎯ OH	10.0

Table 1.7: The structures and IC_{50} values of some anandamide transport inhibitors (Piomelli *et al*., 1999).

MAFP also exhibits cannabimimetic activity by irreversibly binding to the CB1 receptor with a higher affinity than anandamide. Although MAFP is an anandamide analogue with four *cis* double bonds, a recent publication has demonstrated that saturated methyl fluorophosphonate analogues are also potent inhibitors of FAAH (Martin *et al*., 2000). The most potent of the series had a saturated 12 carbon chain, inhibited FAAH with an IC_{50} of 3.0 nM and was a high-affinity CB1 ligand.

Other potent FAAH inhibitors include the sulphonyl fluorides and the trifluoromethyl ketones. The most potent sulphonyl fluoride compounds are saturated fatty acid analogues and, like the methyl fluorophosphonates, have IC_{50} values in the low nanomolar range (Deutsch *et al*., 1997b). The trifluoromethyl ketones are less potent than the methyl fluorophosphonates and sulphonyl

fluorides. The most potent of these compounds possesses the oleic acid carbon chain, but saturated analogues have similar IC_{50} values (Boger *et al*., 1999). The most potent FAAH inhibitors to date, however, were only described recently. These α-keto N4 oxazolopyridine compounds possess IC_{50} values as low as 140 pM and are analogues of oleamide (Boger *et al*., 2000). The structures and IC_{50} values of synthetic FAAH inhibitors are summarized in **table 1.8**.

Compound	IC_{50} (nM)	Reference
MAFP	2.5	Deutsch *et al*., 1997c
$H_3C(H_2C)_7$-R	15.0	Martin *et al*., 2000
$H_3C(H_2C)_{11}$-R	3.0	Martin *et al*., 2000
$H_3C(H_2C)_{15}$-R	78.0	Martin *et al*., 2000
$H_3C(H_2C)_{17}$-R	48.0	Martin *et al*., 2000
$H_3C(H_2C)_{11}$-R^1	3.0	Deutsch *et al*., 1997b
$H_3C(H_2C)_{13}$-R^1	6.0	Deutsch *et al*., 1997b
$H_3C(H_2C)_{15}$-R^1	7.0	Deutsch *et al*., 1997b
$H_3C(H_2C)_{17}$-R^1	4.0	Deutsch *et al*., 1997b
	460	Boger *et al*., 1999
$H_3C(H_2C)_8$-R^2	600	Boger *et al*., 1999
$H_3C(H_2C)_{16}$-R^2	1200	Boger *et al*., 1999
	2.3	Boger *et al*., 2000
	0.57	Boger *et al*., 2000
	0.14	Boger *et al*., 2000
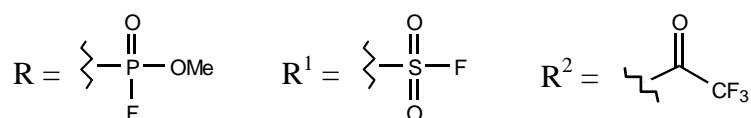
Table 1.8: The structures and IC_{50} values of fatty acid amide hydrolase inhibitors.

It can be seen from this section that there are a large number of structurally diverse cannabimimetic compounds. The next section describes some of the pharmacological effects of cannabinoids and the potential therapeutic applications of drugs that enhance or inhibit the endocannabinoid system.

1.8 Pharmacological Effects and Therapeutic Potential of Cannabimimetic Compounds

Cannabinoid receptor ligands and modulators of endocannabinoid metabolism have numerous pharmacological effects throughout the body. In the nervous system, most, but certainly not all, actions of cannabinoid agonists are due to their influence on the transmission of nerve impulses. An essential feature of neurotransmission is the influx of Ca^{2+} into the pre-synaptic terminal by the activation of voltage-gated calcium channels. This increase in the intracellular concentration of Ca^{2+} induces vesicles containing neurotransmitter molecules to fuse with the pre-synaptic membrane, releasing the neurotransmitter in to the synaptic cleft. Diffusion of the neurotransmitter across the synaptic cleft to the post-synaptic membrane and binding to the appropriate receptors induces depolarization of the post-synaptic membrane and propagation of the nerve impulse. As mentioned in **section 1.2.3**, cannabinoids inhibit several different voltage-gated calcium channels *via* the CB1 receptor, thus preventing calcium influx into the pre-synaptic terminal and subsequent neurotransmitter release and nerve transmission. Cannabinoids have been shown to inhibit the release of glutamate (Shen *et al*., 1996), dopamine (Schlicker *et al*., 1996; Burkey *et al*., 1997), noradrenaline (Schlicker *et al*., 1996) and acetylcholine (López-Redondo *et al*., 1997; Carta *et al*., 1998) and this mechanism possibly underlies a majority of the observed acute effects of cannabinoids including analgesia, reduced locomotor activity and memory deficits. In the immune system, however, there are a number of mechanisms by which cannabinoids exert their effects. The following sections describe the most promising therapeutic targets for the use of cannabimimetic drugs, although there are many other pharmacological effects that have no direct clinical applications at present.

1.8.1 Pain

Cannabis is well known for its analgesic properties and there are a number of synthetic cannabinoid receptor agonists such as CP-55,940 that rival the analgesic potency of morphine. The mechanisms for cannabinoid-induced analgesia are now being elucidated and it is becoming apparent that they involve cannabinoid receptors on central and peripheral neurones as well as interaction with the opioid system. The central analgesic effects of cannabinoids have been demonstrated in both the brain and spinal cord. In the brain, the periaqueductal gray (PAG) area is involved in the processing of pain, with the ventral PAG involved in the control of pain by endogenous opioid compounds. However, the mediators of analgesia in the lateral and dorsal PAG were unknown. When the tails of laboratory rats are exposed to thermal pain, the observed pain response is tail flicking. Walker and co-workers electrically stimulated the lateral and dorsal PAG of rats exposed to thermal pain and observed antinociception. This analgesic effect was concurrent with the release of anandamide from the PAG and was blocked by SR141716A, suggesting that activation of the CB1 receptor is involved in the modulation of pain in the PAG (Walker *et al.*, 1999). In addition, when pain was induced in the hind paws by injection of formalin, anandamide release occurred in the dorsal and lateral PAG, implying that endocannabinoids are involved in pain suppression. Pain suppression by endogenous cannabinoids has also been demonstrated in the spinal cord. When peripheral inflammation was induced by injection of carrageenin into rat hind paws, spinally administered anandamide inhibited nociceptive transmission by spinal neurones. This inhibitory effect was blocked in the presence of SR141617A, indicating that this effect was mediated by CB1 cannabinoid receptors (Harris *et al.*, 2000). When SR141716A was administered to carrageenin-inflamed rats in the absence of anandamide, nociceptive responses were not affected. However, a previous study demonstrated that SR141716A, but not SR144528, facilitated nociceptive transmission in non-inflamed rats (Chapman, 1999). Together, these data suggest that endocannabinoids are involved in the tonic control of pain in the spinal cord by activation of CB1 receptors but this endogenous spinal cannabinoid tone is reduced following carrageenin-induced inflammation. Whether this effect is due to a decrease in the

number of CB1 receptors or an increase in endocannabinoid degradation remains to be seen.

In the periphery, one mechanism of pain control is the release of opioid peptides by immune cells. These peptides then bind to opioid receptors resulting in analgesia. It has been shown that there is also a peripheral regulation of pain response by endogenous cannabinoids. When pain is induced in rat hind paws by injection of formalin, there is an immediate pain response, peaking after about five minutes, followed by a sustained pain response which begins after ten to fifteen minutes. Co-injection of formalin and anandamide blocked the first phase of pain, but not the second phase, while WIN 55-212,2 and HU-210 blocked both phases (Calignano *et al*., 1998). The inability of anandamide to suppress the second phase of pain was thought to be due to its rapid inactivation as the hydrolysis-resistant analogue (*R*)-methanandamide also blocked both phases. This blockade of the pain response by cannabinoids was antagonized by SR141716A, but not by SR144528 or the opioid receptor antagonist naloxone, suggesting a CB1 receptor-mediated mechanism. The peripheral nature of this effect was demonstrated by intra-venous and intra-peritoneal injection of anandamide. The antinociceptive effect of anandamide was reduced 100-fold by i.v. injection and totally abolished by i.p. administration. Furthermore, palmitoylethanolamide, which does not bind to the CB1 or CB2 receptors, blocked both phases of the pain response when co-injected with formalin. This effect was abolished by SR144528 but not by SR141716A or naloxone, suggesting an interaction with CB2-like receptors on peripheral nerves. When equal amounts of anandamide and palmitoylethanolamide were co-injected with formalin, the antinociceptive effect was 100 times more pronounced than administration of each compound alone, implicating participation of both CB1 and CB2-like receptors in the control of peripheral pain. When SR141716A or SR144528 were co-administered with formalin, a hyperalgesic response was observed, suggesting that locally generated anandamide and palmitoylethanolamide play a role in controlling the initiation of pain. The hyperalgesic effect of SR141716A has also been observed by other researchers (Strangman *et al*., 1998).

In addition to cannabinoid regulation of pain that is independent of the opioid system, interaction between the two systems does occur. When Δ^9-THC was administered daily to rats i.p. for five days, it was observed that mRNA levels of the opioid peptide precursors prodynorphin and proenkephalin were elevated in the spinal cord compared to animals treated with the vehicle (Corchero *et al*., 1997). This has implications for combined cannabinoid and opioid drug therapies to control pain. A review of the interaction between the cannabinoid and opioid systems can be found elsewhere (Manzanares *et al*., 1999).

In summary, it is now becoming apparent that endogenous cannabinoid compounds are involved in the control of pain initiation. The peripheral administration of cannabinoids or inhibitors of endocannabinoid uptake and hydrolysis has the potential of relieving pain without undesirable psychotropic effects. The involvement of CB2-like receptors also offers the possibility of specific agonists for these receptors, totally removing the potential for effects on the CNS. Indeed, the CB2-selective agonist HU-308 has been shown to be an analgesic in the formalin model of pain without causing any psychotropic effects, presumably by binding to CB2-like receptors (Hanus *et al*., 1999). In addition, the non-psychotropic cannabinoid CT-3 (**figure 1.15**) is currently undergoing development as a potent, orally active analgesic, although its exact mechanism of action is unknown (Dajani *et al*., 1999).
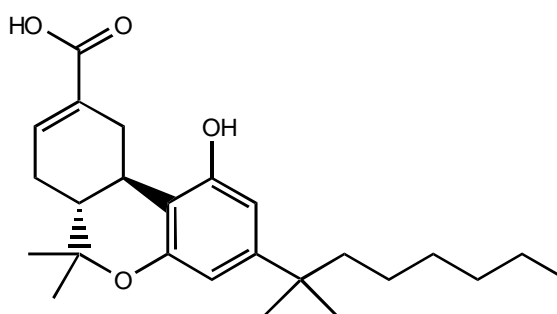
Figure 1.15: The structure of CT-3, a non-psychotropic cannabinoid with analgesic and anti-inflammatory activity.

1.8.2 Multiple Sclerosis

Multiple sclerosis (MS) is an autoimmune disease of the CNS caused by progressive damage or destruction of the myelin sheath surrounding nerves in the

brain and spinal cord. This demyelination results in the disruption of nerve transmission which is manifested by numerous symptoms including numbness, tremors, weakness, pain, seizures and paralysis. Anecdotal evidence has shown that cannabis can be effective at relieving the symptoms of MS where prescription drugs have failed, but it was only recently that the therapeutic potential of cannabinoids to alleviate the symptoms of MS was rationalized scientifically. One important study in this area investigated the effect of anandamide on astrocytes isolated from mice infected with Theiler's murine encephalomyelitis virus (TMEV), a model of MS which results in immune-mediated demyelination. IL-6 is a cytokine that has anti-inflammatory and immunosuppressive effects and has been shown to suppress demyelination in the TMEV model of MS. Anandamide was shown to induce IL-6 production by astrocytes infected with TMEV and this effect was potentiated by arachidonyl trifluoromethyl ketone, an inhibitor of FAAH. In addition, the specific CB1 receptor antagonist SR141716A attenuated the effect of anandamide on IL-6 production, suggesting that this effect is CB1 receptor-mediated (Molina-Holgado *et al*., 1998). A more recent study has implicated both the CB1 and CB2 receptors in alleviating the symptoms of MS. Using mice with chronic relapsing experimental allergic encephalomyelitis (CREAE), a model of MS, cannabinoid compounds were shown to quantitatively reduce tremor and spasticity (Baker *et al*., 2000). The relative involvement of CB1 and CB2 receptors in alleviating the symptoms of CREA appears complex. The CB1 receptor antagonist SR141716A and the CB2 receptor antagonist SR144528 both inhibited the ability of WIN 55-212,2 to inhibit tremor but, when administered alone, the antagonists exhibited distinguishable effects. Administration of SR141716A to animals with mild spasticity, but no tremor, increased spasticity compared to control animals and also induced tremor. When SR144528 was administered alone, a small increase in spasticity was observed. However, when animals treated with SR141716A were subsequently given SR144528, the spasticity was even more pronounced than in those animals treated with SR141716A alone. The fact that administration of cannabinoid receptor antagonists by themselves worsens the symptoms of CREAE indicates that endogenous cannabinoids play a role in controlling the symptoms of this disease. These data also indicate that the CB1 receptor has a role in the control of tremor while both cannabinoid receptors are involved in the control of spasticity. This

may pave the way for the development of synthetic compounds to treat the symptoms of MS. Although the CB1 receptor appears dominant in regulating the tremor and spasticity of MS, drugs that act *via* the CB1 receptor would inevitably produce psychotropic effects. It may be possible to partially alleviate symptoms with CB2-selective agonists or by increasing the levels of endocannabinoids with anandamide uptake and FAAH inhibitors. This would obviously be preferable to the illegal use of cannabis by many MS sufferers that occurs at present.

1.8.3 Neuroprotection

Cannabinoids may have a therapeutic role to play in the prevention of neuronal death caused by oxygen or glucose depletion, common following stroke or heart attack. This mechanism of damage is thought to involve the release of the neurotransmitter L-glutamate and it is also known that activation of pre-synaptic CB1 receptors by cannabinoid agonists inhibits Ca^{2+} influx and subsequent L-glutamate release in the hippocampus (Shen *et al*., 1996). Therefore, the hypothesis that cannabinoid compounds could exert neuroprotective effects was tested by Nagayama *et al*. (1999). Ischemia was induced in laboratory rats and the effect of WIN 55-212,2 on neuronal survival determined. When administered i.p. 40 minutes before ischemia, WIN 55-212,2 dose-dependently increased neuronal survival compared to control animals although it appeared to become neurotoxic at the highest concentrations tested. This effect was antagonized by SR141716A which had no effect when administered alone, suggesting a CB1 receptor-mediated mechanism of neuroprotection. However, in cultured cortical neurones, the neuroprotective effect of cannabinoids was not as straightforward. WIN 55-212,2 and anandamide both protected cells from death caused by ischemia and hypoglycaemia, but Δ^9-THC did not. Pre-treatment with SR141716A or SR144528 did not antagonize the neuroprotective effect, suggesting a mechanism that is independent of both cannabinoid receptors. Although there may be more than one mechanism responsible for the neuroprotective effects of cannabinoids, there is real therapeutic potential for cannabinoid use to improve the neurological outcome of patients that suffer stroke or cardiac arrest.

1.8.4 Septic Shock

Septic shock is a condition that can be caused by bacterial infection, trauma and ischemia, inducing the production of the pro-inflammatory cytokine tumour necrosis factor α (TNFα). The heightened levels of TNFα result in fever, sickness, hypotension, stimulation of pituitary and stress hormones, haemorrhage of the GI tract and lungs and, ultimately, death. There are no drugs currently available that are effective in treating septic shock, but a synthetic cannabinoid compound is now undergoing phase II clinical trials for severe head injury. This compound, dexanabinol (HU-211) (**figure 1.16**), is an enantiomer of the potent synthetic cannabinoid HU-210, but is non-psychotropic and has no significant affinity for the cannabinoid receptors. When septic shock was induced in rodents by administration of the bacterial endotoxin lipopolysaccharide (LPS), HU-211 rescued a high percentage of the animals from death. *In vitro*, it was demonstrated that HU-211 markedly decreased TNFα production by cells exposed to LPS, though the mechanism of its action are unclear (Gallily *et al.*, 1997). Currently, it is not known if the effects of HU-211 are totally receptor-independent or if it is acting at an, as yet, undiscovered cannabinoid receptor. Nevertheless, HU-211 may prove to be a very important drug for the treatment of septic shock, which is a major cause of mortality in intensive care units worldwide.
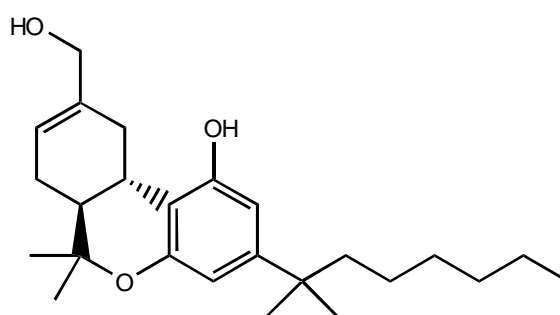
Figure 1.16: The structure of HU-211, a non-psychotropic cannabinoid effective in the treatment of septic shock.

1.8.5 Inflammation

Another historical use of cannabis is the treatment of inflammation. It is now clear that there are a number of mechanisms by which cannabinoids exert their anti-inflammatory effects, and these are predominantly due to activation of CB2

receptors. One of the first studies suggesting that CB2 receptors are involved in the anti-inflammatory actions of cannabinoids was performed with the murine T-cell line EL4.IL-2. In untreated cells, cAMP causes the activation of protein kinase A which, in turn, activates specific transcription factors that subsequently induce the transcription of genes encoding the pro-inflammatory cytokine interleukin-2 (IL-2) which is involved in both humoral and cell-mediated immune response. When cells were pre-treated with Δ^9-THC, forskolin-stimulated cAMP synthesis was inhibited and subsequent transcription and secretion of IL-2 was also decreased. This effect was concentration-dependent and, as Northern blotting showed the presence of the CB2 receptor but not CB1, was assumed to be mediated by CB2 (Condie *et al.*, 1996). However, at the time of this study, the CB2 receptor antagonist SR144528 had not been developed and, therefore, the role of CB2 was only speculative.

A further mechanism for the anti-inflammatory effects of cannabinoids was demonstrated in the macrophage cell line RAW 264.7. When these cells were exposed to LPS, there was an increase in the nuclear binding of the transcription factor NF-κB/Rel which resulted in an increase in expression of inducible nitric oxide synthase (iNOS). iNOS catalyses the synthesis of nitric oxide (NO) which is involved in the cytolytic function of macrophages. Pre-treatment of these cells with Δ^9-THC inhibited the LPS-induced up-regulation of NO production by inhibition of the cAMP cascade (Jeon *et al.*, 1996), thereby down-regulating T-cell cytolytic activity. Again, this work was done before the development of a CB2 receptor antagonist and, although CB2 receptor mRNA, but not CB1 receptor mRNA, was detected in these cells, it can only be implied that CB2 receptor activation caused this suppression.

Further work published before the development of a CB2 receptor antagonist investigated the effect of cannabinoid receptor ligands on pulmonary inflammation in mice. Inhalation of LPS caused a macrophage-mediated inflammatory response, apparent by massive recruitment of neutrophils and release of TNFα. Both Δ^9-THC and WIN 55-212,2 reduced neutrophil recruitment and TNFα production with WIN 55-212,2 being more effective, consistent with its higher affinity for the CB2 receptor. The effects of anandamide and palmitoylethanolamide were not as pronounced. Anandamide reduced TNFα and

neutrophil recruitment only at the lowest concentration tested, while palmitoylethanolamide decreased TNFα only at the highest concentration and did not affect neutrophil levels (Berdyshev *et al.*, 1998). This suggests that anandamide and palmitoylethanolamide act at different receptors and, considering its lack of affinity for the CB1 and CB2 receptors, palmitoylethanolamide possibly exerts this effect by interaction with CB2-like receptors.

More recently, a pro-inflammatory effect of cannabinoids has been described using HL60 cells, a human promyelocytic cell line that expresses the CB2 receptor, but not the CB1 receptor. In these cells, CP-55,940 was shown to up-regulate the synthesis of the α-chemokine interleukin-8 (IL-8) and the β-chemokine monocyte chemotactic protein-1 (MCP-1). Both IL-8 and MCP-1 are pro-inflammatory and have been detected in a number of conditions including asthma, rheumatoid arthritis and inflammatory bowl disease. The CP-55,940-stimulated synthesis of these chemokines was abolished by pre-treatment with pertussis toxin, suggesting the involvement of a $G_{i/o}$-coupled GPCR, and antagonized by SR144528, implicating activation of CB2 or CB2-like receptors (Jbilo *et al.*, 1999).

Cannabinoids undoubtedly have anti-inflammatory properties but the full extent of their actions within the immune system remains to be elucidated. The CB2 receptor is emerging as a target for anti-inflammatory drugs, and the recently described CB2-selective agonists are likely to be able to exert anti-inflammatory effects without the psychotropic affects of non-selective cannabinoids. Indeed, the synthetic cannabinoid HU-308 has been shown to be inactive at the CB1 receptor, yet has an anti-inflammatory effect due to its high affinity for the CB2 receptor (Hanus *et al.*, 1999). This is also true for the orally active anti-inflammatory cannabinoid CT-3. This compound is non-psychotropic, although the exact mechanism of its anti-inflammatory action is unknown (Dajani *et al.*, 1999). There is also the potential for the development of novel therapeutic strategies to reverse cannabinoid-induced production of IL-8 and MCP-1. If an inverse agonist could down-regulate these chemokines, it may find applications in autoimmune diseases.

1.8.6 Cancer

It is now becoming apparent that both endogenous and exogenous cannabinoids possess anti-cancer activity through receptor-independent and receptor-mediated mechanisms. The first potential anti-cancer mechanism is the induction of apoptosis (programmed cell death) by a cannabinoid receptor-independent route. Δ^9-THC has been shown to induce apoptosis in murine splenocytes and peritoneal macrophages by a dual mechanism involving two intracellular proteins (Zhu *et al.*, 1998). The first of these, caspase-1, is involved in the processing of interleukin-1β (IL-1β), a cytokine implicated in the induction of apoptosis, from immature IL-1β to mature IL-1β. Δ^9-THC increased caspase-1 levels in these cell types, hence increasing IL-1β processing. The second protein is encoded by the gene Bcl-2 and is involved in suppression of apoptosis. Δ^9-THC inhibited transcription of Bcl-2, thus attenuating the protection from apoptosis. However, from this evidence it is not clear whether these effects are mediated by cannabinoid receptors or not as the effects of cannabinoid receptor antagonists on Δ^9-THC-induced apoptosis were not studied. However, another study has shown that Δ^9-THC-induced apoptosis is unlikely to be due to activation of cannabinoid receptors. Using human prostate cancer (PC-3) cells, Δ^9-THC was shown to induce apoptosis in a dose-dependent manner. However, the synthetic aminoalkylindole WIN 55-212,2, which is more potent and efficacious than Δ^9-THC at both cannabinoid receptors, failed to induce apoptosis in PC-3 cells. Moreover, the CB1 receptor antagonist AM251 failed to antagonize the effects of Δ^9-THC. Pre-treatment of the cells with pertussis toxin also had no effect on Δ^9-THC-induced apoptosis, suggesting that GPCRs are not involved in this mechanism (Ruiz *et al.*, 1999).

There is also evidence that cannabinoids can exhibit anti-tumoural activity *via* cannabinoid receptors. An *in vivo* study to investigate the effect of cannabinoids on malignant gliomas in rats demonstrated that when Δ^9-THC or WIN 55-212,2 were injected directly in to the tumour, there was a significant reduction in the size of the tumour in comparison to rats injected with the vehicle (Galve-Roperh *et al.*, 2000). WIN 55-212,2 was more effective than Δ^9-THC and was active at lower doses (10 % of the Δ^9-THC dose), consistent with the relative affinities of the two compounds for the cannabinoid receptors. In addition, Δ^9-THC, WIN 55-

212,2, CP-55,940 and HU-210 were all shown to induce apoptosis in cultured rat glioma C6 cells. When cannabinoid receptor antagonists were added to the assay system, neither the CB1-selective antagonist SR141716A nor the CB2-selective antagonist SR144528 attenuated the apoptotic effect when added alone. However, when the two antagonists were added together, the effect of the cannabinoid receptor agonists was reversed, suggesting a synergistic mechanism involving both cannabinoid receptors. Further investigations in to the mechanism of cannabinoid-induced apoptosis showed that accumulation of ceramide and activation of the extracellular signal-regulated kinase (ERK) cascade, both implicated in apoptosis, were induced by Δ^9-THC.

Further anti-tumoural actions of cannabinoids have been described in human breast cancer cells (HBCCs). In the EFM-19 and MCF-7 cell lines, anandamide, 2-AG, (*R*)-methanandamide and HU-210 were all shown to inhibit proliferation in a concentration-dependent manner. This effect was not due to cell toxicity or apoptosis and was inhibited by the CB1 receptor antagonist SR141716A (De Petrocellis *et al*., 1998). Furthermore, EFM-19 cells were shown to synthesize both anandamide and oleamide and express FAAH. Both compounds inhibited proliferation of the cells with IC_{50} values of 2.1 and 11.3 µM, respectively, and when an ineffective concentration of oleamide was incubated with anandamide, the anti-proliferative effect of anandamide was enhanced. The effects of both compounds were attenuated by SR141716A, suggesting a CB1-dependent mechanism of action. These data also suggest that oleamide exerts its effects by inhibition of FAAH, thus increasing the amount of anandamide available to bind to the CB1 receptor (Bisogno *et al*., 1998). A more in-depth study has revealed the potential signalling mechanisms for the anti-proliferative action of anandamide in HBCCs. In these cells, prolactin and nerve growth factor (NGF) induce proliferation by activating the prolactin receptor (PRLr) and the high affinity *trk* NGF receptor, respectively. Anandamide was shown to down-regulate PRLr and *trk* NGF receptor expression in MCF-7 HBCCs, thereby inhibiting their proliferation. This effect was antagonized by the SR141716A, implicating activation of the CB1 receptor, and was caused by the inhibition of adenylate cyclase and activation of MAPK signalling (Melck *et al*., 1999a). Furthermore,

oleamide also potentiated the anti-proliferative effect of anandamide in these cells, again suggesting enhancement of activity *via* the inhibition of FAAH.

The data described above show that cancer chemotherapy is a potential therapeutic application of cannabinoids and cannabimimetic compounds, although the exact cellular mechanisms of action still require full elucidation. As described previously, cannabinoids are also immunosuppressive and may affect the body's defences against cancer, though many of the immunosuppressive effects appear to be mediated *via* the CB2 cannabinoid receptor. The anti-tumoural effects, however, are predominantly CB1 receptor-mediated and, therefore, CB1-selective cannabinoid agonists may prove to be effective anti-tumoural drugs.

1.8.7 Schizophrenia

The causes of schizophrenia are not well understood, but there is evidence to suggest that dysfunction of the endogenous cannabinoid system may be a causative factor. An example of this is the examination of visual illusionary perception in non-schizophrenic patients before and after intoxication with Δ^9-THC. It was found that Δ^9-THC induced abnormalities in perception that were similar to those exhibited by schizophrenic patients, suggesting a role for the CB1 receptor in this process (Emrich *et al*., 1997). More recently, it has been shown that levels of anandamide and palmitoylethanolamide are significantly higher in the cerebrospinal fluid of schizophrenics compared to non-schizophrenic subjects (Leweke *et al*., 1999). Although wider ranging studies must be performed to confirm this and to elucidate the mechanisms by which these compounds affect schizophrenia, CB1 antagonists may prove to be novel therapeutics in alleviating the symptoms of this condition. Indeed, the selective CB1 receptor antagonist SR141716A is currently undergoing phase IIa clinical trials as a potential treatment for schizophrenia (Kendall, 2000).

1.8.8 Hypertension

It is well established that cannabis causes a reduction in blood pressure and the mechanisms by which this occurs are now, at least partially, understood. It is now apparent that the endothelium of blood vessels is an important regulator of vascular tone and there are two major endogenous species implicated in this

process. The first, endothelium-derived relaxant factor (EDRF), has been identified as nitric oxide while the identity of the second species remains unclear. This species is known as the endothelium-derived hyperpolarizing factor (EDHF) and causes hyperpolarization or repolarization of the endothelium *via* the activation of K^+ channels, resulting in vasodilation. Both NO and EDHF are released from the vasculature by treatment with the acetylcholine receptor agonist carbachol. However, when NO synthesis was blocked, carbachol caused dose-dependent relaxations in the rat mesenteric arterial bed that were antagonized by SR141716A. This suggests that EDHF may act *via* CB1 receptors and, therefore, may be an endogenous cannabinoid (Randall *et al*., 1996). Furthermore, thin layer chromatography analysis of the effluent from perfused mesenteries that had been pre-incubated with [^{3}H]-arachidonic acid revealed a compound that co-eluted with synthetic anandamide. The production of this compound was increased by carbachol treatment, suggesting that anandamide, or a very closely related compound, may be an EDHF. However, there is also evidence that suggest that anandamide is not an EDHF. Plane *et al.* (1997) demonstrated that anandamide caused smooth muscle relaxation in the rat mesenteric artery but this relaxation, and that caused by EDHF, was not inhibited by SR141716A nor mimicked by HU-210 or WIN 55-212,2. However, further work by Randall *et al.* (1997) comparing the pharmacology of anandamide and EDHF strengthened the hypothesis that anandamide is an EDHF. The anandamide-induced and EDHF-mediated relaxations of the isolated rat mesentery were both blocked by high K^+ and opposed by blockading K^+ channels. Putative EDHF inhibitors also inhibited anandamide-induced and EDHF-mediated relaxation, showing that the two species have very similar pharmacological profiles. This apparent relationship between the EDHF and anandamide has also been demonstrated in the coronary vasculature of the rat (Randall & Kendall, 1997).

Further evidence that anandamide may be an endogenous mediator of vascular tone was demonstrated using the anandamide uptake inhibitor AM404. Systemic blood pressure in anaesthetized guinea-pigs was decreased by anandamide and this effect was antagonized by SR141716A, implicating a CB1 receptor-dependent mechanism. The anandamide-mediated decrease in blood pressure was independent of the autonomic nervous system and significantly prolonged by the AM404, suggesting that the anandamide transporter is present in the vasculature

and is one mechanism by which the vasodilatory effects of anandamide are terminated (Calignano *et al*., 1997). However, evidence now suggests that, although anandamide causes dilation of the vasculature, it is unlikely to be an EDHF. In the rat mesenteric arterial bed, EDHF-mediated vasorelaxations were inhibited by the selective CB1 receptor antagonist LY320135 but were insensitive to SR141716A, SR144528 and AM630. In addition, anandamide-induced vasorelaxations were insensitive to LY320135, suggesting that anandamide is not an EDHF and that a CB1-like receptor, but not CB2 receptors, may have a role in EDHF-mediated vasorelaxations (Harris *et al.*, 1999; Harris, unpublished data). Further evidence exists that EDHF acts at an, as yet, unidentified cannabinoid receptor. The non-psychotropic cannabinoid abnormal cannabidiol (**figure 1.17**) does not bind to the CB1 cannabinoid receptor but causes SR141716A-sensitive hypotension and vasodilation in mice. This compound also induces these effects in mice lacking the CB1 receptor or both the CB1 and CB2 receptors. In addition, the vasodilation caused by abnormal cannabidiol is not affected by blockade of NO and is abolished by removal of the endothelium (Járai *et al*., 1999). Together these data suggest that abnormal cannabidiol is an agonist of a CB1-like receptor located within the endothelium and induces NO-independent vasodilation in the mesentery, consistent with the release of an EDHF.
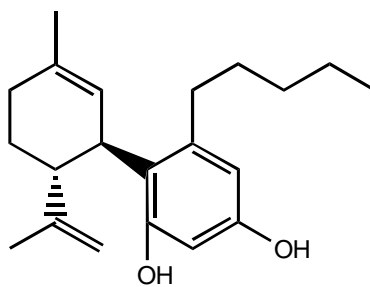
Figure 1.17: The structure of abnormal cannabidiol, a non-psychotropic hypertensive compound.

Finally, evidence is now emerging that suggests 2-AG may be an EDHF. When carbachol was applied to the rat aorta, 2-AG levels were found to be five times higher than in control experiments and, when the endothelium was removed, no change in 2-AG levels was measured. In addition, when exogenous 2-AG was administered the mean arterial blood pressure was significantly reduced (Mechoulam *et al*., 1998). Although further investigations are necessary to

determine the role of 2-AG in endothelium-dependent vasorelaxations, the CB1-like receptor implicated in the actions of LY320135 and abnormal cannabidiol may be an endogenous 2-AG receptor.

Thus, it appears that endogenous cannabinoids, and particularly 2-AG, play a role in the maintenance of vascular tone, possibly *via* an as yet undiscovered CB1-like receptor in the endothelium. Specific agonists for this receptor as well as inhibitors of endocannabinoid uptake and hydrolysis have real therapeutic potential as anti-hypertensive drugs.

1.8.9 Summary

The effects of cannabinoids and cannabimimetics described above show that there is great potential for drugs that activate the cannabinoid receptors or increase endocannabinoid signalling by inhibiting uptake or hydrolysis. The increasing evidence indicating the existence of distinct CB1-like and CB2-like receptors also provides the possibility that specific agonists or antagonists of these receptors could become clinically important in the future. This would be especially significant if the positive therapeutic potential of cannabimimetics can be uncoupled from undesirable psychoactive effects as has been observed for compounds such as HU-308 and CT-3.

1.9 Aims and Objectives

At the time this research was started, elucidation of the endogenous cannabinoid system was at a relatively early stage. Although the cannabinoid receptors and FAAH had been discovered, the anandamide transporter had yet to be described and there was no evidence of CB1- and CB2-like receptors. In addition, there were few selective ligands for either cannabinoid receptor and only one antagonist, SR141716A. Nevertheless, it was obvious that there was great therapeutic potential in modulators of endocannabinoid signalling. Therefore, the aim of this research was to develop cannabimimetic drugs that could act as

pharmacological tools or therapeutic agents by acting as cannabinoid receptor ligands, whether agonists or antagonists, or inhibitors of FAAH. The following chapter describes the design and synthesis of these compounds. Subsequent chapters describe the analysis of the effects of these compounds, if any, on endocannabinoid signalling, namely their ability to bind to the cannabinoid receptors and inhibit both anandamide uptake and fatty acid amide hydrolase.

Chapter 2:

Chemical Synthesis

2.1 Introduction

As part of a strategy to develop potential cannabimimetic agents, three classes of target compound were proposed. This chapter describes the rationale behind the development of these novel species and the methodologies employed for their synthesis.

2.1.1 Aryl Ethanolamides

Anandamide is the ethanolamide derivative of arachidonic acid. With this in mind, it was hypothesized that the ethanolamides of compounds that mimic arachidonic acid may display cannabimimetic activity. Aspirin (**figure 2.1**) is a non-steroidal anti-inflammatory drug that competes for binding to cyclooxygenase (COX) enzymes with arachidonic acid, the natural substrate of COX. Preliminary evidence from the University of Nottingham showed that, at a concentration of 30 μM, aspirin ethanolamide displaced 23 % of specific [^{3}H]-CP-55,940 binding to rat cerebellar membranes and, therefore, this compound possessed some affinity for the CB1 receptor (Millns, unpublished data). Computer modelling studies have shown that in order to bind to the CB1 receptor, the carbon chain of anandamide must be folded and that this folding is energetically favourable (Thomas *et al*., 1996). Therefore, the affinity of aspirin ethanolamide for the CB1 receptor may be at least partly explained by the distribution of negative charge in its benzene ring mimicking the "pocket" of negative charge formed by the double bonds of anandamide on the folding of its carbon chain.

In addition to this preliminary data, there is also evidence in the literature of drugs with actions that overlap between COX enzyme inhibition and the endogenous cannabinoid system. Firstly, the development of the aminoalkylindole pravadoline and related compounds as described in **section 1.7.1** demonstrated that inhibitors of COX enzymes could bind to the CB1 cannabinoid receptor (Bell *et al*., 1991). Relatively minor structural alterations of these compounds abolished their COX inhibition while dramatically increasing their CB1 affinity (Dambra *et al*., 1992). More recently it has been shown that the NSAID ibuprofen (**figure 2.1**) and its related compounds inhibit FAAH in rat brain (Fowler *et al*., 1997a; Fowler *et al*., 1997b), thereby exerting a cannabimimetic effect by increasing endogenous

cannabinoid levels. Moreover, this inhibition occurs at pharmacologically relevant concentrations with IC_{50} values between 50 and 650 µM.
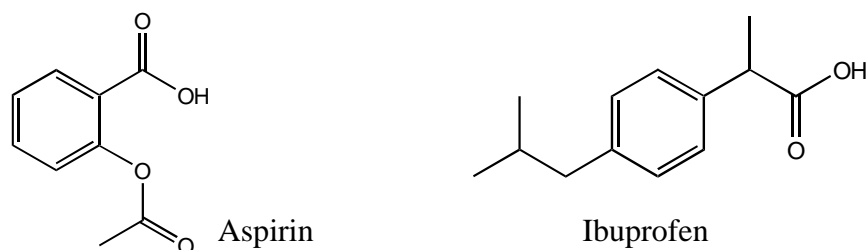
Figure 2.1: The structures of the NSAIDs aspirin and ibuprofen.

Based on the preliminary binding data for aspirin ethanolamide and the hypothesis of an interaction between NSAIDs and their derivatives and endocannabinoid signalling, the synthesis of aryl ethanolamides (AEs) with the general structure shown in **figure 2.2** was proposed.
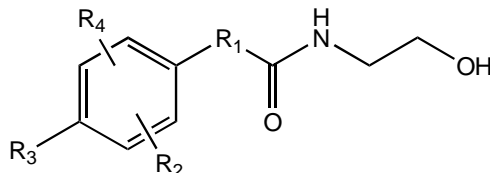
Figure 2.2: The general structure of potential aryl ethanolamide cannabimimetics. R_1-R_4 represent substituent groups.

As nothing was known about the structural requirements for AE binding to cannabinoid receptors, if any, it was necessary to include some structural diversity in their synthesis in order to elucidate any structure-activity relationships. To achieve this, target compounds were designed using commercially available starting materials that provided diversity in the substituent groups on the benzene ring and the presence or absence of a "spacer" between the benzene ring and the ethanolamide group. The initial novel target compounds are shown in **table 2.1**. If any of these compounds mimicked anandamide by showing affinity for the

cannabinoid receptors, it would also be likely that they would act as substrates for the anandamide transporter and FAAH. Therefore, the aryl ethanolamides had the potential to exert cannabimimetic activity in three ways, namely activation of the cannabinoid receptors and elevation of endocannabinoid levels by acting as competitive inhibitors of endocannabinoid transport and hydrolysis.

Compound	R_1	R_2	R_3	R_4
AE1	CH=CH	H	OH	H
AE2	CH=CH	H	H	H
AE3	-	H	H	H
AE4	CH_2	H	H	H
AE5	CH_2-CH_2	H	H	H
AE6	CH-CH_3	H	H	H
AE7	CH_2	3-OH	H	H
AE8	-	3- CH_3O	H	5- CH_3O
AE9	-	3-Cl	H	H
AE10	-	2- CH_3O	H	6- CH_3O
AE11	-	2- CH_3O	CH_3O	H
AE12	CH-OH	H	H	H
AE13	CH_2	H	Ph	H
AE14	Naphthyl-	-	-	-

Table 2.1: Target aryl ethanolamide compounds.

2.1.2 Phosphinic Acids

Phosphinic acids are phosphorus-containing species based on the tetrahedral parent compound phosphinic acid. Phosphinic acid itself exists in equilibrium with phosphonous acid but, as shown in **figure 2.2**, due to the stability of the phosphoryl group, the equilibrium lies well to the left.

Phosphinic acid
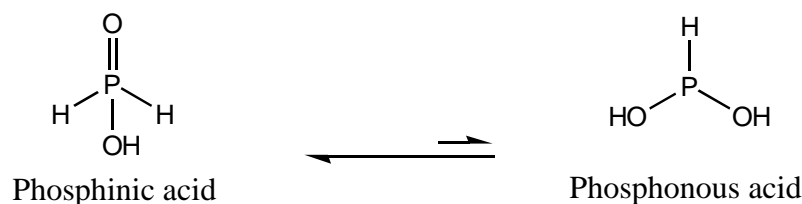
Phosphonous acid

Figure 2.2: The structures and equilibrium between phosphinic acid and phosphonous acid.

A therapeutically significant use of phosphinic acid derivatives is the inhibition of amidase-catalysed amide bond hydrolysis. This process proceeds *via* a tetrahedral transition state as depicted in **figure 2.3** and, as the phosphinic acid moiety is itself tetrahedral, it can act as a stable mimic of this intermediate structure. If the amide bond of a natural enzyme substrate is replaced with a phosphinic acid moiety, the resulting compound can act as a transition state enzyme inhibitor, competing with the natural substrate at the active site (Bartlett & Kezer, 1984; Bartlett *et al*., 1990).
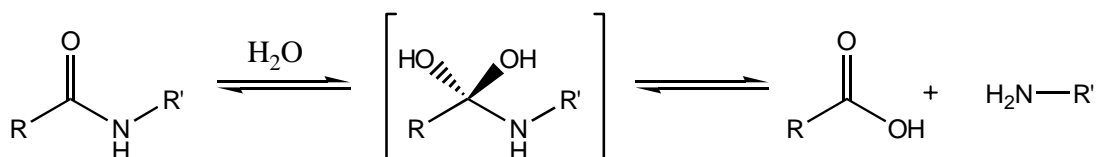
Figure 2.3: Proposed mechanism of amide bond hydrolysis.

It was proposed that the ability of phosphinic acids to act as transition state enzyme inhibitors could be used to develop cannabimimetic compounds that inhibit the ability of FAAH to hydrolyse endogenous cannabinoids. To this end, two classes of phosphinic acid, the phenyl- and alkylphosphinic acids, were designed.

Phenylphosphinic Acid Derivatives

The phenylphosphinic acid (PPA) template (see **table 2.2**) is based on that of aryl ethanolamides, with the amide bond replaced by the phosphinic acid moiety.

Since AEs are potential cannabinoid receptor ligands and may themselves competitively inhibit FAAH, the phosphinic acid moiety should confer resistance to FAAH, making these compounds more potent at both targets. In addition to the inclusion of the phosphinic acid group, the PPA compounds are structurally different to the aryl ethanolamides. A report in the literature, published after the completion of AE synthesis, demonstrated that the hydroxyl group of anandamide is not necessary for CB1 receptor affinity and, in fact, is slightly detrimental (Sheskin *et al*., 1997). It was also shown that anandamide analogues with *N*-alkyl groups including propyl, butyl, isopropyl and isobutyl have higher affinity for the CB1 receptor than the parent compound. For this reason, the target PPA compounds shown in **table 2.2** include these alkyl substituents as well as the hydroxypropyl group which was designed as a direct mimic of anandamide itself. As nothing was known about the interactions, if any, of this type of species with the endogenous cannabinoid system, the synthesis of compounds PPA2, PPA5 and PPA7 was also attempted. If biologically active, the long alkyl chains should offer increased lipophilicity, which may be important for transport across biological membranes.
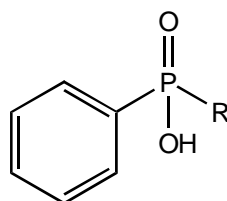
Compound	R
PPA1	Butyl
PPA 2	Decyl
PPA 3	3-Hydroxypropyl
PPA 4	Isobutyl
PPA 5	Octadecyl
PPA 6	Isopropyl
PPA 7	Hexadecyl
PPA8	Propyl

Table 2.2: Target phenylphosphinic acid derivatives.

<u>Alkylphosphinic Acid Derivatives</u>

The ultimate aim of alkylphosphinic acid synthesis was the development of anandamide analogues in which the amide bond is replaced with the phosphinic acid moiety. In theory, such compounds would mimic the ability of anandamide to bind to the cannabinoid receptors and act as substrates of the anandamide transporter. In addition, these compounds would be stable to hydrolysis and act as transition state FAAH inhibitors, thereby having a longer duration of action than anandamide *in vivo* and increasing endocannabinoid levels. However, in order to utilize commercially available starting materials and develop an effective synthetic methodology, it was decided that saturated alkylphosphinic acid compounds would be synthesized before incorporation of unsaturated carbon chains was attempted. The target alkylphosphinic acid compounds shown in **table 2.3** also have cannabimimetic potential, however. The di-substituted compound APA6, for example, is the alkylphosphinic acid analogue of palmitoylethanolamide, albeit lacking the hydroxyl group. As described previously, palmitoylethanolamide is now thought to act at peripheral CB2-like receptors and has been shown to be a substrate for FAAH, competing with anandamide (Tiger *et al*., 2000). Compounds such as APA6 that are analogous to endogenous fatty acid amides should, in theory, also compete for FAAH binding while being resistant to hydrolysis themselves. It was shown in **section 1.7.3** that there are a number of existing saturated synthetic FAAH inhibitors, namely the sulphonyl fluorides, the trifluoromethyl ketones and the methyl fluorophosphonates. These compounds potently inhibit FAAH with IC_{50} values as low as 3 nM and, therefore, analogous alkylphosphinic acids have the potential to exhibit similar pharmacological effects with the added possibility of affinity for the cannabinoid receptors.

$$\begin{array}{c} O \\ \parallel \\ P \\ R \diagup \mid \diagdown R' \\ OH \end{array}$$
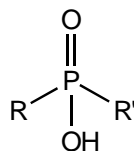
Compound	R	R'
APA1	Decyl	H
APA2	Hexadecyl	H
APA3	Octadecyl	H
APA4	Decyl	Decyl
APA5	Decyl	Butyl
APA6	Hexadecyl	Butyl
APA7	Octadecyl	Butyl

Table 2.3. Target alkylphosphinic acids.

The remainder of this chapter describes the methodologies utilized to synthesize the three classes of potential cannabimimetics and the results that were obtained.

2.2 Experimental Methods

2.2.1 Aryl Ethanolamides

A simple disconnection of the aryl ethanolamides showed that they could be synthesized by the reaction of the appropriate carboxylic acid with ethanolamine. To achieve this, it was necessary to activate the carboxylic acid, thereby making it susceptible to nucleophilic attack by the amine. Two different methodologies were employed for aryl ethanolamide synthesis and are described below.

Acid Chloride Strategy

A common method used to activate a carboxylic acid is to convert it to its acid chloride derivative. This species can then undergo attack by a nucleophile, in this case ethanolamine, to form a new amide bond (**scheme 2.1**).
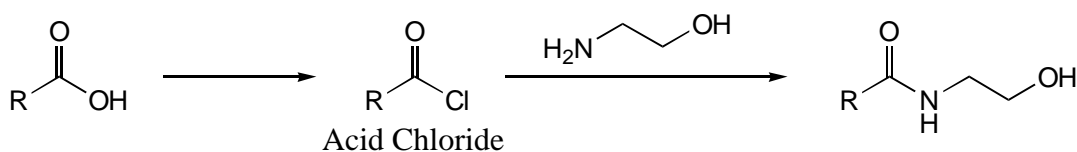
Scheme 2.1: Acid chloride strategy of aryl ethanolamide synthesis. R = aryl.

It was proposed that this activation step should be carried out by the reaction of the carboxylic acid with an excess of oxalyl chloride. The advantage of this method is that the oxalic acid by-product of the reaction decomposes to liberate carbon monoxide and carbon dioxide, thus driving the reaction forward. Hence, for these reactions, the carboxylic acid was dissolved in an appropriate solvent and stirred with a slight molar excess of oxalyl chloride for between 30 minutes and 3 hours, with the progress of the reaction periodically monitored by thin layer chromatography (TLC) for disappearance of the carboxylic acid starting material. Acid chlorides are sensitive to moisture, undergoing hydrolysis back to the carboxylic acid so, to counter this problem, glassware was oven-dried and dry solvents were used. In order to prevent atmospheric water affecting the reaction, either a silica guard tube or a dry, inert atmosphere was employed. A mechanism for this reaction is proposed in **scheme 2.2**.
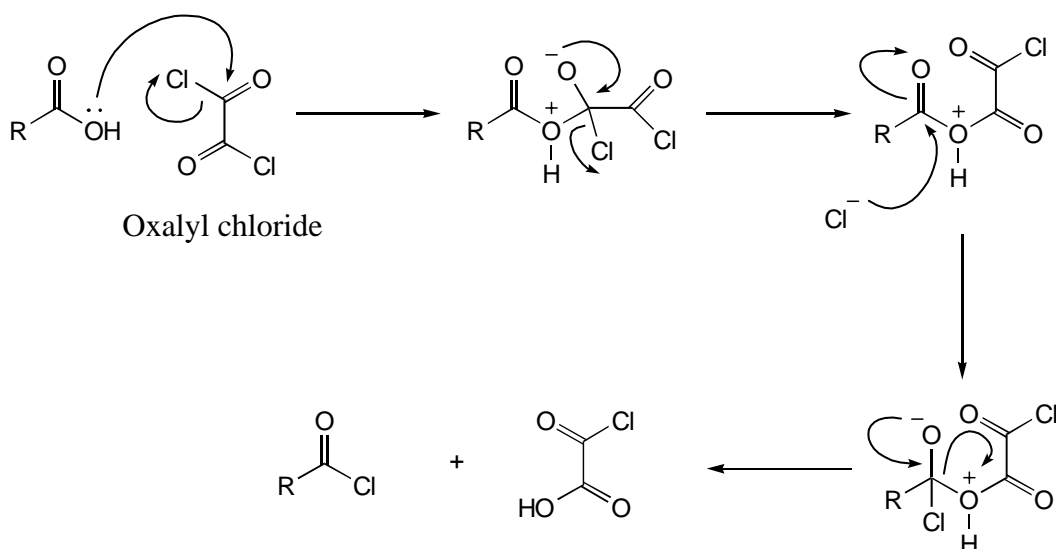
Scheme 2.2. Proposed mechanism for the reaction of a carboxylic acid with oxalyl chloride.

62

After the initial reaction with oxalyl chloride, synthesis of the aryl ethanolamide was attempted by the addition of excess ethanolamine to the reaction mixture and stirring for between 20 minutes and 2 hours (**scheme 2.3**), again monitoring the reaction by TLC.
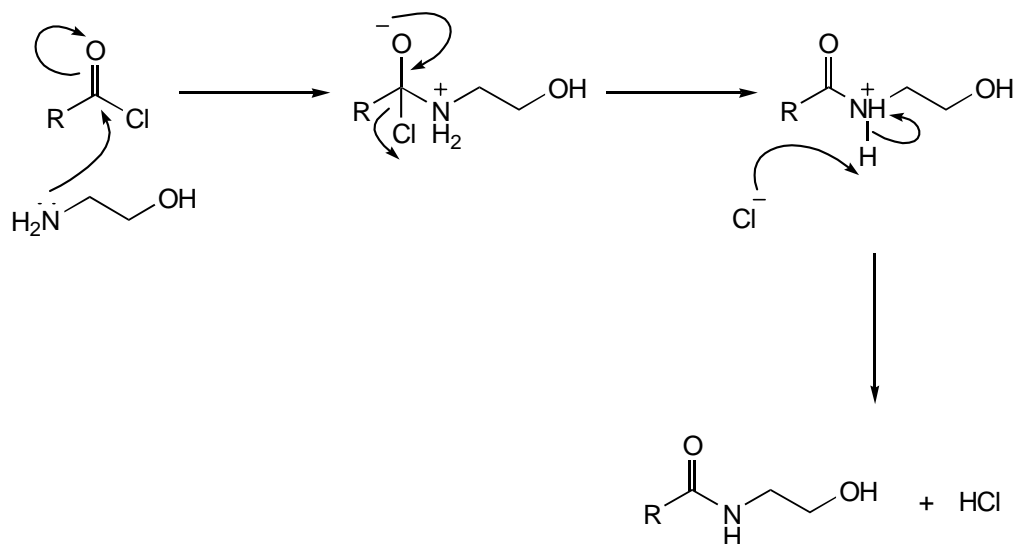
Scheme 2.3: Proposed mechanism of the reaction of ethanolamine with an acid chloride.

On completion of the reaction, the solution was washed with aqueous acid and base to remove basic and acidic impurities, respectively, and the crude product analysed by TLC and ^{1}H nuclear magnetic resonance (NMR) spectroscopy. In ^{1}H NMR spectra, ethanolamide protons appear as a quartet and an adjacent, downfield, triplet at approximately δ 3.0 to 4.0 ppm. If these peaks were observed in the NMR spectrum, the crude product was purified by flash column chromatography.

If a synthesis proved to be unsuccessful, it was likely that the acid chloride had not formed in the first step, possibly because due to the carboxylic acid not being a strong enough nucleophile to react effectively with oxalyl chloride. In an attempt to drive the reaction forwards, two different approaches were taken. The first was to simply increase the reaction time, while the second was the use of *N,N*-dimethylformamide (DMF) as a catalyst as shown in **scheme 2.4**.
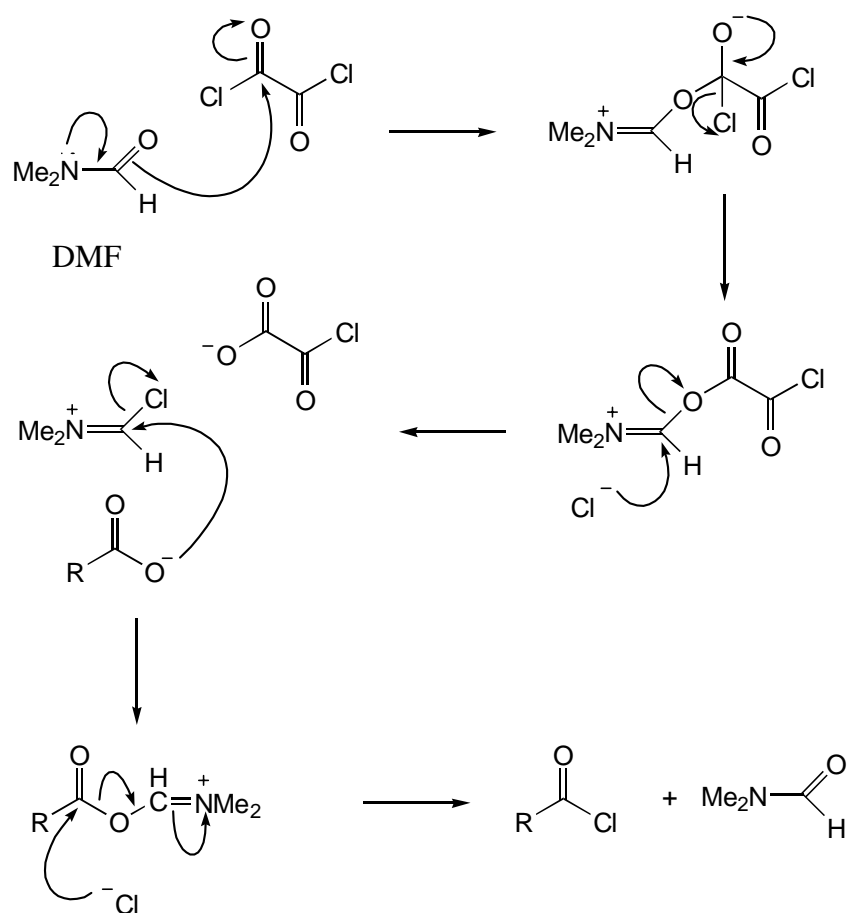
Scheme 2.4: Proposed mechanism of DMF-catalysed acid chloride synthesis using oxalyl chloride.

Another possible detrimental effect on the synthesis was the reaction of ethanolamine with unreacted oxalyl chloride. Although the excess of ethanolamine used should have "mopped up" the oxalyl chloride, it, along with the reaction solvent, was removed *in vacuo* in some syntheses to prevent unwanted side-reactions. The crude acid chloride residue was then redissolved in an appropriate solvent before addition of excess ethanolamine.

Coupling Strategy

An alternative method employed in amide bond formation is the use of coupling agents, so called because they couple a carboxylic acid and an amine together *via*

an intermediate that is more susceptible to electrophilic attack than the parent acid. Using a coupling agent, amide bond synthesis can occur in two ways. When a coupling agent is reacted with a carboxylic acid, an *O*-acyl urea is formed. The first possible route of amide bond synthesis is the direct reaction of an amine with this species. The alternative route involves a second carboxylic acid molecule reacting with the *O*-acyl urea to form a symmetric anhydride, which can then react with the amine to form an amide bond. Both routes are likely to occur to varying extents when using a coupling agent and are depicted in **scheme 2.5**.
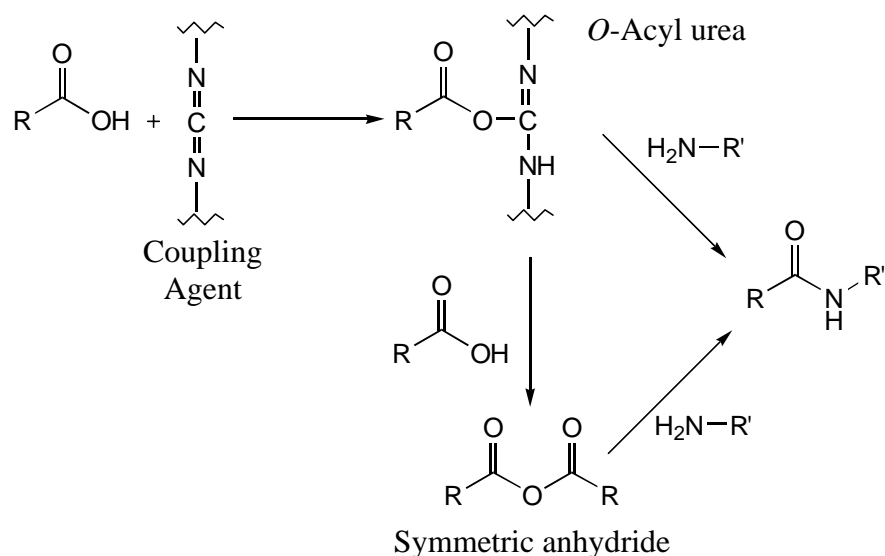
Scheme 2.5: Coupling strategy of aryl ethanolamide synthesis.

For some compounds, where the oxalyl chloride method proved unsuccessful, this reaction was attempted with the coupling agent 1-(3-dimethylaminopropyl)-3-ethycarbodiimide hydrochloride (EDC). A mechanism for this reaction is proposed in **scheme 2.6**.

For these reactions, the carboxylic acid was dissolved in an appropriate solvent and stirred with an excess of EDC for between 5 minutes and 1 hour. Excess ethanolamine was then added to the reaction mixture and stirred for 30 minutes to 19 hours. A silica guard tube was employed for the duration of the reactions, which were monitored by TLC.
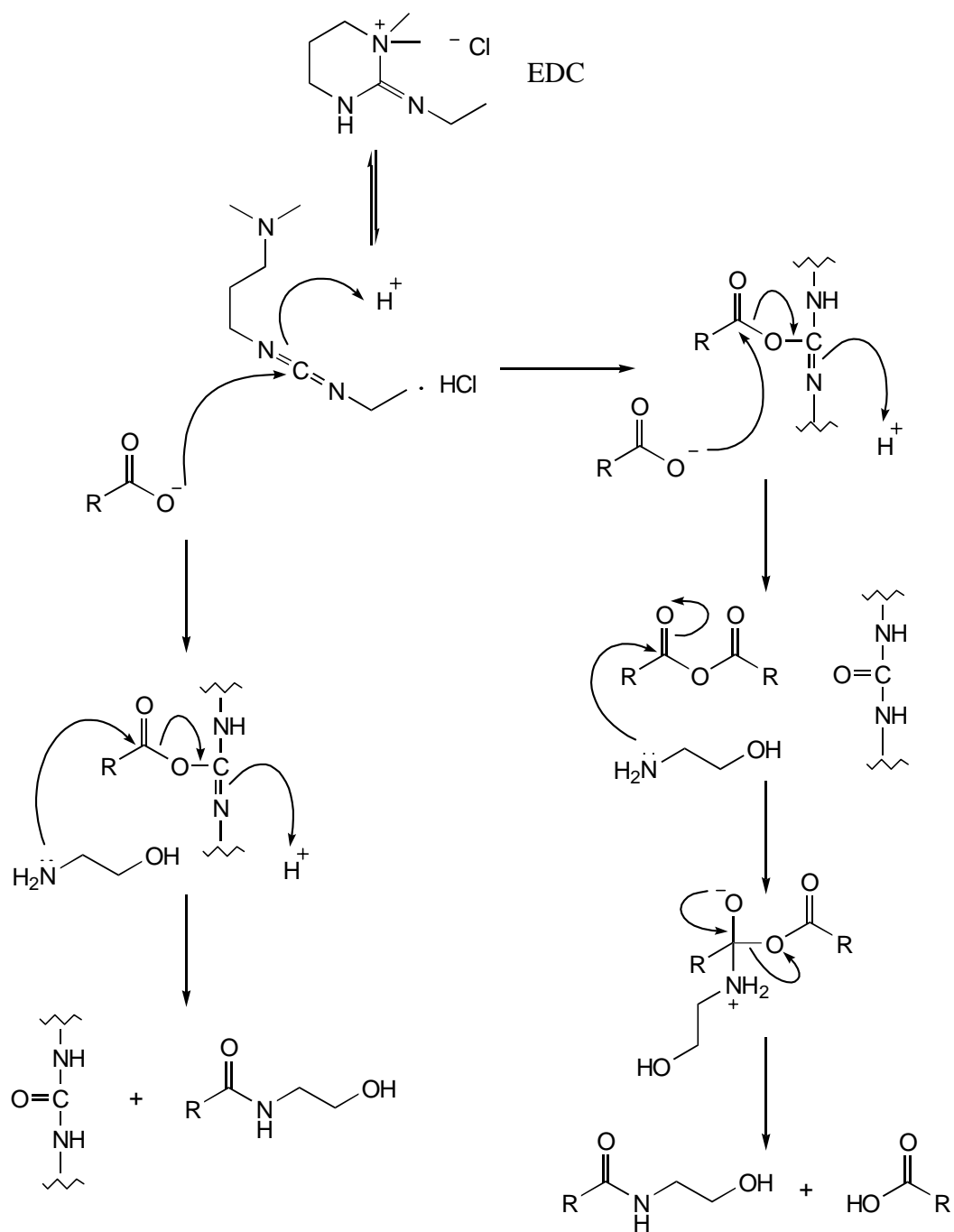
Scheme 2.6: Mechanism of aryl ethanolamide synthesis using the coupling agent EDC.

Precipitated by-products were filtered off, the solution washed with aqueous base and the crude product analysed by TLC and ^{1}H NMR spectroscopy. If the

ethanolamide product was evident, the crude product was purified by flash column chromatography.

A problem that can occur in reactions of this type is the formation of *N*-acylureas, which reduce the yield of the desired product. These species form by inter- or intramolecular rearrangements (**scheme 2.7**) which may be reduced by the introduction of a catalyst to the reaction.

Intramolecular   Intermolecular
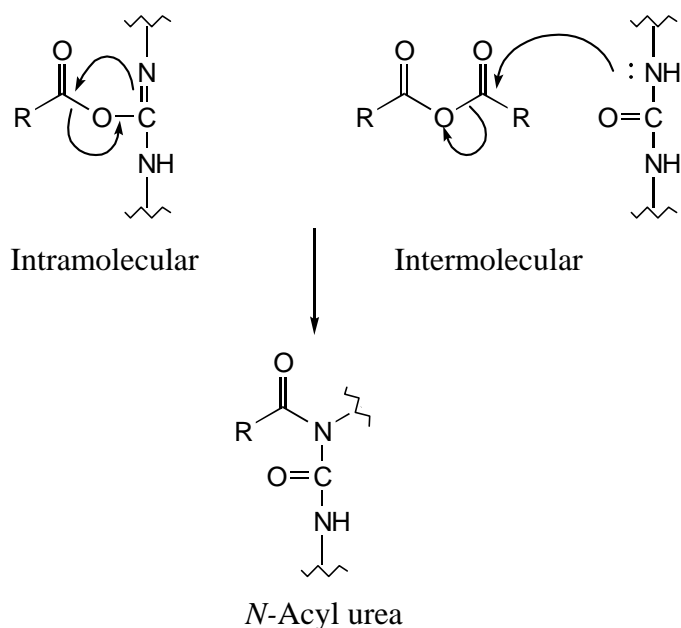
N-Acyl urea

Scheme 2.7: Mechanisms of intra- and intermolecular *N*-acylurea formation when using coupling agents.

Two catalysts, 1-hydroxybenzotriazole (HOBt) and 4-dimethylaminopyridine (DMAP), were employed in these reactions to reduce *N*-acylurea occurrence. These compounds react with the *O*-acylurea and symmetric anyhdride as soon as they form, thereby reducing the formation of the *N*-acylurea. The intermediates formed by these reactions are more susceptible to nucleophilic attack by ethanolamine than the anhydride itself and, thus, the reaction is also catalysed (**schemes 2.8** and **2.9**).
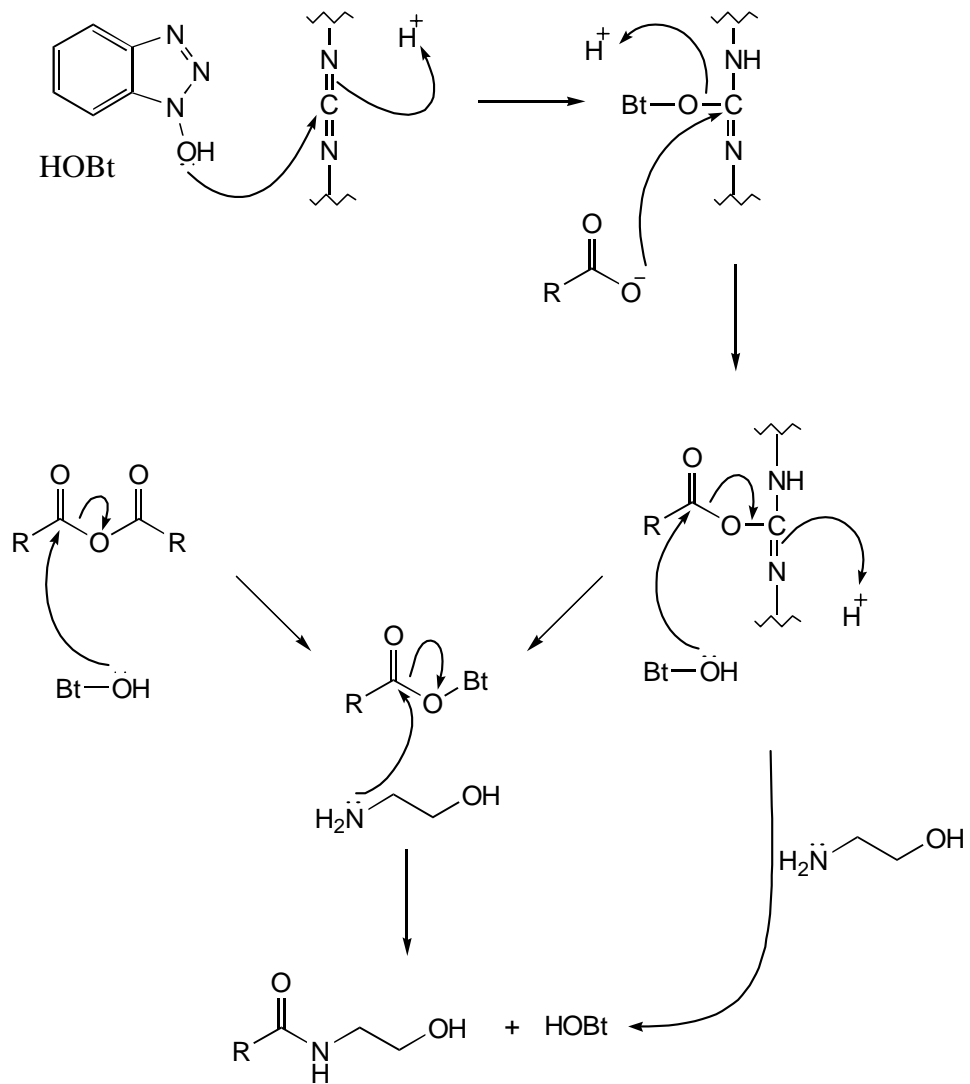
Scheme 2.8: Mechanism of HOBt catalysis in the EDC coupling reaction.
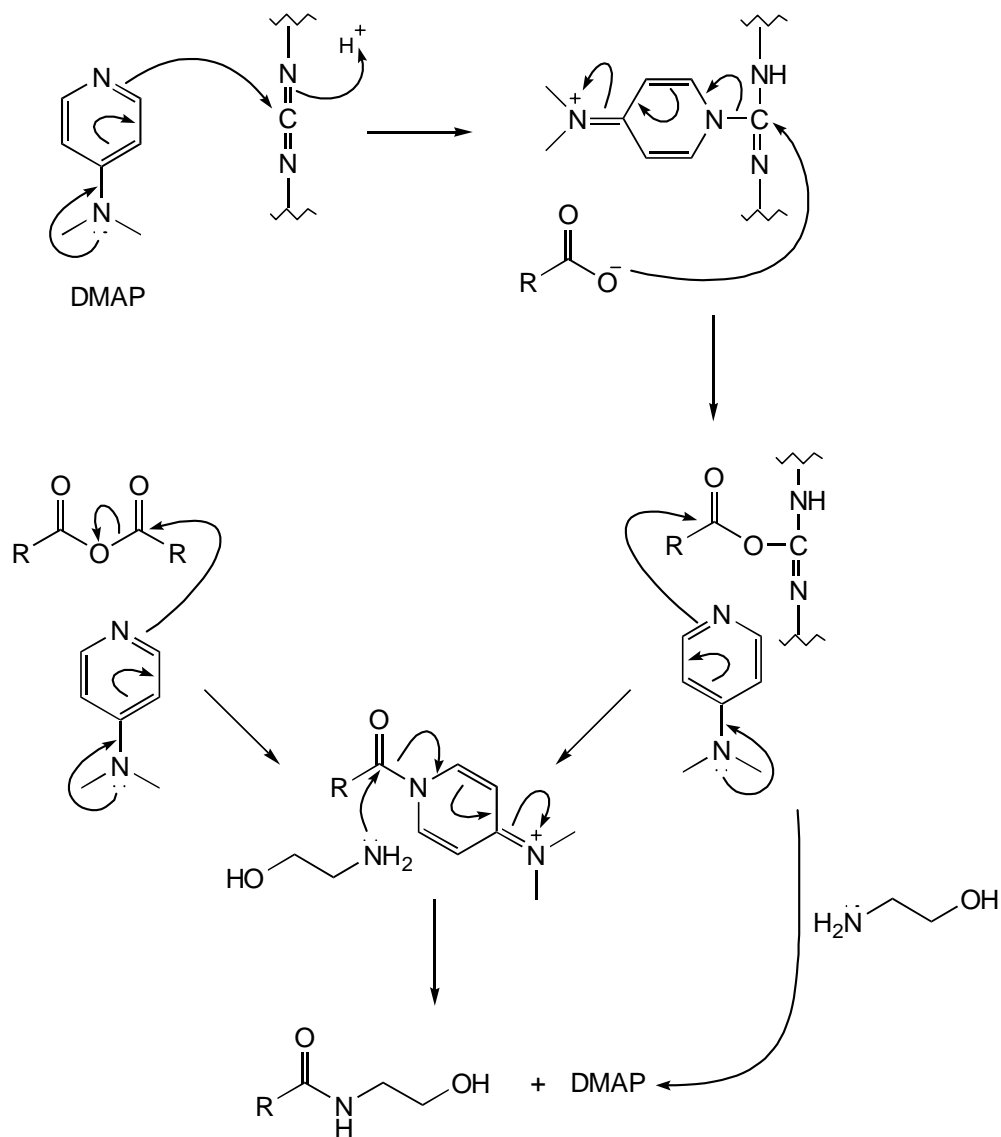
Scheme 2.9: Mechanism of DMAP catalysis in the EDC coupling reaction.

The results of both the acid chloride and coupling strategies for aryl ethanolamide synthesis are described in **section 2.3.1**.

2.2.2 Phenylphosphinic Acids

Until recently, the formation of phenylphosphinic acid derivatives was limited by the lack of a suitable methodology for their synthesis under mild conditions. However, Boyd and co-workers developed a flexible synthetic strategy in which phenylphosphinic acid is silylated in the presence of a base to *bis*(trimethylsilyl)

phenylphosphonite (BTSPP). This trivalent species can then undergo nucleophilic attack to form a new carbon-phosphorus bond when reacted with various electrophilic species (Boyd *et al.*, 1996). In order to synthesize the PPA derivatives shown in **table 2.2**, BTSPP was generated *in situ* by stirring a solution of phenylphosphinic acid with diisopropylethylamine (DIPEA) and trimethylsilyl chloride (TMSCl) for up to 3 hours. BTSPP was then stirred with the appropriate alkyl iodide and the intermediate washed with aqueous acid to hydrolyse the silyl groups. The only exception to this was PPA3, where 3-bromopropan-1-ol was used instead of an alkyl iodide. DIPEA was used in preference to other bases as its steric bulk reduces the risk of side-reactions between the base and electrophile. Since BTSPP is pyrophoric, these reactions were performed under an inert atmosphere. The mechanism of this synthetic route is shown in **scheme 2.10**.
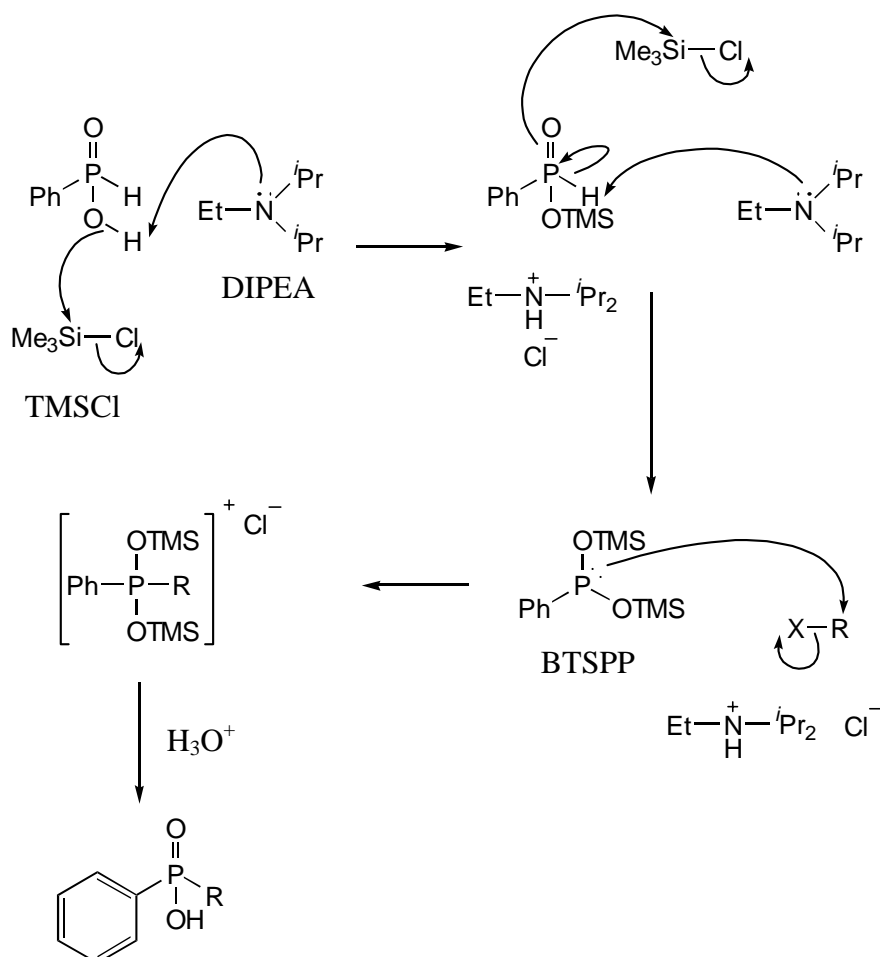
Scheme 2.10: Mechanism of the synthesis of phenylphosphinic acid derivatives *via* the formation of BTSPP. R = alkyl, X = I or Br.

One problem encountered in the purification of phosphinic acids is that they interact with silica and, therefore, conventional chromatographic techniques can not be used. Because of this, it was important that the reactions were driven to completion in these syntheses. When a crude product was obtained, it was analysed by ^{1}H and ^{31}P NMR spectroscopy. In ^{1}H NMR spectra, any remaining phenylphosphinic acid produced a distinctive P-H doublet between δ 6.0 and δ 9.0 ppm with a large coupling constant of 500-600 Hz, and a single ^{31}P peak at approximately δ 25-30 ppm. Alkyl-substituted PPAs gave a single ^{31}P peak at approximately δ 40-50 ppm. If a phenylphosphinic acid peak was evident, the reaction had not reached completion and repeat reactions were performed in which reaction time and equivalents of reagents were altered to drive the reaction forwards. The results of the phenylphosphinic acid syntheses are described in **section 2.3.2**.

2.2.3 Alkylphosphinic Acids

Until recently, the most common method of phosphinic acid synthesis was the Arbuzov reaction. This reaction involves the nucleophilic displacement of an appropriate leaving group, usually a halide, from carbon by a substituted phosphonite ester, resulting in a phosphinate ester. As depicted in **scheme 2.11**, subsequent acidic hydrolysis of the ester forms the free phosphinic acid.
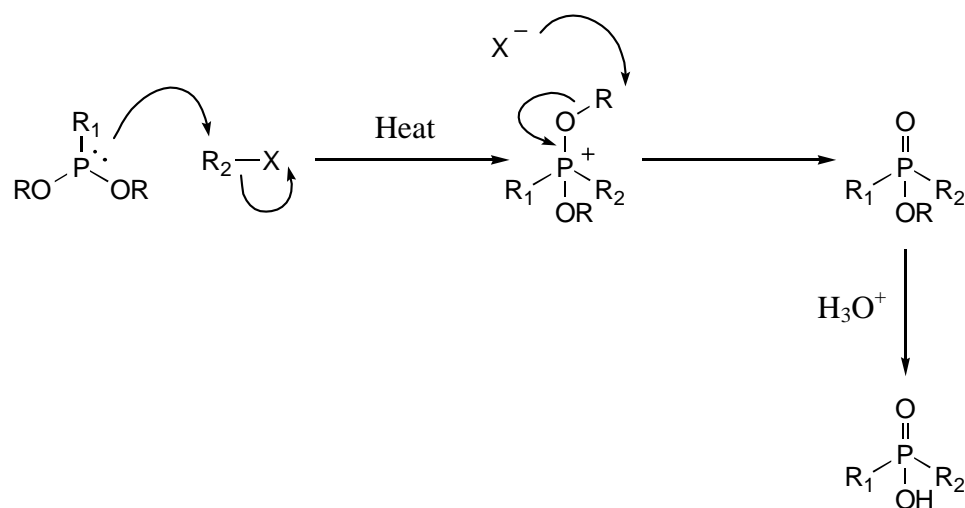
Scheme 2.11: Phosphinic acid synthesis *via* the Arbuzov reaction. R, R$_1$, R$_2$ = alkyl, X = halide.

71

However, the Arbuzov reaction is limited by the restricted availability of phosphonite starting materials and the high temperatures of 120-160 °C that are required. These temperatures mean that the starting material, halide and product must be thermally stable to withstand these harsh conditions. Recently, however, a flexible methodology was developed for phosphinic acid synthesis under mild conditions (Boyd *et al.*, 1990; Boyd *et al.*, 1994). In this methodology, similar to that used in the synthesis of phenylphosphinic acid derivatives, ammonium phosphinate is reacted with hexamethyldisilazane (HMDS) to silylate the oxygen atoms and form the reactive, trivalent *bis*(trimethylsilyl)phosphonite (BTSP). Nucleophilic attack by BTSP on an alkyl halide results in the displacement of the halide ion and formation of a new carbon-phosphorus bond.

In the synthesis of alkylphosphinic acid compounds, shown in **scheme 2.12**, ammonium phosphinate was heated with 1.1 equivalents of HMDS for 2-3 hours at 110-120 °C to generate BTSP, which was then stirred at room temperature with the appropriate alkyl iodide. For the synthesis of mono-substituted alkylphosphinic acids, the reaction was terminated at this step by washing with aqueous acid to hydrolyse the silyl groups. However, for the synthesis of di-substituted alkylphosphinic acids, more HMDS was added to the reaction solution at this point. Instead of acting as a silylating agent, HMDS now acts as a hindered base to deprotonate the intermediate and allow nucleophilic attack at a second alkyl iodide. After stirring with the second iodide, the silyl groups were hydrolysed with aqueous acid to liberate the di-substituted product. As with BTSPP, BTSP is pyrophoric so the reactions were performed under an inert atmosphere.

Alkylphosphinic acids, like the phenylphosphinic acids, could not be purified by normal silica chromatography, so these reactions needed to be driven as far as possible towards completion. In addition to the problem of reactions being incomplete, the major possible problem with mono-substituted alkylphosphinic acid synthesis was the reaction proceeding too far, resulting in unwanted di-substitution. The possible problems in the synthesis of di-substituted species were more diverse, however.

72
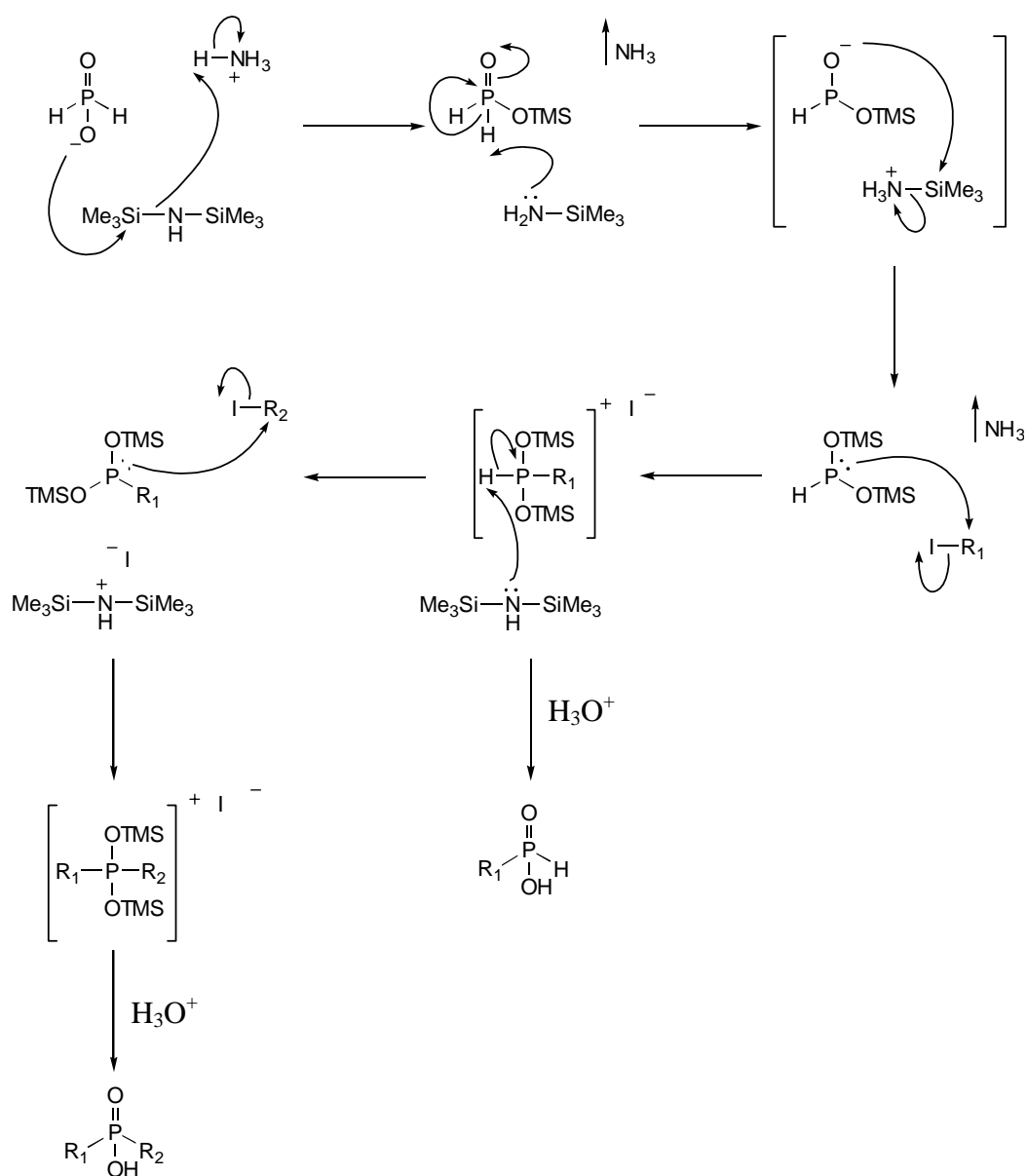
Scheme 2.12: Mechanism of the synthesis of mono- and di-substituted alkylphosphinic acids *via* the formation of BTSP.

In addition to remaining ammonium phosphinate and the presence of mono-substituted product, the synthesis of the asymmetric compounds could result in both symmetric and asymmetric di-substitution. To ascertain the extent of reactions, products were analysed by NMR spectroscopy. In ^{31}P NMR spectra, ammonium phosphinate appeared as a single peak at δ 9-10 ppm, while mono-

and di-substituted APAs appeared as single peaks at δ 39-42 ppm and δ 61-64 ppm, respectively. If undesirable phosphorus peaks were evident, the reaction times and reagent quantities were adjusted accordingly in an attempt to rectify the problem. Fortunately, since ammonium phosphinate is water soluble, small amounts could be removed by aqueous washing if it was observed in the spectra. The results of the alkylphosphinic acid syntheses are described in **section 2.3.3**.

2.2.4 Physical Measurements

The physical characteristics of the successfully synthesized novel target compounds were fully evaluated by melting point analysis, NMR spectroscopy, mass spectroscopy and elemental analysis. These data and general experimental methodologies are described in **appendix A**. Representative NMR and mass spectra are shown in **appendix B**.

2.3 Results and Discussion

2.3.1 Aryl Ethanolamides

The synthesis of the target aryl ethanolamide compounds was largely unsuccessful despite numerous attempts with varied reaction conditions. Of the fourteen target compounds, only five were synthesized successfully.

Acid Chloride Strategy

The results obtained from reactions using the acid chloride strategy are summarized in **table 2.4**. It is evident from these results that there is no definitive set of conditions that can be used for aryl ethanolamide synthesis and the reaction must be tailored to the individual carboxylic acid starting materials. For instance, of the successful syntheses, two of the four compounds required DMF catalysis whereas AE5 was successful with or without the catalyst. AE3 and AE4 are structurally very similar to AE5 and AE6, but the former compounds were not successfully synthesized despite attempts using similar conditions to those that proved successful for the latter. The successful synthesis of compound AE9 with a relatively high yield can be easily explained. The chlorine atom on the benzene

ring has an electron withdrawing effect and, therefore, makes the carboxylic acid and subsequent acid chloride more susceptible to nucleophilic attack. On the other hand, the failure to synthesize the methoxy derivatives may be due to these groups having an electron donating effect, thereby making the acid chloride less susceptible to nucleophilic attack. A similar effect caused by the double bonds in AE1 and AE2 may be responsible for their failure.

Coupling Strategy

The results of reactions performed using the EDC coupling strategy are shown in **table 2.5**. Although this strategy was not explored as thoroughly as the acid chloride strategy, it is apparent that there is no pattern relating to the success of synthesis and conditions used. The only successful reaction, AE13, was performed using DMAP and stirring overnight. This reaction time resulted in only a slightly increased yield when compared to stirring for 4 hours. AE1 and AE2 were totally unsuccessful, presumably due to the double bond adjacent to the acid functionality affecting the acid chloride reactivity. AE3 and AE4 are the most structurally similar compounds to the successfully synthesized AE13 and would be expected to be synthesized successfully too. The use of catalysis in the attempted syntheses of AE3 proved to have no beneficial effect. The aryl ethanolamide was formed after stirring overnight with and without catalyst, but analysis by TLC showed there were numerous, close impurities meaning purification by flash column chromatography was not possible. This was also the case in the synthesis of AE4. As with the acid chloride strategy, the electron donating effect of the methoxy groups of AE8 were likely to be the reason for the failed synthesis.
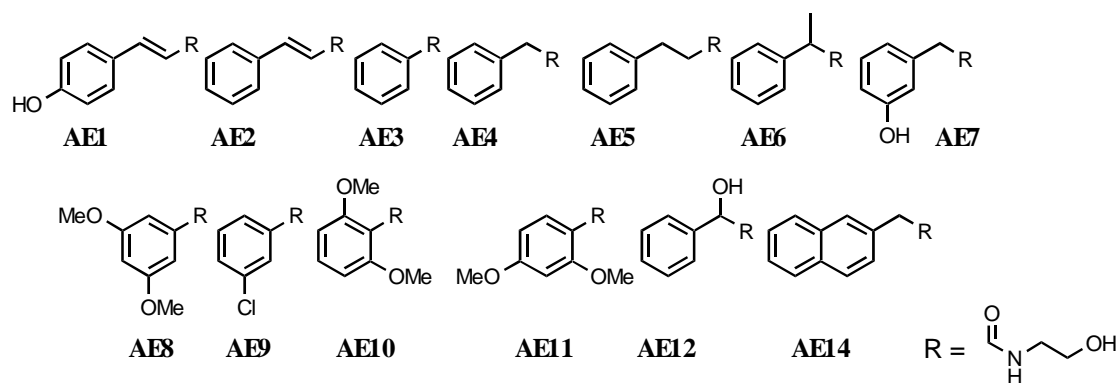
Compound	Oxalyl Chloride (Equiv.)	Time[1]	Ethanolamine (Equiv.)	Time	DMF[2] (Equiv.)	Outcome[3]
AE1	1.91	1 hr[a]	5.46	20	1.28	c
AE1	1.53	2 hrs	3.27	¾ hr	0	c
AE2	1.38	1 hr	2.95	1½ hrs	0	c
AE2	1.38	½ hr	2.95	½ hr	cat.	d
AE3	1.4	¾ hr[a]	2.84	¾ hr	0	e
AE3	1.4	¾ hr	2.84	½ hr	1.59	e
AE3	1.4	1¾ hrs[b]	2.84	2 hrs	1.59	d
AE3	1.14	½ hr[a]	2.84	1¾ hrs	1.11	d
AE4	1.27	1½	2.71	½ hr	1.42	d
AE4	1.27	1½	2.71	½ hr	0	f
AE5	1.4	1½	3.0	1½ hrs	0	g (26 %)
AE5	1.4	1 hr[a]	3.0	1¼ hrs	cat.	e
AE5	1.4	1 hr[a,b]	3.49	¾ hr	cat.	g (45 %)
AE6	1.4	1½	3.0	1¾ hrs	0	g (62 %)
AE7	1.42	½ hr	3.03	¾ hr	0	e
AE8	1.27	1 hr	3.03	¾ hr	0	c
AE8	1.27	1¼ hrs[b]	3.03	2 hrs	0	h
AE9	1.46	½ hr	3.64	2 hrs	0	c
AE9	1.09	½ hr[a]	3.12	1½ hrs	1.22	g (71 %)
AE10	1.27	1 hr	3.03	½ hr	0	h
AE11	1.27	1 hr	3.03	¾ hr	0	c
AE12	1.42	1 hr	3.03	½ hr	0	e
AE14	1.3	¾ hr[b]	4.3	¾ hr	0	h
AE14	1.3	3 hrs[b]	2.78	1 hr	cat.	g (49 %)

1. a = Solvent removed prior to addition of ethanolamine, b = inert atmosphere. 2. cat. = Catalytic amount, typically 2 drops. 3. c = Crude product formed, but not the desired AE, d = minute trace of ethanolamide protons, e = no product, f = impurity remained after columning, g = successful synthesis and purification (overall % yield), h = "product" was the starting material.

Table 2.4. Results of reactions using the acid chloride strategy.
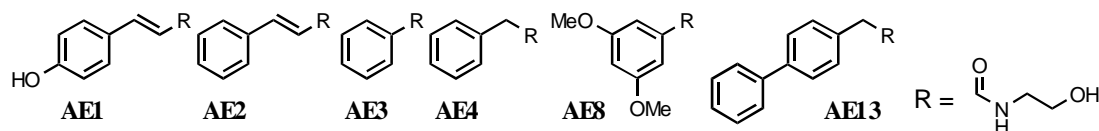
Compound	EDC (Equiv.)	Time[1]	Ethanolamine (Equiv.)	Time[2]	Catalyst[3] (Equiv.)	Outcome[4]
AE1	2.9	1hr	5.46	o/n	0	a
AE2	1.39	½ hr	4.43	1½ hrs	0	a
AE2	1.19	10	1.48	o/n	0	b
AE3	1.27	¾ hr	2.84	½ hr	0	b
AE3	1.21	0[a]	1.62	¾ hr	H, 1.31	b
AE3	1.11	1½ hrs	1.22	2 hrs	D, cat.	b
AE3	1.21	5 mins	1.22	o/n	0	c
AE3	1.27	10	1.22	o/n	0	c
AE3	1.27	¼ hr	1.27	o/n	D, cat.	c
AE4	1.21	2½ hrs	2.71	¾ hr	0	d
AE4	1.21	40	1.36	o/n	0	c
AE8	1.20	0[a]	3.03	2 hrs	H, 1.43	a
AE8	1.20	25	1.82	o/n	0	b
AE13	1.11	0[a]	1.38	4 hrs	D, cat.	e (42 %)
AE13	1.11	¼ hr	2.12	o/n	D, cat.	e (53 %)

1. a = EDC and ethanolamine added together. 2. o/n = Overnight. 3. H = HOBt, D = DMAP, cat. = catalytic amount (micro spatula tip). 4. a = Crude product formed, but not the desired AE, b = no product, c = numerous spots on TLC of crude product. Too close to separate, d = ^{1}H NMR showed only a minute trace of ethanolamide protons, e = successful synthesis and purification (overall % yield).

Table 2.5. Results of reactions using the EDC coupling strategy.

2.3.2 Phenylphosphinic Acids

Optimisation of these reactions took some time to achieve. Initial studies involved the attempted synthesis of PPA1 and these results are summarized in **table 2.6**. The methodology of Boyd *et al.* (1994) suggested that BTSPP should be stirred with the appropriate electrophile for 12-24 hours so, in attempts 1 and 2, butyl iodide and BTSPP were stirred together for 20½ hours. Neither reaction proved to be successful although, as expected, using 1.0 equivalents resulted in the reaction going further towards completion than 0.5 equivalents. Increasing the reaction

time and iodide concentration in attempts 3 and 4 showed a promising shift towards the product, but starting material still remained. It was postulated that this was because all of the phenylphosphinic acid was not being converted to BTSPP so, in attempts 5 and 6, reaction time with DIPEA and TMSCl was increased to 3 hours and in attempt 5, the iodide reaction was refluxed at 50 °C in order to attempt to drive the reaction forwards. The fact that appreciable amounts of phenylphosphinic acid were still present after these reactions indicated that the determining factor was iodide reaction time. Attempts 7 and 8 were run in parallel with reaction times of 65 and 153 hours, respectively. Attempt 7 went very close to completion with a small amount of phenylphosphinic acid remaining, while attempt 8 resulted in a single product peak at δ 45.42 in the ^{31}P NMR spectrum. With this result in mind, the remaining PPA derivatives were attempted by reacting phenylphosphinic acid (14.1 mmol) with DIPEA (31.0 mmol) and TMSCl (31.5 mmol) for 3 hours and the appropriate electrophile for 7 days or more. The results of these reactions are summarized in **table 2.7**.

Although the experimental conditions resulted in the desired products and disappearance of phenylphosphinic acid, there were still two factors affecting product purity. In the literature, Boyd *et al*. (1996) suggested that washing with 2M hydrochloric acid was sufficient to hydrolyse the remaining TMS groups. However, ^{1}H NMR spectra of the crude products often revealed a strong TMS peak at approximately δ 0 ppm. To hydrolyse these groups effectively, the crude material was resuspended in wet methanol, stirred for 1½ to 2 hours and the solvent then removed *in vacuo*.

Attempt	DIPEA (Equiv.)	TMSCl (Equiv.)	Time (hrs)	Iodide (Equiv.)	Time (hrs)	Outcome
1	2.2	2.18	2	0.5	21½	Phenylphosphinic acid present in approximate ratio of 4:3 with product.
2	2.2	2.18	2	1	21½	Phenylphosphinic acid present in approximate ratio of 1:2 with product.
3	2.2	2.18	2¼	1.5	48	Phenylphosphinic acid present in approximate ratio of 1:5 with product.
4	2.2	2.18	2¼	2.0	48	Phenylphosphinic acid present in approximate ratio of 1:7 with product.
5	2.2	2.18	3	1.5	20½[1]	Appreciable amount of phenylphosphinic acid remaining.
6	2.49	2.52	3	1.5	20¾	Appreciable amount of phenylphosphinic acid remaining.
7	2.2	2.18	$2^{1}/_{3}$	2.0	65	Near completion.
8	2.2	2.18	$2^{1}/_{3}$	2.0	153	Reaction complete, but excess iodide present. Impurity removed with base/acid wash. ^{31}P peak at δ 45.42.

1. Refluxed at 50 °C.

Table 2.6: Results of attempted PPA1 syntheses.

Compound	Electrophile (Equiv.)	Time (hrs)	Outcome[1]	Overall % Yield	^{31}P NMR (δ)
PPA1	2.0	153	a	74	45.42
PPA2	2.0	163	a	66	47.63
PPA3	2.04	164	b	-	-
PPA4	1.98	211½	a	21	47.49
PPA5	1.16	163	a	63	48.34
PPA6	1.14	185¾	c	-	-
PPA7	1.49	167½	d	-	-
PPA7	1.49	259½	a	79	48.60
PPA8	1.17	164	d	-	-
PPA8	1.17	284½	a	68	46.86

1. a = Pure product by ^{1}H and ^{31}P NMR after base/acid wash, b = ^{1}H and ^{31}P NMR indicates no phosphorus-containing product, c = no product, d = some phenylphosphinic acid remaining.

Table 2.7: Results of attempted phenylphosphinic acid syntheses.

The second problem encountered was that of alkyl iodide remaining in the crude product, evident from an excess number of protons in the ^{1}H NMR spectra. To solve this, a work up procedure was developed to remove any impurities from the product. After initial washing with hydrochloric acid to partly hydrolyse the TMS groups, this aqueous phase was removed and replaced with 1M sodium hydroxide solution. As the alkylphosphinic acid products were acidic in nature, they were extracted into the basic aqueous layer, leaving any organic impurities in the solvent, which was then discarded. The product was then liberated by addition of excess 2M hydrochloric acid and redissolved in clean solvent. This procedure effectively removed impurities and resulted in clean products.

As can be seen from **table 2.7**, the attempted syntheses of PPA3 and PPA6 failed. The use of 3-bromo-1-propanol in the attempted synthesis of PPA3 may have been an important factor as alkyl bromides are less reactive than their corresponding iodide. In addition, there may have been competition between carbons 1 and 3 in the nucleophilic attack by BTSPP, although this does not explain the total lack of any form of "product". A possible reason for the failure of PPA6 is the production of propene gas as proposed in **scheme 2.13**. This would

explain the lack of success in this synthesis although, as in the synthesis of PPA3, regenerated phenylphosphinic acid should have been evident in the NMR spectra.
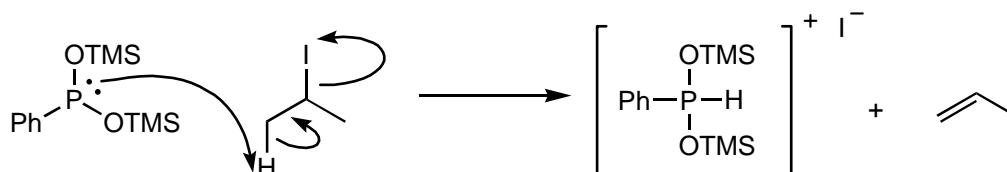
Scheme 2.13: Proposed mechanism to explain the failure of PPA6 synthesis.

2.3.3 Alkylphosphinic Acids

As mentioned in **section 2.2.3**, the main problem in the synthesis of alkylphosphinic acids is optimising the reaction conditions to obtain the desired product without the formation of unwanted substitutions. This was especially problematical in the synthesis of asymmetric, di-substituted phosphinic acids where it was theoretically possible to obtain two types of mono-substituted product and two types of symmetrical, di-substituted product as well as the target compound. Therefore, determining the optimum reaction conditions was vital for successful APA synthesis.

<u>Mono-Substituted Alkylphosphinic Acids</u>

Decylphosphinic Acid (APA1):
The initial attempts at mono-substituted APA synthesis were on target compound APA1. The results for this compound are summarized in **table 2.8**. As can be seen in attempts 1 to 3, increasing the iodide reaction time increased the amount of di-substituted product formed. Attempts 4 to 6 were performed in order to compare the HMDS silylating method with the TMSCl method employed for phenylphosphinic acid syntheses.

Attempt	Silylating Method[1]	Time (hrs)	Iodide (Equiv.	Time (hrs)	Outcome[2]
1	a	2½	0.90	20	d. Approximate 15:1 ratio of product to ammonium phosphinate. Large TMS peak.
2	a	3	0.90	92	d,f. No ammonium phosphinate remaining. Approximate 12:1 ratio of product to di-substituted.
3	a	3	0.86	162	d. As above, but approximately 8:1.
4	b	3	0.82	46	d,f. Approximate 3:1 ratio of desired product to ammonium phosphinate.
5	c	3	0.82	47	e. Similar to attempt 4, but some di-substitution.
6	a	3	0.82	47	e. As above, though less di-substitution.

1. a = 1.10 equivalents of HMDS, b = 2.20 equivalents of DIPEA for 15 mins then 2.20 equivalents of TMSCl, c = 2.20 equivalents of NEt₃ for 15 mins then 2.20 equivalents of TMSCl.
2. d = Purification by base/acid extraction, e = washed with 2M HCl, f = stirred with methanol for 1½-2 hrs to hydrolyse TMS groups.

Table 2.8: Results of attempted syntheses of decylphosphinc acid (APA1).

The reduced iodide concentration and intermediate reaction time employed proved to be more successful, and the results show that in the TMSCl reactions, triethylamine (NEt₃) is a more effective base than DIPEA. However, the HMDS method resulted in less di-substituted product and, despite the fact that synthesis of pure APA1 was not achieved, this method appeared to be the best route to mono-substituted APAs.

Hexadecylphosphinic Acid (APA2):
The results of attempted APA2 synthesis are shown in **table 2.9**. The first attempted synthesis was carried out using less iodide than in the APA1 syntheses

in order to prevent di-substitution occurring. This strategy proved successful, although the overall yield was quite low. Attempts were made to rectify this in subsequent reactions by optimising reaction conditions. Attempt 2 appears to be anomalous as the desired product was not formed, while changing to the TMSCl silylating method in attempt 3 produced the desired product, although a large amount of ammonium phosphinate remained.

Attempt	Silylating Method[1]	Time (hrs)	Iodide (Equiv.	Time (hrs)	Outcome[2]
1	a	2	0.75	22¾	c. Pure product obtained with 20 % overall yield.
2	a	3½	0.8	311	c. Oil formed and did not crystallize on refrigeration.
3	b	3	0.8	44½	d,e. Significant amounts of ammonium phosphinate remaining. Stirring overnight with water did not remove it.
4	b	3	0.8	48	d,e,f. Pure product obtained with 7 % overall yield.
5	b	3	0.87	66	d,e,g. Pure product obtained with 11 % overall yield.
6	a	3	0.9	189	d,e,g. Pure product obtained with 26 % overall yield.

1. a = 1.10 equivalents of HMDS, b = 2.20 equivalents of DIPEA for 15 mins then 2.20 equivalents of TMSCl. 2. c = Purification by base/acid extraction, d = washed with 2M HCl, e = stirred with methanol for 1½-2 hrs to hydrolyse TMS groups, f = sodium salt purification method, g = ethyl acetate wash.

Table 2.9: Results of attempted syntheses of hexadecylphosphinic acid (APA2).

At this point, two different purification methods were attempted. In attempt 4, it was noticed that when performing the basic extraction (as described for the PPA derivatives) on hexadecylphosphinic acid, a thick, white precipitate formed. This was assumed to be the insoluble sodium salt, so the precipitate was filtered off, dissolved in methanol and acidified with excess 2 M hydrochloric acid to yield the

alkylphosphinic acid, also a thick, white precipitate. The product was then resuspended in dichloromethane, washed, dried and the solvent removed to yield the pure product. However, the yield was low so, in the final two reactions, an attempt was made to find a solvent in which the impurities were soluble and the product insoluble. Hexane appeared to be the most suitable solvent, so it was used to wash the crude product to yield the pure alkylphosphinic acid in higher yields.

Octadecylphosphinic Acid (APA3):

These reactions were performed in parallel with those for APA2 and the results are summarized in **table 2.10**.

Attempt	Silylating Method[1]	Time (hrs)	Iodide (Equiv.)	Time (hrs)	Outcome[2]
1	a	3½	0.75	92	c. No phosphorus peak evident in ^{31}P spectrum.
2	a	3½	0.80	312	c. Small product peak plus ammonium phosphinate.
3	b	3	0.80	44½	d,e. Ammonium phosphinate remaining after work up.
4	b	3½	0.89	48	d,e,f. Pure product obtained with 4 % overall yield.
5	b	3	0.89	66	d,e,g. Pure product obtained with 15 % overall yield.
6	a	3	0.92	138	d,e,g. Pure product obtained with 26 % overall yield.

1. a = 1.10 equivalents of HMDS, b = 2.20 equivalents of DIPEA for 15 mins then 2.20 equivalents of TMSCl. 2. c = Purification by base/acid extraction, d = washed with 2M HCl, e = stirred with methanol for 1½-2 hrs to hydrolyse TMS groups, f = sodium salt purification method, g = ethyl acetate wash.

Table 2.10: Results of attempted syntheses of octadecylphosphinic acid (APA3).

Di-Substituted Alkylphosphinic Acids

Synthesis of these compounds proved more problematical than the mono-substituted alkylphosphinic acids. The first compound attempted, APA4, was the most straightforward as it was symmetrical and, therefore, there was no danger of unwanted di-substitutions. The results for this analogue are shown in **table 2.11**. The first attempt, stirring with each addition of iodide overnight, as described in the literature, was unsuccessful with no di-substituted product evident in the ^{31}P NMR spectrum and some remaining ammonium phosphinate. It was thought that deprotonation of the second intermediate was not occurring effectively so, to try and rectify this, the reaction time of the second addition of HMDS was increased. This led to a slight improvement with some di-substitution evident, so reaction times at all stages were increased, resulting in a greater ratio of di-substituted product to mono-substituted by-product. To try and increase this ratio further, the second iodide reaction time was almost doubled in attempt 4, leading to a much improved ratio in favour of the desired product. In the final attempt, the silylating time was increased and a longer reaction time also applied to the first iodide. Although mono-substituted product was still evident, this reaction was the most effective of the five attempts.

Despite the failure to synthesize APA4, the asymmetrical phosphinic acid derivatives were attempted beginning with APA5, also shown in **table 2.11**. The first reaction employed standard literature conditions but with longer reaction times for the two iodides. This resulted in a much more successful ratio of di-substituted to mono-substituted products than the previous attempts with APA4. This was likely to be caused by the deprotonation of the second intermediate species being easier to achieve in this reaction due to the reduced electron donating effect of the butyl group in comparison to the decyl group. Increasing the iodide reaction times further in the second attempt led to an almost complete conversion to the di-substituted product, although some mono-substitution remained.

It was now evident that total di-substitution was unlikely to be achieved in this one-pot reaction due to the fine line between mono-alkylating the ammonium phosphinate in the first step and creating unwanted, symmetrical di-substitution.

Compound	HMDS (Equiv.)	Time (hrs)	First Iodide (Equiv.)	Time (hrs)	Base Used[1] (Equiv.)	Time (hrs)	Second Iodide (Equiv.)	Time (hrs)	Outcome
APA4	1.01	2	1.01	21	a, 1.01	2	1.01	21	No di-substituted product. Mostly mono-substituted with some ammonium phosphinate.
APA4	1.10	2	1.09	22	a, 1.10	2½	1.09	24	Small amount of di-substitution. No starting material remaining, mostly mono-substitution.
APA4	1.10	2½	1.09	66	a, 1.10	3	1.09	44½	Approximate 3:2 ratio of mono- to di-substituted species.
APA4	1.10	3	1.06	68	a, 1.10	2	1.06	83½	Approximate 1:3 ratio of mono- to di-substituted species.
APA4	1.10	4	1.06	93	a, 1.03	2½	1.06	70	Approximate 1:4 ratio of mono- to di-substituted species.
APA5	1.10	2¾	Butyl, 1.11	44	b, 1.10	3¾	Decyl, 1.06	43	Approximate 1:7 ratio of mono- to di-substituted species.
APA5	1.04	3	Butyl, 1.10	68	a, 1.06	2	Decyl, 1.06	83½	Almost complete reaction. Small amount of mono-substitution remaining.

1. a = HMDS, b = DIPEA.

Table 2.11: Results of attempted syntheses of APA4 and APA5.

For the final two asymmetrical di-substituted alkylphosphinic acids, APA6 and APA7, the one-pot method was initially attempted with mixed success. In an attempt to remove the possibility of unwanted side-reactions in the synthesis of APA6 and APA7, it was decided that a different approach would be taken. As described above, the mono-substituted compounds hexadecylphosphinic acid (APA2) and octadecylphosphinic acid (APA3) were successfully synthesized and purified. Using these compounds as starting materials for the synthesis of APA6 and APA7 and an analogous method to that employed in the synthesis of phenylphosphinic acid derivatives, unwanted substitutions would not be possible. The results of the attempted syntheses of APA6 and APA7 are shown in **table 2.12**. In an attempt to silylate heaxadecylphosphinic acid, the DIPEA/TMSCl method was employed followed by the reaction with excess butyl iodide. Although not as effective as the initial result with the one-pot synthesis, this method did appear promising. In order to improve the amount of target compound, the iodide concentration was doubled to 3.06 molar equivalents. However, the result was opposite to that expected and, even when the reaction was refluxed with 2.04 equivalents, the outcome was not as favourable as the initial reaction. Similarly, the attempted synthesis of APA7 by this route was also only a limited success. Based on the large proportion of starting materials remaining, it was thought that the deprotonation of these compounds by DIPEA was not occurring effectively due to the electron donating power of the hexadecyl and octadecyl substituents. Unfortunately, due to time constraints, it was not possible to investigate the outcome of these reactions using stronger bases in the deprotonation step.
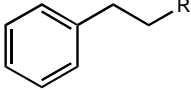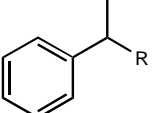
2.4 Summary

In summary, five aryl ethanolamide, six phenylphosphinic acid and two alkylphosphinic acid target compounds were successfully synthesized (see **table 2.13**). These target compounds were subsequently analysed for any cannabimimetic effects and the following chapters describe their evaluation at the CB1 and CB2 cannabinoid receptors, the anandamide transporter and fatty acid amide hydrolase.

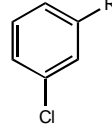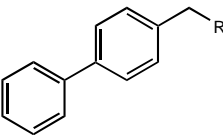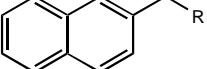| Compound	Silylating Method[1]	First Iodide (Equiv.)	Time (hrs)	Base Used[2] (Equiv.)	Time (hrs)	Second Iodide (Equiv.)	Time (hrs)	Outcome
APA6	a	Butyl, 1.05	93	a, 1.10	2½ hrs	1.10	70	No ammonium phosphinate remaining. Approximate 1:9 ratio of mono- to di-substituted product.
APA6	b	-	-	-	-	1.53	141	Approximate 1:2 ratio of mono- to di-substituted product.
APA6	b	-	-	-	-	3.06	143	Approximate 13:1 ratio of mono- to di-substituted product.
APA6	b	-	-	-	-	2.04	139[3]	Approximate 1:1 ratio of mono- to di-substituted product.
APA7	a	Butyl, 1.09	117	b, 1.05	3½ hrs	1.10	168	No phosphorus peak in ^{31}P NMR spectrum.
APA7	b	-	-	-	-	2.80	143	Approximate 6:1 ratio of mono- to di-substituted product.

1. a = 1.10 equivalents of HMDS at 110-120 °C for 3½ to 4 hours, b = DIPEA for 15 mins then TMSCl for 3 hrs using hexadecyl- or octadecylphosphinic acid as starting material. 2. a = HMDS, b = DIPEA. 3. Refluxed at 40 °C.

Table 2.12: Results of attempted syntheses of APA6 and APA7.

Compound	Structure	Yield (%)
AE5		45
AE6		62
AE9		71
AE13		49
AE14		53
PPA1	R^1 —— Butyl	74
PPA2	R^1 —— Decyl	66
PPA4	R^1 —— Isobutyl	21
PPA5	R^1 —— Octadecyl	63
PPA7	R^1 —— Hexadecyl	79
PPA8	R^1 —— Propyl	68
APA2	R^2 —— Hexadecyl	26
APA3	R^2 —— Octadecyl	26
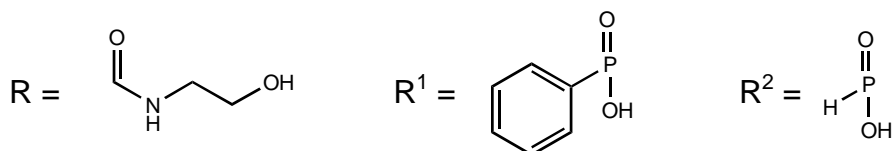
Table 2.13: Summary of the successfully synthesized target compounds.

Chapter 3:

CB1 Receptor Binding Studies

3.1 Introduction

Radioligand binding assays have proved invaluable in the study of receptors. Competition assays are the most widely used of the radioligand binding techniques and enable the affinity of a drug for a receptor to be determined as well as the elucidation of receptor number and the kinetics of ligand-receptor interactions. Radioligand binding also enables the measurement of receptor activation upon drug binding and the accurate determination of receptor distribution within different tissues. In order to investigate the ability of the novel aryl ethanolamide and phosphinic acid compounds to bind to and activate the CB1 receptor, two different radioligand binding assays were employed.

3.1.1 Competition Assays

Competition assays, sometimes referred to as displacement assays, are so called because they measure the ability of an unlabelled compound to compete for a binding site occupied by radiolabelled ligand. Radioligands bind specifically to receptors and non-specifically to other proteins and components of the assay system, so a means of determining the specific binding is required. This is achieved by incubating the radioligand and a cell or tissue preparation containing the receptor of interest with a high concentration of an unlabelled receptor ligand, thus displacing the specifically bound radioligand. The radioactivity of the remaining, non-specifically bound ligand can then be measured and specific binding calculated by subtracting this from the radioactivity in the absence of competing ligand. This type of assay was used to determine whether the aryl ethanolamide and phosphinic acid test compounds displayed affinity for the CB1 receptor by displacing radiolabelled cannabinoid receptor ligands.

3.1.2 GTP-γ-S Binding Assays

As shown in **figure 1.2**, when a G protein-coupled receptor is in its active state, GTP is bound to its G_α subunit and, subsequently, signalling is terminated by hydrolysis of GTP to GDP by an inherent GTPase activity. GTP-γ-S is a hydrolysis-resistant synthetic analogue of GTP. Therefore, when a GPCR is

activated by agonist binding in the presence of GTP-γ-S, it displaces GDP and the G protein is persistently activated. To measure the extent of GPCR activation by a compound, [^{35}S]-GTP-γ-S binding assays can be used. The extent of receptor activation is determined by the difference between basal [^{35}S]-GTP-γ-S binding and binding in the presence of the compound. Non-specific binding of [^{35}S]-GTP-γ-S is determined as described for competition assays, using a saturating concentration of unlabelled GTP-γ-S. It was decided to investigate the effects of the test compounds on [^{35}S]-GTP-γ-S binding to brain membranes for two reasons. First, if any of the compounds displayed affinity for the CB1 receptor, the [^{35}S]-GTP-γ-S assay would indicate whether they were receptor agonists or antagonists. Second, if the compounds did not display CB1 receptor affinity, the [^{35}S]-GTP-γ-S assay would indicate whether they activated any other GPCRs in the brain.

3.2 Experimental Methods

3.2.1 Competition Assays

Cultured cells transfected with CB1 are often used in cannabinoid research but, since the CB1 receptor is highly expressed in the CNS, membrane homogenates from rat cerebellum or whole brain were used in this work. This section describes the preparation of these tissues and their use in competition assays to investigate the affinity, if any, of the test compounds for the CB1 receptor.

Membrane Preparation:

Frozen cerebella or whole brains taken from male Wistar or hooded Lister rats were thawed, weighed and homogenized in 10 volumes of ice-cold buffer (50 mM Tris; pH 7.0) using a Polytron homogenizer. The homogenate was centrifuged at 30,000g at 4 °C for 10 minutes, the supernatant layer was discarded and the pellet manually re-homogenized in ice-cold buffer using a glass/teflon homogenizer. The centrifugation and re-homogenization procedure was repeated twice more and

the final membrane pellet resuspended in 10 volumes of ice-cold buffer. Aliquots of the membrane homogenate were frozen at -20°C until required.

Competition Assay Procedure:

The assay procedure described below, a slight adaptation of that described by Compton *et al.* (1993), was used routinely within the School of Biomedical Sciences. In this procedure, the use of bovine serum albumin (BSA) in the buffers was necessary to overcome a particular problem encountered with the use of cannabinoids. These compounds are notoriously lipophilic and tend to adhere to glass and plastics. BSA acts as a carrier for the cannabinoids, keeping them in solution and reducing unwanted interactions with the assay vessel and membrane lipids. The assay protocol was initially verified by producing a concentration-response curve for HU-210 displacement of [^{3}H]-CP-55,940 from rat cerebellum membranes as follows:

[^{3}H]-CP-55,940 (180.0 Ci/mmol) was dissolved in drug buffer (50 mM Tris; pH 7.0, 2 mM EDTA, 5 mM MgCl$_2$, 5.0 mg/ml BSA) and the radioactivity of a 50 μl sample measured using liquid scintillation spectroscopy. Dilutions were made to give 65,000 dpm per 50 μl aliquot, resulting in an assay concentration of approximately 0.16 nM [^{3}H]-CP-55,940. HU-210 was initially dissolved in ethanol to 200 times the desired assay concentration and then diluted 10 times in drug buffer. Aliquots (50 μl) of radioligand solution were added to polystyrene test tubes followed by 50 μl of blank buffer (drug buffer with 10 % v/v ethanol) or HU-210 solution and 850 μl of assay buffer (50 mM Tris; pH 7.0, 2 mM EDTA, 5 mM MgCl$_2$, 0.2 mg/ml BSA). To initiate the assay, 50 μl of membrane preparation were added to each tube, the tubes vortexed and incubated at 37 °C for 30 minutes. Membranes were harvested on to Whatman GF/B filter mats, pre-soaked in drug buffer for 30 minutes, using wash buffer (50 mM Tris; pH 7.0, 2 mM EDTA, 5 mM MgCl$_2$, 0.5 mg/ml BSA) at 4 °C on a Brandel cell harvester. Individual filter circles were transferred to insert vials and 4 ml of Packard Emulsifier-Scintillator Plus added to each. After standing overnight, the vials were vortexed and radioactivity measured on an LKB Rackbeta liquid scintillation counter. Each assay condition was assayed in triplicate and non-specific binding determined in the presence of 10 μM HU-210.

Receptor Solubilization:

As mentioned above, binding of radioligand to sites other than the receptor of interest is a problem encountered with this type of assay. In an attempt to increase the ratio of specific to non-specific radioligand binding, solubilization of the CB1 receptor was attempted. In theory, this crude purification procedure should reduce the contribution of non-specific binding from the membrane preparation.

Aliquots of rat cerebellum membrane homogenate were thawed, manually re-homogenized using a glass/teflon homogenizer and kept on ice when not used. Solubilization of receptors was attempted by mixing 700 µl of membrane preparation and 700 µl of solubilization buffer (10 mM Tris; pH 7.0, 20 % w/v glycerol, 1 % w/v 3-[(3-Cholamidopropyl)dimethylammonio]-1-propane sulphonate (CHAPS)), vortexing three times over a 15 minute period and centrifuging at 36,000*g* at 4 °C for 15 minutes. The supernatant layer was removed and saved as soluble fraction 1 and the pellet re-suspended in 700 µl of buffer (10 mM Tris; pH 7.0) by brief sonication using an MSE Soniprep 150 ultrasonic disintegrator. Solubilization and centrifugation were repeated as described above and the supernatant saved as soluble fraction 2.

To determine whether this solubilization procedure had been effective, the total and non-specific binding of 0.52 nM [³H]-SR 141716A, a selective CB1 receptor antagonist, (56.0 Ci/mmol) to untreated membranes and the two soluble fractions was compared. This was performed using the methodology described above with 10 µM CP-55,940 to determine the non-specific binding of the radioligand. In addition, the effect of pre-soaking filter mats in drug buffer or polyethylenimine (PEI) solution (0.3 % w/v; pH 10.0) were compared, as PEI treatment has been shown to be effective for retention of soluble receptors, possibly due to an ionic charge effect (Bruns *et al*., 1983). All conditions were measured in triplicate and assays were repeated on a further occasion.

Displacement of [³H]-CP-55,940 from CB1 by Test Compounds:

The ability of the test compounds to bind to the CB1 receptor was assayed using the simple particulate homogenate and the protocol described above. [³H]-CP-

55,940 was used as the radioligand, 10 μM HU-210 used to determine non-specific binding and the test compounds were assayed at 1, 10 or 100 μM, depending on solubility. The compounds were initially dissolved in ethanol and diluted in drug buffer as previously described for HU-210. For these assays, whole rat brain membrane homogenate was used and each concentration of compound tested in triplicate using a minimum of two different tissue sources.

Note: PPA1 became accidentally contaminated and was not used in the CB1 receptor competition assay or the assays described hereafter.

3.2.2 GTP-γ-S Binding Assays

As with the CB1 receptor displacement assay, the GTP-γ-S binding assay was routinely used within the School of Biomedical Sciences. In this protocol, a slight variation of the method described by Traynor & Nahorski (1995), brain membranes were pre-treated with theophylline to reduce the basal level of [^{35}S]-GTP-γ-S binding. The antagonist theophylline occupies the G protein-coupled adenosine A_1 receptor (Bruns, 1981), which is activated by endogenous adenosine in the membrane homogenate. Pre-treatment with theophylline therefore reduces unwanted [^{35}S]-GTP-γ-S binding. However, unlike the CB1 displacement assays, the GTP-γ-S binding assay protocol initially involved the use of BSA-free buffers.

The assay was verified by producing a concentration response curve for HU-210-stimulated [^{35}S]-GTP-γ-S binding to rat cerebella membranes. Assays with and without BSA in the buffers were performed in parallel to investigate whether including BSA would increase the signal to noise ratio. The tissue preparation and assay procedure are described below.

Membrane Preparation:
Frozen cerebella form male Wistar or hooded Lister rats were thawed, weighed and homogenized in 40 volumes of ice-cold buffer (50 mM Tris; pH 7.4, 100 mM NaCl, 10 mM $MgCl_2$) using a Polytron homogenizer. The homogenate was centrifuged at 33,000g for 15 minutes at 4 °C, the supernatant discarded and the

pellet manually re-homogenized in ice-cold buffer using a glass/teflon homogenizer. The centrifugation and re-homogenization procedure was repeated twice more with the final pellet resuspended in 10 volumes of ice-cold buffer. Aliquots were frozen at -20 °C until required.

General Assay Procedure:

[^{35}S]-GTP-γ-S (20 mM, 1000 Ci/mmol) was diluted in assay buffer (50 mM Tris; pH 7.4, 100 mM NaCl, 10 mM MgCl$_2$, ± 0.2 mg/ml BSA) to 893 nM. GTP-γ-S was dissolved to 5 mM in distilled water and 50 µl of this solution diluted to 500 µM with 50 µl of ethanol and 400 µl of drug buffer (50 mM Tris; pH 7.4, 100 mM NaCl, 10 mM MgCl$_2$, ± 5 mg/ml BSA). HU-210 was dissolved in ethanol to 500 times the desired assay concentration and then diluted 10-fold in drug buffer. Aliquots of membrane homogenate were thawed and a membrane mixture was prepared with 150 µl of theophylline solution (100 mM in distilled water), 150 µl GDP solution (10 mM in distilled water) and 375 µl membrane homogenate, made up to 15.6 ml with assay buffer. This mixture was vortexed and left to stand at room temperature for 20 minutes prior to its use in the binding assay.

Aliquots of [^{35}S]-GTP-γ-S solution (460 µl) were placed in polystyrene test tubes and 20 µl of blank buffer (drug buffer with 10 % v/v ethanol), GTP-γ-S solution or HU-210 solution were added in triplicate. The assay was initiated by adding 520 µl of membrane mixture and the tubes were vortexed and incubated at 25 °C for 45 minutes. Membranes were harvested on to Whatman GF/B filter mats and washed with distilled water at 4 °C on a Brandel cell harvester. Individual filter circles were then transferred to insert vials and 4 ml of Packard Emulsifier-Scintillator Plus added to each. After standing overnight, the vials were vortexed and radioactivity measured on an LKB Rackbeta liquid scintillation counter.

Comparison of GDP Concentrations:

The preliminary results from the [^{35}S]-GTP-γ-S binding assays indicated that buffers containing BSA were the most effective, so they were adopted for the remaining assays. However, it was also decided to investigate the effect of GDP concentration on CP-55,940-stimulated binding of [^{35}S]-GTP-γ-S as this has

previously been shown to affect this assay (Griffin *et al.*, 1998). Rat whole brain membranes were prepared in the same way as the cerebella membranes and the assay performed using GDP at 50 or 100 μM and CP-55,940 at concentrations between 5 nM and 1 μM. As the radioactivity present in the membranes in the initial assays was lower than expected, possibly due to radioactive decay, the assay concentration of [^{35}S]-GTP-γ-S was doubled to 0.82 μM and the amount of membrane homogenate used was also doubled. Otherwise, the procedure used was the same as described above.

*The Effect of Test Compounds on [^{35}S]-GTP-γ-S Binding to Brain Membranes:*
The comparison of GDP concentrations demonstrated that the use of 50 μM gave the higher binding above basal, so this concentration was used to assay the test compounds for their ability to stimulate [^{35}S]-GTP-γ-S binding to rat brain membranes. The assays were performed in the presence of 0.82 μM [^{35}S]-GTP-γ-S as described above, but with the following alterations. First, test compounds were initially diluted to 200 times the desired assay concentration in ethanol and then diluted 10-fold in drug buffer. Assay concentrations were 1, 10 or 100 μM with 50 μl of the solution added to the assay mixture. Second, CP-55,940 was used at 1 μM as a positive control. Finally, the membrane mixture was prepared as described above, except that 600 μl of brain membrane homogenate were used and 500 μl of the mixture was added to each assay tube. All assays were performed using triplicate concentrations in two different brain membrane homogenates.

3.3 Results and Discussion

3.3.1 Competition Assays

The initial competition assay of [^{3}H]-CP-55,940 from rat cerebella membranes by HU-210 is represented in **figure 3.1**. These data clearly demonstrate that the assay procedure used was valid, with a concentration-dependent displacement of the radioligand by HU-210. From this data it was also possible to make a rough of

estimate of the K_i value of HU-210. Using the Cheng-Prusoff equation (Cheng & Prusoff, 1973), $IC_{50} = K_i (1 + L/K_d)$ where L is the concentration of [³H]-CP-55,940 and K_d is the dissociation constant of CP-55,940 at the CB1 receptor. The concentration of [³H]-CP-55,940 in the assay was 0.16 nM and, using GraphPad Prism, the IC_{50} of HU-210 was determined as 2.69 nM. From the literature, the K_d of CP-55,940 in rat cerebellum membranes was reported as 0.52 nM (Kearn *et al.*, 1999) and, hence, the K_i of HU-210 was calculated to be approximately 2.06 nM. Obviously this value was obtained from very limited experimental data but, in comparison to the K_i values for HU-210 summarized in **table 1.2**, is of the same order of magnitude suggesting that this assay was an effective measure of [³H]-CP-55,940 displacement from the CB1 receptor.
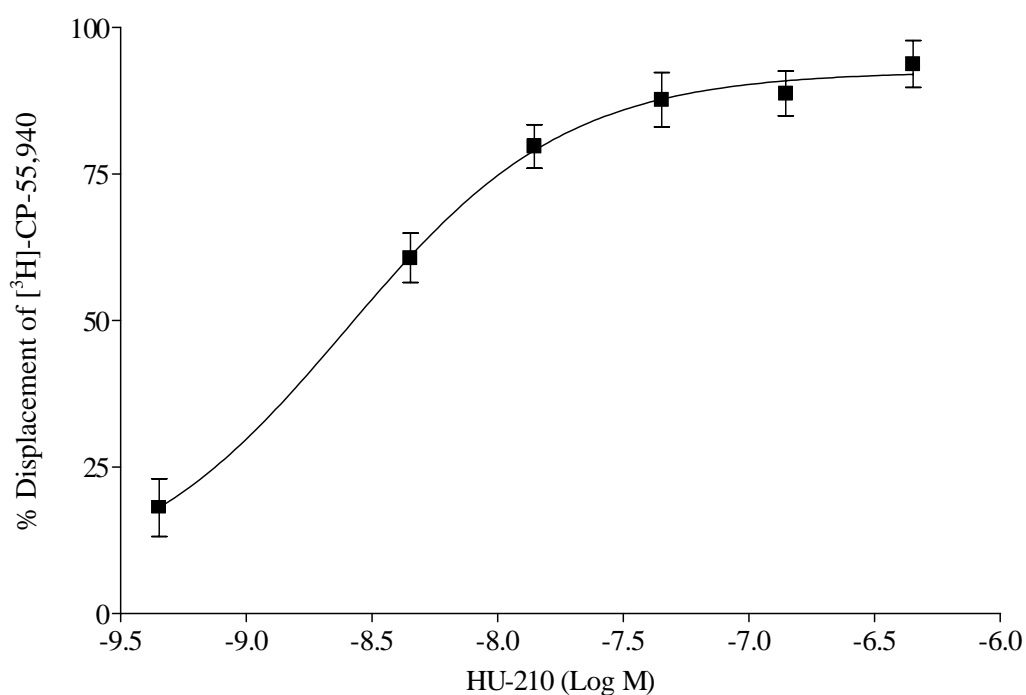
Figure 3.1: The displacement of specifically bound [³H]-CP-55,940 from rat cerebellum membranes by HU-210. Data are expressed as the mean ± SEM of three determinations of displacement and were fitted by non-linear regression using GraphPad Prism.

The results of the subsequent attempted solubilization of the CB1 receptor are shown in **figure 3.2**. As would be expected, there was very little difference between the specific and non-specific binding of [³H]-SR 141716A to the un-

treated membranes when comparing buffer- and PEI-soaked filter mats. The amount of specifically bound radioligand was slightly higher using buffer-soaked filters with 31.1 ± 0.4 % specific binding compared to only 21.9 ± 1.6 % using PEI-soaked filters. When comparing the effect of filter pre-treatments on the soluble fractions, it is clear that the PEI-soaked filters retained a greater amount of the soluble protein. However, it is also apparent that the solubilization procedure greatly reduced the amount of bound radioligand and all but eliminated specific binding. This suggests that a large proportion of the membrane homogenate, including the CB1 receptor, was insoluble under these conditions. Repeated assays produced very similar results and, therefore, this approach was abandoned.
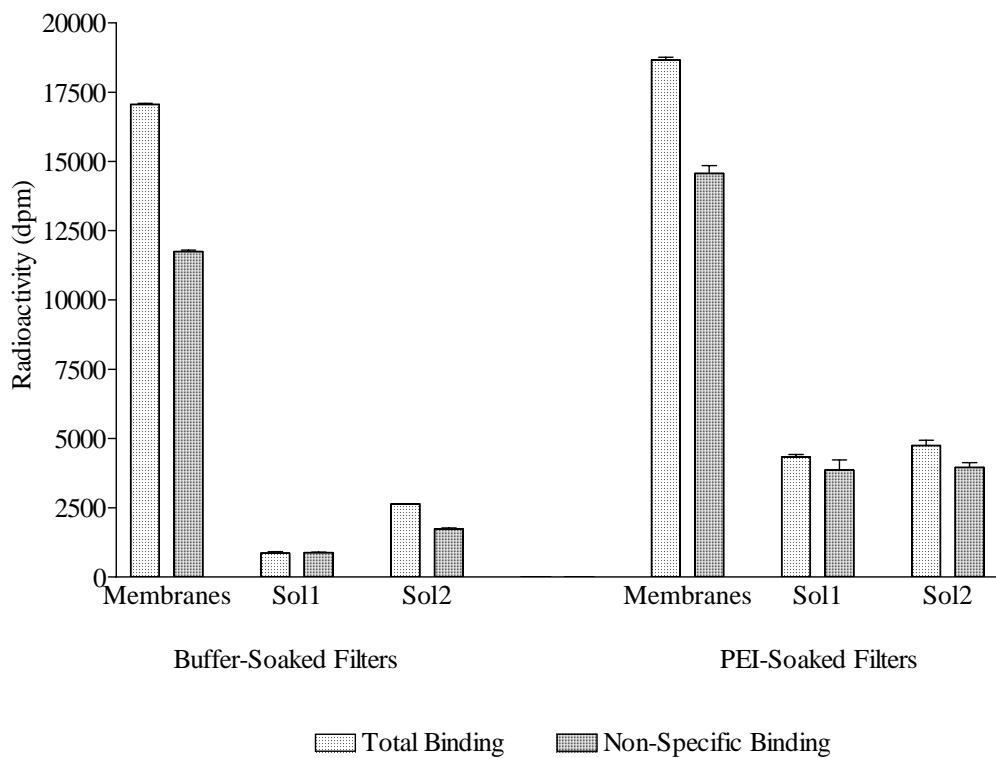
Figure 3.2: The effect of solubilization and filter pre-treatment on the total and non-specific binding of [^{3}H]-SR141716A to rat cerebellum membranes. Data are expressed as the mean $\pm$ SEM of three determinations of [^{3}H]-SR141716A binding at each assay condition.

Using the original assay protocol with washed membranes, the affinity of the test compounds for the CB1 receptor was measured by their ability to displace [³H]-CP-55,940. The results of these assays are shown in **figures 3.3** and **3.4** and it is clear from these data that none of the compounds had a strong affinity for the CB1 receptor, with high concentrations of compound being required to produce even a small percentage displacement.
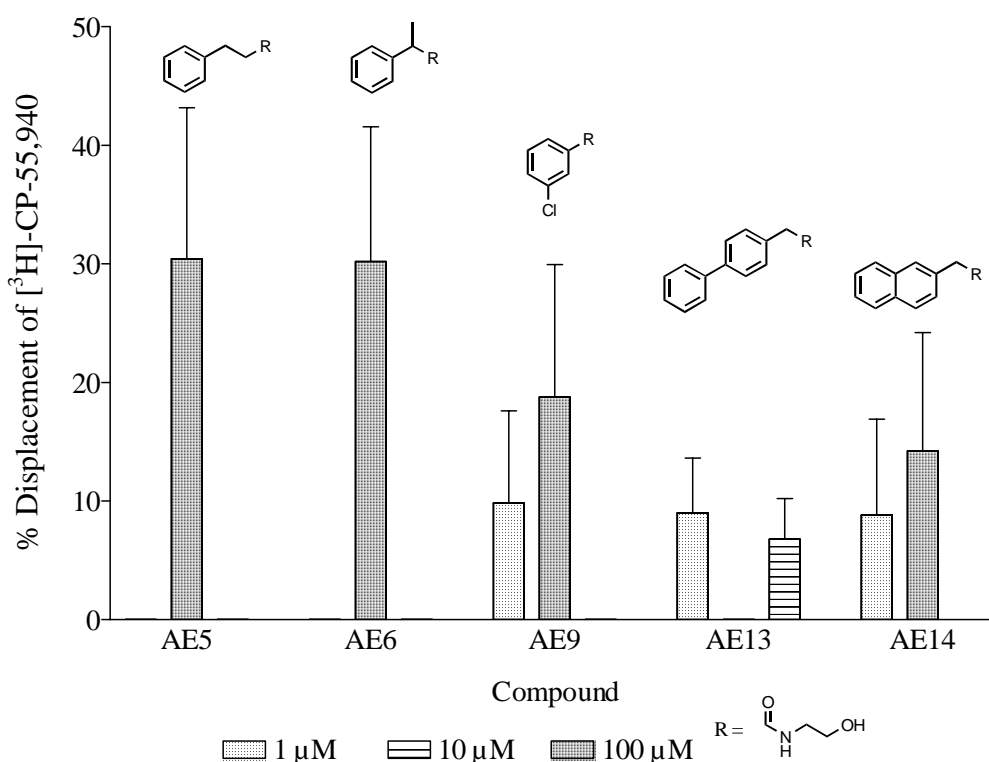
Figure 3.3: The displacement of [³H]-CP-55,940 from rat brain membranes by aryl ethanolamide test compounds. Data are expressed as the mean ± SEM of three (AE5 and AE6) or four (AE9 and AE14) independent experiments. Each concentration of AE13 was assayed in two different membrane homogenates and the data is expressed as mean ± SEM of the triplicate concentrations from these single experiments.

The aryl ethanolamides AE5 and AE6 proved to have the highest receptor affinity, displacing 30.4 and 30.2 % of the specifically bound radioligand, respectively, at 100 μM. With IC_{50} values of >100 μM, the K_i values of AE5 and AE6 at the CB1

receptor can be roughly estimated using the Cheng-Prusoff equation. Assuming a K_d of 0.52 nM for CP-55,940 as described above, these two aryl ethanolamides have K_i values of >76.5 μM, very high when compared with the cannabinoid receptor ligands described in **section 1.7.1**. From this limited data it appears that, for the aryl ethanolamides, a single benzene ring and a spacer between it and the ethanolamide group confers greatest affinity. However, the large standard errors for most data prevent any firm conclusions being drawn for these compounds.
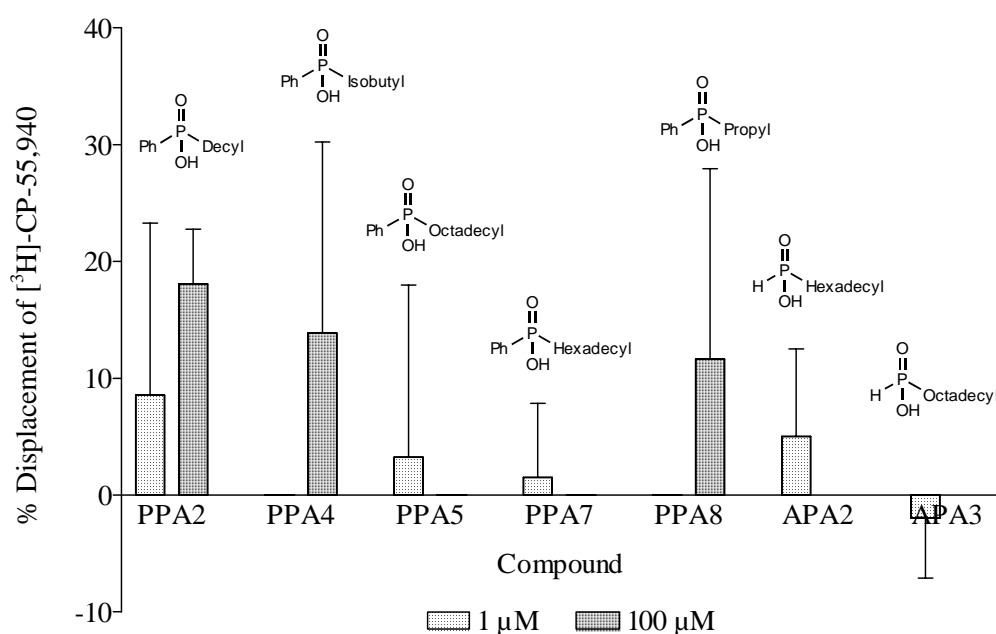
Figure 3.4: The displacement of [^{3}H]-CP-55,940 from rat brain membranes by phosphinic acid test compounds. Data are expressed as the mean ± range of two independent experiments (PPA2, PPA5, PPA7 and APA3) or the mean ± SEM of three independent experiments (PPA4, PPA8 and APA2).

The phosphinic acids demonstrated even lower affinity for CB1 receptors than the aryl ethanolamides, with a maximum displacement of 18.1 % using PPA2 at 100μM. The inactivity of the phosphinic acids is not entirely unexpected, however, as they were primarily designed as transition state enzyme inhibitors of FAAH rather than cannabinoid receptor ligands.

3.3.2 GTP-γ-S Binding Assays

The results of the initial assay to investigate the effect of including BSA in the buffers are shown in **figure 3.5**. It is apparent that with the use of BSA, the maximum percentage binding of [^{35}S]-GTP-γ-S above basal was greater than in the BSA-free assay. If BSA were acting as a carrier of HU-210 in the assay, the concentration-response curve should have been shifted to the left and the maximum [^{35}S]-GTP-γ-S binding should have been the same no matter which buffer was used. The fact that the curve was not shifted to the left, but that the maximum effect was increased is not easily explained. One possibility is that BSA is acting as an allosteric effector of the CB1 receptor G protein complex, increasing the overall signal compared to the BSA-free system. This would have important repercussions for cannabinoid research, as most *in vitro* work has been performed in the presence of BSA. The mechanism of this interaction requires further investigation. The increased [^{35}S]-GTP-γ-S binding afforded by BSA, however, led to the adoption of these assay conditions.
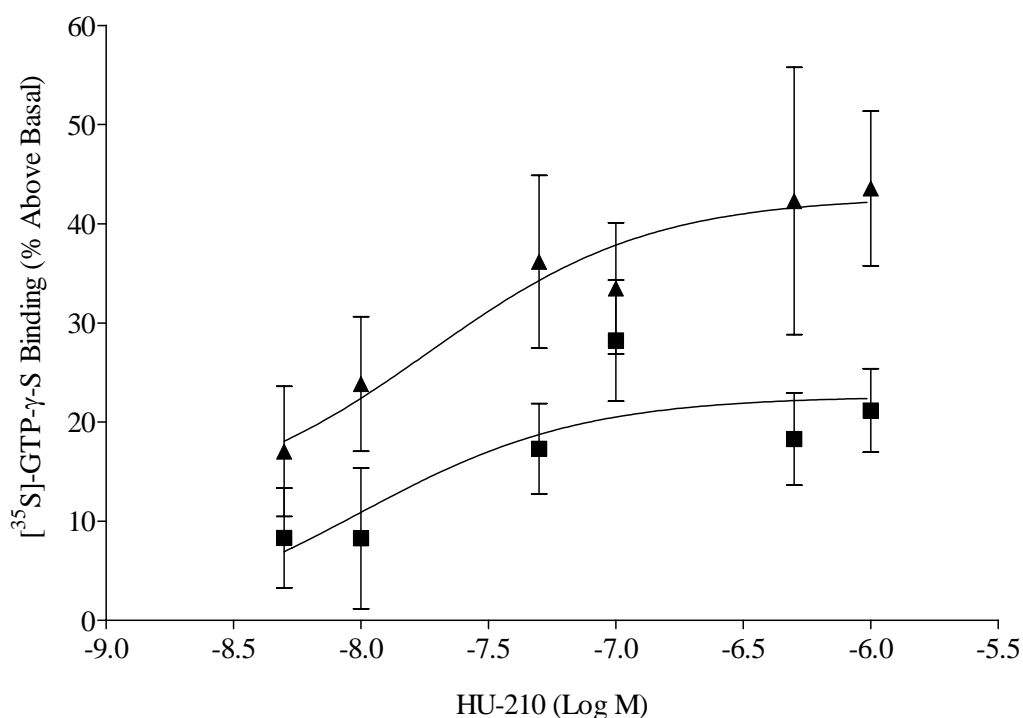
Figure 3.5: HU-210-stimulated [^{35}S]-GTP-γ-S binding to rat cerebellum membranes using normal (■) and BSA (▲) buffers. Data are expressed as the mean ± SEM of three determinations of [^{35}S]-GTP-γ-S binding and were fitted by non-linear regression using GraphPad Prism.

The next investigation of assay conditions was the comparison of CP-55,940-stimulated [^{35}S]-GTP-γ-S binding to rat whole brain membranes in the presence of 50 or 100 μM GDP. These results are shown in **figure 3.6**. Again, it is clear that the concentration-response curve with 50 μM GDP displayed a greater maximum effect than that performed in the presence of 100 μM GDP. The curves, generated by GraphPad Prism, have maxima of 47.8 and 36.0 % [^{35}S]-GTP-γ-S binding above basal for 50 and 100 μM GDP, respectively. As the binding of guanine nucleotides to G proteins is a dynamic process, this result suggests that increasing the GDP concentration shifts the equilibrium in favour of GDP binding and, therefore, [^{35}S]-GTP-γ-S binding is reduced. For this reason, the lower concentration of GDP was used in subsequent assays as it was in the original assay.
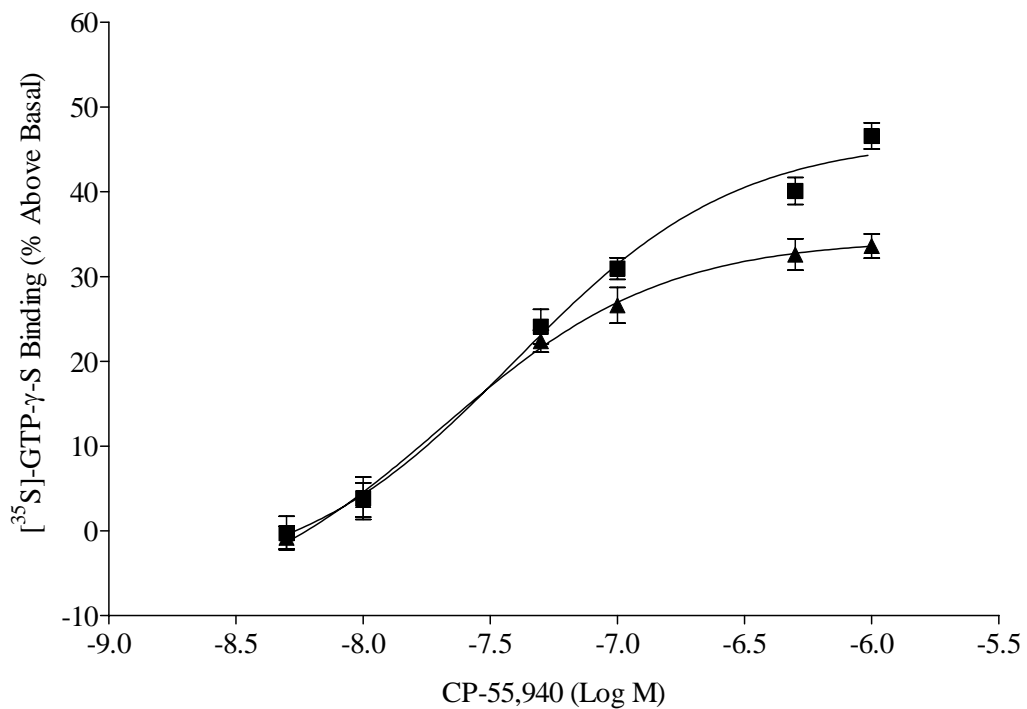
Figure 3.6: CP-55,940-stimulated [^{35}S]-GTP-γ-S binding to rat brain membranes using 50 μM (■) and 100 μM (▲) GDP. Data are expressed as the mean ± SEM of three determinations of [^{35}S]-GTP-γ-S binding and were fitted by non-linear regression using GraphPad Prism.

Since none of the test compounds showed any appreciable affinity for CB1 receptors in the [³H]-CP-55,940 displacement assays, little effect would be expected for [³⁵S]-GTP-γ-S binding unless the compounds activate other GPCRs in the brain. The results of [³⁵S]-GTP-γ-S binding assays with the test compounds are shown in **figure 3.7**.
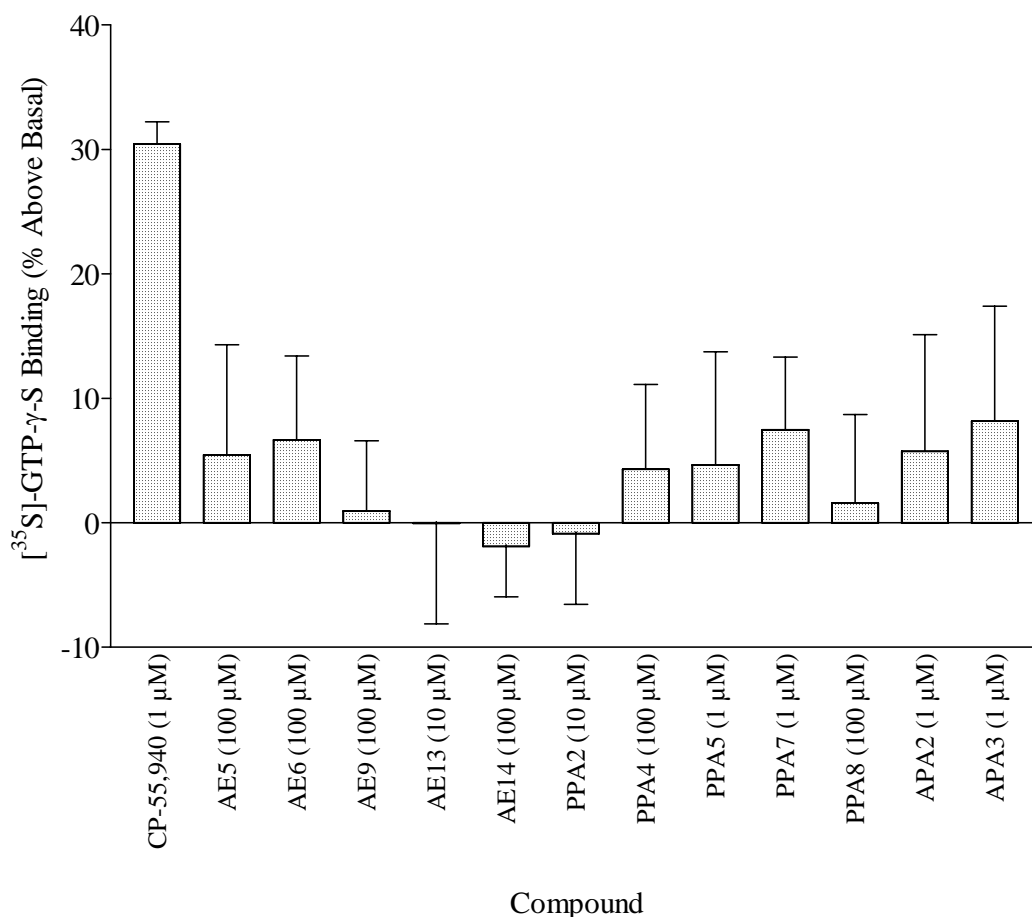
Figure 3.7: The effect of test compounds on [³⁵S]-GTP-γ-S binding to whole rat brain membranes. Data are expressed as the mean ± range of two independent experiments using different membrane homogenates, except the data for CP-55,940 which is the mean ± SEM of thirteen assays.

These results clearly show that, within error, none of the compounds activated GPCRs in rat brain or the CB1 receptor in particular. This latter point correlates with the result of the CB1 competition assays. Of course, the lack of increased [³⁵S]-GTP-γ-S binding compared to basal in the presence of these compounds does not rule out the possibility that they may be antagonists of other GPCRs. In

order to demonstrate this hypothetical effect, it would first be necessary to show that these compounds displace radioligands that are specific for other GPCRs from brain membranes. Due to the sheer number of such receptors, this would be a difficult and time-consuming task, well beyond the scope of this research.

In summary, none of the target compounds showed any significant affinity for the CB1 cannabinoid receptor and did not activate any other GPCRs in the rat brain. The next chapter describes the development of a cannabinoid receptor competition assay in porcine spleen and the subsequent evaluation of the test compounds for CB2 receptor affinity.

Chapter 4:

CB2 Receptor Binding Studies

4.1 Introduction

Most examples of CB2 binding assays in the literature have involved the use of transfected cells, while little work has been carried out on the native receptor. For this reason, porcine spleen membranes were used as a high density source of CB2 receptors in order to develop CB2 receptor competition and agonist-stimulated GTP-γ-S binding assays. After the initial characterization, these assays would then be used to examine the effects of the novel aryl ethanolamide and phosphinic acid test compounds. The spleen was chosen as it has been reported to have relatively high levels of CB2 expression (Galiègue *et al*., 1995), and pig spleen was chosen because of its size and, hence, the amount of tissue which could be readily prepared. The major problem in using spleen, or any other tissue preparation, instead of transfected cells is that the immune cells on which the CB2 receptor is expressed also express CB1 receptors (Schatz *et al*., 1997), albeit at much lower levels. Cannabinoid ligands will, therefore, bind to both receptors and the data produced will reflect overall cannabinoid binding, and not specifically CB2 binding. For the test compounds, however, the effect of CB1 receptors should not be greatly relevant as none of the compounds tested had CB1 affinity and, therefore, any effects in these assays should be solely from CB2 receptors. The following section describes the preparation of porcine spleen membranes and their use in the development of the competition and GTP-γ-S assays.

4.2 Assay Development

4.2.1 Competition Assays

Membrane Preparation:

Spleens from male or female Modern White hybrid pigs, less than 6 months old, were obtained from a local abattoir (G. Wood and Sons, Clipstone, Notts.). The tough, fibrous outer membrane was removed with forceps and the internal red pulp scraped out and placed in ice-cold buffer (50 mM Tris; pH 7.0, 2 mM EDTA, 5 mM $MgCl_2$). The tissue suspension was centrifuged at 2,000g at 4 °C for 10 minutes, the supernatant was removed and the wet weight of tissue measured. The

tissue was then homogenized in 10 volumes of ice-cold buffer containing 10 % (w/v) sucrose using a Polytron homogenizer and the homogenate centrifuged at 1,000g at 4 °C for 10 minutes. The supernatant was diluted with an equal volume of ice-cold, sucrose-free buffer and this mixture was then centrifuged at 33,000g at 4 °C for 15 minutes. The pellets were manually re-homogenized in ice-cold buffer using a glass/teflon homogenizer and the centrifugation and re-homogenisation process was repeated twice more with the final re-homogenisation in 40 volumes of buffer with respect to the original wet weight. Aliquots of the spleen membrane preparation were frozen at -20 °C until required.

Preliminary Binding Assays:

As the CB2 receptor density in the spleen membrane preparation was unknown, it was first necessary to determine the levels of total and non-specific binding using varying amounts of tissue in order to find the optimum conditions. The assay procedure was the same as that described for the CB1 competition assays, using 0.18 nM [^{3}H]-CP-55,940 as the radioligand and 10 μM HU-210 to determine non-specific binding. Each determination of total and non-specific binding was performed in triplicate using 100 μl of spleen membrane homogenate in a total assay volume of 1 ml. Where necessary, the tissue was diluted with buffer or concentrated by centrifugation at 9,000g at 4 °C for 5 minutes then re-suspension of the pellet in the appropriate volume of buffer. After incubation for 30 minutes at 37 °C, membranes were harvested as previously described using distilled water at 4 °C and the radioactivity then measured. As is evident from **figure 4.1**, increasing the tissue concentration resulted in an increase in the total binding of [^{3}H]-CP-55,940 to the membranes. Similarly, an increase in non-specific binding would be expected but this was not evident. This resulted in a steady increase of specific binding peaking with 41.9 % specific binding in the 400 % concentrated tissue preparation. A possible reason for this was thought to be filter binding of the [^{3}H]-CP-55,940. This potential problem is addressed below.

Since specific cannabinoid binding to spleen membranes had been successfully demonstrated, the next assays performed in the assay development were concentration-response curves for CP-55,940 displacement of [^{3}H]-CP-55,940. Duplicate assays were performed as above with triplicate concentrations of CP-

55,940 and 100 μl of 400 % spleen membrane homogenate. Non-specific binding was determined using 10 μM of the unlabelled ligand. The results of these experiments are shown in **figure 4.2**.
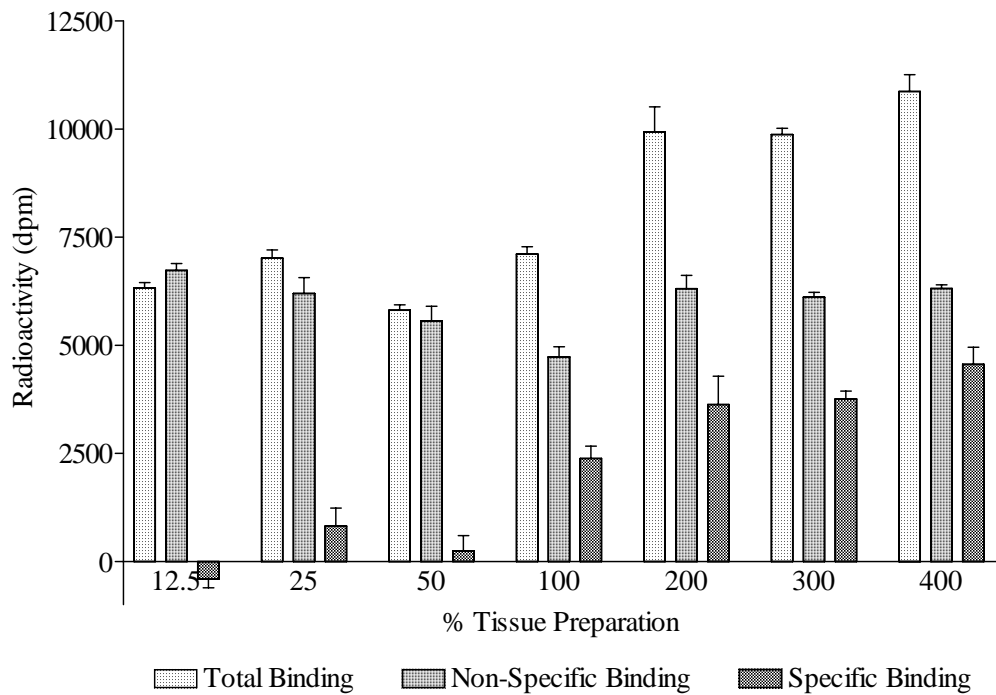
Figure 4.1: The effect of spleen membrane concentration on the binding of [³H]-CP-55,940. Data are expressed as the mean ± SEM of three determinations of binding in the presence or absence of 10 μM CP-55,940.
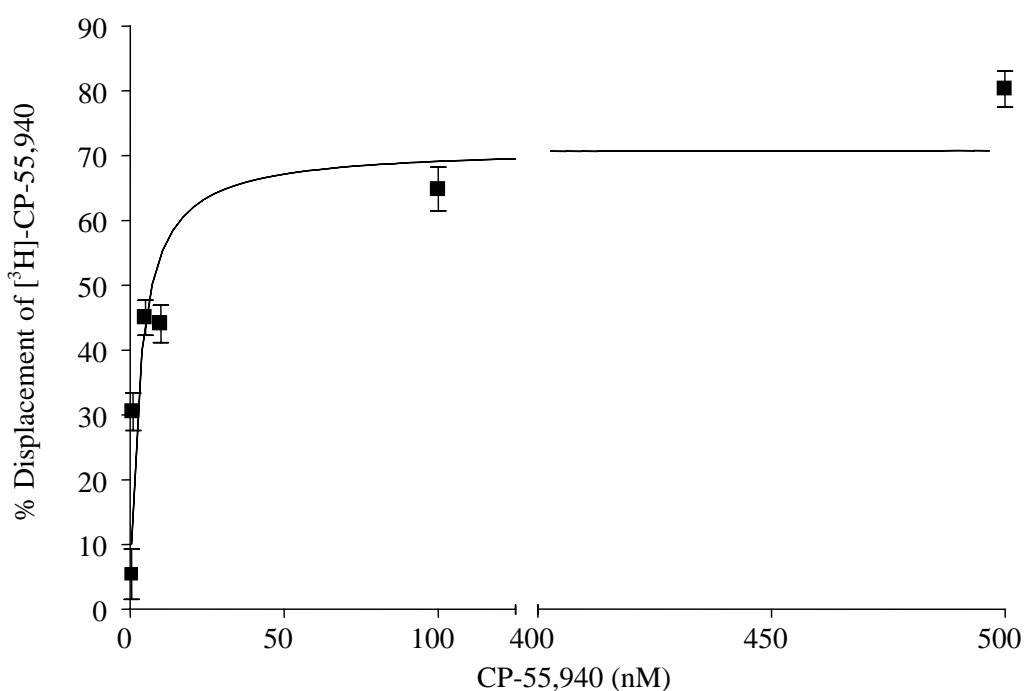
Figure 4.2: Displacement of [^{3}H]-CP-55,940 from spleen membranes by CP-55,940. Data are expressed as the mean ± SEM of three separate determinations of displacement for each concentration of CP-55,940.

Although the displacement of [^{3}H]-CP-55,940 did not reach 100 %, these assays clearly demonstrate a concentration-dependent displacement of the radioligand from porcine spleen membranes by CP-55,940. The possibility that the [^{3}H]-CP-55,940 was adhering to the filters was tested by examining the total and non-specific "binding" in the absence of spleen membranes. It is apparent from **figure 4.3** that there was significant, albeit non-displaceable, binding of the radioligand to the filter mats and, in an attempt to rectify this, a centrifugation-based competition assay was performed to harvest the membranes.
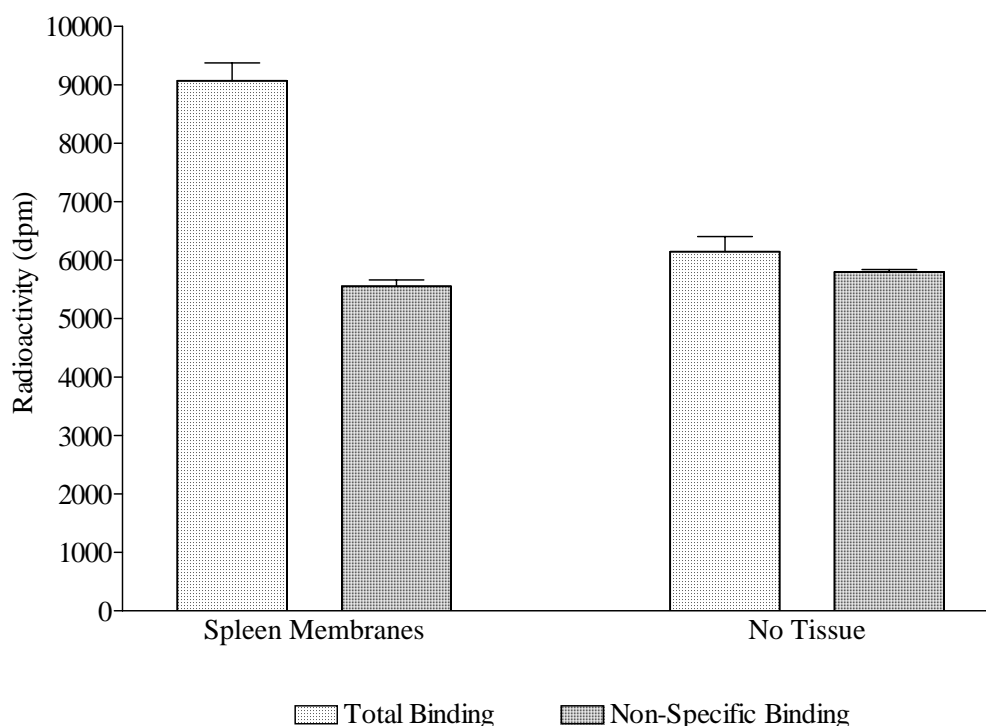
Figure 4.3: The total and non-specific binding of [^{3}H]-CP-55,940 in competition assays with and without spleen membranes. Data are expressed as the mean ± SEM of three determinations of specific and non-specific binding in the presence or absence of spleen membranes.

Centrifugation Assay:

Assays were performed to determine total and non-specific binding of [^{3}H]-CP-55,940 to 0, 100, 200 and 400 % concentrations of spleen membrane homogenate, with 10 μM HU-210 to determine the non-specific binding. The procedure was performed in microcentrifuge tubes with triplicate determinations at each spleen concentration as described above. After incubation, the membranes were pelleted by centrifugation at 36,000g for 2 minutes at 4 °C to eliminate the use of filters. To remove free radioligand from the assay solution, the supernatant was aspirated and the pellets then washed with 1 ml of buffer (50 mM Tris; pH 7.0, 2 mM EDTA, 5 mM MgCl$_2$). To digest the pellets, 50 μl of aqueous NaOH solution (1 M) was added to each before vortexing. The solutions were neutralized with 50 μl of aqueous HCl solution (1 M) and 1 ml of scintillation fluid added to each tube.

After standing overnight, the tubes were vortexed and radioactivity was measured. As is shown in **figure 4.4**, this assay did not prove to be more advantageous than the filtration procedure. Despite the evidence of specific binding to the spleen homogenates, there was significant adherence of [^{3}H]-CP-55,940 to the microcentrifuge tubes and this binding was displaceable by HU-210.

In a further attempt to reduce unwanted binding of [^{3}H]-CP-55,940, solubilization of the spleen membranes was performed. It was hoped that with CB2 being structurally dissimilar to CB1, the procedure would possibly be more successful than the previous attempts. This procedure was essentially the same as described for the CB1 receptor (**section 3.2.1**), except only one soluble fraction was obtained from the tissue.
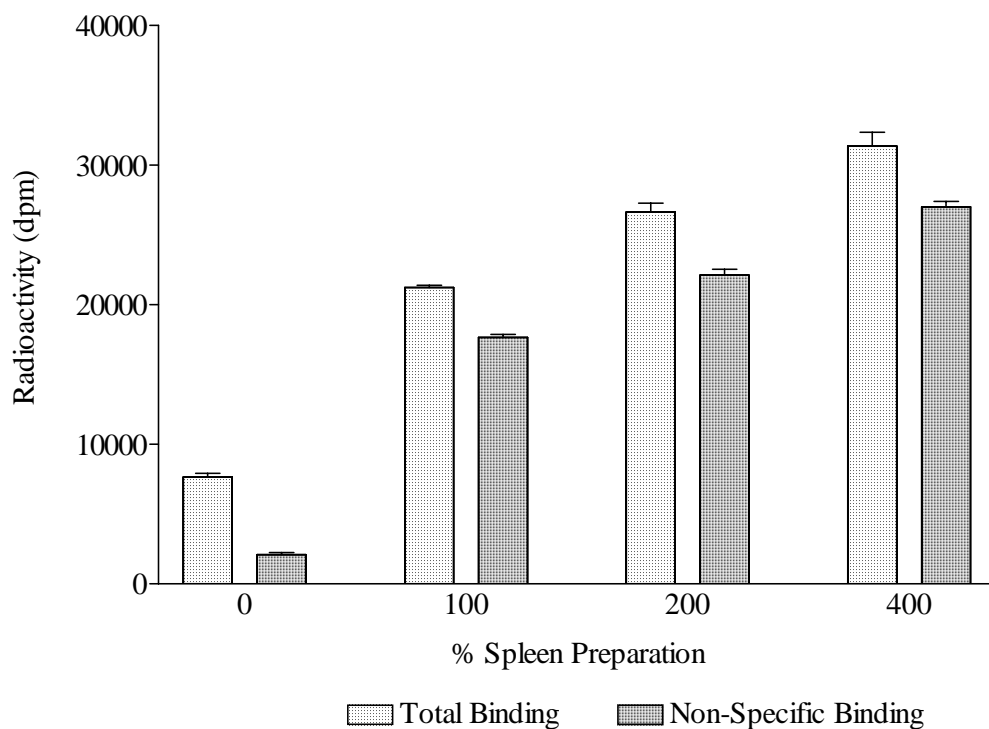
Figure 4.4: The effect of spleen membrane concentration on the binding of [^{3}H]-CP-55,940 in a centrifugation assay. Data are expressed as the mean ± SEM of three determinations of specific and non-specific binding at each concentration of spleen membrane preparation.

Assays were performed to compare the binding of [3H]-CP-55,940 to 100 μl of either untreated membrane homogenate, solubilized protein or a blank containing no tissue. The effect of pre-soaking filters in drug buffer and PEI solution was also examined and these results are shown in **figure 4.5**. It is clear that there was significant binding of [3H]-CP-55,940 to both sets of filters and this binding was more than doubled in PEI-soaked filters compared to BSA-soaked. The fact that the non-specific "binding" in both blanks was greater than the total binding may be due to the high concentration of HU-210 employed displacing radioligand from the assay tube walls, therefore making more available to adhere to the filters. The level of [3H]-CP-55,940 binding to the filters makes it difficult to comment on the results from the membrane and soluble fraction assays with any confidence.
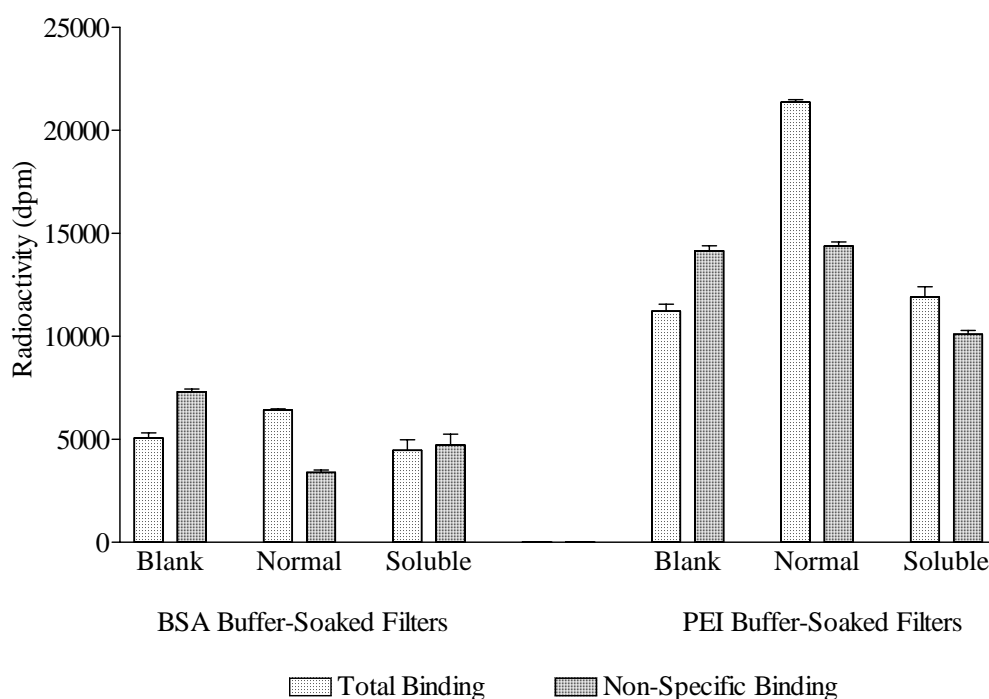
Figure 4.5: The effect of solubilization of spleen membranes and filter pre-treatment on the total and non-specific binding of [3H]-CP-55,940. Data are expressed as the mean ± SEM of three determinations of total and non-specific binding for each assay condition.

PEI-soaked filters appeared to retain more membrane homogenate than BSA-soaked filters. The soluble fractions, however, exhibited less specific binding of the radioligand than the un-treated membranes, suggesting that, as for CB1, CB2

was insoluble using these conditions. For this reason, attempts at solubilizing the CB2 receptor were abandoned at this point, as was the idea of pre-soaking filters in PEI as this seemed to promote non-specific [^{3}H]-CP-55,940 filter binding.

In this development procedure, membranes retained on filters had been rinsed with distilled water since this had been successful with the brain GTP-γ-S binding assays. For the final assays in the development of the CB2 displacement assay, the use of cold water and wash buffer containing 0.5 mg/ml BSA to wash the membranes was compared. Assays were performed to investigate [^{3}H]-CP-55,940 binding with and without 100 µl of un-diluted membrane homogenate as described above followed by harvesting on to Whatman GF/B filters, pre-soaked in drug buffer (containing 5 mg/ml BSA) for 30 minutes.
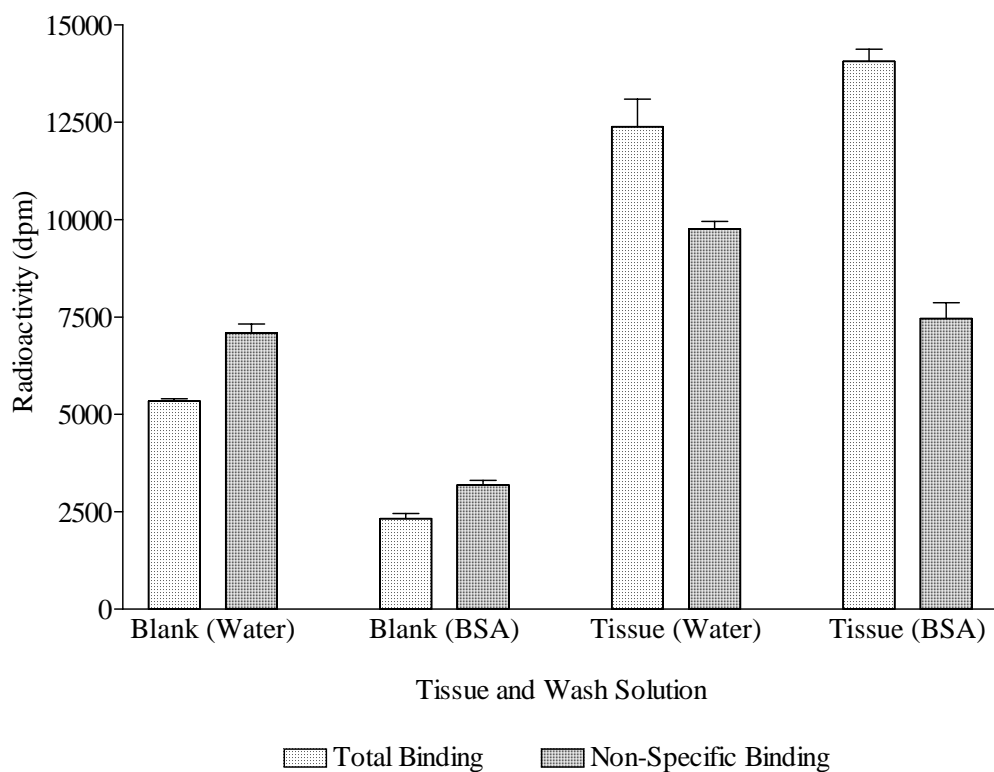

Figure 4.6: The effect of wash solution on the total and non-specific binding of [^{3}H]-CP-55,940 to spleen membranes. Data are expressed as the mean ± SEM of three determinations of total and non-specific binding for each assay condition.

It is evident from **figure 4.6** that the use of wash buffer containing BSA caused a significant reduction in [^{3}H]-CP-55,940 sticking to the filter mat and, in the presence of tissue, reduced non-specifically bound radioligand. Assuming that [^{3}H]-CP-55,940 binds to the filter homogeneously, this effect should not detrimentally affect the outcome of binding assays. As a result of these initial assays, it was decided that centrifugation assays or solubilization of the tissue would not provide any advantage over the standard competition assay using a particulate membrane preparation. Investigation of cannabinoid and test compound binding to spleen membranes was, therefore, performed using 100 µl of un-diluted membrane homogenate and the membranes then washed with BSA wash buffer at 4 °C as described for CB1 competition assays.

4.2.2 GTP-γ-S Binding Assay

The GTP-γ-S binding assay routinely used in the School of Biomedical Sciences had not been performed in spleen tissue, so some initial experiments were required to determine the optimum conditions. Total, non-specific and HU-210-stimulated [^{35}S]-GTP-γ-S binding to spleen membranes was measured in triplicate using GDP concentrations of 12.5, 25, 50 and 100 µM. The procedure used was the same as that described for brain (**section 3.2.2**), with [^{35}S]-GTP-γ-S at an assay concentration of 0.45 µM and 250 µl of spleen membrane homogenate used in the membrane mixture. HU-210 was used at 1 µM. The assay volume of 1 ml consisted of 480 µl of [^{35}S]-GTP-γ-S solution, 20 µl of either blank assay buffer, GTP-γ-S solution or HU-210 solution and 500 µl of membrane mixture.

Figure 4.7 shows representative data from these experiments in comparison to a positive control of rat brain membranes using the same conditions. It is evident that, in the brain membranes, HU-210 caused an increase in [^{35}S]-GTP-γ-S binding. However, this was not observed in the porcine spleen membrane preparation, suggesting that the receptor density was simply too low for an effective GTP-γ-S binding assay using this tissue. Previously published data investigating [^{3}H]-CP-55,940 binding in peripheral tissues showed that, in the red pulp of the spleen, the specific binding of [^{3}H]-CP-55,940 was 44 fmol/mg wet weight tissue compared to 143 fmol/mg in the brain (Lynn & Herkenham, 1994).
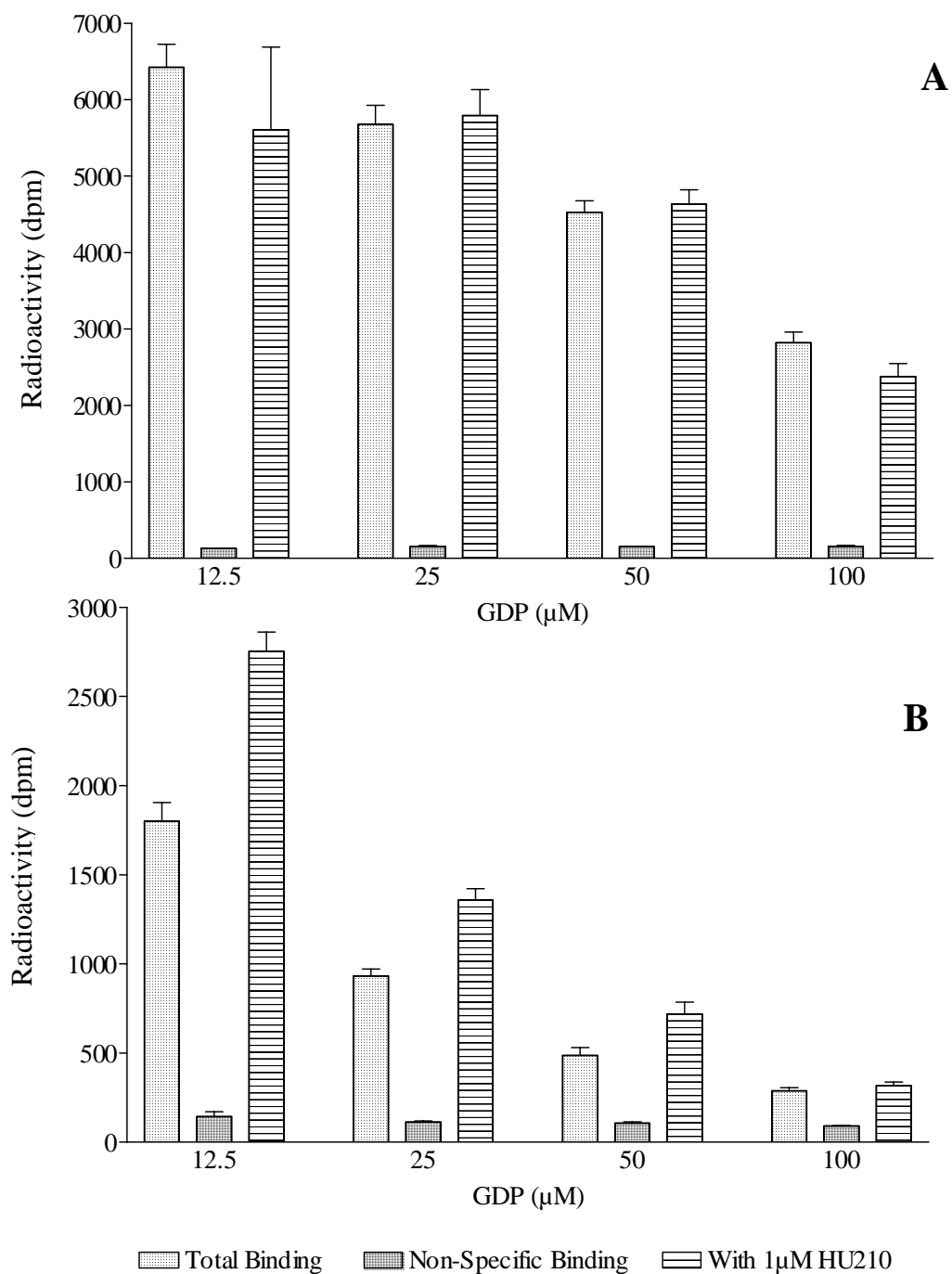
Figure 4.7: The effect of GDP concentration on HU-210-stimulated [^{35}S]-GTP-γ-S binding to porcine spleen (**A**) and rat brain membranes (**B**). Data are expressed as the mean ± SEM of three determinations of total, non-specific and HU-210-stimulated binding at each concentration of GDP.

Another study, using RT-PCR to analyse the expression of cannabinoid receptors in different tissues showed that the brain contains 72 times more cannabinoid receptor mRNA compared to spleen (Schatz *et al.*, 1997). With this in mind, the results of the spleen GTP-γ-S binding assays are not unexpected, considering the fact that CP-55,940-stimulated binding of [^{35}S]-GTP-γ-S to brain membranes was only 30.4 % above basal (**figure 3.7**). This assay was not pursued further due to this lack of cannabinoid-stimulated GTP-γ-S binding in porcine spleen membranes.

4.3 Experimental Methods

With the development of an effective cannabinoid competition assay using porcine spleen membrane homogenate, it was then possible to determine the receptor number in this tissue preparation, the binding affinity of a number of cannabinoid receptor ligands and the affinity, if any, of the test compounds for the CB2 receptor. The following sections describe how this was achieved.

4.3.1 Determination of Receptor Number and Affinity for CP-55,940

Competition assays where the competing compound employed is the same as the radioligand can be used to determine the receptor number (B_{max}) and the affinity of the receptor for the radioligand (K_d) (DeBlasi, *et al.* 1989). According to the Cheng-Prusoff equation:

$$IC_{50} = K_c \ (1 + L/K_h)$$

where IC_{50} is the concentration of unlabelled compound required to displace 50 % of specifically bound radioligand, K_c and K_h are the dissociation constants of the unlabelled and radiolabelled ligands, respectively, and L is the concentration of radioligand (Cheng & Prusoff, 1973). Assuming that the radioligand and unlabelled ligand have equal receptor affinity (i.e. K_d), then $K_c = K_h = K_d$. Therefore, using the Cheng-Prusoff equation:

$$IC_{50} = K_d \ (1 + L/K_d)$$

$$= K_d + L \qquad \textbf{(a)}$$

$$\text{so} \quad K_d = IC_{50} - L \qquad \textbf{(b)}$$

Also, according to the law of mass action:

$$B_{max} = B_0 (K_d + L)/L$$

where B_0 is the specific binding of the radioligand. Substituting (**a**):

$$B_{max} = B_0\, IC_{50}/L \qquad \textbf{(c)}$$

Since B_0 and IC_{50} can be determined experimentally, equations (**b**) and (**c**) can be used to define B_{max} and K_d.

It would have been desirable to perform these assays with a CB2-specific radioligand and corresponding unlabelled ligand, but these were not available when this work was performed. Instead, it was decided to define binding to both cannabinoid receptors using [^{3}H]-CP-55,940 which possesses almost equal affinity for CB1 and CB2 (Showalter *et al.*, 1996). Assays were performed to measure the displacement of a single concentration of [^{3}H]-CP-55,940 from spleen membranes by increasing concentrations CP-55,940 (0.03 to 300 nM) using the protocol described below. Each drug concentration was assayed in triplicate and each assay was performed in spleen membrane homogenates from three different animals. The adaptation of the assay was carried out to allow for the use of repeat dispensing pipettes, but drug solutions and buffers (containing BSA) were made up as described previously.

General Assay Procedure:

[^{3}H]-CP-55,940 (180.0 Ci/mmol) was dissolved in drug buffer (50 mM Tris; pH 7.0, 2 mM EDTA, 5 mM MgCl$_2$, 5.0 mg/ml BSA) to a concentration of 3.25 nM and then diluted to 0.65 nM in assay buffer (50 mM Tris; pH 7.0, 2 mM EDTA, 5 mM MgCl$_2$, 0.2 mg/ml BSA). Aliquots (250 μl) were placed in polystyrene test tubes with 500 μl of assay buffer and 50 μl of blank buffer or unlabelled drug solution then added. Assays were initiated by addition of 200 μl of spleen membrane homogenate (diluted 1:1 with assay buffer), the tubes vortexed and then incubated at 37 °C for 30 minutes. Non-specific binding of the radioligand was determined using HU-210 at a concentration of 10 μM. Membranes were harvested on to Whatman GF/B filter mats, pre-soaked in drug buffer for 30

minutes, using wash buffer (50 mM Tris; pH 7.0, 2 mM EDTA, 5 mM $MgCl_2$, 0.5 mg/ml BSA) at 4 °C on a Brandel cell harvester. Individual filter circles were placed in insert vials, 4 ml of Packard Emulsifier-Scintillator Plus added to each and left overnight. The vials were then vortexed and radioactivity measured on an LKB Rackbeta liquid scintillation counter. For accurate determination of the [³H]-CP-55,940 assay concentration, the mean value of radioactivity from three 250 µl aliquots of radioligand solution was determined and the assay concentration calculated.

Protein Concentration Assay:

In order to determine B_{max}, it was necessary to determine the protein concentration in the spleen membrane homogenates used in the assays. This was achieved using a variation of the method described by Bradford (1976):

Aliquots of each spleen membrane homogenate were diluted to 4, 2, 1 and 0.5 % of the original with buffer (50 mM Tris; pH 7.0, 2 mM EDTA, 5 mM $MgCl_2$) containing NaOH at a final concentration of 0.5 M in each solution. These solutions were assayed against BSA standards from 1.95 µg/ml to 4 mg/ml, each containing the same concentrations of buffer and NaOH as the spleen samples. Triplicate aliquots of the standards and quadruplicate aliquots of the spleen membrane samples (10 µl) were placed on a 96 well plate with 12 blanks of buffer containing 0.5 M NaOH. Coomassie blue dye (200 µl) was added to each well and, after allowing a minimum of 2 minutes for the colour to develop, optical densities were measured at a wavelength of 595 nm using a Dynation MRX microplate reader. The protein concentrations of the samples were calculated by fitting the sample optical densities to the BSA standard curve generated by non-linear regression (one site binding) using GraphPad Prism.

Coomassie Blue Dye:

Coomassie Brilliant Blue G (100 mg) was dissolved in 50 ml of 95 % ethanol and 100 ml of 85 % orthophosphoric acid added. The solution was made up to 1 litre with distilled water, filtered and stored in a well stoppered bottle at room temperature.

Data Analysis:

The amount of radioligand bound to the membranes was calculated and expressed as fmol/mg protein. This was plotted against the concentration of unlabelled CP-55,940 (log M) and a sigmoidal dose-response curve for each homogenate was generated by non-linear regression using GraphPad Prism. B_0 values were determined by subtracting the minimum from the maximum of each curve and these, along with the IC_{50} values generated by the program, were used to calculate B_{max} and K_d values for each tissue homogenate. The final values were expressed as the means ± SEMs of the three assays. As the spleen membranes contained both CB1 and CB2, the B_{max} and K_d represent the total number of cannabinoid binding sites and the affinity of combined spleen cannabinoid receptors for CP-55,940.

4.3.2 Determination of K_i Values for Other Cannabinoid Ligands

When the K_d had been determined for [^{3}H]-CP-55,940 binding to porcine spleen cannabinoid receptors, it was possible to determine the equilibrium binding constants (K_i) for other cannabinoid ligands in this tissue preparation. In the Cheng-Prusoff equation, the K_d of CP-55,940 is equivalent to K_h, and K_i is equivalent to K_c, so:

$$IC_{50} = K_i (1 + L/K_d)$$

Rearranging gives:

$$K_i = IC_{50}/(1 + L/K_d)$$

Assays were performed to generate concentration-response curves of [^{3}H]-CP-55,940 displacement from spleen membranes by HU-210, SR141716A, SR144528 and anandamide. The assays were performed in triplicate as described above but, since anandamide is hydrolysed by FAAH, assays were performed to compare its ability to displace [^{3}H]-CP-55,940 from normal and PMSF-treated membranes. This PMSF pre-treatment was performed as described below.

Treatment of Spleen Membranes with PMSF:

PMSF was dissolved in ethanol to a concentration of 6 mM and then diluted 10 times in assay buffer. Equal volumes (3.5 ml) of spleen membrane homogenate and either PMSF solution or assay buffer containing 10 % ethanol were vortexed together, incubated at room temperature for 30 minutes and then centrifuged at 19,000g for 2 minutes. The supernatant was aspirated, the pellet washed with 5 ml of assay buffer and then re-suspended in the original volume of buffer.

Data Analysis:

The percentage displacement of specifically bound [^{3}H]-CP-55,940 from the membranes was plotted against the concentration of unlabelled cannabinoid (log M) and a sigmoidal concentration-response curve generated by non-linear regression using GraphPad Prism. The IC$_{50}$ value generated by the program was used to calculate the K$_i$ value for that compound and the final K$_i$ value was determined by calculating the mean ± SEM for the three individual assays. The K$_i$ for CP-55,940 was also determined in this way using the data generated in the CP-55,940 versus [^{3}H]-CP-55,940 assays.

4.3.3 Determination of the Affinity of Test Compounds for the CB2 Receptor

The affinity of the test compounds for the CB2 receptor was determined by their ability to displace [^{3}H]-CP-55,940 from porcine spleen membranes. Each compound was assayed as described above (**section 4.3.1**) using triplicate concentrations of either 10 or 100 μM in three different spleen membrane homogenates.

4.4 Results and Discussion

4.4.1 Determination of Receptor Number and Affinity for CP-55,940

The results of [^{3}H]-CP-55,940 displacement from spleen membranes by CP-55,940 are shown in **figure 4.8**. The combined data from the three assays produced a K$_d$ for [^{3}H]-CP-55,940 of 1.55 ± 0.34 nM, and a B$_{max}$ of 678.5 ± 129.5

fmol/mg protein and these values compare well with data in the literature (**table 4.1**), especially the results of Hillard *et al.* (1999) which were also obtained using native spleen cannabinoid receptors, albeit from the rat. The small differences between the values described here and the other cited literature values are readily explained. The fact that the B_{max} in the spleen membranes is lower than that reported by other groups, excluding Hillard *et al.*, is likely to be due to this work being done using the endogenous receptor as opposed to transfected receptors where the receptor number is artificially high. Therefore, no direct comparisons can be made between this work and the B_{max} values described in the literature. As K_d is a property of the receptor, the B_{max} has no bearing on it. One possible reason for the difference in K_d values is the presence of CB1 in the spleen membranes used in this work. However, in species other than the pig, it is known that the CB1 receptor is expressed at much lower levels than the CB2 receptor.
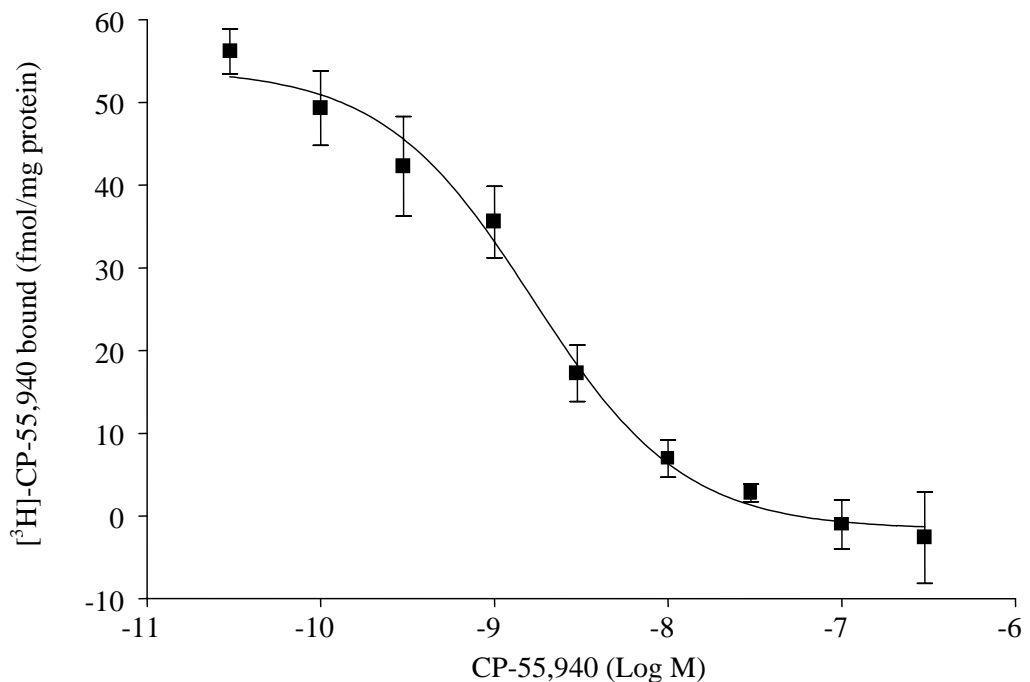
Figure 4.8: Displacement of specifically bound [^{3}H]-CP-55,940 from spleen membranes by CP-55,940. Data are expressed as the mean ± SEM of three independent experiments.

The lower affinity of the receptor population for CP-55,940 described here is likely to be caused by species variation. The only CB2 receptors that have been

cloned at this time are the human, rat and murine receptors. The murine receptor (mCB2) is 13 amino acids shorter than the human equivalent (hCB2) with the two sharing 82 % overall identity. In binding studies with the hCB2 and mCB2 receptors expressed in COS-3 cells, [^{3}H]-CP-55,940 was displaced by CP-55,940 with IC_{50} values of 3.2 ± 0.8 nM and 5.6 ± 0.5 nM for the two receptors, respectively. This indicates that mCB2 has a slightly lower affinity for CP-55,940 than hCB2 (Shire *et al*., 1996). It has also recently been shown that the cloned rat CB2 receptor exhibits a different binding profile for a number of cannabinoid receptor ligands in comparison to the hCB2 and mCB2 receptors (Griffin *et al*., 2000). It is likely that the porcine CB2 receptor also exhibits a slightly different binding profile compared to the human, rat and mouse CB2 receptors, explaining the slight variation between the K_d in porcine spleen membranes and the data summarized in **table 4.1**, using cells transfected with hCB2.

K_d (nM)	B_{max} (pmol/mg protein)	Receptor Source
0.49 ± 0.11	4.69 ± 0.58	hCB2 in CHO cells (Rinaldi-Carmona *et al*., 1998)
0.88 ± 0.09	1.55 ± 0.39	hCB2 in HEK-293 cells (Tao *et al*., 1999)
0.96 ± 0.24	2.42 ± 0.38	hCB2 in CKL cells (CHO with krox24 reporter) (Portier *et al*., 1999)
0.46 ± 0.06	2.88 ± 0.19	hCB2 in CCL cells (CHO with cAMP reporter) (Portier *et al*., 1999)
0.64 ± 0.05	27.4 ± 6.15	rCB2 in HEK-293 cells (Griffin *et al*., 2000)
0.73 ± 0.20	9.9 ± 1.60	mCB2 in HEK-293 cells (Griffin *et al*., 2000)
0.87 ± 0.08	5.8 ± 0.67	hCB2 in HEK-293 cells (Griffin *et al*., 2000)
2.8 ± 0.4	0.57 ± 0.02	Rat spleen membranes (Hillard *et al*., 1999)

Table 4.1: Previously reported K_d and B_{max} values determined by CP-55,940 displacement of [^{3}H]-CP-55,940 from the CB2 receptor.

4.4.2 Determination of K_i Values for Other Cannabinoid Ligands

The results of cannabinoid displacement of [3H]-CP-55,940 from spleen membranes are shown in **figure 4.9**. These data show that, in this system, the affinities of the compounds is in the order HU-210 > CP-55,940 > SR144528 > SR141716A > anandamide. It is also clear that pre-treatment of the spleen membranes with PMSF had no effect on the ability of anandamide to displace [3H]-CP-55,940. This suggests that FAAH is not present in the spleen or that the levels are too low to significantly hydrolyse anandamide in the time available during the assay. Data from Katayama *et al.* (1997) indicates that FAAH activity with respect to anandamide hydrolysis is 0.13 ± 0.06 nmol/min/mg protein in rat spleen compared to 4.36 ± 0.28 nmol/min/mg in the liver. Despite the inevitable species variation, this difference in distribution is likely to be similar in the pig.

In **table 4.2**, the K_i values obtained in these experiments are compared with those published in the literature. It is evident that the values obtained using porcine spleen membranes are consistent with the literature values, although most of these were determined using cells transfected with hCB2. The only two compounds that appear significantly different, however, are the two antagonists, SR141716A and SR144528. The reasons for these differences are likely to be due to the fact that these were the only receptor-selective compounds tested. The presence of CB1 in the spleen membranes is likely to have caused the lower than expected K_i value for SR141716A while, at the same time, causing a higher than expected K_i value for SR144528. However, Rinaldi-Carmona *et al.* (1998) determined that SR144528 had a K_i value of 0.30 ± 0.38 nM in rat spleen microsome membranes compared to 4.55 ± 1.1 nM in this work. Since both preparations contained CB1 and CB2, it is most likely that the differences in the values are due to inter-species differences in receptor structure and binding.
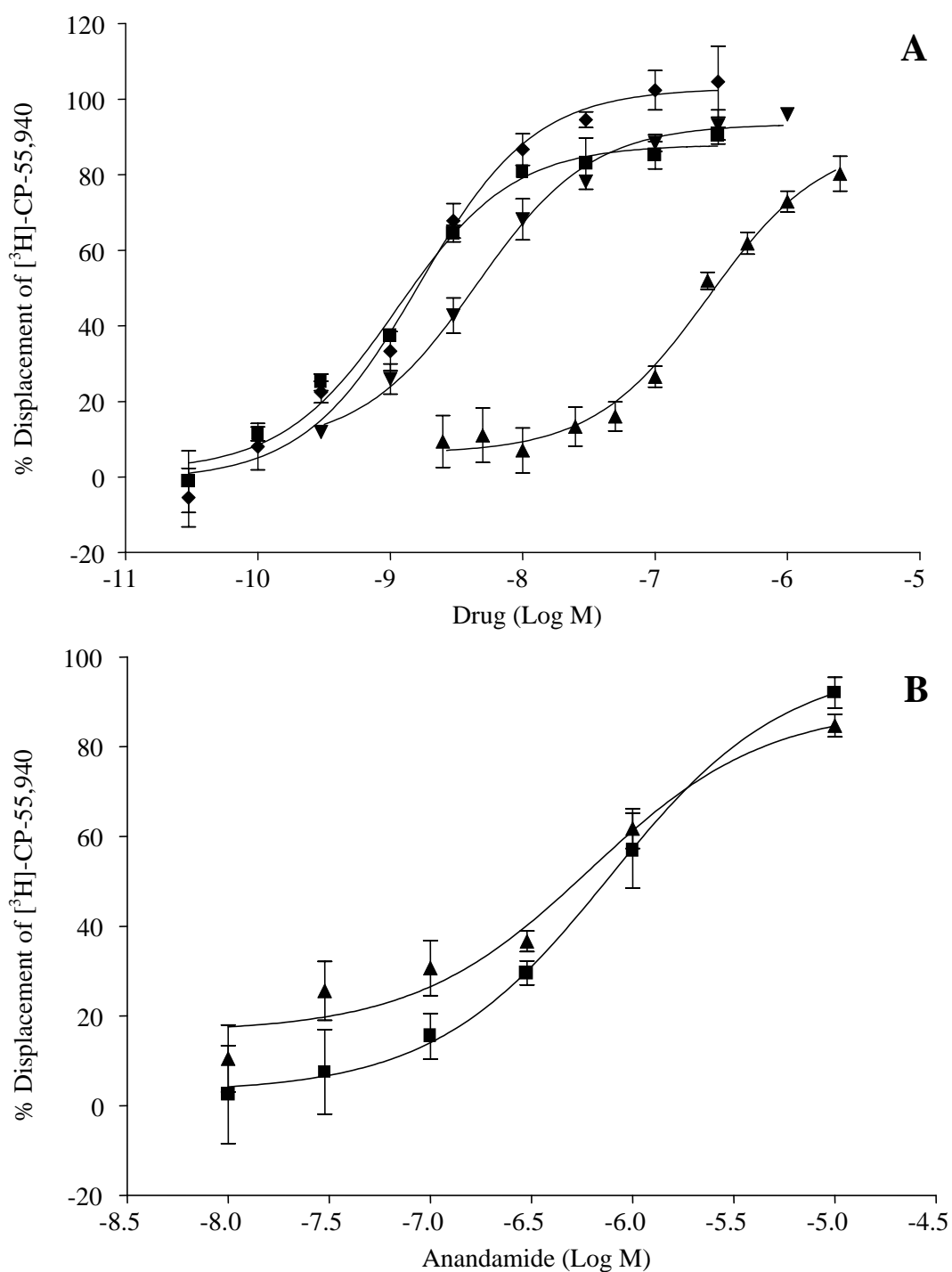
Figure 4.9: The displacement of [³H]-CP-55,940 from porcine spleen membranes by various cannabinoid ligands. **A**. HU-210 (■), CP-55,940 (◆), SR144528 (▼) and SR141716A (▲). **B**. The effect of membrane pre-treatment with PMSF (▲) compared to un-treated membranes (■). Data are expressed as the mean ± SEM of three independent experiments.

| Compound	K_i (nM)	Literature K_i (nM)	Receptor Source
CP-55,940	1.55 ± 0.31	0.69 ± 0.02	hCB2 in CHO cells (Showalter *et al.*, 1996)
		2.55 ± 0.19	hCB2 in mouse AtT-20 cells (Felder *et al.*, 1995)
		7.2 ± 2.4	Rat spleen sections (Lynn & Herkenham, 1994)
		0.75 ± 0.08	hCB2 in HEK-293 cells (Tao *et al.*, 1999)
		0.64 ± 0.06	rCB2 in HEK-293 cells (Griffin *et al.*, 2000)
		0.73 ± 0.20	mCB2 in HEK-293 cells (Griffin *et al.*, 2000)
HU-210	1.02 ± 0.24	0.22 ± 0.18	hCB2 in CHO cells (Showalter *et al.*, 1996)
		0.60 ± 0.13	hCB2 in mouse AtT-20 cells (Felder *et al.*, 1995)
SR141716A	236.7 ± 25.1	702 ± 62	hCB2 in CHO cells (Showalter *et al.*, 1996)
		973 ± 280	hCB2 in mouse AtT-20 cells (Felder *et al.*, 1995)
SR144528	4.55 ± 1.1	0.30 ± 0.38	Rat spleen microsome membranes (Rinaldi-Carmona *et al.*, 1998)
		0.60 ± 0.13	
		0.30 ± 0.14	hCB2 in CHO cells (Rinaldi-Carmona *et al.*, 1998)
		0.08 ± 0.02	rCB2 in HEK-293 cells (Griffin *et al.*, 2000)
			mCB2 in HEK-293 cells (Griffin *et al.*, 2000)
Anandamide	693 ± 26 641 ± 178 (PMSF)	371 ± 102	hCB2 in CHO cells (Showalter *et al.*, 1996)
		1940 ± 240	hCB2 in mouse AtT-20 cells (Felder *et al.*, 1995)
		306 ± 48	hCB2 in HEK-293 cells (Tao *et al.*, 1999)
		1930	Mouse spleen membranes (Lin *et al.*, 1998)
		$> 10\ \mu M$	rCB2 in HEK-293 cells (Griffin *et al.*, 2000)

Table 4.2: The K_i values of cannabinoid receptor ligands at porcine spleen cannabinoid receptors in comparison to K_i values from the literature.

The values for porcine spleen are represented as the mean $\pm$ SEM of three independent experiments.

4.4.3 The Affinity of Test Compounds for Porcine Spleen Cannabinoid Receptors

The results of [^{3}H]-CP-55,940 displacement from porcine spleen membranes by the novel test compounds are shown in **figure 4.10**.
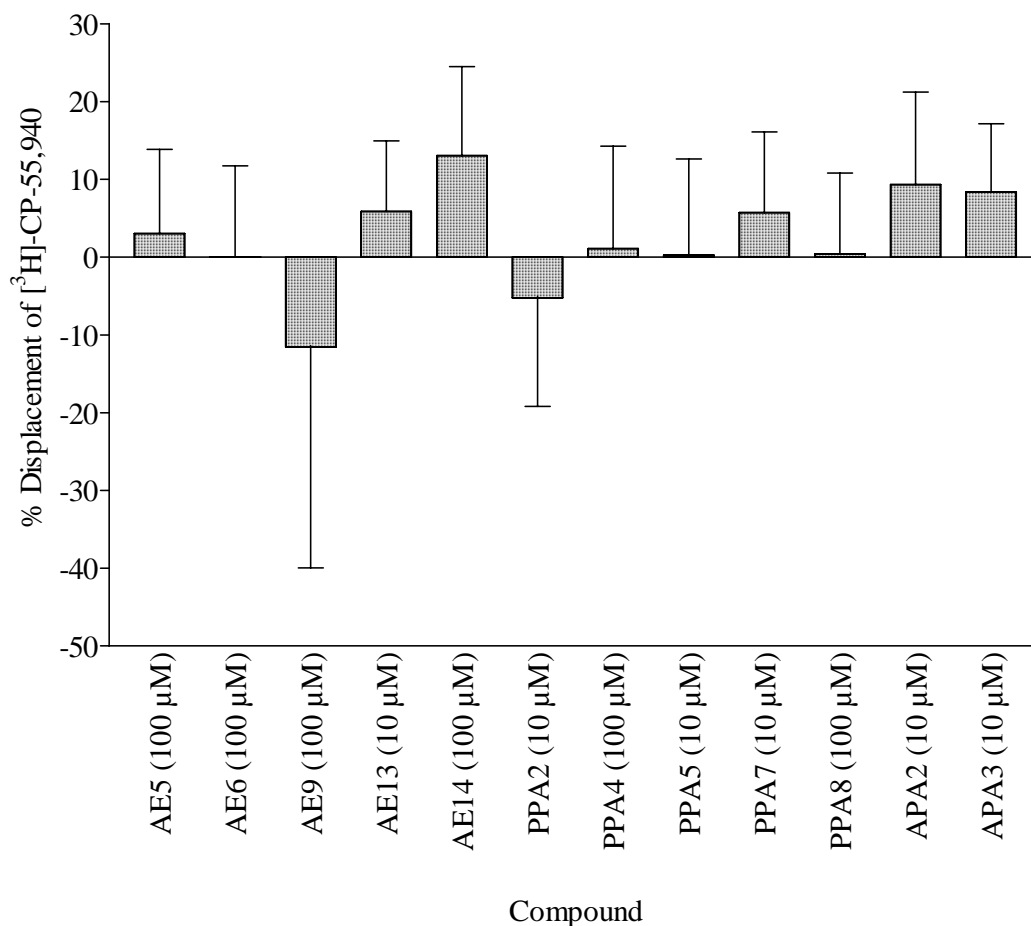
Figure 4.10: The displacement of [^{3}H]-CP-55,940 from porcine spleen membranes by aryl ethanolamide and phosphinic acid test compounds. Data are expressed as the mean ± SEM of three independent experiments.

It is apparent from these results that none of the test compounds had any affinity for the CB2 receptor and, unlike the results at the CB1 receptor, no speculation can be made about any structure-activity relationships. However, despite these disappointing results, the cannabinoid binding profile of porcine spleen

cannabinoid receptors has been characterized and shown to be similar to the binding profiles of the cloned human, rat and murine CB2 receptors. The next chapter describes the investigation of the effect of these compounds on the anandamide transport mechanism. It was hoped that the lack of affinity of the test compounds for the receptors would not preclude activity at this target. Indeed, the anandamide transport inhibitor AM404 possesses only low affinity for the CB1 cannabinoid receptors with a K_i value of 1.76 ± 0.14 µM (Beltramo *et al*., 1997).

Chapter 5:

Anandamide Uptake Studies

5.1 Introduction

In order to explore the effects of the aryl ethanolamides and phosphinic acids on anandamide uptake, a cell line possessing the endocannabinoid transporter was required. The mouse neuroblastoma cell line N18TG2 was available in the School of Biomedical Sciences and, although previously shown to accumulate [³H]-anandamide (Deutsch & Chin, 1993), the anandamide transport system has not been fully characterized in this cell type. The following section describes the culture of these cells, the uptake experiments used to determine the presence of the anandamide transport system and subsequent studies to investigate the effect of the novel test compounds

5.2 Experimental Methods

5.2.1 Cell Culture

The cell culture work was performed in a laminar flow cabinet using sterile techniques throughout. All solutions were sterile unless otherwise stated and were pre-warmed to 37 °C in order to prevent the cells being exposed to temperature shock.

Initial Cell Culture:

N18TG2 cells were thawed from storage at -80 °C, suspended in culture medium (90 % DMEM, 9 % FBS and 1 % 200 mM L-glutamine) and, to remove the freezing solution, were centrifuged at 400g for 15 minutes. The supernatant was aspirated, the pellet re-suspended in 10 ml of culture medium and the suspension transferred to a 25 cm^2 culture flask. The cells were then incubated at 37 °C in an atmosphere of 95 % O_2 and 5 % CO_2. When the cells had reached confluence, they were dislodged from the flask with 5 ml of trypsin solution (0.25 % w/v). This solution was not sterile, so it was added to the flask through a 0.2 μm filter in order to remove any microbial contaminants. The cell suspension was transferred to a universal tube and the flask washed with 5 ml culture medium which was combined with the cell suspension and centrifuged at 400g for 5 minutes. The supernatant was aspirated and the tube "flicked" to break up the cell pellet which

was then re-suspended in 5 ml of culture medium and transferred to a 75 cm^2 culture flask. A further 5 ml of medium was added to the flask to give an overall split of 1:3 and the cells were incubated as described above.

Cell Viability Test:

In order to test the viability of the cells, trypan blue dye was used. This is an exclusion dye which is only taken up by dead or dying cells, turning them blue. Equal volumes of cell suspension and dye were mixed together and 10 µl of the mixture placed on a counting chamber and examined using phase contrast microscopy. The number of colourless, viable cells and dead or dying cells were counted in a 25 by 25 grid and percentage viability calculated.

Cell Maintenance:

It was observed that EDTA was at least as effective as trypsin at dislodging the cells so, when the cells had reached confluence, the culture medium was aspirated and the cells dislodged from the flask with 10 ml of EDTA solution (0.5 mM in Dulbecco's PBS). As with the trypsin solution, this solution was not sterile, so it too was added to the flask through a 0.2 µm filter. The cell suspension was then transferred to a universal tube, and the flask washed with 5 ml of culture medium which was combined with the cell suspension. The tube was then centrifuged at 400*g* for 5 minutes, the supernatant aspirated and the cell pellet re-suspended in 6 ml of medium. A 1:3 split was performed by transferring 2 ml of the suspension back to the original culture flask and making the volume up to 10 ml with culture medium. The remaining 4 ml of cell suspension was split in to two new flasks in a total volume of 10 ml per flask and all three flasks incubated as described above. Cells were passaged every 2 to 3 days, or when confluent, and new culture flasks were used after every third or fourth passage to prevent the selection of cells that were resistant to EDTA treatment.

Cell Plating:

When cells were required for anandamide uptake assays, a 1:3 split was performed and the remaining 4 ml of cell suspension was made up to 25 ml with culture medium. The cell suspension was then plated at 1 ml per well on a 24 well

culture plate and incubated as described above.

Cell Storage:

In case the cells became infected, it was necessary to have a supply of frozen, healthy cells that could be thawed and cultured. To achieve this, at passage 2, the cells were dislodged, transferred to a universal tube and the flask washed as described above. 5 ml of the suspension were transferred to a second universal tube with 5 ml of medium, resulting in this tube containing one third of the cells. The cells were then pelleted and the second tube used for a 1:3 split. The pellet from the first tube was re-suspended in 4 ml of freezing solution (10 % DMSO, 90 % FBS) and 1 ml aliquots were gradually lowered in to liquid nitrogen for storage.

5.2.2 Anandamide Uptake Assays

The high-affinity anandamide transporter described in rat neurones and astrocytes by Beltramo *et al.* (1997) is temperature-dependent, saturable and inhibited by AM404 and the prostaglandin E_2 transport inhibitor bromocresol green. In order to establish the presence of the uptake mechanism in N18TG2 cells, it was necessary to perform assays to demonstrate these characteristics. The effect of temperature and inhibitors on anandamide accumulation in to the cells was examined by performing anandamide concentration-response assays to measure its accumulation at 0 °C and at 37 °C in the absence or presence of AM404 and bromocresol green. An anandamide concentration-response assay was also performed at 37 °C in a cell-free system to determine whether experiments would be affected by adherence of the anandamide to the culture plate. This assay was performed in the absence or presence of AM404 to ascertain whether any adherence was displaceable by this inhibitor. Finally, the effect of time on anandamide uptake by N18TG2 cells was examined by performing time course assays using a single concentration of anandamide in the absence or presence of AM404.

For these assays, cells were incubated with unlabelled anandamide containing 0.5 % (v/v) of [^{3}H]-anandamide (223 Ci/mmol) as a tracer. The amount of anandamide accumulated could then be calculated by lysing the cells and

measuring the radioactivity present in the lysate. The aqueous solutions of anandamide used in the assays contained 2-hydroxy-β-cyclodextrin (β-CD) as this has previously been shown to improve anandamide's solubility (Jarho *et al*., 1996). Also, since these cells express the CB1 receptor, it was necessary to displace any membrane-bound anandamide by washing the cells with BSA-containing buffer before lysis to prevent it affecting the results.

General Assay Procedure:

N18TG2 cells were grown to confluence on 24 well culture plates as described above and placed on a plate warmer at 37 °C. The culture medium was aspirated and replaced with 500 μl of Tris-Krebs' buffer (20 mM Tris; pH 7.4, 130 mM NaCl, 5 mM KCl, 1.2 mM $MgCl_2$, 2.5 mM $CaCl_2$, 10 mM glucose) pre-warmed to 37 °C and the cells allowed to equilibrate for at least 10 minutes. The buffer was then aspirated and replaced with 500 μl of pre-warmed assay buffer (Tris-Krebs' with 1 % (w/v) β-CD) containing the appropriate concentrations of anandamide and [^{3}H]-anandamide. The cells were incubated for 10 minutes and the incubations terminated by aspiration of the buffer. The cells were then washed carefully with 2 x 500 μl of Tris-Krebs' buffer containing 0.1 % (w/v) BSA at room temperature and lysed with 500 μl of aqueous HCl solution (1 M). The lysates were transferred to scintillation vials and each well washed with 500 μl of distilled water which was combined with the corresponding lysate. 8 ml of scintillation fluid was added to each tube, the tubes vortexed and radioactivity measured on an LKB Rackbeta liquid scintillation counter.

Comparison of Anandamide Uptake at 0 and 37 °C:

Assays were performed as described above with triplicate anandamide concentrations of 6.25 to 100 nM containing 0.03 to 0.5 nM [^{3}H]-anandamide. For the assay at 0 °C, the culture plate, Tris-Krebs' buffer and assay buffers were cooled on ice. The 37 °C assay was performed in the presence or absence of AM404 and bromocresol green at 10 μM and 20 μM, respectively.

Cell-Free Assay:

The assay was performed as above with duplicate anandamide concentrations in

the presence or absence of 10 μM AM404.

Time Point Assay:

This assay was performed essentially as above using 50 nM anandamide containing 0.25 nM [^{3}H]-anandamide with or without 10 μM AM404. Assay durations of 5, 10, 20 and 40 minutes were employed.

When the transport mechanism had been studied, the aryl ethanolamides and phosphinic acids were included in the general assay to investigate whether they affected anandamide accumulation. The compounds were dissolved in ethanol and assay solutions made up with 50 nM anandamide containing 0.25 nM [^{3}H]-anandamide and 10 μM of the test compound with a final ethanol concentration of 0.5 %. Duplicate assays were performed as described above, except that the incubations continued for 20 minutes, with triplicate concentrations each of a blank containing anandamide only, a positive control of anandamide containing 10 μM AM404 and the test compounds.

Data Analysis:

The mean ± SEM anandamide accumulation was plotted against anandamide concentration or time and curves were generated by non-linear regression (one site binding) using GraphPad Prism. To determine the significance of inhibition by AM404 and bromocresol green, the data from assays using these compounds was compared to the control conditions using un-paired t tests. For the test compound assays, the accumulation in the presence of test compound was compared to that of the control containing anandamide only and the percentage inhibition calculated.

5.2.3 Protein Concentration Assay

In order to calculate the rate of anandamide accumulation by the cells (pmol/min/mg protein), it was necessary to determine the amount of protein in the wells of the culture plates. N18TG2 cells were grown to confluence on a 24 well plate as described above and the plate placed on a plate warmer at 37 °C. Since the culture medium was protein-rich, it was necessary to remove as much as

possible to prevent it affecting the assay for cellular protein. To achieve this, the medium was aspirated and the wells then washed with 1 ml of pre-warmed Tris-Krebs' buffer which was replaced with a further 1 ml of buffer. 1 ml of aqueous NaOH solution (1 M) was then added to each well and left for 10 minutes to allow the cellular protein to be digested. BSA standards from 1.95 µg/ml to 4 mg/ml were assayed in triplicate, each containing the same concentrations of NaOH and Tris-Krebs' buffer as the samples. The assay procedure and calculation of protein concentration was the same as described in **section 4.3.1**.

5.3 Results and Discussion

5.3.1 Cell Viability

Cell viability was tested after the initial culture from frozen and after passage number 7. The initial viability was approximately 75 %, increasing to a mean of 92 ± 1.5 % in the three flasks tested after passage 7.

5.3.2 Characterization of Anandamide Uptake

The data from the preliminary anandamide uptake assays were expressed as pmol/min/well due to an unforeseen problem with the protein concentration assay. The comparison of anandamide uptake at 0 and 37 °C, shown in **figure 5.1**, demonstrated that there was a temperature- and concentration-dependent accumulation of anandamide in the N18TG2 cells, indicating the presence of the anandamide transporter. In addition, this accumulation was significantly inhibited by the anandamide transport inhibitor AM404, further supporting this interpretation. Performing the uptake assay in the absence of cells (**figure 5.2**) showed a concentration-dependent adherence of anandamide to the plastic of the culture plate, which was displaced by AM404. However, the amount of anandamide that adhered to each well was very small in comparison to that accumulated by the cells, and this effect was ignored in subsequent assays. Confirming the results of Beltramo *et al.* (1997) in rat neurones and astrocytes, **figures 5.3** shows that anandamide uptake was time-dependent in N18TG2 cells. However, contradicting the results of Beltramo *et al*, **figure 5.4** shows that anandamide accumulation by N18TG2 cells was not significantly inhibited by

bromocresol green. Un-paired t-tests comparing anandamide accumulation in the absence and presence of this compound (20 μM) gave P values of > 0.1 at all anandamide concentrations.

Although the scope of these experiments was limited, the results clearly show that N18TG2 cells possess a temperature- and time-dependent anandamide uptake mechanism that is inhibited by AM404. However, it is apparent from the graphs that the range of anandamide concentrations used was not sufficient to allow the determination of V_{max}. It is also evident that there was inconsistency between the experiments. This can be seen when comparing the rates of anandamide uptake in the absence of inhibitor in **figures 5.1** and **5.4**. The most likely reasons for this inconsistency are variations in the confluency of the cells and slight differences in the culture medium used in the different passages. It is clear though, that in order to properly characterize the kinetics of this uptake mechanism in this cell type, numerous repeats of these assays should be performed.

Since V_{max} was not determined, these preliminary results can not be compared directly with those of Beltramo *et al*. However, it does appear that there are differences in the kinetics of the uptake mechanism of N18TG2 cells compared to that of rat neurones and astrocytes. In these cells, K_m values were determined as 32 nM and 320 nM, respectively. In comparison, it is apparent from **figures 5.1** and **5.4** that the K_m for N18TG2 lies between these two values. There is also a difference between the time courses in rat neurones and astrocytes when compared with N18TG2 cells. Beltramo *et al.* found that anandamide accumulation reached 50 % of the maximal rate within about 4 minutes. In contrast, **figure 5.3** shows that in the N18TG2 cells, this time is much greater. This is possibly due to variation in the transporter number between the different cell types.
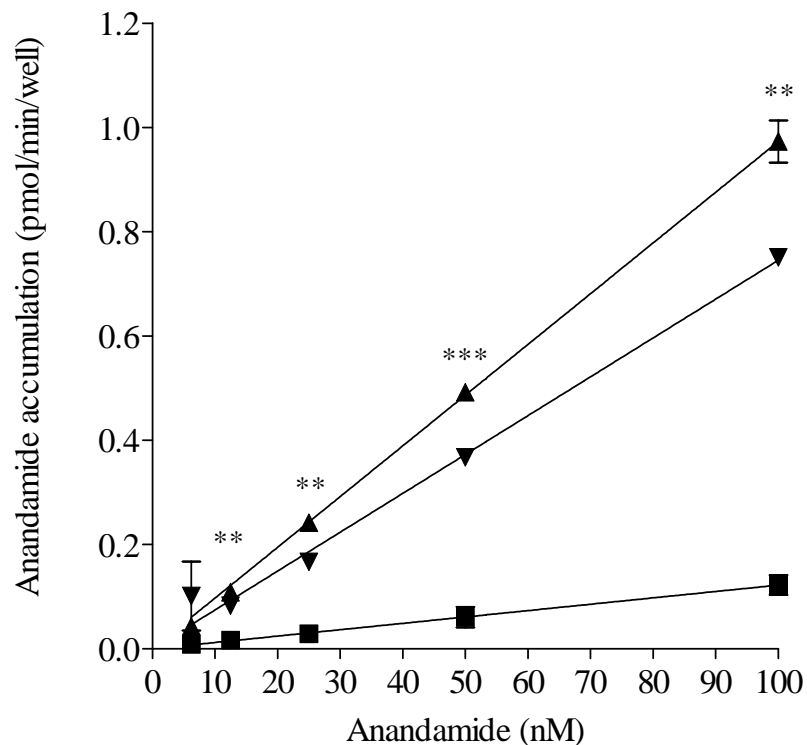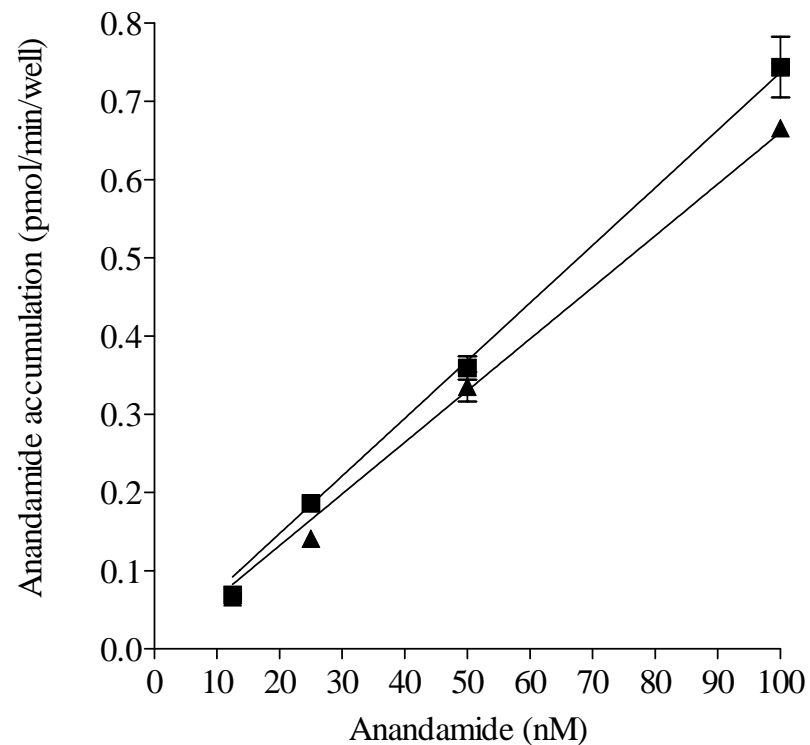
Figure 5.1: Accumulation of anandamide by N18TG2 cells at 0 °C (■) and at 37 °C in the absence (▲) and presence (▼) of 10 μM AM404. Data are expressed as the mean ± SEM of six (0 °C) or three (37 °C) determinations of uptake, and were fitted by non-linear regression (one-site binding) using GraphPad Prism. Rates of anandamide uptake at 37 °C in the presence and absence of AM404 were compared using un-paired t-tests (** P < 0.01, *** P < 0.001).
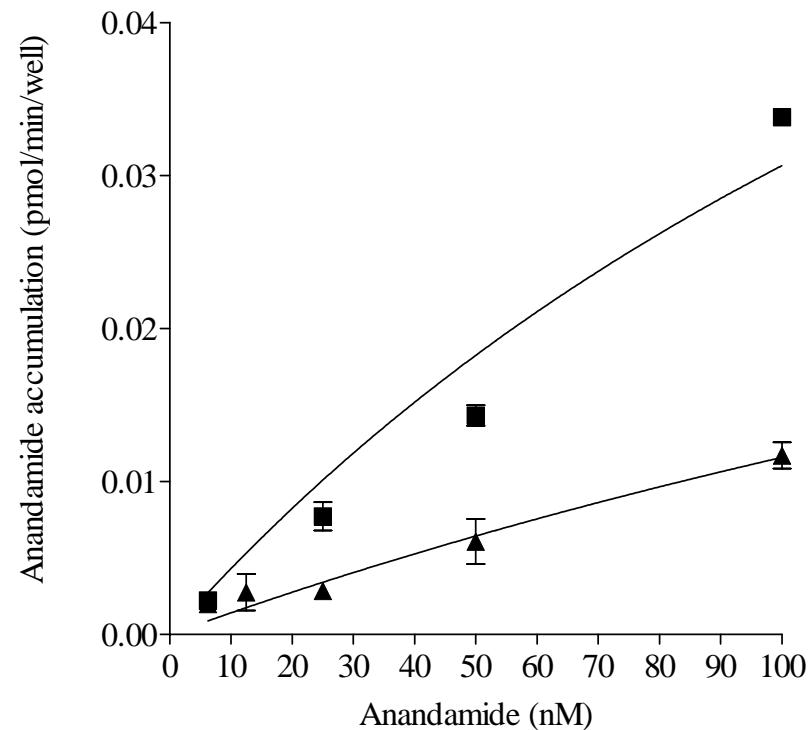
Figure 5.2: Adherence of anandamide to the plastic of a culture plate at 37 °C in the absence (■) and presence (▲) of 10 μM AM404. Data are expressed as the mean ± range of two determinations of uptake at each concentration and were fitted by non-linear regression (one-site binding) using GraphPad Prism.
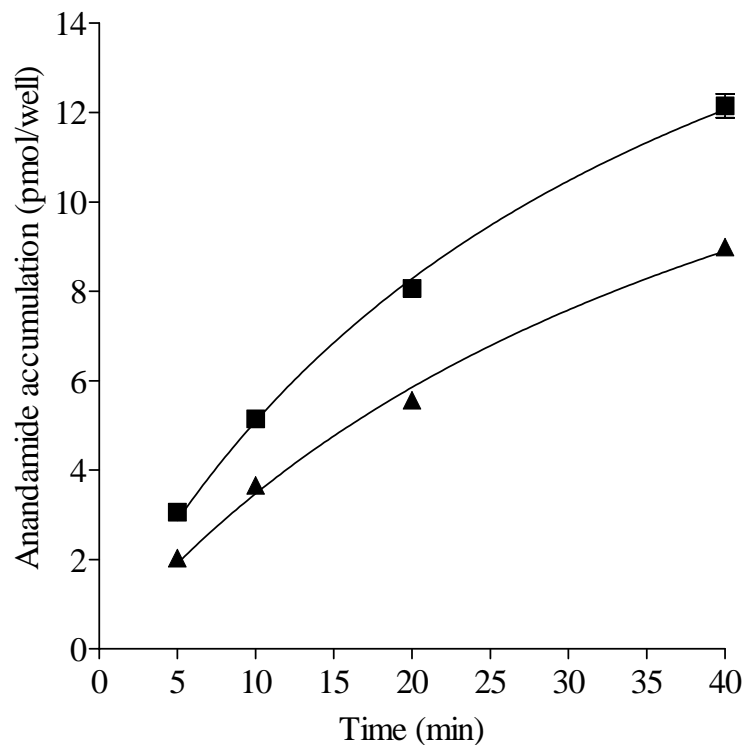
Figure 5.3: The effect of incubation time on anandamide uptake by N18TG2 cells at 37 °C in the absence (■) and presence (▲) of 10 μM AM404. Data are expressed as the mean ± SEM of three determinations of uptake at each time point and were fitted by non-linear regression (one-site binding) using GraphPad Prism.

Figure 5.4: The accumulation of anandamide by N18TG2 cells at 37 °C in the absence (■) and presence (▲) of 20 μM bromocresol green. Data are expressed as the mean ± SEM of three determinations of uptake at each concentration and were fitted by non-linear regression (one-site binding) using GraphPad Prism. Rates of anandamide uptake in the presence and absence of bromocresol green were compared using un-paired t-tests.

5.3.3 The Effect of Test Compounds on Anandamide Uptake

As the results described above indicated that N18TG2 cells possess an anandamide transport system, the effect of the aryl ethanolamides and phosphinic acids on uptake were investigated. The results in **figure 5.5** show that, when compared to the anandamide control, AM404 inhibited anandamide uptake by 30.3 ± 10.0 % at a concentration of 10 μM, while none of the other compounds tested had any inhibitory effect at the same concentration within experimental error. The only compound that showed any activity was PPA2. This compound has a long carbon chain and a benzene ring and therefore, structural similarities with AM404, but this could also be claimed for PPA5 and PPA7. Therefore, it is likely that this compound had no real effect on anandamide uptake, though studies at higher concentrations would be required to confirm this. It is possible, however, that there are multiple endocannabinoid transport systems. If this were the case, the relatively poor inhibition of anandamide uptake by AM404 and bromocresol green could be due to potent inhibition of a single transporter. It is therefore hypothetically possible that one or more of the test compounds could demonstrate this selectivity.

Although the test compounds failed to bind to either CB1 or CB2 and to affect anandamide uptake, the next chapter describes the investigation of their potential effects on FAAH using a novel spectrophotometric assay for FAAH activity. It was hoped that this would be the most likely successful target for these compounds due to the known inhibition by ibuprofen and other NSAIDs and the similarities between the alkylphosphinic acids and existing FAAH inhibitors.
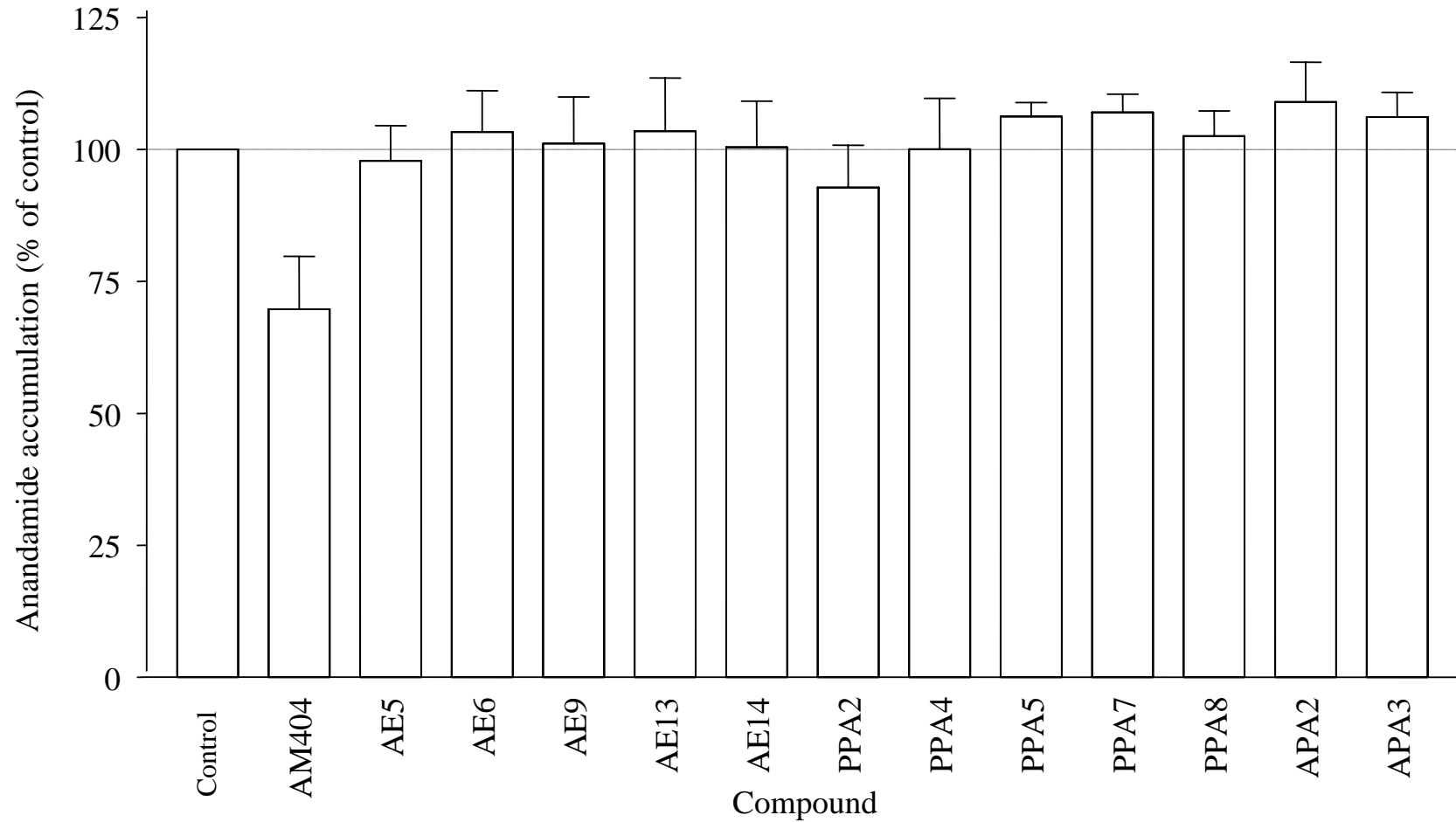
Figure 5.5: The effect of the test compounds and AM404 on anandamide accumulation in to N18TG2 cells. All compounds were assayed at 10 μM and data represent the mean ± SEM of six determinations of uptake for the test compounds and 12 determinations for AM404.

Chapter 6:

Fatty Acid Amide Hydrolase Studies

6.1 Introduction

6.1.1 Existing Assays for Fatty Acid Amide Hydrolase Activity

The majority of assays for FAAH activity described in the literature involve the use of either radiochemicals, chromatography, or both. In radiochemical FAAH assays, a radiolabelled substrate is incubated with the enzyme and, after extraction of reaction products from the mixture, the radioactive reaction product is separated from any remaining labelled substrate. This separation is achieved by TLC (Deutsch & Chin, 1993), mini-column chromatography (Desarnaud *et al*., 1995) or reverse-phase high performance liquid chromatography (RP-HPLC) (van der Stelt *et al*., 1997; Maccarrone *et al*., 1999), followed by measurement of the radioactivity present in the relevant band, fraction or peak. Alternatively, if an ethanolamide FAAH substrate is used, the compound can be radiolabelled with ^{14}C on the ethanolamine portion. After incubation of this substrate with the enzyme, addition of an organic solvent causes the ethanolamine to partition in the aqueous phase, while any unreacted substrate is retained in the organic phase. The aqueous phase is then removed and liquid scintillation counting is performed, eliminating the use of chromatography (Omeir *et al*., 1995).

The other commonly used FAAH assays are based purely on chromatography. The first methodology involves the incubation of an unsaturated FAAH substrate with the enzyme followed by extraction of the reaction products. RP-HPLC is then used to separate and quantify substrate and products by detection of the carbon-carbon double bonds (Lang *et al*., 1996). The second method is another HPLC-based assay in which an ethanolamide substrate is incubated with FAAH and the products then extracted from the assay mixture. The ethanolamine produced by the reaction is derivatized by reaction with *o*-phthaldialdehyde to form an isoindole which can then separated by RP-HPLC and detected at a wavelength of 230 nm (Qin *et al*., 1998).

All of these assays have drawbacks in that they are either expensive due to the use of radiolabelled substrates, time-consuming because of the chromatographic analysis, or both. These problems are especially compounded by the need to assay multiple samples, but only two examples of FAAH assays exist in the literature

that do not possess either of these drawbacks. First, the activity of FAAH has been measured using an ion-specific electrode to detect the ammonia generated by oleamide hydrolysis (Patterson *et al*., 1996). Second, a fluorescent displacement assay has been described which measures either the arachidonic acid or oleic acid generated by hydrolysis of anandamide or oleamide, respectively (Thumser *et al*., 1997). In this method, the generation of the fatty acid displaces DAUDA (11-(5-dimethylamino naphthalenesulphonyl)-undecanoic acid), a fluorescent fatty acid analogue, from fatty acid binding protein (FABP) and the decrease in fluorescence is used to determine the rate of hydrolysis by FAAH. Both of these methods have drawbacks, however. The ammonia electrode method involves the use of large (10 ml) assay volumes due to the physical size of the electrode. The fluorescence assay has two problems associated with it. First, the FABP must be extracted from either rat liver or *E. coli* expressing the recombinant protein, then purified and delipidated for use in the assay. Second, because anandamide and oleamide also bind to the FABP, the assay system requires calibration in order to discount the effects of these ligands binding to the FABP.

6.1.2 A Novel FAAH Assay

Due to the drawbacks of existing assays, it was decided that a totally novel approach would be taken to develop an effective, cheap and rapid FAAH assay that could be performed without specialized equipment. To achieve this, a spectrophotometric assay was developed using the first known substrate of FAAH, oleamide. To measure the rate of ammonia generation upon oleamide hydrolysis, a dual-enzyme assay was proposed using FAAH and L-glutamate dehydrogenase (GDH) as shown in **scheme 6.1**.
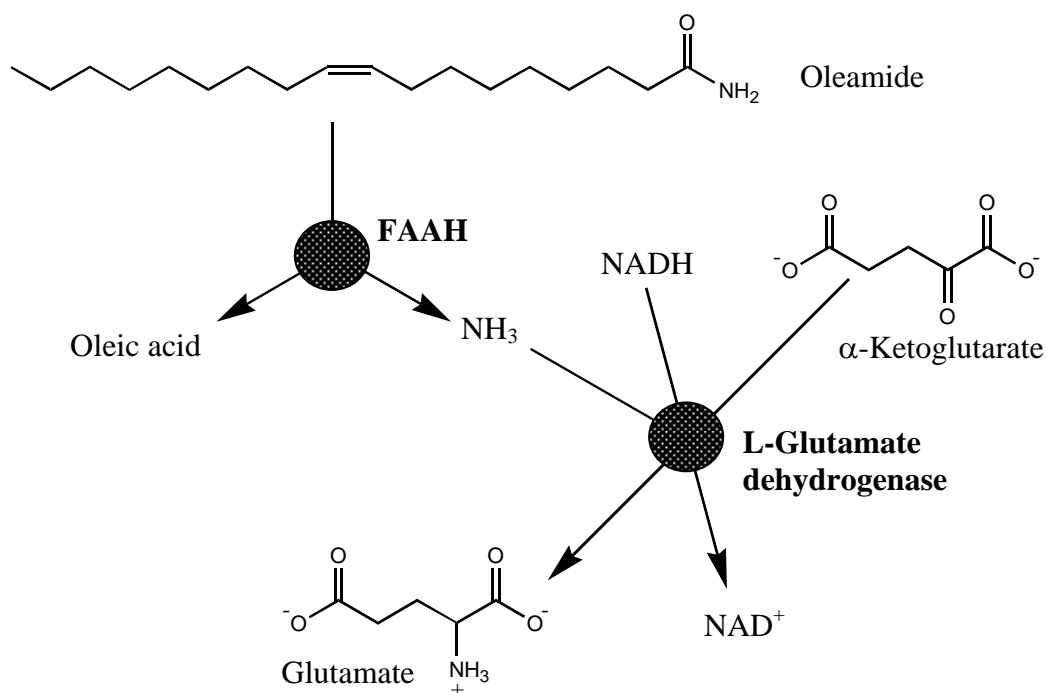
Scheme 6.1: Dual-enzyme assay to measure the ammonia generated by FAAH-catalysed oleamide hydrolysis.

As shown above, GDH catalyses the condensation of α-ketoglutarate (α-KG) and ammonia to form glutamate, using NADH as a co-factor. NADH has a high molar extinction at 340 nm and, therefore, its oxidation to NAD^+ can readily be followed using a spectrophotometer. Since ammonia and NADH are equimolar in this reaction, the ammonia generated by FAAH-catalysed hydrolysis of oleamide and the reduction in absorbance at 340 nm are directly proportional. The following section describes how this theoretical assay system was developed and optimized.

6.2 Assay Development

6.2.1 Glutamate Dehydrogenase Reaction

Before attempting to combine the two enzymes in one assay, it was first necessary to optimize the conditions of the GDH assay. Using commercially available bovine L-glutamate dehydrogenase, the method of Bergmeyer & Beutler (1985) was adapted for use in cuvettes as shown in **table 6.1**. These adapted conditions

will henceforth be referred to as the "normal" assay conditions. ADP was present in this assay system as it is a known allosteric activator of GDH.

Solution	Assay Concentration According to Bergmeyer	Assay Volume According to Bergmeyer (ml)	Adapted Assay Concentration	Adapted Assay Volume (μl)
Triethanolamine	155 mM		156 mM	
α-Ketoglutarate	11 mM	1.00	11 mM	140
ADP	0.56 mM		0.67 mM	
β-NADH	186 μM	0.10	222 μM	14
NaHCO$_3$	3.70 mM		3.75 mM	
GDH*	7.4 kU/dm^3	0.02	6.7 kU/dm^3	2
Water	-	2.00	-	244
Ammonia sample	up to 150 μM	0.10	160 μM	50
Total Volume		**3.22 ml**		**450 μl**

Table 6.1: Assay components, volumes and concentrations for the glutamate dehydrogenase reaction. * 1 Unit = the amount of enzyme that will oxidize 1.0 μmole of α-KG in the presence of ADP at 25 °C, pH 7.8.

Another factor known to affect GDH activity is the magnesium ion concentration, although there are conflicting accounts of its effects. For example, Fahien *et al.* (1990) reported that, in the absence of ADP, Mg^{2+} inhibited bovine GDH activity while, in the presence of ADP, Mg^{2+} behaved as an activator. However, Bailey *et al.* (1982), also using bovine GDH, showed that, up to 5 mM, Mg^{2+} had no effect on GDH activity or the role of ADP in its regulation.

<u>Preliminary Assays</u>

With the conflicting accounts of the effect of ADP and Mg^{2+}, it was necessary to investigate the effects of these factors by performing assays in their presence and absence. To confirm that the assay concentrations used by Bergmeyer & Beutler were indeed the most effective, assays were also performed with varying amounts of α-ketoglutarate, NADH and GDH in comparison to the normal assay conditions.

Normal Assay Procedure:

Assay solutions were made up by placing 140 μl of solution A (71.4 mM α-ketoglutarate, 4.3 mM ADP, 500 mM triethanolamine; pH 8.0), 14 μl of solution B (7.1 mM β-NADH, 120.6 mM $NaHCO_3$), 2 μl of GDH solution (1600 kU/dm^3, 50 % glycerol solution) and 244 μl of distilled water in acrylic cuvettes.

Solutions were stirred and gently shaken for at least 10 minutes to allow equilibration prior to placing the cuvettes in a Beckman DU650 spectrophotometer. Absorbance was monitored at 340 nm until constant and the reactions then initiated by the addition of 50 μl of ammonium acetate solution (1.4 mM) to give an assay concentration of 160 μM. Solutions were mixed by stirring and absorbance automatically measured every 38 seconds for up to 30 minutes. Each assay was conducted at room temperature and consisted of four test cuvettes and two cuvettes containing a blank of distilled water added in place of ammonium acetate solution.
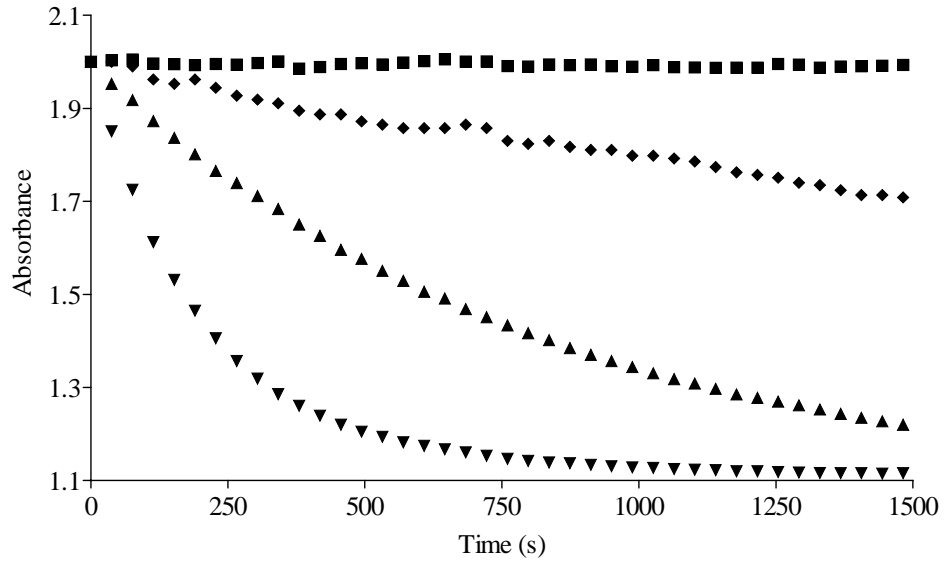
Variation of Assay Conditions:

Assays were performed as described above with the following variations in the assay conditions: high (1.1 mM) or low (0.4 mM) NADH, high (22.2 mM) or low (1.1 mM) α-KG, high (66.7 kU/dm^3) or low (0.7 kU/dm^3) GDH, 1 mM Mg^{2+} with ADP, 1 mM Mg^{2+} without ADP or the absence of both Mg^{2+} and ADP. For assays containing Mg^{2+}, the distilled water in the normal assay was replaced with $MgCl_2$ solution (1.8 mM).

Results:

The results in **figures 6.1** and **6.2** show the effect of altering α-KG, NADH and enzyme concentrations on the rate of the GDH reaction. It is clear that lower than normal concentrations of these species reduced the reaction rate. As expected, increasing the amount of enzyme increased the rate, but a higher than normal concentration of α-KG did not affect the reaction. Unfortunately, due to the absorbance reading going off the scale of the spectrophotometer, a higher concentration of NADH could not be assayed. The effects of ADP and Mg^{2+} on the GDH reaction are shown in **figure 6.3** and **table 6.2**. These data confirm the activation of glutamate dehydrogenase by ADP and show that Mg^{2+} has an inhibitory effect on the reaction rate. The initial reaction rate in the presence of ADP (i.e. normal assay conditions) is double that of the assay in its absence.
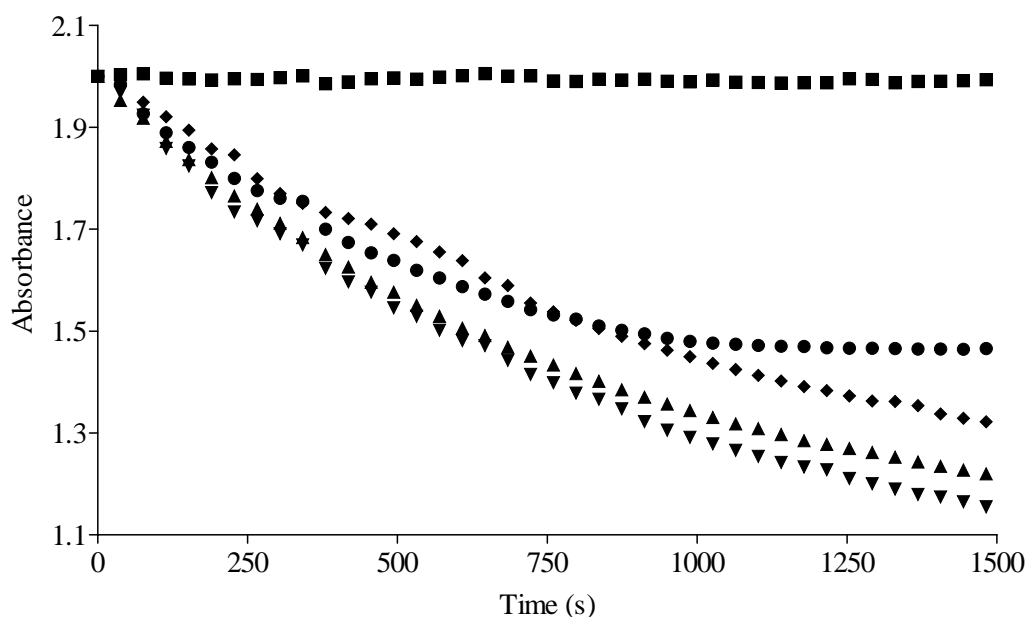
Figure 6.1: Representative data from a single experiment, showing the effect of different concentrations of α-ketoglutarate and NADH on the rate of the GDH reaction. Blank (■), normal assay conditions (▲), high α-KG (▼), low α-KG (◆) and low NADH (●). For visualisation, all data were normalized so that the absorbance reading at 0 seconds was 2.0.

Figure 6.2: Representative data from a single experiment, showing the effect of different concentrations of enzyme on the rate of the GDH reaction. Blank (■), normal assay conditions (▲), high GDH (▼) and low GDH (◆). For visualisation, all data were normalized so that the absorbance reading at 0 seconds was 2.0.
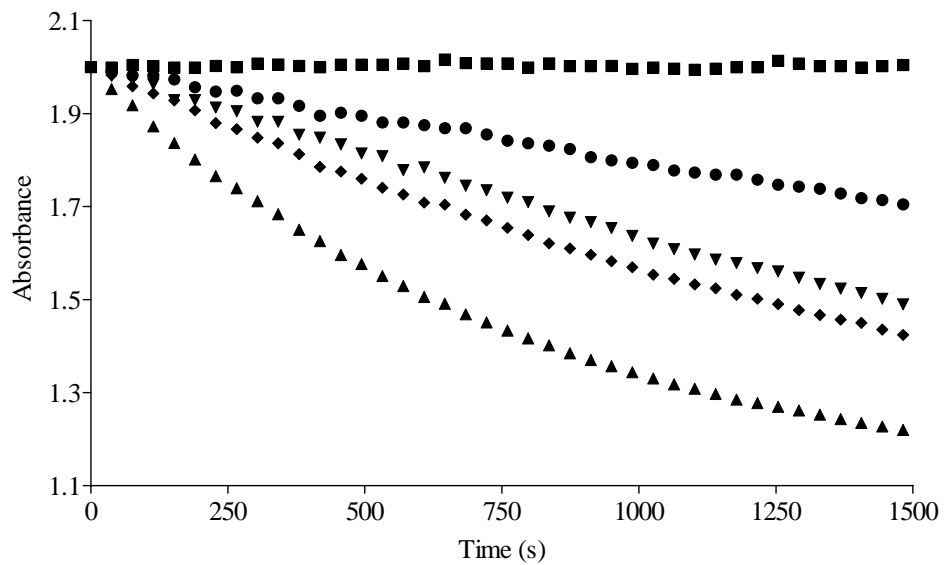
Figure 6.3: Representative data from a single experiment, showing the effect of the presence or absence of ADP and Mg^{2+} on the rate of the GDH reaction. Blank (■), normal assay conditions (▲), +ADP/+Mg^{2+} (▼), -ADP/-Mg^{2+} (◆) and -ADP/+Mg^{2+} (●). For visualisation, all data were normalized so that the absorbance reading at 0 seconds was 2.0.

Conditions	Rate (Abs/sec)	Relative Rate
Normal (+ADP/-Mg^{2+})	-1.02 x 10^{-3}	1
-ADP/-Mg^{2+}	-5.13 x 10^{-4}	0.50
+ADP/+Mg^{2+}	-3.86 x 10^{-4}	0.38
-ADP/+Mg^{2+}	-2.21 x 10^{-4}	0.22

Table 6.2: The effect of ADP and Mg^{2+} on initial GDH reaction rate. Rates were determined by linear regression (0 to 228 seconds) of the data from **figure 6.3** using GraphPad Prism and the blank rate subtracted from each.

When ADP and 1 mM Mg^{2+} were both present, the initial rate was approximately one third that of the normal assay, showing the negative effect of the ADP-metal complex. However, with Mg^{2+} alone, the inhibitory effect was even greater, with the initial rate reduced to one fifth of the optimum.

These results demonstrate that the assay conditions adapted from Bergmeyer & Beutler were indeed optimal for this assay. The reaction rate could have been dramatically increased by increasing the enzyme concentration but this would be unnecessary and wasteful. In contrast to the results of Fahien *et al.* (1990), these results showed that the ADP/Mg^{2+} complex was not activating, but inhibitory. This also contradicts the findings of Bailey *et al.* (1982) who found Mg^{2+} did not alter either the activity of GDH or the effect of ADP. With these results in mind, the assay conditions shown in **table 6.1** were adopted for the subsequent assays.

Ammonium Acetate Concentration-Response Assay

To show that the GDH assay could be used to detect variable concentrations of ammonia, an ammonium acetate concentration-response assay was performed. The protocol was as described for the normal assay procedure, using ammonium acetate at assay concentrations between 1 and 160 μM. Each concentration was assayed in duplicate against blanks containing water only. Reaction rates were linear up to at least 5 minutes, so the initial rate at each concentration was determined by linear regression of the data from 0 to 304 seconds using GraphPad

Prism. Reaction rates were plotted against concentration and the results of this assay are shown in **figure 6.4**. These data clearly show that, as expected, the rate of GDH reaction was dependent on ammonium acetate concentration and was linear using these assay conditions. With this demonstration, it was then possible to combine GDH and FAAH in one assay to test the proposed spectrophotometric FAAH assay.
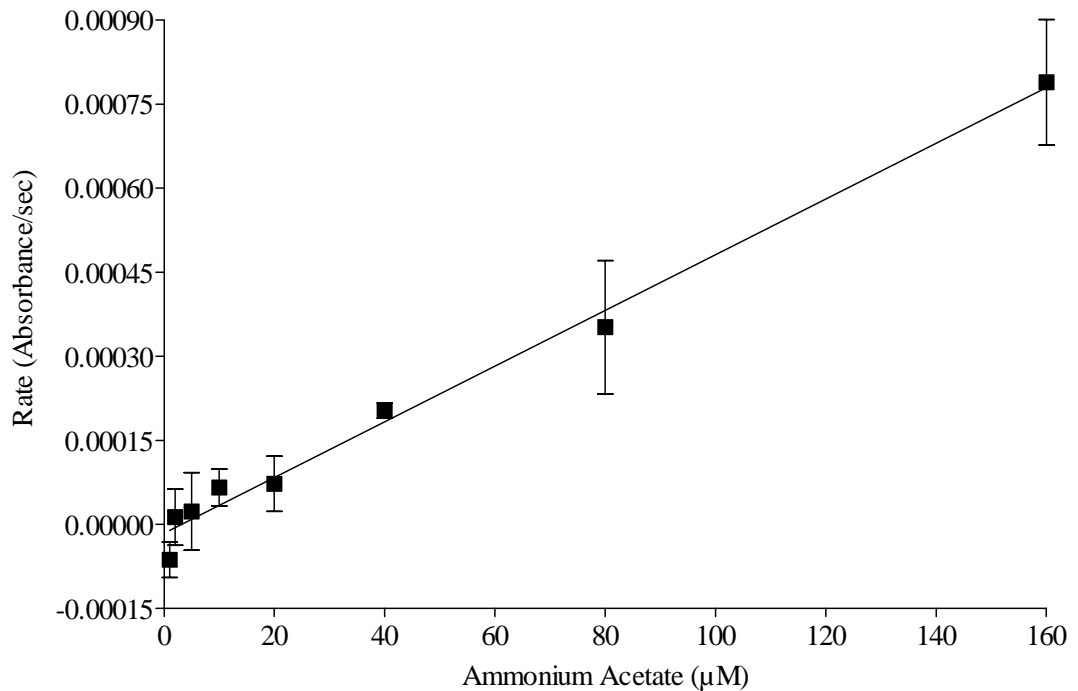
Figure 6.4: Representative data showing the effect of increasing ammonium acetate concentration on the rate of GDH-catalysed glutamate formation. Data are expressed as the mean ± range of two determinations of rate and were fitted by linear regression using GraphPad Prism.

6.2.2 FAAH Assays

<u>Preliminary Assays</u>

FAAH is highly expressed in the brain (Desarnaud *et al*., 1995) and liver (Katayama *et al*., 1997) so, due to the immediate availability of rat liver microsomes, liver was chosen for this work. The first attempt at combining the two enzyme sources in one assay was unsuccessful as the absorbance was off the

scale of the spectrophotometer, probably due to light scattering by the cloudy assay solution. To overcome this, the microsomes were solubilized as described below and the assays repeated.

Tissue Solubilization:

Frozen rat liver microsomes (13.25 mg protein/ml in 250 mM sucrose, 5 mM EDTA, 20 mM Tris; pH 8.0) were prepared by an adaptation of the method described by Kamath *et al*. (1971) and kindly provided by Mr Kishan Jassi. Equal volumes of thawed microsome preparation and microsome buffer containing 1 % (w/v) of the detergent t-octylphenoxypolyethoxy ethanol (TX-100) were placed on ice and vortexed three times over a period of 15 minutes, then centrifuged at 9,000g for 5 minutes at 4 °C. The supernatant, containing the soluble protein, was removed and used in the subsequent assays.

FAAH Assay Procedure:

Assay solutions were made up by placing 140 μl of solution A, 14 μl of solution B, 2 μl of enzyme solution and 40 μl of solubilized microsomes in acrylic cuvettes and making the volume up to 448 μl with microsome buffer. The procedure used was then exactly as described above for the GDH reaction with the assay initiated by adding 2 μl of ethanolic oleamide stock (36 mM), giving an assay concentration of 160 μM. Blank cuvettes contained the same assay components as the test cuvettes, but 2 μl of ethanol was added instead of oleamide solution.

The results of the initial FAAH assay are shown in **figure 6.5**. This example of typical experimental data demonstrates that the reaction rate in the blank and test sample were linear for the duration of the assay. The blank showed a small decrease in absorbance due to the inevitable presence of endogenous ammonia in the microsome preparation, but this was eclipsed by the much larger reaction rate in the presence of oleamide. These data indicate that oleamide was hydrolysed by FAAH, with the resulting ammonia utilized by GDH. The linearity of these data may be due to the FAAH reaction being the rate-limiting step in this system, presumably because the pH and temperature of the assay were not optimal for this enzyme.

151
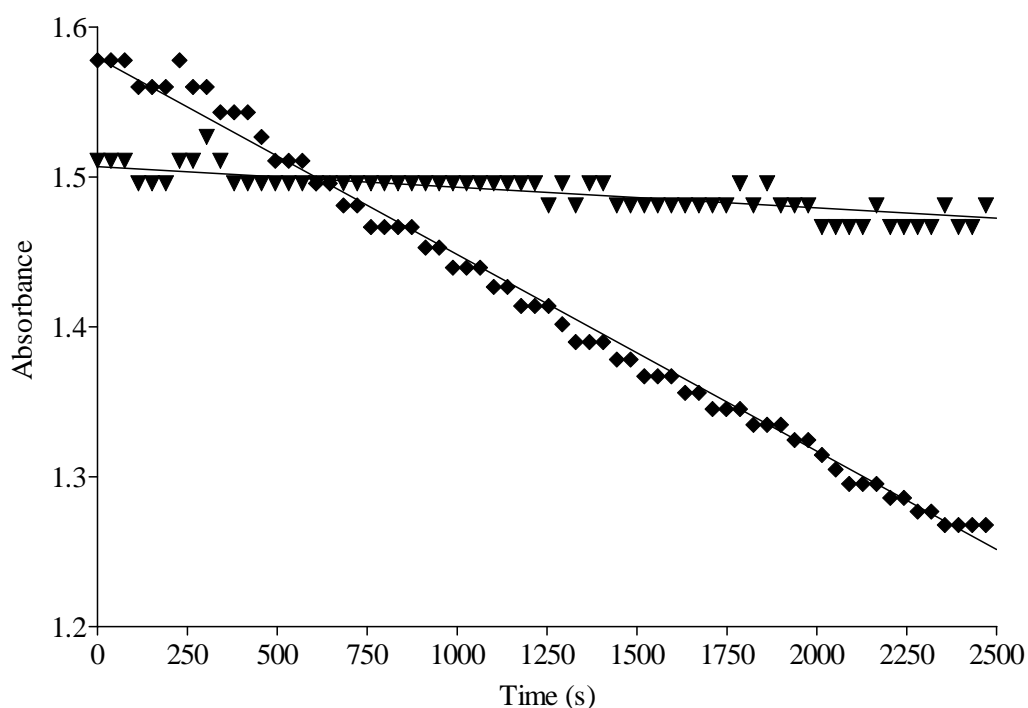
Figure 6.5: Representative experimental data from the preliminary FAAH assays using solubilized rat liver microsomes with an ethanolic blank (▼) or 160 μM oleamide (◆). Data were fitted by linear regression using GraphPad Prism.

Oleamide Concentration-Response Assay

To demonstrate further that this assay was working as predicted, a limited oleamide concentration-response assay was performed. The procedure was as described for the preliminary FAAH assay, with oleamide at assay concentrations of 10 to 320 μM. Each concentration was assayed in duplicate against ethanolic blanks.

Data Analysis:

As with the previous assays, the rate of oleamide hydrolysis was linear for the duration of the experiments, so rates were determined by linear regression of the data from 0 to 4560 seconds. The rate of reaction in nmol/min was then calculated as described below and the data fitted by non-linear regression using GraphPad Prism.

152

The absorbance of a chromophore is linked to its concentration by the Beer-Lambert equation:

$$A = \varepsilon \, c \, l$$

where A = absorbance, ε = the molar extinction coefficient, c = the concentration of the chromophore and l = the path length of the cuvette. In this system, the molar extinction coefficient of NADH = 6220 M^{-1} cm^{-1} and the path length of the cuvette = 1 cm. Therefore,

$$A = 6220 \, c$$

As the absorbance in these assays decreased with time, the slopes generated by GraphPad Prism were negative with units of A/sec so:

$$-1(\text{slope} \times 60) = 6220 \, c/min$$

$$c/min = -1((\text{slope} \times 60)/6220)$$

Finally, to convert the rate from moles/dm^3/min to nmol/min:

$$nmol/min = -1((\text{Slope} \times 60 \times 450 \times 10^{-6} \times 1 \times 10^{9})/6220)$$

$$= -1((\text{Slope} \times 27 \times 10^{6})/6220)$$

Results:

The results of the preliminary oleamide concentration-response assay are shown in **figure 6.6**. These data show that the rate of oleamide hydrolysis was concentration -dependent, confirming that this assay may be an effective method to measure FAAH activity.
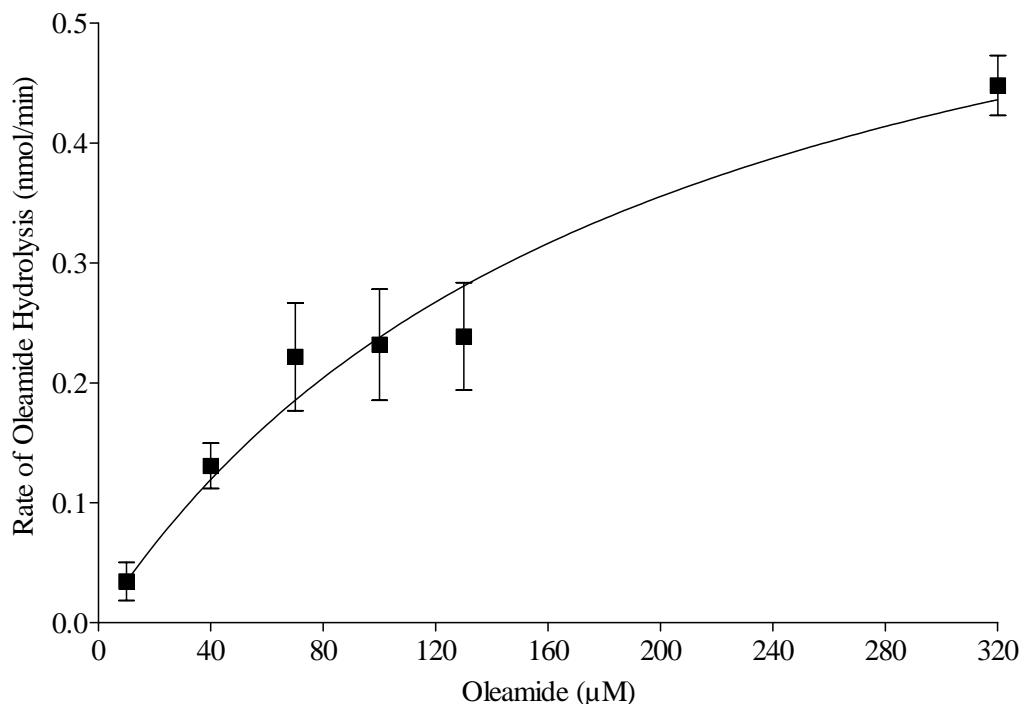
Figure 6.6: The effect of concentration on FAAH-catalysed oleamide hydrolysis by solubilized rat liver microsomes using a spectrophotometric FAAH assay. The data represent the mean ± range of two determinations of rate and were fitted by non-linear regression using GraphPad Prism.

Comparison of Rat Liver Microsomes and Liver Plasma Membranes

To simplify the overall assay procedure, it was decided that rat liver membranes would be assayed for FAAH activity as their preparation is simpler than that of microsomes. Therefore, the rate of hydrolysis of 160 μM oleamide by FAAH was compared in solubilized preparations from rat liver microsomes and rat liver membranes to determine whether the membranes were a viable FAAH source.

Assay Procedure:

Rat liver membranes were prepared as described for the brain membrane preparation in **section 3.2.1**, and kindly provided by Professor David Kendall. Assays were performed as described for the previous rat liver microsome FAAH assays, with 40 μl of solubilized microsomes or membranes in duplicate against blanks containing ethanol instead of oleamide solution. Slopes were generated as previously described using data from 0 to 1026 seconds and the rate of oleamide

154

hydrolysis calculated as nmol/min/mg protein. The microsome preparation was provided at a known protein concentration of 13.25 mg/ml and the protein concentration of the membrane preparation was determined using the adapted method of Bradford (1976), as described in **section 4.3.1**. The protein concentrations used to determine the rate of oleamide hydrolysis in each tissue preparation were the pre-solubilization concentrations.

Results:

The results of this assay are shown in **figure 6.7**. It is clear from this figure that there was no difference in the FAAH activity present in solubilized rat liver membrane or microsome preparations. Although the protein concentrations used to determine rates were the pre-solubilization concentrations, it is reasonable to assume that the efficiency of FAAH solubilization by TX-100 was the same in both preparations. In light of these results, it was decided that, because of the ease of preparation, rat liver membranes would be used instead of rat liver microsomes in subsequent assays.
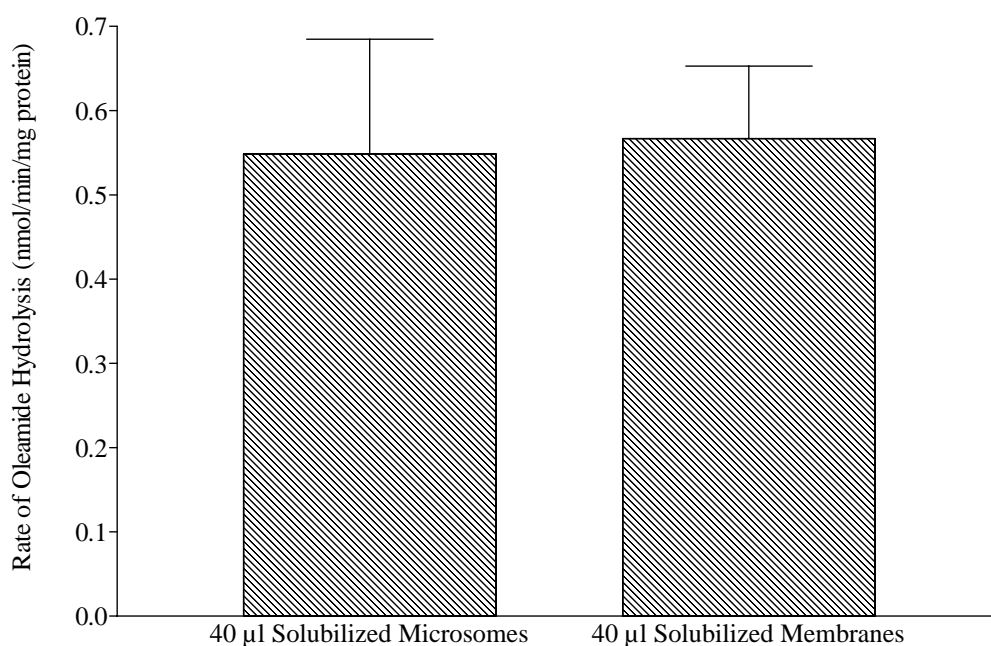
Figure 6.7: Comparison of the rate of FAAH-catalysed hydrolysis of 160 μM oleamide in solubilized preparations of rat liver microsomes and membranes. Data represent the mean ± range of two determinations of rate. Protein concentrations were determined prior to solubilization of the tissue preparations.
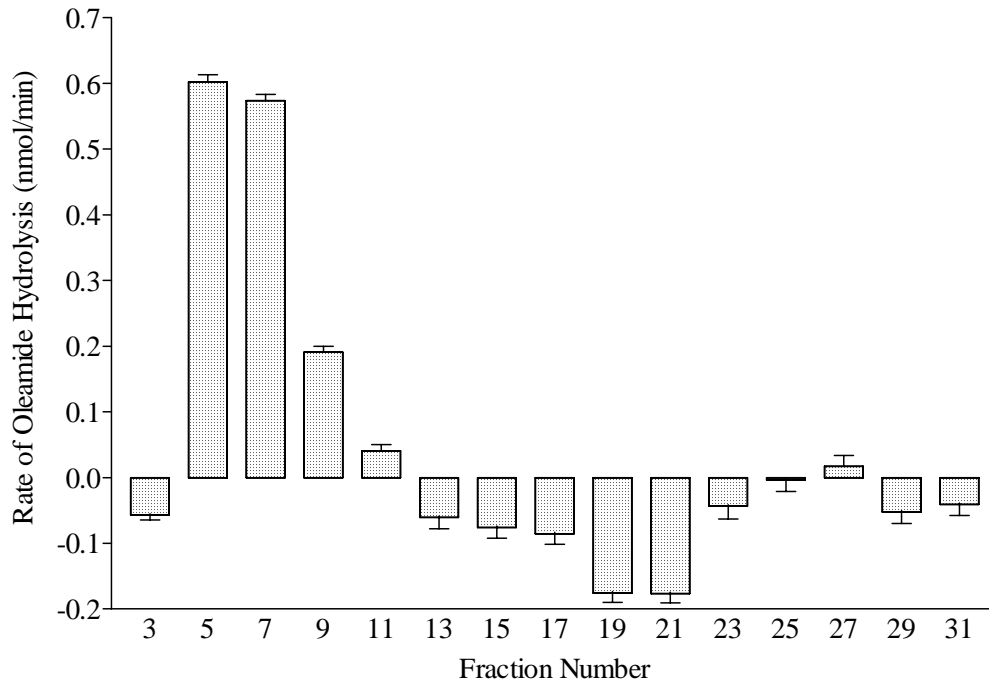
Crude Purification of FAAH Activity

In an attempt to enrich the FAAH activity in the liver membrane homogenate, a crude purification procedure was employed using a BioRad Econo-Pac High Q anion exchange column.
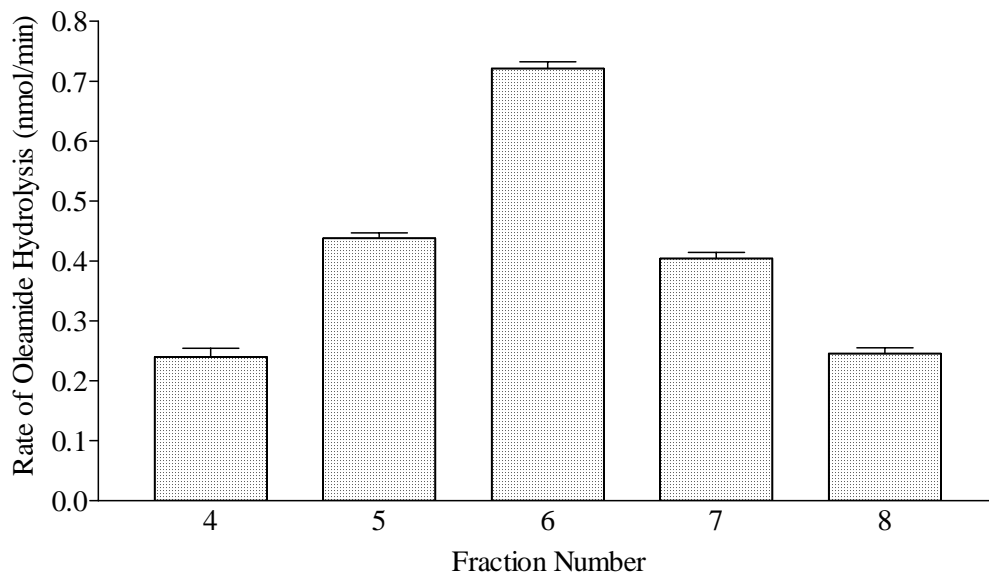
Purification and Assay Procedures:

Distilled water was passed through the column for 1 hour at 1 ml/min followed by column buffer (1 mM EDTA, 0.1% (w/v) TX-100, 20 mM HEPES; pH 7.2) for 2 hours at 1 ml/min. Rat liver membrane homogenate was solubilized as described at the beginning of this section, using an equal volume of solubilization buffer (1 mM EDTA, 1% (w/v) TX-100, 20 mM HEPES; pH 7.2). The solubilized protein solution (5 ml) was then passed through the column at 1 ml/min. A linear gradient of 50 mM to 1 M ammonium acetate was employed to desorb bound material, which was collected as 32 x 2.5 ml fractions. FAAH assays were then performed using 50 μl aliquots of the samples with column buffer making up the bulk of the assay volume. In these assays, all cuvettes contained oleamide at a concentration of 160 μM and, in the blanks, the tissue was replaced by 50 μl of buffer.

Results:

From the results shown in **figure 6.8**, it is apparent that FAAH activity was not eluted as a sharp band, with activity present in fractions 4 to 11. A subsequent experiment (**figure 6.9**) showed that fraction 6 contained the highest FAAH activity, possessing an oleamide hydrolysis rate of 0.72 ± 0.01 nmol/min. Significant enzyme activity was also evident in fractions 4, 5, 7 and 8. However, with the failure of this procedure to separate the FAAH activity in to a single fraction, no further purification was attempted. For simplicity, it was decided to routinely use solubilized homogenate without an additional purification step.

Figure 6.8: The FAAH activity present in the alternate fractions collected during the attempted purification of the enzyme using an ion exchange column.

Figure 6.9: The FAAH activity present in fractions 4-8, collected during the attempted purification of the enzyme using an ion exchange column.

FAAH Assays Using Rat Liver Crude Particulate Fraction

To simplify further the overall procedure, it was decided to attempt FAAH assays with the crude particulate fraction (CPF) of rat liver. The preparation of this tissue homogenate, more straightforward than liver membrane preparation, and its subsequent use in FAAH assays is described below.

Preparation of Rat Liver Crude Particulate Fraction (CPF):

Freshly dissected liver from Wistar or hooded Lister rats was roughly chopped with scissors, weighed and homogenized in 10 volumes of ice-cold buffer (1 mM EDTA, 50 mM Tris; pH 7.4) using a Polytron homogenizer. The homogenate was centrifuged at 1,000g for 5 minutes at 4 °C, and the supernatant was then centrifuged at 36,000g for 20 minutes at 4 °C. The resulting pellet was then suspended in 4 volumes (original wet weight) of ice-cold buffer and manually re-homogenized with a glass/teflon homogenizer. Aliquots of the CPF (1 ml) were frozen at -80 °C until required.

Assay Procedure:

Assays were performed to assess the FAAH activity in solubilized preparations from rat liver CPF. Solubilization was performed as described above using equal volumes of rat liver CPF and buffer (1 mM EDTA, 50 mM Tris; pH 7.4) containing 1 % (w/v) TX-100 and 100 µl of the soluble protein was used in each assay. The assay procedure was as described above, with CPF buffer as the bulk of the assay volume. The hydrolysis of 160 µM oleamide was measured in quintuplicate against blanks containing no oleamide and rates determined as previously described.

Results:

The rate of oleamide hydrolysis in this solubilized tissue was calculated as 0.98 ± 0.08 nmol/min, i.e. greater than that in soluble liver microsomes or membrane homogenate. Subsequently, an oleamide concentration-response assay was performed with oleamide at 1 to 160 µM, with each concentration assayed in duplicate. To calculate the rate of hydrolysis of oleamide in this assay, the protein

concentration of the solubilized tissue was measured using an adaptation of the method of Bradford (1976) as described in **section 4.3.1**. Rates were then expressed as nmol/min/mg protein and the results are shown in **figure 6.10**. These data demonstrate that, as in solubilized rat liver membranes, there was a concentration -dependent FAAH activity in solubilized preparation of rat liver CPF.
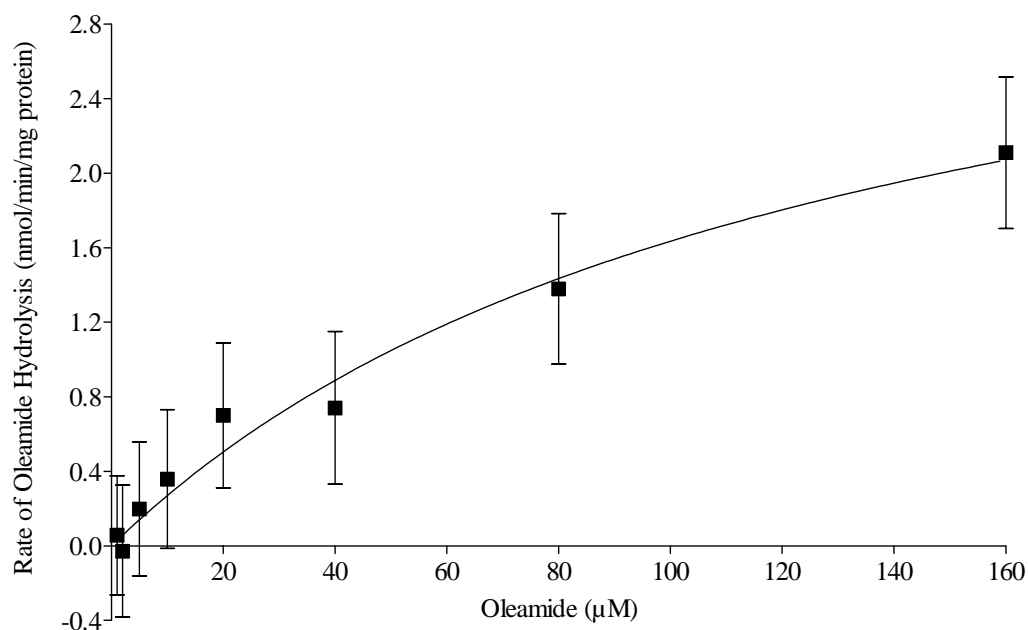
Figure 6.10: Representative data showing the effect of oleamide concentration on its FAAH-catalysed hydrolysis using solubilized rat liver crude particulate fraction. Data represent the mean ± range of two determinations of hydrolysis rate and were fitted by non-linear regression using GraphPad Prism.

All of the results described above demonstrate that the novel assay combining FAAH and GDH does work, largely as predicted. The next section describes the detailed validation of this assay system.

6.3 Assay Validation

To ensure that this assay system was a valid method of measuring FAAH activity, it was necessary to demonstrate that the enzyme kinetics measured were comparable with those reported using existing assays and that activity was concentration-dependently inhibited by known FAAH inhibitors.

6.3.1 Oleamide Concentration-Response Assays

Although these assays had been performed as part of the assay development process, they were of limited value due to the low number of replications and variations in the assay conditions. To rectify this, assays were performed using the following, definitive, protocol.

FAAH Assay Procedure:

Assay solutions were made up by placing 140 µl of solution A (71.4 mM α-ketoglutarate, 4.3 mM ADP, 500 mM triethanolamine; pH 8.0), 14 µl of solution B (7.1 mM β-NADH, 120.6 mM $NaHCO_3$), 2 µl of GDH solution (1600 kU/dm^3, 50 % glycerol solution), 192 µl of CPF buffer (1 mM EDTA, 50 mM Tris; pH 7.4) and 100 µl of solubilized preparation of rat liver CPF in acrylic cuvettes. Solutions were stirred, gently shaken for at least 10 minutes to allow equilibration and then the cuvettes were placed in a Beckman DU650 spectrophotometer. Absorbance was monitored at 340 nm until it was constant and the reactions were initiated by the addition of 2 µl of ethanolic oleamide solution. Solutions were mixed by stirring and absorbance automatically measured every 38 seconds for up to 2500 seconds. Each assay was conducted at room temperature and consisted of five test cuvettes and one cuvette containing a blank of ethanol instead of oleamide solution. Oleamide was assayed at concentrations ranging from 3.75 to 120 µM, with each concentration measured in triplicate. Three assays were performed using liver CPF from three separate rats.

Data Analysis:

The protein concentration of each solubilized tissue was determined as described previously and slopes were calculated for each assay by linear regression of the data (0 to 494 seconds) using GraphPad Prism. The slope of the blank was then subtracted from that of the test samples and the rate of oleamide hydrolysis calculated using the equation described in **section 6.2.2**. Rates were then plotted against concentration and the data fitted by non-linear regression to a rectangular hyperbola using GraphPad Prism.

The two defining values usually quoted when referring to enzyme kinetics are V_{max}, the maximum rate, and K_m, the Michaelis constant, which is the concentration of substrate at which the reaction rate is half the V_{max}. Non-linear regression analysis of the data by GraphPad Prism generated K_m and V_{max} values for each experiment. The means ± SEMs of these data were calculated from three experiments.

Results:

The combined data from the three experiments are shown in **figure 6.11**. The V_{max} and K_m values for oleamide hydrolysis by FAAH were calculated as 5.73 ± 0.44 nmol/min/mg protein and 103.8 ± 13.0 μM, respectively and data described in the literature are shown in **table 6.3** for comparison. Although V_{max} values for oleamide hydrolysis by FAAH have not been reported in the literature, the rate at a single concentration has been determined in comparison to that of anandamide. Using purified FAAH, the rate of hydrolysis of 100 μM oleamide was shown to be 242 ± 20 nmol/min/mg protein compared to 333 ± 30 nmol/mg/protein with 100 μM anandamide (Cravatt *et al*., 1996). This demonstrates that, although anandamide is the preferred substrate of the enzyme, the rate for oleamide hydrolysis is similar to that for anandamide. In comparison with the V_{max} values in **table 6.3**, the maximum rate described for these experiments is of the same order of magnitude.
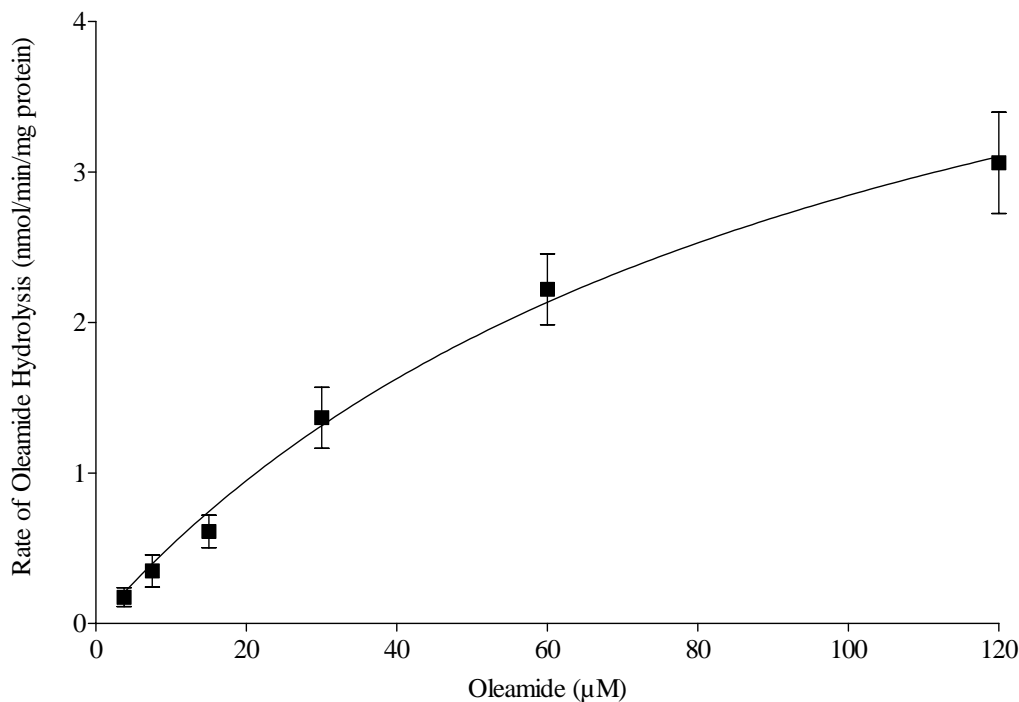
Figure 6.11: The effect of concentration on FAAH-catalysed oleamide hydrolysis in solubilized rat liver crude particulate fraction. Data are expressed as the mean ± SEM of three independent experiments.

However, the K_m value of 103.8 ± 13.0 μM obtained with the present assay was higher than the previously reported data, but of the same order of magnitude. These differences may well be due to pH and temperature effects. Although the V_{max} was defined using this spectrophotometric assay, the concentration of oleamide required to achieve this may have been greater than that needed to achieve the maximum rate under the optimum conditions. For this reason, the concentration necessary to achieve half the maximal rate, i.e. K_m, would also be higher. These results suggest that this spectrophotometric assay of FAAH activity was effective but, to confirm this, it was necessary to validate further the assay by studying the effects of known FAAH inhibitors. This validation procedure is described in the following section.

Tissue	Substrate	K_m (μM)	V_{max} (nmol/min /mg protein)	Reference
Rat brain microsomes	Anandamide	12.7 ± 1.8	5.63 ± 0.20	Desarnaud *et al.*, 1995
Over-expression in COS-7 cells	Anandamide	18	132	Kurahashi *et al.*, 1997
Rat brain microsomes	Anandamide	2.78 ± 0.51	1.40 ± 0.06	Lang *et al.*, 1999
Human brain	Anandamide	2 ± 0.2	0.800 ± 0.075	Maccarrone *et al.*, 1998
Solubilized rat liver plasma membranes	Oleamide	31 ± 3	N.D.	Patricelli *et al.*, 1998
Rat liver membranes	Oleamide	5 ± 2	N.D.	Patterson *et al.*, 1996

Table 6.3: Previously reported values of K_m and V_{max} for fatty acid amide hydrolase. N.D. = Not determined.

6.3.2 FAAH Inhibitor Studies

If the results observed using the novel spectrophotometric assay system were truly due to the hydrolysis of oleamide by FAAH, known inhibitors of the FAAH should inhibit the enzyme in a concentration-dependent manner. To demonstrate this, the effects of methylarachidonyl fluorophosphonate (MAFP), PMSF and anandamide on the assay were investigated. MAFP is a potent, selective and irreversible inhibitor of FAAH, while PMSF is a broad spectrum serine protease inhibitor, which has also been shown to inhibit FAAH irreversibly. As anandamide is a substrate of FAAH, it was also included in this work as a

competitive inhibitor of oleamide hydrolysis. It is also possible that the products of anandamide hydrolysis would inhibit FAAH.

FAAH Inhibitor Assays

Assays were performed essentially as described for the oleamide concentration-response assays, except the volume of buffer in the assay solution was reduced from 192 to 190 μl. When the absorbance of the initial assay solution was constant, 2 μl of ethanolic inhibitor was added to each cuvette followed by 2 μl of oleamide solution. The assay solutions were then stirred and absorbance measured against one blank containing neither inhibitor nor oleamide and a second blank containing oleamide but no inhibitor. Oleamide was present in the assay at 100 μM, while MAFP was assayed at concentrations between 10 nM and 1 μM, PMSF between 3.125 and 50 μM and anandamide between 10 and 320 μM. Each inhibitor concentration was assayed in triplicate using rat liver CPFs from three different animals.

Data Analysis:

Slopes were calculated as described previously and the blank containing neither inhibitor nor oleamide subtracted from the test samples. The percentage inhibition of oleamide hydrolysis was then calculated by comparing the inhibitor samples with the second blank containing oleamide but no inhibitor. The mean $\pm$ SEM inhibition was calculated from the triplicate inhibitor concentrations was then plotted against concentration (log M) and a variable slope sigmoidal curve fitted by non-linear regression using GraphPad Prism. The IC_{50} values generated for each tissue by the program were combined as the mean $\pm$ SEM.

Results:

Representative curves generated by these assays are shown in **figure 6.12**. The validity of this assay was confirmed by the concentration-dependent inhibition of FAAH-catalysed oleamide hydrolysis by these compounds. As predicted, the order of potency was MAFP > PMSF > anandamide, with IC_{50} values of 264 $\pm$ 49 nM, 17 $\pm$ 3 μM and 171 $\pm$ 40 μM for the three compounds, respectively. These values for MAFP and PMSF are higher than expected, as can be observed when

they are compared to IC_{50} values described in the literature (**table 6.4**). There is no reported IC_{50} value for inhibition of FAAH activity by anandamide. There are two possible explanations of these discrepancies. Firstly, as mentioned before, the kinetics of inhibition may have been affected by the lower than optimal pH and temperature employed in this assay. Secondly, it was thought that the lack of preincubation of the inhibitors with FAAH may have affected these results, as methods described in the literature involve preincubating the inhibitors with the enzyme preparations for times of 10 to 20 minutes. The investigation of this possibility is described below.
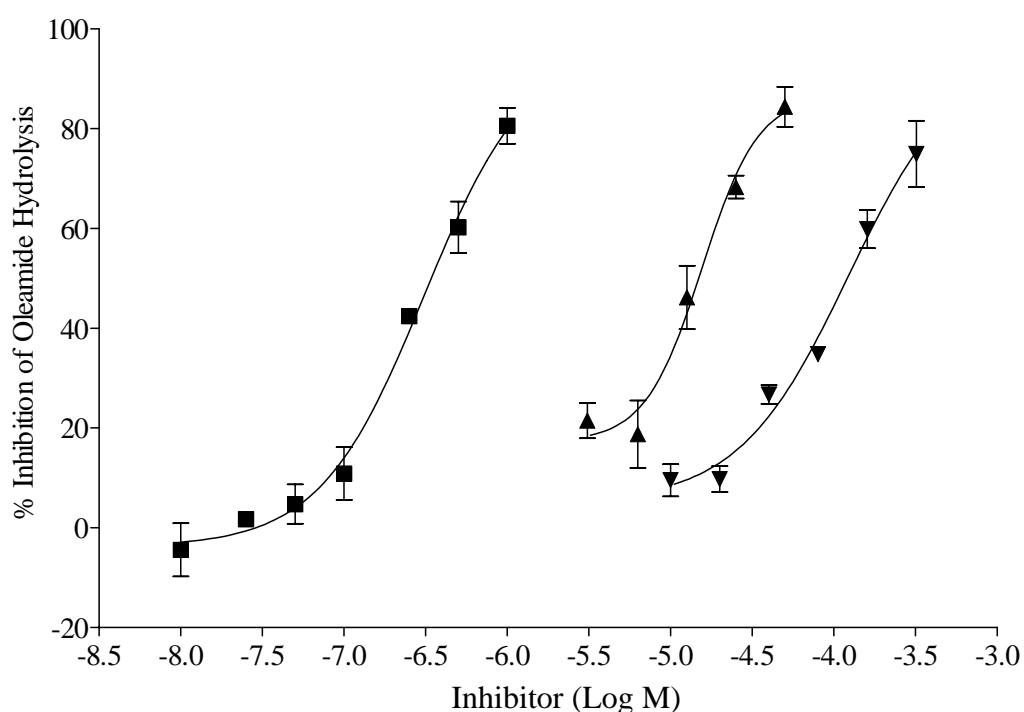
Figure 6.12: Representative data showing the effect of MAFP (■), PMSF (▲) and anandamide (▼) on the FAAH-catalysed hydrolysis of 100 μM oleamide in solubilized rat liver CPF. Data are expressed as the mean ± SEM of three determinations of percentage inhibition.

Tissue	Substrate	Compound	IC$_{50}$	Reference
N18TG2, approx. 10x FAAH purification	100 μM anandamide	MAFP	3 nM	De Petrocellis *et al.*, 1997
RBL-1, approx. 10x FAAH purification	100 μM anandamide	MAFP	1 nM	De Petrocellis *et al.*, 1997
Rat brain homogenate	30 μM anandamide	PMSF	290 nM	Deutsch *et al.*, 1997b
Rat brain membranes minus cerebellum	2 μM anandamide	PMSF	3.7 μM	Fowler *et al.*, 1997

Table 6.4: Previously reported IC$_{50}$ values for inhibition of FAAH activity by MAFP and PMSF.

Preincubation Assays

To investigate the effect of preincubating FAAH with an inhibitor, the enzyme preparation was preincubated with 10 μM PMSF for different periods of time.

Assay Procedure:

The assay procedure was essentially as described above for the inhibitor studies. The effect of 10 μM PMSF on the hydrolysis of 100 μM oleamide was studied with preincubation times 10, 20 and 30 minutes in comparison to no preincubation. Each condition was assayed in triplicate with three different solubilized rat liver CPF preparations. The percentage inhibition of oleamide hydrolysis was calculated and the combined mean ± SEM plotted against preincubation time. To determine whether preincubation significantly affected the inhibition of enzyme activity, one-way analysis of variance was performed on the data. P values were determined by comparing the level of inhibition in preincubated samples with the control using GraphPad Prism.

Results:

The results of the preincubation assays are shown in **figure 6.13**. It is clear that preincubation of FAAH with 10 µM PMSF caused a significant increase in the inhibition of the FAAH-catalysed hydrolysis of 100 µM oleamide compared to the control. This may at least partially explain the higher than expected IC_{50} values reported above.
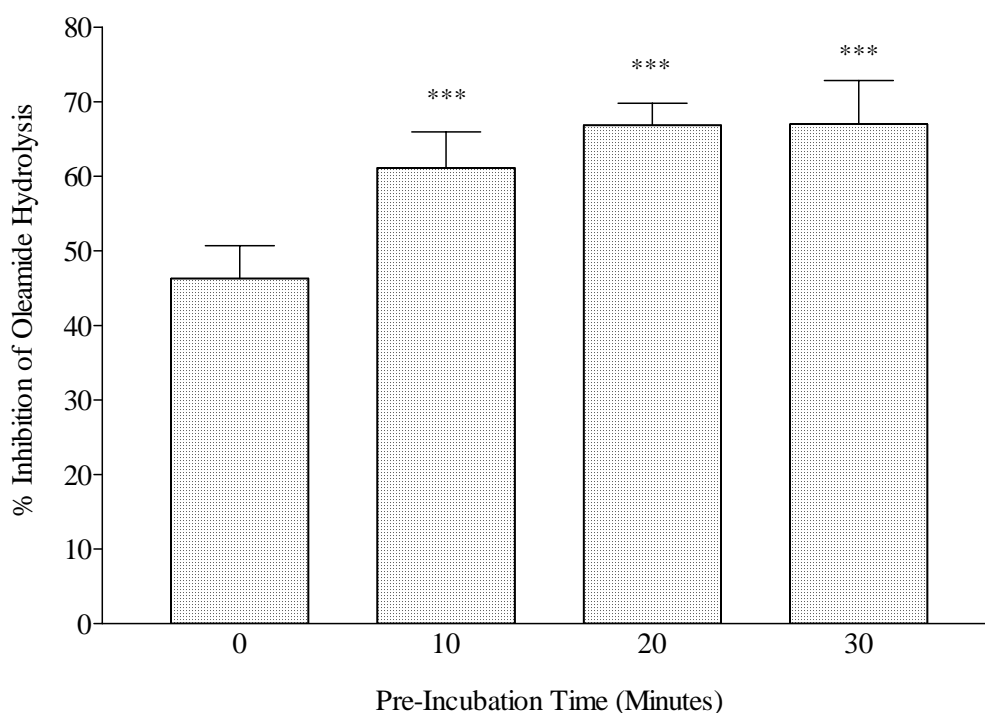
Figure 6.13: The effect of preincubation with 10 µM PMSF on the FAAH-catalysed hydrolysis of 100 µM oleamide in solubilized rat liver CPF. Data are expressed as the mean ± SEM of three independent experiments and were analysed by one-way ANOVA (*** $P < 0.0001$).

The Effect of FAAH Inhibitors on Glutamate Dehydrogenase

To complete the validation of this assay, it was necessary to demonstrate that the observed inhibition of oleamide hydrolysis was not due to the inhibition of glutamate dehydrogenase activity.

Assay Procedure:

Using the solutions described in **section 6.3.1**, 140 μl of solution A, 14 μl of solution B, 192 μl of buffer (1 mM EDTA, 50 mM Tris; pH 7.4) and 2 μl of GDH solution were placed in acrylic cuvettes. Solutions were stirred then gently shaken for at least 10 minutes to allow equilibration and the cuvettes then placed in a Beckman DU650 spectrophotometer. Absorbance was measured at 340 nm and, when constant, 2 μl of ethanol or ethanolic inhibitor solution was added to the cuvettes followed by 100 μl of buffer or ammonium acetate solution (0.45 mM in buffer). Solutions were stirred and absorbance then automatically measured every 38 seconds for up to 30 minutes. Assays consisted of two blank cuvettes, two control cuvettes to measure the GDH reaction rate and two cuvettes to examine the effect of the FAAH inhibitor. Triplicate assays were performed with each inhibitor using MAFP, PMSF and anandamide at assay concentrations of 1, 100 and 320 μM, respectively.

Data Analysis:

Absorbance was plotted against time. Reaction rates were linear up to 300 seconds, so the slopes of the curves were determined from 0 to 266 seconds by linear regression of the data using GraphPad Prism. Initial reaction rates (nmol/min/mg protein) were calculated as described above and the rates of the blanks subtracted from those of the test samples. The rate of the GDH reaction in the presence and absence of FAAH inhibitor was calculated as the mean ± SEM of the combined data and the rate in the presence of inhibitor was then expressed as a percentage of the control rate. To determine whether the reaction rate in the presence of FAAH inhibitor was significantly different from the control rate, the data were analysed by paired t-tests using GraphPad Prism.

Results:

The effect of FAAH inhibitors on the rate of the GDH reaction is shown in **table 6.5**, which clearly demonstrates that none of the inhibitors tested had a significant effect on GDH activity. These data confirm that the observed, concentration-dependent inhibition of oleamide hydrolysis by these compounds was not due to

an effect on GDH and, therefore, finally confirmed that the assay procedure was an effective means of measuring FAAH activity.

FAAH Inhibitor	Control Rate (nmol/min/mg protein)	Rate with Inhibitor (nmol/min/mg protein)	% of Control	P Value
MAFP (1 μM)	205 ± 2	199 ± 2	96.9 ± 1.4	0.069
PMSF (100 μM)	202 ± 2	200 ± 2	99.1 ± 1.3	0.161
Anandamide (320 μM)	226 ± 3	228 ± 3	100.7 ± 1.8	0.182

Table 6.5: The effect of FAAH inhibitors on the rate of GDH-catalysed glutamate production using 100 μM ammonium acetate. Data represent the mean ± SEM of three independent experiments with each inhibitor and were analysed by paired t-tests using GraphPad Prism.

With the completion of the assay validation, it was it was decided to perform one more investigation using this spectrophotometric procedure. To test its versatility, the assay was used to examine FAAH activity in various tissue preparations in order to determine whether there might be tissue-dependent differences, perhaps indicating the existence of more than one form of the enzyme. These experiments are described below.

6.4 Comparison of FAAH Activity in Different Tissue Preparations

The activity of FAAH has been shown to be broadly similar in brain and liver although, as described in **section 1.5.4**, there is evidence for the existence of other enzymes that hydrolyse endocannabinoids. However, most work published

concerning FAAH has involved the use of either solubilized or untreated tissue preparations and no direct comparisons have been made between the two. The original isolation and protein sequencing of FAAH was carried out using soluble protein from rat liver membranes, obtained by treatment with TX-100. This solubilization was used to characterize the FAAH activity in the assays described above, but no consideration was given to any FAAH activity that might be present in the pellet of insoluble protein that remained after solubilization. In the work described below, the FAAH activity in the solubilized and insoluble protein from the crude particulate fraction of rat liver and rat brain was examined.

Preparation of Crude Particulate Fractions:

Frozen livers or brains from Wistar or hooded Lister rats were thawed, weighed and homogenized in 10 volumes of ice-cold buffer (1 mM EDTA, 50 mM Tris; pH 7.4) using a Polytron homogenizer. The homogenate was centrifuged at 1,000g for 5 minutes at 4 °C, and the supernatant was then centrifuged at 36,000g for 20 minutes at 4 °C. The resulting pellet was then suspended in 4 volumes (original wet weight) of ice-cold buffer and manually re-homogenized with a glass/teflon hgomogenizer. Aliquots of the CPF (1 ml) were frozen at -80 °C until required.

Preparation of Soluble and Insoluble Protein Solutions from Rat Liver and Brain CPFs:

Equal volumes of either rat liver or brain crude particulate fraction and solubilization buffer (1 mM EDTA, 50 mM Tris; pH 7.4, 1 % (w/v) TX-100) were mixed, placed on ice and vortexed three times in a fifteen minute period. The mixture was then centrifuged at 9,000g for 5 minutes at 4 °C and the supernatant retained as the soluble protein solution. The insoluble protein was then resuspended, with the aid of sonication, in the original volume of TX-100-free buffer.

Assay of FAAH Activity:

Using the solutions described in **section 6.3.1**, 140 μl of solution A, 14 μl of solution B, 2 μl of GDH solution, 192 μl of buffer and 100 μl of soluble or insoluble protein were placed in acrylic cuvettes and stirred. The solutions were

gently shaken for at least 10 minutes to allow equilibration and then placed in a Beckman DU650 spectrophotometer. Absorbance was measured at 340 nm until constant and the assay initiated by the addition of 2 μl of ethanol or ethanolic oleamide solution (22.5 mM). The solutions were stirred and absorbance automatically measured every 38 seconds for up to 30 minutes at room temperature. Each assay consisted of two blank cuvettes containing ethanol and four test cuvettes containing oleamide. Duplicate assays were performed with both soluble and insoluble protein.

Data Analysis:

The concentration of protein in each tissue solution was determined using the adaptation of the Bradford method (1976) as described in **section 4.3.1**. Rates of oleamide hydrolysis were calculated from the slopes generated by linear regression of the data from 0 to 494 seconds using GraphPad Prism. The mean blank rate in each assay was subtracted from the observed rate for each sample and the mean ± SEM rate of hydrolysis calculated using the data from the duplicate assays.

Results:

The results of this assay are shown in **figure 6.14**. The rates of oleamide hydrolysis using solubilized protein were 3.29 ± 0.08 and 1.05 ± 0.11 nmol/min/mg protein in liver and brain, respectively. This contrasts with the rates observed using the insoluble protein which, for liver and brain, were 10.52 ± 0.18 and 12.58 ±0.60 nmol/min/mg protein. This suggests that the majority of FAAH activity in both rat liver and brain was not solubilized by treatment with TX-100 and remained bound to the plasma membrane. The FAAH activity in the insoluble liver protein was 3.2 times greater than that in the solubilized protein whereas, for brain, the insoluble protein possessed an activity 12.0 times greater than that found in the soluble protein. These results may indicate that the fifteen minute period used for the solubilization of the protein from these tissues was not adequate to achieve effective solubilization. Alternatively, the data may be evidence for the existence of two or more different FAAH activities in rat liver and brain. If this is the case, the activity evident in the insoluble protein

preparations may be more strongly anchored to the plasma membrane than the activity in the soluble preparations. The observed ratios of activities may also be indicative of a variation in the expression of these hypothetical enzymes in the two organs. In order to investigate the possible existence of multiple FAAH activities in these tissues, additional characterization would be required and this, unfortunately, was beyond the scope of this work.
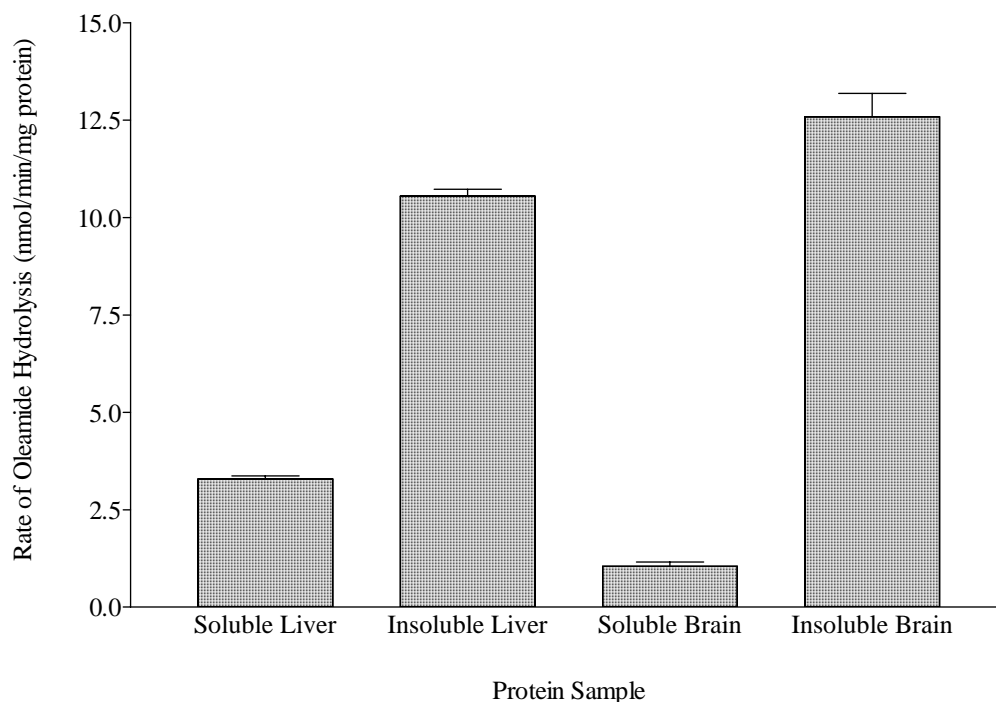
Figure 6.14: The rate of FAAH-catalysed hydrolysis of 100 μM oleamide in solubilized and insoluble protein solutions from rat liver and brain crude particulate fraction. Data represent the mean ± SEM of eight determinations of the hydrolysis rate.

Unlike existing procedures, the spectrophotometric nature of this assay gave it the potential for high-throughput screening (HTS) of compounds for inhibition of FAAH activity. The next section describes the adaptation of the assay for use on a 96 well microtiter plate for the purpose of HTS.

6.5 Adaptation of the FAAH Assay for Use on a Microtiter Plate

Inhibition of FAAH results in an increase in the levels of endogenous cannabinoids and, therefore, it is a potential drug target. However, screening large numbers of compounds for potential inhibitors using existing assays of FAAH activity would be impractical and expensive. The adaptation of this spectrophotometric assay for use on a 96 well (or greater) microtiter plate format would enable the cheap and rapid HTS of compound libraries for their effect on FAAH. Although the sensitivity of the spectrophotometric assay is not sufficient to detect very low levels of FAAH inhibition, the aim of HTS is to identify potent inhibitors and this would be easily achievable.

As the key process in the assay was the use of GDH to detect the ammonia generated by FAAH-catalysed oleamide hydrolysis, it was first necessary to demonstrate that the GDH assay could be adapted for use on a microtiter plate. This procedure is described in the following section.

6.5.1 Measurement of GDH Activity Using a Microtiter Plate Assay

To adapt the GDH methodology for use on a microtiter plate, the major alteration required was a reduction of the assay volume from 450 to 200 μl. To achieve this, the solutions used in the assay were adapted so that the assay concentrations of the individual components were the same as those in the spectrophotometer assay, despite the altered volumes used in this assay.

GDH Microtiter Plate Assay Procedure:

The assay solution was made up by placing 4.5 ml of solution A (49.38 mM α-ketoglutarate, 2.96 mM ADP, 691.36 mM triethanolamine; pH 8.0), 600 μl of solution B (7.41 mM β-NADH, 125.15 mM NaHCO$_3$), 9.4 ml of buffer (1 mM EDTA, 50 mM Tris; pH 7.4) and 500 μl of GDH solution (1600 kU/dm^3 stock in 50 % glycerol diluted to 284.4 kU/dm^3 with buffer) in a universal tube. The solution was thoroughly mixed by vortexing and 150 μl of the mixture placed in

each well of a 96 well microtiter plate. The absorbance of the solutions was measured at 340 nm on a Dynatech MR5000 microplate reader and, when constant, 50 μl of buffer or ammonium acetate solution (12.5 to 800 μM, in buffer) was added to the assay solutions with a multi-tip pipette. The plate was then shaken for 10 seconds and the absorbance of each well was measured every 30 seconds for 5 minutes. Of the eight rows on the plate, one row contained the buffer blank while the other seven each contained a different concentration of ammonium acetate.

Data Analysis:

For each of the eight assay conditions, the wells were treated individually. Absorbance was plotted against time and the slopes of the lines were determined by linear regression using GraphPad Prism. As the concentration of protein in the GDH solution was known, slopes were converted to reaction rates using the equation described in **section 6.2.2** and the mean ± SEM rate was determined from the twelve repeats of each assay condition. The rate at each concentration of ammonium acetate was then determined by subtracting the blank rate from the observed rate. Reaction rate was plotted against ammonium acetate concentration and the data fitted by linear regression using GraphPad Prism.

Results:

The results of this assay are shown in **figure 6.15**, in comparison to those obtained using the spectrophotometer assay.
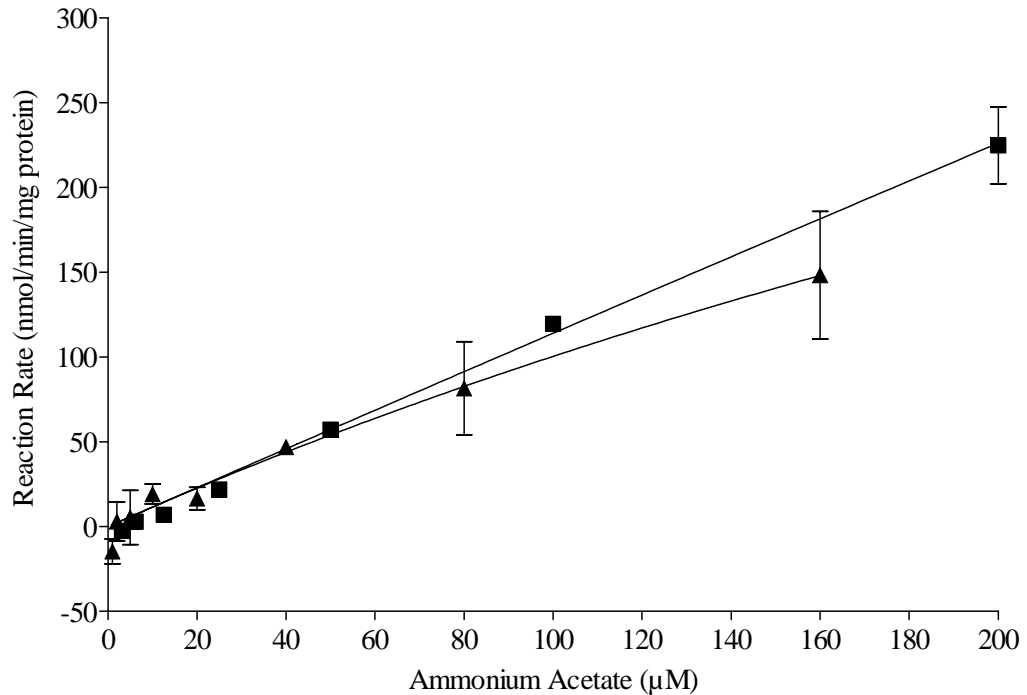
Figure 6.15: Comparison of the effect of ammonium acetate concentration on the rate of GDH-catalysed glutamate formation using spectrophotometer (▲) and microtiter plate (■) assays. Data are expressed as the mean ± range of two determinations of rate (spectrophotometer assay) or the mean ± SEM of twelve determinations of rate (microtiter plate assay) and were fitted by linear regression using GraphPad Prism.

The reproducibility between these two sets of data clearly demonstrates that the spectrophotometric GDH assay could be effectively adapted for use on a microplate reader. The next logical step, therefore, was to investigate whether the same reproducibility existed for the FAAH spectrophotometer assay.

6.5.2 Measurement of FAAH Activity Using a Microtiter Plate Assay

Preliminary Assays

The spectrophotometric FAAH assays were initiated by the addition of 2 µl of ethanolic oleamide solution. To scale down this amount of oleamide solution for use in the microtiter plate assay, it would have been necessary to add 0.89 µl of

ethanolic solution to each well. This was not readily achievable with any accuracy, so it was decided to dilute ethanolic oleamide in buffer before addition to the assays. This proved impossible to achieve as the oleamide consistently precipitated out of solution when diluted in buffer. This problem was not encountered in the spectrophotometer assay as the presence of TX-100 kept it in solution. To counter this problem, the ethanolic oleamide solution was diluted in buffer containing TX-100 and, to limit the amount of the detergent in the assay, tissue was not solubilized and was used directly in the assay. This was achieved as described below.

Assay Procedure:

Frozen aliquots of rat liver CPF were thawed and a tissue solution made up by mixing 2.2 ml of tissue homogenate with 2.8 ml of buffer (1 mM EDTA, 50 mM Tris; pH 7.4). Oleamide was dissolved to appropriate concentrations in ethanol and 20 µl of the ethanolic solution, or ethanol for the blank solution, was diluted by the addition of 980 µl of buffer containing 1 % (w/v) TX-100. Assay solutions were made up by adding 450 µl of solution A, 60 µl of solution B, 50 µl of GDH solution, 500 µl of oleamide solution and 440 µl of buffer in a test tube. The solutions were thoroughly mixed by vortexing and 150 µl of each solution placed in the wells of one column of a 96 well microtiter plate. The absorbance of the solutions was measured at 340 nm on a Dynatech MR5000 microplate reader and, when constant, 50 µl of tissue solution was added to the assay solutions with a multi-tip pipette. The plate was then shaken for 10 seconds and the absorbance of each well was measured every 30 seconds for 5 minutes. The microtiter plate layout consisted of one column of eight blank solutions and six columns containing oleamide at assay concentrations of 3.75 to 200 µM.

Data Analysis:

The absorbance of each well was plotted against time and the rate of reaction (absorbance/sec) was determined by linear regression using GraphPad Prism. The mean ± SEM rate was calculated from the eight repeats of each assay condition and the rate at each concentration of oleamide was then determined by subtracting the blank rate from the observed rate. The concentration of oleamide was plotted

against the rate of hydrolysis and the data fitted by non-linear regression (one-site binding) using GraphPad Prism.

Results:

The results of this preliminary FAAH microtiter plate assay are shown in **figure 6.16**. It is clear from these data that this preliminary assay was not successful. The reason for this undesirable result was unclear, although one factor that may have affected the outcome was the concentration of TX-100 present. In this assay, the TX-100 concentration was 0.245 % (w/v), compared to 0.111 % in the spectrophotometer FAAH assay. Both of these concentrations exceed the critical micelle concentration, the concentration of detergent at which micelles spontaneously form in solution. It is possible that the presence of micelles could cause light scattering, therefore affecting absorbance reading, although this did not appear to have any detrimental effects on the spectrophotometer assay. However, the absorbance readings from the microtiter plate assay were lower than the corresponding spectrophotometer assay because of the smaller path length involved. Any effects of light scattering by micelles would, therefore, have a greater effect on the plate assay than the spectrophotometer assay. This, combined with the higher TX-100 concentration, may be the reason for the failure of this preliminary assay. The next section describes how this problem was investigated using oleamide solutions with different concentrations of detergent.
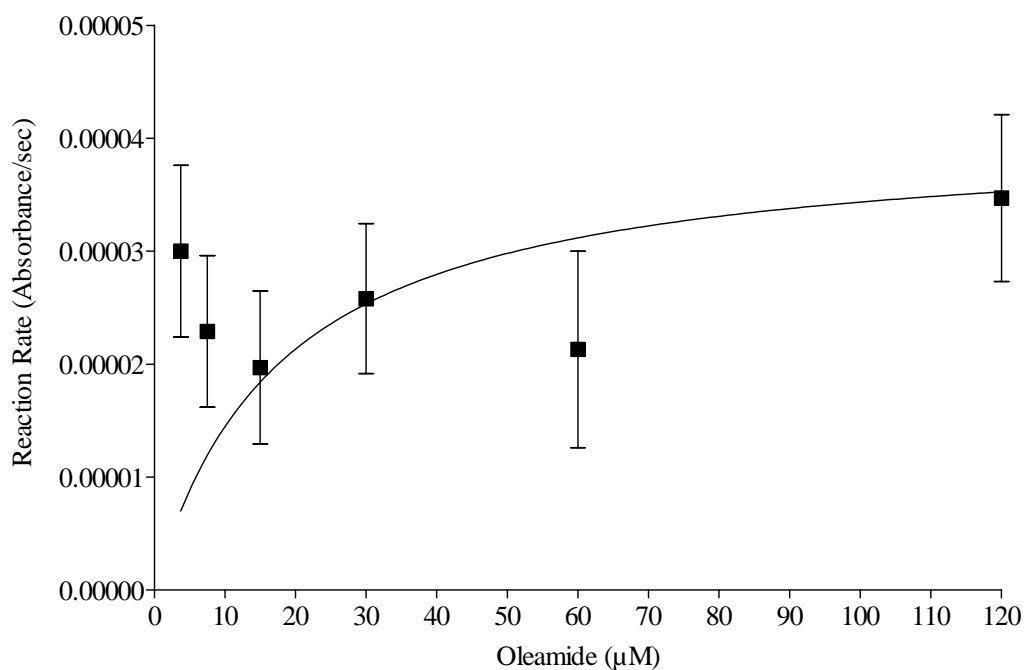
Figure 6.16: The effect of oleamide concentration on the rate of FAAH-catalysed oleamide hydrolysis using a microtiter plate assay. Data are expressed as the mean ± SEM of eight determinations of rate and were fitted by non-linear regression (one-site binding) using GraphPad Prism.

Comparison of Oleamide Solutions and Tissue Preparations

The method of oleamide solubilization described for the preliminary microtiter plate assay (solution one) was compared against an oleamide solution with significantly less TX-100. This solution (solution two) was made by diluting 200 μl of the appropriate concentration of ethanolic oleamide with 1.8 ml buffer containing 1 % (w/v) TX-100. This solution was then diluted five-fold in detergent-free buffer. Both oleamide solutions were then assayed using neat or solubilized rat liver crude particulate fraction to determine which appeared most effective.

Assay Procedure:

Two initial assay solutions were made up by placing 2.25 ml of solution A, 300 μl of solution B and 250 μl of GDH solution in universal tubes. For assays using neat

tissue, 1.1 ml of rat liver CPF and 3.6 ml of buffer was added to the initial assay solution. For assays using solubilized tissue, rat liver CPF was solubilized as previously described and 2.2 ml of this solution and 2.5 ml of buffer was added to the initial solution. Solutions were thoroughly mixed by vortexing and 150 μl of each solution placed in the relevant wells of a 96 well microtiter plate. The absorbance of the solutions was measured at 340 nm on a Dynatech MR5000 microplate reader and, when constant, 50 μl of the appropriate oleamide solution or blank solution was added with a multi-tip pipette. The plate was then shaken for 10 seconds and the absorbance of each well was measured every 30 seconds for 5 minutes. Each of the two oleamide solutions and their corresponding blank solutions were assayed in both neat and solubilized rat liver CPF with oleamide concentrations of 60 and 120 μM. Eight determinations of oleamide hydrolysis rate were made for each assay condition and rates of oleamide hydrolysis were determined as described for the preliminary FAAH microtiter plate assay.

Results:

The data in **figure 6.17** show the effect of the oleamide and tissue solutions on the rate of oleamide hydrolysis by FAAH in comparison with typical data from the standard FAAH spectrophotometer assay. It is apparent from this data that the use of oleamide solution two, with the reduced level of TX-100, resulted in a greatly reduced blank rate compared to the rate of hydrolysis in the presence of oleamide. Assays A and C, with the highest levels of detergent, were ineffective. Of the remaining microtiter plate assays, assay D showed the greatest correlation with the data from the spectrophotometer assay. The distinction between the two oleamide concentrations was greater in this assay, suggesting that solubilization of the rat liver CPF was more effective than the use of the neat tissue preparation. This was not unexpected, as the conditions in assay D were the closest to those used in the spectrophotometer assay.
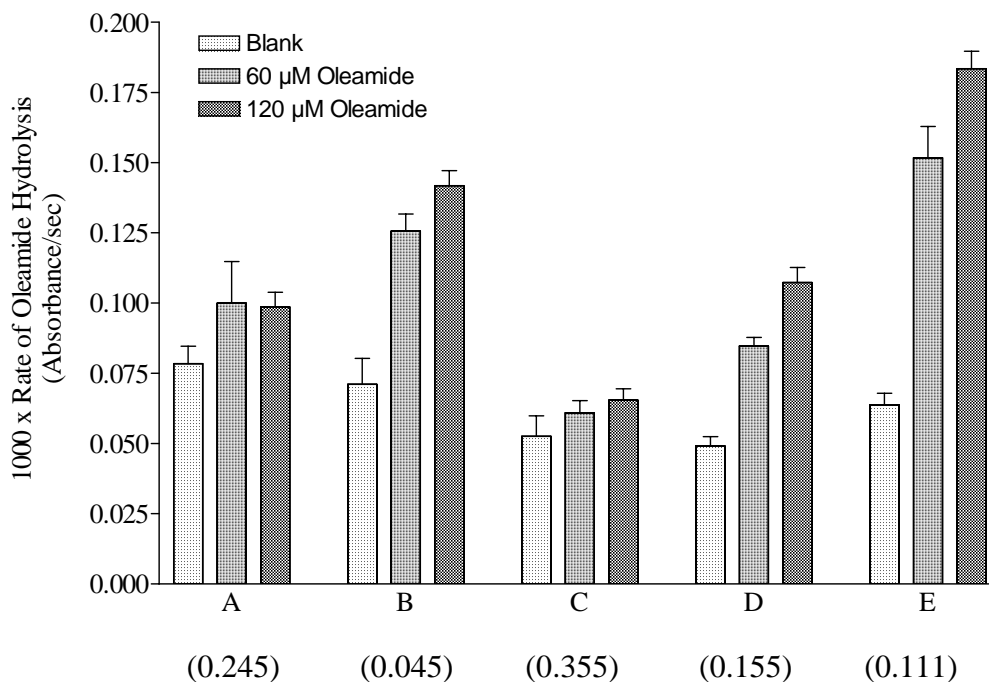
Figure 6.17: The rate of FAAH-catalysed oleamide hydrolysis in microtiter plate assays using oleamide solutions one and two with neat (A and B) or solubilized (C and D) tissue, compared to data obtained from a typical FAAH spectrophotometer assay (E). Data are expressed as the mean ± SEM of eight determinations of rate for the plate assay and three determinations for the spectrophotometer assay. The numbers in brackets represent the TX-100 concentration in each assay.

To determine whether these conditions were also effective at lower oleamide concentrations, concentration-response assays were performed. Quadruplicate determinations of the rate of oleamide hydrolysis were made at oleamide assay concentrations of 3.75 to 120 µM using three different solubilized rat liver CPFs. Reaction rates (absorbance/sec) were determined as described above and plotted against oleamide concentration. The results of these assays are shown in **figure 6.18**. It is clear from these data that there was no evident relationship between the concentration of oleamide and the rate of its hydrolysis by FAAH using the microtiter plate assay. The rates of hydrolysis at the lower oleamide concentrations were not distinguishable from one another, making any kinetic

analysis impossible so, due to these disappointing results and time constraints, no further kinetic investigations were undertaken using this FAAH assay procedure. However, as the main aim of this adaptation was the high throughput screening of potential FAAH inhibitors, the effect of PMSF on the rate of hydrolysis of oleamide by FAAH was examined as described below.
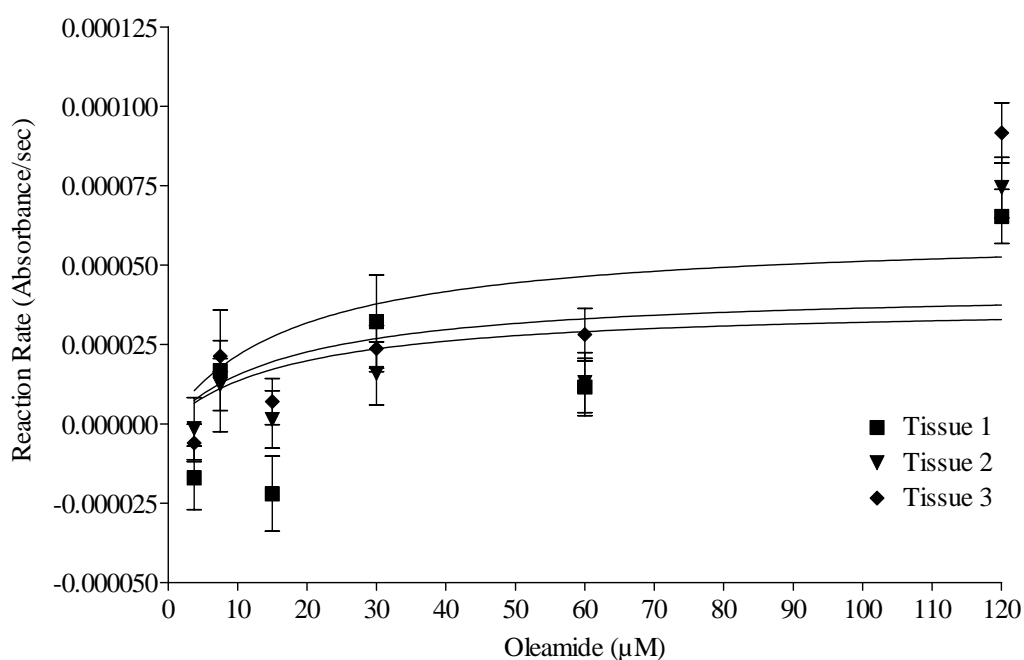
Figure 6.18: The effect of oleamide concentration on the rate of FAAH-catalysed oleamide hydrolysis using adapted microtiter plate assays. Data are expressed as the mean ± SEM of four determinations of rate and were fitted by non-linear regression (one-site binding) using GraphPad Prism.

6.5.3 Investigation of the Effect of PMSF on FAAH Activity Using a Microtiter Plate Assay

If this assay was to be used to screen a library of compounds for potential potent inhibitors of FAAH activity, it would only be necessary to examine the effect of the compounds on the hydrolysis of a single concentration of oleamide. If a potential FAAH inhibitor was identified, more detailed kinetic studies could then be undertaken using the spectrophotometer FAAH assay or a "traditional" assay

for FAAH activity. The use of higher oleamide concentrations appeared to be the only effective measure of the rate of FAAH-catalysed oleamide hydrolysis in the attempted microtiter plate assays so, to investigate the viability of using this assay for HTS, the effect of 10 μM PMSF on the rate of hydrolysis of 100 μM oleamide by FAAH was investigated. This concentration of oleamide was chosen so a direct comparison could be made between this assay and the spectrophotometer assays with PMSF, which also used oleamide at 100 μM.

Assay Procedure:

Frozen rat liver crude particulate fraction was thawed and solubilized with an equal volume of buffer (1 mM EDTA, 50 mM Tris; pH 7.4) containing 1 % TX-100 (w/v), as described previously. Oleamide was dissolved to 20 mM in ethanol, diluted ten-fold with buffer containing 1 % TX-100 (w/v) and this solution was then diluted five-fold in detergent-free buffer. PMSF was dissolved to 1 mM in ethanol, then assay solutions made by combining 900 μl of solution A, 120 μl of solution B, 100 μl of GDH solution, 880 μl of solubilized rat liver crude particulate fraction, 960 μl of buffer and 40 μl of ethanol or PMSF solution in a test tube. This solution was mixed by vortexing and 150 μl per well placed in a 96 well microtiter plate. After 30 minutes preincubation of PMSF with FAAH, the absorbance of the solutions was measured at 340 nm on a Dynatech MR5000 microplate reader and, when constant, 50 μl of oleamide solution or oleamide-free blank solution was added with a multi-tip pipette. The plate was then shaken for 10 seconds and the absorbance of each well was measured every 30 seconds for 5 minutes. Assays consisted of eight wells containing blank solutions, eight wells with oleamide and eight wells with oleamide and PMSF. Triplicate assays were performed using rat liver CPFs from three different animals.
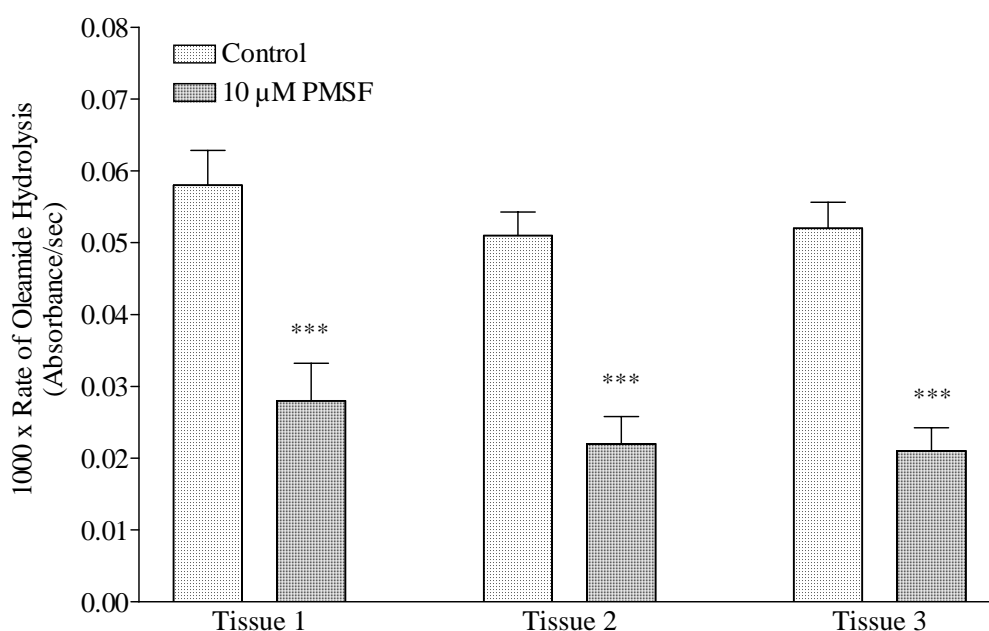
Data Analysis:

The absorbance of each well was plotted against time and the rate of reaction (absorbance/min) determined by linear regression of the data using GraphPad Prism. The mean ± SEM rate was calculated from the eight determinations at each assay condition and the blank rate subtracted from the observed rates of hydrolysis for oleamide and oleamide in the presence of PMSF. To test if the rate

of oleamide hydrolysis in the presence of PMSF was significantly different from that of the control, data were analysed with un-paired t tests using GraphPad Prism.

Results:

The effect of 10 μM PMSF on the FAAH-catalysed hydrolysis of 100 μM oleamide in the microtiter plate assay is shown in **figure 6.19**. These data show that PMSF significantly inhibited FAAH activity. The mean inhibition of oleamide hydrolysis in the three experiments was 55.96 ± 1.90 % which compares well with the spectrophotometer assay, where 10 μM PMSF inhibited the hydrolysis of 100 μM oleamide by 34.35 ± 1.45 %. The difference in inhibition can be explained by the lack of preincubation of PMSF with FAAH prior to the spectrophotometer assays. These results give clear evidence that this microtiter plate assay can be used for the HTS of libraries of compounds for inhibitors of FAAH activity.


Figure 6.19: The effect of 10 μM PMSF on the rate of FAAH-catalysed hydrolysis of 100 μM oleamide using a microtiter plate assay. Data represent the mean ± SEM of eight determinations of hydrolysis rate and were analysed using un-paired t-tests (*** $P < 0.0001$).

The final investigations using this novel assay system concerned the examination of the effects of the aryl ethanolamide and phosphinic acid test compounds on FAAH activity. These experiments are described below.

6.6 Investigation of the Effects of Test Compounds on FAAH Activity

The effects of the novel test compounds on the hydrolysis of 100 μM oleamide by FAAH were examined using the same methodology described for the known inhibitors of the enzyme. Each compound was tested in triplicate at an assay concentration of 10 or 100 μM, depending on their solubility in ethanol, and duplicate assays were performed using solubilized preparations of rat liver CPFs from two different animals. After subtracting the blank slope from the test slopes, the percentage inhibition of oleamide hydrolysis by each compound was calculated by comparison with the control rate. The mean ± range percentage inhibition was then calculated. The results from these assays are shown in **figure 6.20**.

It is clear from these data that, as with the other potential targets investigated, the test compounds had no effect on the rate of FAAH-catalysed oleamide hydrolysis. These results are especially disappointing considering that the two alklylphosphinic acids were designed to be the phosphinic acid analogues of known FAAH inhibitors. This suggests that the phosphinic acid moiety is not a transition state inhibitor of the hydrolysis of endocannabinoids and oleamide by FAAH.
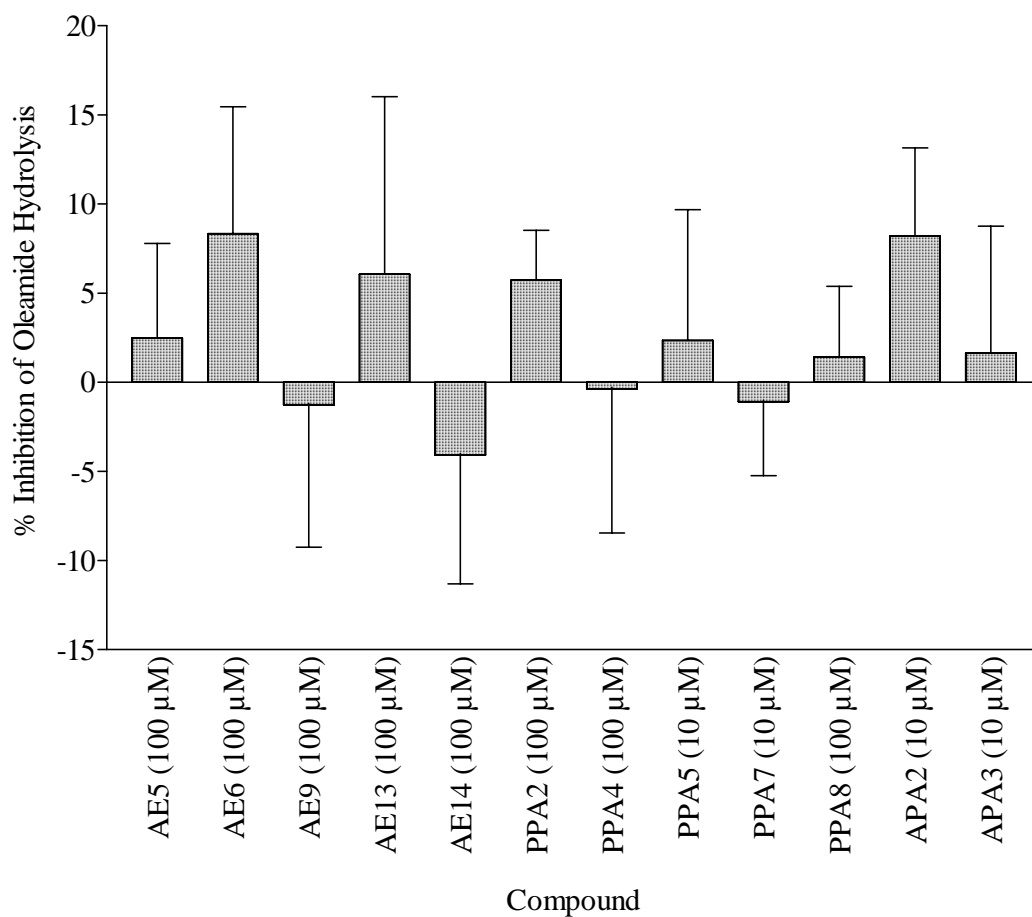
Figure 6.20: The effect of the novel aryl ethanolamide and phosphinic acid test compounds on the FAAH-catalysed hydrolysis of 100 μM oleamide. Data are expressed as the mean ± range of two independent experiments, each performed with triplicate concentrations of test compound.
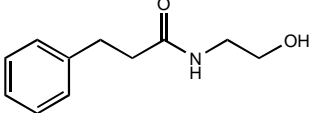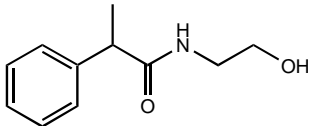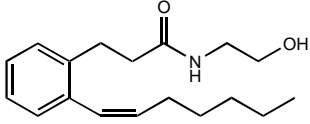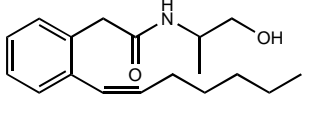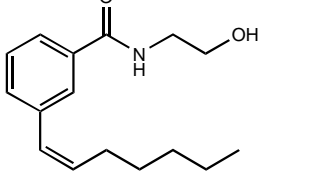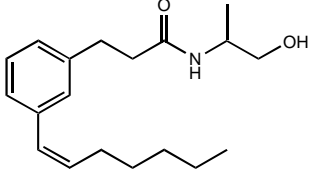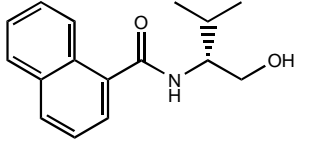
Chapter 7:

Summary and General

Discussion

7.1 CB1 Receptor Binding Studies

It is clear from the data presented in **chapter 3** that the novel aryl ethanolamide and phosphinic acid compounds synthesized during this research had very little or no affinity for the CB1 receptor. The only two compounds that exhibited even low CB1 receptor affinity were the aryl ethanolamides AE5 and AE6, although the approximate K_i value for both compounds was >76.5 μM. In rat brain membranes, no increase in $[^{35}S]$-GTP-γ-S binding was observed above basal levels in the presence of the target compounds suggesting that, in addition to the CB1 receptor, the target compounds did not activate any other GPCRs in this tissue. Of course, this does not rule out the possibility that these compounds are antagonists of other GPCRs, but the investigation of this possibility was beyond the scope and aims of this work. This lack of pharmacological activity is not entirely unexpected for the alkylphosphinic acid compounds. The lack of unsaturation in the alkyl chains of APA2 and APA3 resulted in these compounds being analogous to saturated fatty acid amides which do not possess CB1 receptor affinity. The incorporation of carbon-carbon double bonds in the alkyl chain, as was the ultimate aim for these compounds, may result in an increased CB1 receptor affinity, although this is purely speculative.

Despite these disappointing results, research published since the completion of this work has shown that the aryl ethanolamide template was a valid target for the synthesis of potential cannabimimetic drugs. Berglund *et al.* (2000) synthesized a series of monocyclic and bicyclic alkyl amide cannabinoid receptor ligands, structurally very similar to the aryl ethanolamide compounds described in this thesis. The structures of some of these compounds and their K_i values at the CB1 and CB2 receptors are shown in **table 7.1**. It is apparent from these data, that the compounds described by Berglund *et al.* were generally selective for the CB1 receptor. Structurally, when compared to the aryl ethanolamides, it is clear that affinity for the cannabinoid receptors is greatly increased by the incorporation of an alkyl chain with a *cis* double bond at the *ortho* or *meta* position of the benzene ring. It can only be assumed that similar structural modifications applied to the

phenylphosphinic acid compounds would also confer affinity for the cannabinoid receptors and resistance to hydrolysis *in vivo*.

Compound	Structure	CB1 K_i (nM)	CB2 K_i (nM)	CB1/CB2 Ratio
AE5		>76.5 µM	-	-
AE6		>76.5 µM	-	-
1		371	474	0.78
2		359	672	0.53
3		38	99	0.38
4		59	305	0.19
5		6800	849	8.00

Table 7.1: The structures and K_i values at the CB1 and CB2 receptors of compounds synthesized by Berglund *et al*. (2000) in comparison to AE5 and AE6.

The development of these novel cannabinoid ligands by Berglund *et al*. offers the possibility that the synthesis of compounds of this type with even higher receptor affinities is possible. No mention was made by these authors, however, of the ability of these cyclic alkyl amides to inhibit anandamide uptake or FAAH. These

compounds would possibly act as modulators of these targets given that they are structural mimics of the endogenous cannabinoids. Therefore, the hypothesis that aryl ethanolamides are potential cannabimimetic drugs has been shown to be valid, although the compounds generated lacked sufficient structural diversity. This cannabimimetic potential may also apply to phenylphosphinic acid compounds.
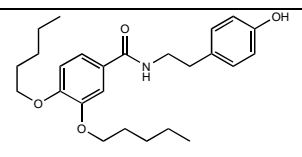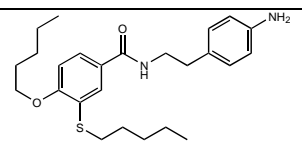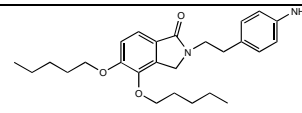

7.2 CB2 Receptor Binding Studies

To date, the porcine CB2 receptor has not been cloned and little research has been performed to elucidate the binding profile of this receptor. The data presented in **chapter 4** demonstrate the development of an effective cannabinoid competition assay using porcine spleen membranes. The K_d of CP-55,940 in this tissue preparation was shown to be 1.55 nM with a B_{max} value of 169 fmol/mg protein. This K_d value compares well with values in the literature using the cloned human, murine and rat CB2 receptors. The K_i values of a number of cannabinoid receptor ligands were determined using this assay system and also compared favourably with data from cloned CB2 receptors. Confirming reports in the literature that there is only a low level of FAAH activity in the spleen, pre-treatment of spleen membranes with PMSF prior to competition assays with anandamide had no effect on the K_i value of this endocannabinoid. The differences in the K_d and K_i values compared to data in the literature are likely to be due to inter-species differences in the CB2 receptors and the unavoidable presence of CB1 receptors in the spleen membranes, albeit at much lower levels than the CB2 receptor. Attempts at developing a $[^{35}S]$-GTP-γ-S binding assay using porcine spleen membranes were unsuccessful, however, presumably due to the low number of cannabinoid receptors in this tissue compared to brain membranes in which $[^{35}S]$-GTP-γ-S binding assays were possible.

The potential affinities of the target compounds for the CB2 receptor was also examined using this assay. The presence of CB1 receptors in the spleen membranes had no effect on these experiments as very little or no affinity for the

CB1 receptor was observed for these compounds. Similarly, this was also the case for the CB2 receptor, with no compound showing even low affinity. As described for CB1 receptor affinity in **section 7.1**, the lack of CB2 receptor affinity exhibited by the alkylphosphinic acid compounds was not unexpected. The endogenous saturated fatty acid amides, of which these compounds are analogues, do not bind to the CB2 receptor, although it would be interesting to examine the effects of these compounds on the postulated CB2-like receptor(s) with which palmitoylethanolamide, itself an saturated species, may interact. It is likely that the lack of unsaturation in these compounds was a major impediment to their ability to bind to the CB2 receptor.

However, since the synthesis of the target aryl ethanolamide and phosphinic acid compounds was completed, a worldwide patent by Japan Tobacco Inc. (1997) disclosed highly selective ligands for the CB2 receptor that were based on an aryl ethanolamide template. Of 391 compounds tested, 32 proved to be potent cannabinoid receptor ligands and some of these species are shown in **table 7.2**.

Structure	CB1 K_i (nM)	CB2 K_i (nM)	CB1/CB2 Ratio
	>3300	0.44	>7500
	>4300	1.9	>2263
	330	0.11	3000

Table 7.2: The structures and K_i values at the CB1 and CB2 cannabinoid receptor of highly selective CB2 receptor ligands developed by Japan Tobacco.

It is evident that these compounds are the most selective CB2 ligands yet and, although their pharmacology has not been examined in detail, they have great therapeutic potential and may inhibit endocannabinoid uptake and degradation. Structurally, these compounds differ from the aryl ethanolamides by the inclusion
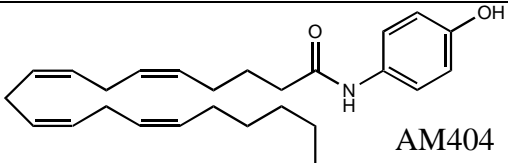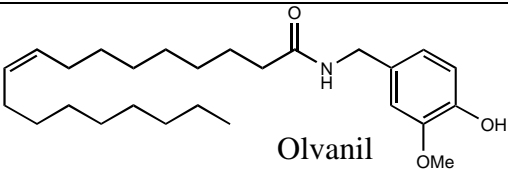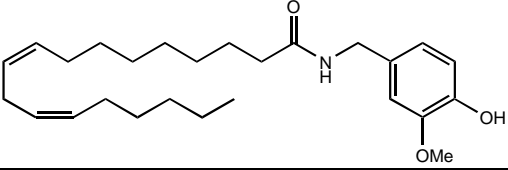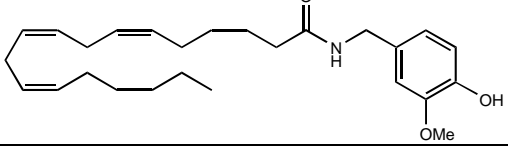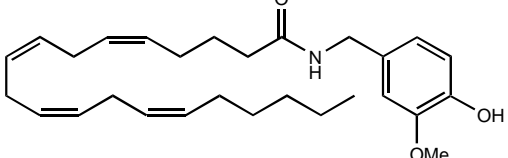
of a substituted phenyl group in place of the hydroxy group and alkyl ester or alkyl sulphide substituents at the *meta* or *para* positions of the benzene ring. The phenylphosphinic acid equivalents of these compounds may also exhibit high affinity for the cannabinoid receptors while being resistant to hydrolysis. Therefore, as for the CB1 receptor, the hypothesis that aryl ethanolamides, and possibly their corresponding phenylphosphinic acids, are potential cannabimimetic drugs has been shown to be valid although more structural diversity was required than in the compounds whose synthesis this thesis describes.

7.3 Anandamide Uptake Studies

Accumulation of anandamide into the mouse neuroblastoma cell line N18TG2 was previously demonstrated by Deutsch & Chin (1993) but, until now, this mechanism had not been characterized. [^{3}H]-Anandamide uptake into cultured N18TG2 cells was shown to be concentration-, time- and temperature-dependent. In addition, this accumulation was inhibited by the selective anandamide transport inhibitor AM404 and the prostaglandin E_2 uptake inhibitor bromocresol green, confirming the characteristics of the anandamide uptake system observed by Beltramo *et al*. (1997) in rat neurones and astrocytes. However, although not fully characterized, the kinetics of anandamide uptake into N18TG2 cells differed from those reported by Beltramo *et al*. The K_m observed in N18TG2 cells fell between the K_m values reported for rat neurone and astrocyte anandamide accumulation and the time taken to achieve 50 % of the maximal rate appeared considerably greater than in these two rat cell types. Nonetheless, the presence of an anandamide uptake system was confirmed in N18TG2 cells, allowing the effects of the aryl ethanolamide and phosphinic acid target compounds on this transporter to be investigated.

None of the target compounds displayed any significant inhibitory effect on anandamide uptake into cultured N18TG2 cells. The only compound that was a possible anandamide uptake inhibitor, PPA2, displays some structural similarities

with AM404. However, higher concentrations of PPA2 than the single 10 µM assay concentration used would be required to confirm any effects. All inhibitors of anandamide uptake described in the literature, with the exception of bromocresol green, show at least some affinity for one or both cannabinoid receptors. Considering the lack of cannabinoid receptor affinity displayed by the compounds synthesized in the course of this research, it is perhaps not surprising that they were not effective in inhibiting anandamide uptake. However, since the chemical synthesis of the target compounds was completed, it has been shown that the vanilloid receptor ligand olvanil and its derivatives inhibit anandamide uptake with IC_{50} values approaching that of AM404. Some of these compounds are shown in **table 7.3**.

Structure	IC_{50} (µM)
AM404	2.2
Olvanil	9.0
	7.0
	5.0
	3.6

**Table 7.3**: The structures and IC_{50} values at the anandamide transporter of AM404 and some of the vanilloid receptor ligands (Melck *et al.*, 1999b).

The structural similarities between these compounds and the long alkyl chain phenylphosphinic acids are obvious. It is entirely possible that incorporation of a *para*-hydroxy group into the benzene ring of PPA5 (octadecylphenylphosphinic acid) and at least one carbon-carbon double bond in the alkyl chain would enable this compound to inhibit anandamide uptake. Unfortunately, the anandamide transporter and its inhibitors were unknown at the time the target compounds were synthesized and, therefore, they were not designed as uptake inhibitors. However, as with the CB1 and CB2 receptor affinity, their lack of structural diversity appears to have severely limited their biological activity.

7.4 Fatty Acid Amide Hydrolase Studies

Chapter 6 describes a novel spectrophotometric assay for rat liver FAAH activity as an alternative to the widely used radiochemical- and HPLC-based assays. Using this methodology, the K_m and V_{max} values for FAAH-catalysed oleamide hydrolysis were determined and found to be similar to values published in the literature. In addition, inhibition of FAAH by MAPF, PMSF and anandamide was observed in a concentration-dependent manner, although the IC_{50} values of these compounds were higher than previously published data. However, "traditional" FAAH assays often involve pre-incubation of the enzyme with an inhibitor prior to initiation of the reaction. Using the spectrophotometric assay, PMSF was pre-incubated with FAAH for up to 30 minutes and this procedure significantly increased the level of inhibition. It was also shown that the levels of FAAH activity in solubilized and insoluble membrane fractions of rat brain and liver were significantly different. This may be due to the presence of more than one FAAH enzyme in these tissues, although further research is required to confirm this. In addition, due to the spectrophotometric nature of this assay, the possibility of scaling down the protocol for use on microtiter plates was examined. Although kinetic analysis of FAAH activity was not readily achievable on a microtiter plate, the assay was shown to have the potential for high-throughput screening of chemical libraries for FAAH inhibitors. This may prove important in the development of novel cannabimimetic drugs.

When the novel aryl ethanolamide and phosphinic acid target compounds were assayed for their ability to inhibit FAAH activity, no biological activity was apparent. The aryl ethanolamides and phenylphosphinic acids were ineffective as ligands for the CB1 and CB2 cannabinoid receptors and, therefore, would not be expected to compete with endogenous fatty acid amides for FAAH. However, although inactive in cannabinoid receptor competition and anandamide uptake assays, it was hoped that the alkylphosphinic acids would inhibit FAAH. These compounds were primarily designed as transition state FAAH inhibitors, being the phosphinic analogues of potent FAAH inhibitors, so these results are especially disappointing. Therefore, it is apparent that the phosphinic acid moiety does not inhibit the transition state of FAAH-catalysed amide bind hydrolysis. As described in **section 1.5.3**, new evidence now supports the proposal that FAAH catalyses the hydrolysis of both amide and ester bonds by a novel mechanism (Patricelli *et al*., 1999; Patricelli & Cravatt, 1999). This novel activity may be a contributary factor in the failure of the alkylphosphinic acid compounds to inhibit oleamide hydrolysis. It is also apparent from existing FAAH inhibitors that a good leaving group, such as a fluorine atom, is necessary for reaction with serine or cysteine residues at the active site of the enzyme. This is demonstrated for the sulphonyl fluoride and methyl fluorophosphonate compounds in **scheme 7.1**.
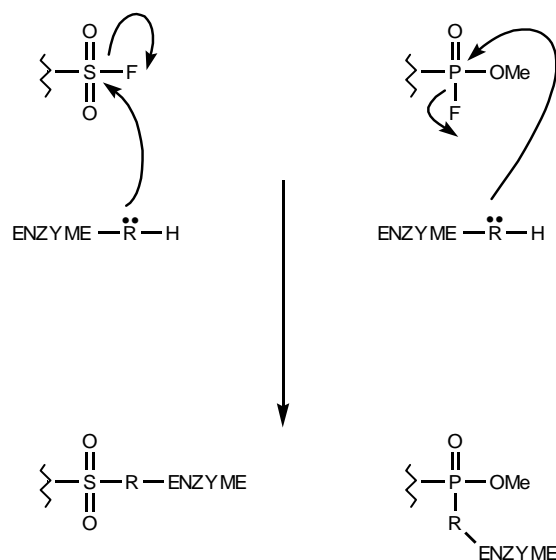
Scheme 7.1: Proposed mechanism by which sulphonyl fluorides and methyl fluorophosphonates inhibit FAAH, demonstrating the importance of a good leaving group (Di Marzo & Deutsch, 1998). R = O or S.

It is likely that modifying APA2 and APA3 by replacing the hydrogen atom or hydroxyl group of the phosphinic acid moiety with a good leaving group would confer the ability to inhibit to FAAH on these compounds. This effect could be increased by the incorporation of at least one carbon-carbon double bond in to the alkyl chain, thereby mimicking FAAH substrates such as oleamide. Such modifications may also impart inhibitory activity on the phenylphosphinic acid compounds, although a deal of work is required to confirm these assumptions.

7.5 Conclusion

None of the novel target compounds described in this thesis proved to be cannabimimetic. It is clear that the limited structural diversity of these compounds compromised their biological activity and, therefore, future work inevitably requires the inclusion of more varied substituent groups into species. However, the potential remains for the development of modulators of endocannabinoid signalling based on the aryl ethanolamide, phenylphosphinic acid and alkylphosphinic acid templates. Compounds analogous to the aryl ethanolamides have already been shown to act as cannabinoid receptor ligands by Berglund *et al.* and Japan Tobacco. There are no reports in the literature, however, of cannabimimetic compounds containing the phosphinic acid moiety, although phosphorus-containing compounds are able to bind to the CB1 receptor and FAAH, demonstrated by the methyl fluorophosphonates which are CB1 receptor agonists and potent FAAH inhibitors (Martin *et al.*, 2000). Therefore, as described in this chapter, structural modifications of the phenylphosphinic and alkylphosphinic acids may confer affinity for the cannabinoid receptors or the ability to inhibit endocannabinoid uptake and FAAH. The activity of these compounds would be enhanced by their metabolic stability, imparting an extended half-life *in vivo*.

Research in to the endocannabinoid system is still at a relatively early stage and it is highly likely that there are targets for cannabimimetic drugs that remain undiscovered. Indeed, there is mounting evidence for the existence of enzymes other than FAAH that catalyse endocannabinoid degradation (Goparaju *et al.*,

1999; Ueda *et al*., 1999) the presence of peripheral CB1-like (Pertwee, 1999) and CB-2 like (Griffin *et al*., 1997; Calignano *et al*., 1998) receptors in the body. To date, these receptors have been implicated in the tumour suppressive effects (De Petrocellis *et al*., 1998), vasodilatory effects (Harris *et al*., 1999; Járai *et al*., 1999) and attenuation of pain responses (Calignano *et al*., 1998) that are modulated by endocannabinoids and may present opportunities for novel therapies. Of particular interest is the dissociation of the potential psychotropic effects of cannabimimetics from their positive therapeutic effects. Peripheral CB1- and CB2-like receptors offer a real possibility of achieving this goal. Therefore, although the novel target compounds described in this thesis possessed no biological activity at the known targets involved in endocannabinoid signalling, it may be that they, or their derivatives, may act as specific ligands for undiscovered components of the endogenous cannabinoid signalling pathways.

Appendix A:

Synthetic Chemistry Protocols

and Physical Data

A1. Physical Measurements

Analytical thin layer chromatography was performed on aluminium-backed Merck silica gel 60 F_{254} plates and visualization of spots achieved using ultraviolet light or potassium permanganate staining. Flash column chromatography was performed using Merck silica gel 60, particle size 0.04-0.063 mm.

Melting point determinations were carried out using Griffin melting point apparatus.

All ^{1}H and ^{31}P NMR spectra were obtained using a Bruker ARX250 nuclear magnetic spectrometer and chemical shifts are quoted as parts per million on the δ scale. Mass spectra were recorded on a Micromass Platform mass spectrometer by Dr Catherine Ortori in the School of Pharmaceutical Sciences, University of Nottingham. Microanalysis was performed by Mr Trevor Spencer in the Microanalysis Laboratory, School of Chemistry, University of Nottingham.

A2. Synthesis of Aryl Ethanolamides

Acid Chloride Strategy

Typical Experimental Protocol:

The appropriate carboxylic acid (3.0 mmol) was dissolved in a suitable solvent (30 to 50 ml) in the presence or absence of DMF (1.50 to 4.77 mmol). The stirred solution was cooled to 0 °C in an ice bath, oxalyl chloride (3.27 to 5.73 mmol) was added and the solution stirred at room temperature under an inert atmosphere or with a silica guard tube for between 30 minutes and 3 hours. After this time, the solution was cooled to 0 °C and ethanolamine (5.40 to 16.50 mmol) added. Stirring was continued for between 20 minutes and 2 hours at room temperature and the solution then washed potassium hydrogen sulphate solution (1 M, 20 ml), saturated sodium hydrogen carbonate solution (20 ml), distilled water (20 ml) and saturated sodium chloride solution (20 ml). The solution was dried over magnesium sulphate, filtered and solvent removed *in vacuo* to yield the crude product, which was purified by flash column chromatography.

The following compounds were synthesized using this methodology:

N-(2-Hydroxyethyl)-3-phenylpropionamide (AE5) as a crude white solid (0.26 g, 40 %), purified by flash chromatography using DCM:MeOH (95:5) as eluent to yield a crystalline white solid (0.17 g, 26 %), R_f 0.30, m.p. 77-79 °C; δ_H (250 MHz, CDCl$_3$) 2.50 (2H, t, J=7.63 Hz, PhC*H$_2$*), 2.97 (2H, t, J=7.63 Hz, PhCH$_2$C*H$_2$*), 3.35 (2H, q, J=5.00 Hz, NHC*H$_2$*), 3.62 (2H, t, J=4.88 Hz, C*H$_2$*OH), 5.97 (1H, s, NH), 7.18-7.32 (5H, m, CH$_2$C$_6$*H$_5$*); *m/z* 194.4 (MH$^+$, 100 %), MH$^+$ requires 194.4. C 67.64; H 7.63; N 6.71 %. C$_{11}$H$_{15}$NO$_2$ requires C 68.37; H 7.82; N 7.25 %.

N-(2-Hydroxyethyl)-2-phenylpropionamide (AE6) as crude yellow oil (0.50 g, 78 %), purified by flash chromatography using DCM:MeOH (95:5) as eluent to yield a pale yellow oil (0.40 g, 62 %), R_f 0.37, δ_H (250 MHz, CDCl$_3$) 1.55 (3H, d, J=7.25 Hz, CH$_3$), 3.34 (2H, m, NHC*H$_2$*), 3.58 (3H, m, C*H*CONHCH$_2$C*H$_2$*OH), 6.08 (1H, s, NH), 7.24-7.40 (5H, m, C$_6$H$_5$); *m/z* 194.4 (MH$^+$, 100%), MH$^+$ requires 194.2. C 68.50; H 7.99; N 7.20 %. C$_{11}$H$_{15}$NO$_2$ requires C 68.37; H 7.82; N 7.25 %.

N-(2-Hydroxyethyl)-3-chlorobenzamide (AE9) as a crude, pale yellow solid (0.45 g, 71 %), purified by flash chromatography using DCM:MeOH (95:5) as eluent to yield a pale yellow crystalline solid (0.45 g, 71 %), R_f 0.22, m.p. 101-103 °C; δ_H (250 MHz, MeOH-d$_4$) 3.67 (2H, t, J=5.63 Hz, NHC*H$_2$*), 3.88 (2H, t, J=5.75 Hz, C*H$_2$*OH), 7.59-8.04 (4H, m, COC$_6$H$_4$Cl); *m/z* 200.3 (MH$^+$, 100%), MH$^+$ requires 200.6. C 54.20; H 5.13; N 6.96 %. C$_9$H$_{10}$NO$_2$Cl requires C 54.15; H 5.05; N 7.02 %.

N-(2-Hydroxyethyl)-2-naphthylacetamide (AE14) as a crude, pale yellow solid (1.09 g, 89 %), purified by flash chromatography using EtOAc as eluent to yield a pale yellow crystalline solid (0.60 g, 49 %), R_f 0.17, m.p. 134-136 °C; δ_H (250 MHz, CDCl$_3$) 2.71 (1H, s, OH), 3.40 (2H, s, CH$_2$CO), 3.69 (2H, t, J=4.75 Hz, NHC*H$_2$*), 3.81 (2H, m, C*H$_2$*OH) 6.32 (1H, s, NH), 7.40 (1H, d, J=9.0 Hz, Naph

C^{3}H), 7.51 (2H, m, Naph C^{6,7}H), 7.75-7.88 (4H, m, Naph C^{1,4,5,8}H); *m/z* 230.1 (MH$^+$), 212.1 (MH$^+$-H$_2$O), MH$^+$ requires 230.3. C 71.14; H 6.62; N 6.00 %. C$_{14}$H$_{15}$NO$_2$ requires C 73.34; H 6.59; N 6.11 %.

Coupling Strategy

Only one compound was successfully synthesized using the EDC coupling strategy. The following is the experimental protocol used in this reaction:

4-Biphenylacetic acid (0.5 g, 2.36 mmol) and EDC (0.5 g, 2.61 mmol) were dissolved in dichloromethane (40 ml) and a catalytic amount of DMAP was added. The solution was stirred at room temperature for 15 minutes, then ethanolamine (5.0 mmol) was added dropwise. The reaction was stirred at room temperature with a silica guard tube for 20 hours then the solution was then washed with hydrochloric acid (2 M, 2 x 30 ml), saturated sodium hydrogen carbonate solution (2 x 30 ml), distilled water (30 ml) and saturated sodium chloride solution (30 ml). The solution was dried over magnesium sulphate and the solvent removed *in vacuo* to yield *N*-(2-hydroxyethyl)-4-biphenylacetamide (AE13) as a crude, pale yellow solid (0.39 g, 65 %) which was purified by flash chromatography using DCM:MeOH (95:5) as eluent to yield a white solid (0.32 g, 53 %), R_f 0.21, m.p. 185-186 °C; δ_H (250 MHz, MeOH-d$_4$) 1.86 (1H, br s, CH$_2$O*H*), 3.44 (2H, q, J=5.0 Hz, NHC*H*$_2$), 3.72 (4H, m, C*H*$_2$CONHCH$_2$C*H*$_2$), 7.29-7.64 (9H, br m, aryl); *m/z* 256.0 (MH$^+$, 100%), MH$^+$ requires 256.3. C 54.20; H 5.13; N 6.96 %. C$_9$H$_{10}$NO$_2$Cl requires C 54.15; H 5.05; N 7.02 %.

A3. Synthesis of Phenylphosphinic Acids

Typical Experimental Protocol:

Phenylphosphinic acid (14.1 mmol) was placed under an inert atmosphere, dissolved in dry dichloromethane (30 ml) and cooled to 0 °C in an ice bath. Diisopropylamine (31.0 mmol) and trimethylsilyl chloride (31.5 mmol) were added, the solution stirred for 3 hrs at room temperature and then cooled to 0 °C. The appropriate electrophile (21.2 mmol) was added, the solution stirred for 7 to

12 days at room temperature and then washed with hydrochloric acid (2M, 5 x 20 ml) and sodium hydroxide solution (1M, 40 ml). The organic phase was discarded and the remaining aqueous phase acidified with hydrochloric acid (2M, 50 ml) to liberate the phenylphosphinic acid. The product was redissolved in dichloromethane (2 x 20 ml) and this organic phase was then washed with distilled water (30 ml) and saturated sodium chloride solution (30 ml). The solution was dried over magnesium sulphate, filtered and the solvent removed *in vacuo* to yield the phenylphosphinic acid. The following compounds were synthesized using this methodology:

Decylphenylphosphinic acid (PPA2) as a white solid (2.26 g, 57 %), m.p. 60-61 °C; δ_H (250 MHz, CDCl$_3$) 0.86 (3H, t, J=3.25 Hz, CH$_3$), 1.17-1.44 (16H, m, CH$_2$-(CH$_2$)$_8$-CH$_3$), 1.69-1.85 (2H, m, P-CH$_2$), 7.38-7.48 (3H, m, Ph C^{3,4,5}H), 7.67-7.75 (2H, m, Ph C^{2,6}H), 9.20 (1H, s, P-OH); δ_P (101 MHz, CDCl$_3$) 47.63; *m/z* 283.2 (MH$^+$, 100%), MH$^+$ requires 283.4. C 66.87; H 9.91 %. C$_{16}$H$_{27}$PO$_2$ requires C 68.06; H 9.64 %.

Isobutylphenylphosphinic acid (PPA4) as a white solid (0.59 g, 21 %), m.p. 64-67 °C; δ_H (250 MHz, CDCl$_3$) 0.91 (6H, d, J=7.5 Hz, CH(CH$_3$)$_2$), 1.71-2.00 (3H, m, CH$_2$CH), 7.35-7.47 (3H, m, Ph C^{3,4,5}H), 7.66-7.74 (2H, m, Ph C^{2,6}H), 10.61 (1H, s, POH); δ_P (101 MHz, CDCl$_3$) 47.49; *m/z* 199.1 (MH$^+$, 100%), MH$^+$ requires 199.2. C 59.76; H 7.42 %. C$_{10}$H$_{15}$PO$_2$ requires C 60.60; H 7.63 %.

Octadecylphenylphosphinic acid (PPA5) as a white solid (3.48 g, 63 %), m.p. 79-82 °C; δ_H (250 MHz, CDCl$_3$) 0.91 (3H, t, J=6.50 Hz, CH$_3$), 1.22-1.46 (32H, m, CH$_2$(CH$_2$)$_{16}$CH$_3$), 1.69-1.90 (2H, m, PCH$_2$), 7.40-7.55 (3H, m, Ph C^{3,4,5}H), 7.67-7.79 (2H, m, Ph C^{2,6}H), 9.48 (1H, s, POH); δ_P (101 MHz, CDCl$_3$) 48.34; *m/z* 395.5 (MH$^+$, 100%), MH$^+$ requires 395.6. C 73.07; H 10.93 %. C$_{24}$H$_{43}$PO$_2$ requires C 73.06; H 10.98 %.

Hexadecylphenylphosphinic acid (PPA7) as a white solid (4.08 g, 79 %), m.p. 73-76 °C; δ_H (250 MHz, CDCl$_3$) 0.88 (3H, t, J=6.5 Hz, CH$_3$), 1.19-1.57 (28H, m, (CH$_2$)$_{14}$CH$_3$), 1.71-1.88 (2H, m, PCH$_2$), 7.38-7.50 (3H, m, Ph C^{3,4,5}H), 7.68-7.76

(2H, m, Ph C^{2,6}H), 7.95 (1H, s, POH); δp (101 MHz, CDCl$_3$) 48.60; *m/z* 367.5 (MH$^+$, 100%), MH$^+$ requires 367.5. C 72.08; H 10.87 %. C$_{22}$H$_{39}$PO$_2$ requires C 72.09; H 10.73 %.

Propylphenylphosphinic acid (PPA8) as a white solid (1.77 g, 68 %), m.p. 85-87 °C; δ$_H$ (250 MHz, CDCl$_3$) 0.88 (3H, t, J=7.50 Hz, CH$_3$), 1.44-1.53 (2H, m, C*H$_2$*CH$_3$), 1.72-1.84 (2H, m, PCH$_2$), 7.25-7.48 (3H, m, Ph C^{3,4,5}H), 7.67-7.75 (2H, m, Ph C^{2,6}H), 11.92 (1H, s, POH); δ$_P$ (101 MHz, CDCl$_3$) 46.86; *m/z* 351.3 ((2M)H$^+$-H$_2$O, 100%), MH$^+$ requires 185.2. C 58.50; H 6.83 %. C$_9$H$_{13}$PO$_2$ requires C 58.69; H 7.11 %.

A4. Synthesis of Alkylphosphinic Acids

Ammonium Phosphinate Synthesis:

Hypophosphorus acid (50 % w/w, 0.27 mmol) was placed in a round-bottomed flask and cooled to 0°C in an ice bath. Concentrated ammonia solution was added dropwise with stirring until in excess, then as much water as possible was removed *in vacuo*. The remaining water was azeotroped with cyclohexane, the mixture removed *in vacuo* and the product dried over phosphorus pentoxide to yield ammonium phosphinate as a white solid in quantitative yield.

Mono-Substituted Alkylphosphinic Acids

Typical Experimental Protocol:

Ammonium phosphinate (2.5 g, 30.1 mmol) and hexamethyldisilazane (33.1 mmol) were heated together at 110-120 °C for 3 hours under an inert atmosphere. The mixture was then cooled to 0 °C, dry dichloromethane (30 ml) and the appropriate alkyl iodide (27.1 mmol) injected and the solution stirred at room temperature for 3 to 7 days. After this time, the solution was filtered, washed with hydrochloric acid (2 M, 3 x 30 ml) and dried over magnesium sulphate. The solvent was then removed *in vacuo* to yield the crude product which was re-

suspended in methanol (40 ml) and stirred for 2 hours. The methanol was then rmoved *in vacuo*, the product washed with ethyl acetate (3 x 30 ml) and filtered. The following compounds were synthesized using this methodology:

Hexadecylphosphinic acid (APA2) as a white solid (1.62 g, 26 %), m.p. 58-61 °C; δ_H (250 MHz, CDCl$_3$) 0.86 (3H, t, J=6.50 Hz, CH$_3$), 1.14-1.81 (30H, m, (C*H$_2$*)$_{15}$CH3), 6.01 and 8.18 (1H, d, J=541.75 Hz, PH), 7.68 (1H, s, POH); δ_P (101 MHz, CDCl$_3$) 41.26; *m/z* 291.7 (MH$^+$, 100%), MH$^+$ requires 291.4. C 66.82; H 12.23 %. C$_{16}$H$_{35}$PO$_2$ requires C 66.17; H 7.63 %.

Octadecylphosphinic acid (APA3) as a white solid (1.98 g, 26 %), m.p. 68-71 °C; δ_H (250 MHz, CDCl$_3$) 0.92 (3H, t, J=6.75 Hz, CH$_3$), 1.22-1.87 (34H, m, (C*H$_2$*)$_{17}$CH3), 6.09 and 8.25 (1H, d, J=541.50 Hz, PH), 4.63 (1H, s, POH); δ_P (101 MHz, CDCl$_3$) 42.09; *m/z* 319.2 (MH$^+$, 100%), MH$^+$ requires 319.5. C 68.04; H 12.65 %. C$_{18}$H$_{39}$PO$_2$ requires C 67.88; H 12.34 %.

A5. Synthesis of Oleamide

Oleic acid (1.70 g, 6.02 mmol) was placed under an atmosphere of dry nitrogen and dissolved in dichloromethane (30 ml). The solution was cooled to 0 °C and oxalyl chloride (1.60 ml, 18.62 mmol) injected with stirring. The solution was stirred for 4 hours at room temperature and the solvent removed under vacuum to yield a pale yellow residue, which was redissolved in dichloromethane (30 ml). Excess aqueous ammonia was slowly added to the stirred solution at 0 °C and stirring was continued for 30 minutes at room temperature. The white precipitate formed was then filtered off and the solution washed with sodium hydroxide solution (1 M, 3 x 20 ml), dried over magnesium sulphate, filtered and solvent removed *in vacuo*. The crude white solid (1.53 g, 90.3 %) was purified by flash column chromatography using EtOAc:hexane (80:20) as eluent to yield oleamide as a white solid (1.23 g, 72.5 %), R_f 0.32, m.p. 76-78 °C; δ_H (250 MHz, CDCl$_3$) 0.90 (3H, t, CH$_3$), 1.28-1.32 (20H, m, (C*H$_2$*)$_4$CH$_2$CH$_2$CO, CH$_3$(C*H$_2$*)$_4$), 1.65 (2H,

t, CH_2CH$_2$CO), 2.02 (4H, d, CH_2CH=CHCH_2), 2.25 (2H, t, CH$_2$CO), 5.36 (2H, t, CH=CH), 5.63 (2H, s, NH$_2$); *m/z* 282.4 (MH$^+$, 100%), MH$^+$ requires 282.5. C 76.88; H 12.53; N 5.06. C$_{18}$H$_{35}$NO requires C 76.81; N 12.53; N 4.98%.

A6. Synthesis of Anandamide

Arachidonic acid (1 g, 3.28 mmol) was placed under an atmosphere of dry nitrogen in a foil-wrapped flask and dissolved in dry benzene (10 ml) and DMF (0.3 ml, 3.90 mmol). The solution was cooled to 0 °C and oxalyl chloride (1.0 ml, 11.64 mmol) injected with stirring. The solution was stirred for 2 hours at room temperature and the solvent removed under vacuum to yield an orange residue, which was re-dissolved in dichloromethane (30 ml). Ethanolamine (2.0 ml, 33.24 mmol) was added slowly to the stirred solution at 0 °C and stirring was continued for 40 minutes at room temperature. The solution was then washed with potassium hydrogen sulphate solution (1 M, 2 x 30 ml), saturated sodium hydrogen carbonate solution (2 x 30 ml), distilled water (30 ml) and saturated sodium chloride solution (30 ml) and dried over magnesium sulphate. The solvent was removed *in vacuo* to yield a crude, pale yellow oil (1.125 g, 98.6 %) which was purified by flash column chromatography using EtOAc as eluent to yield anandamide as a pale yellow oil (0.917 g, 80.3 %), R_f 0.23; δ_H (250 MHz, CDCl$_3$) 0.88 (3H, t, J=6.75 Hz, CH$_3$), 1.25-1.38 (6H, m, (CH_2)$_3$CH$_3$), 1.72 (2H, quin, J=7.50 Hz, CH_2CH$_2$CO), 2.01-2.16 (4H, m, Anan C^{4,16}CH_2), 2.27 (2H, t, J=7.75 Hz, CH_2CO), 2.82 (6H, q, J=5.83 Hz, Anan C$^{7,10,13}H_2$), 3.41 (2H, q, J=4.75 Hz, NHCH_2), 3.72 (2H, t, J=5.00 Hz, CH_2OH), 4.16 (1H, s, OH), 5.27-5.45 (8H, m, 4(CH=CH)), 6.69 (1H, s, NH); *m/z* 348.4 (MH$^+$, 100%), MH$^+$ requires 348.5.

Appendix B:

Selected NMR and Mass Spectra
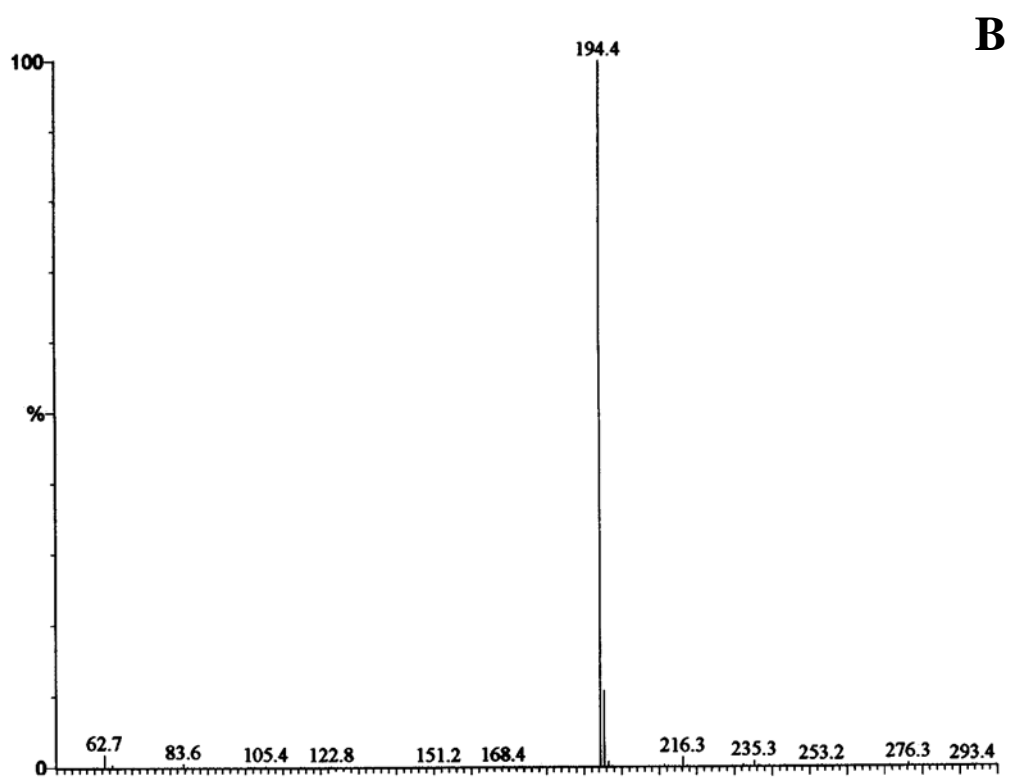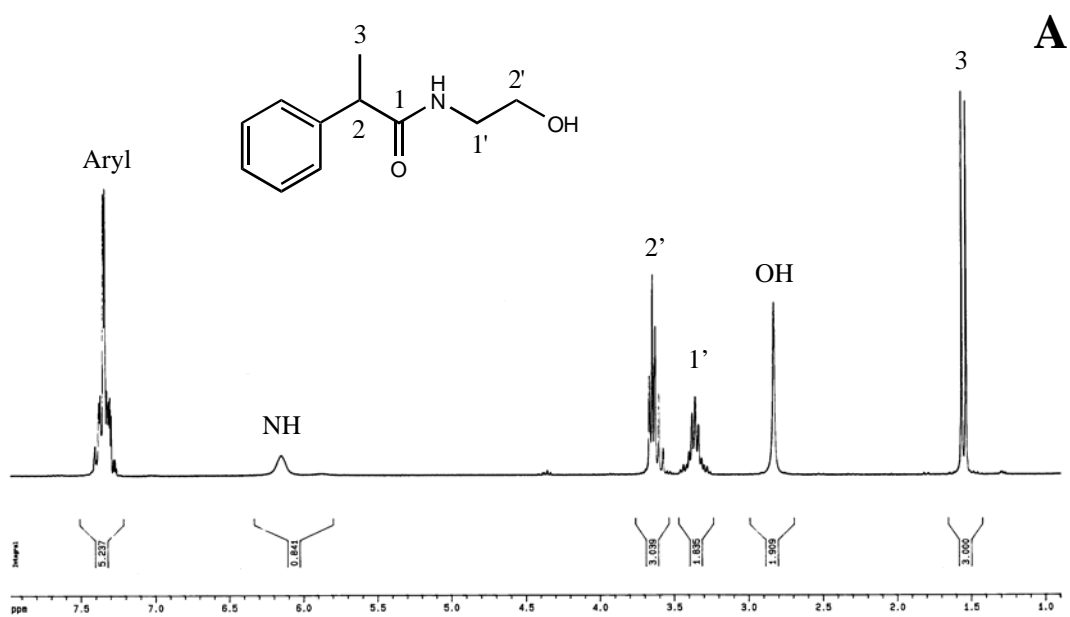
Figure B1: ^{1}H NMR spectrum (**A**) and mass spectrum (**B**) of compound AE6.
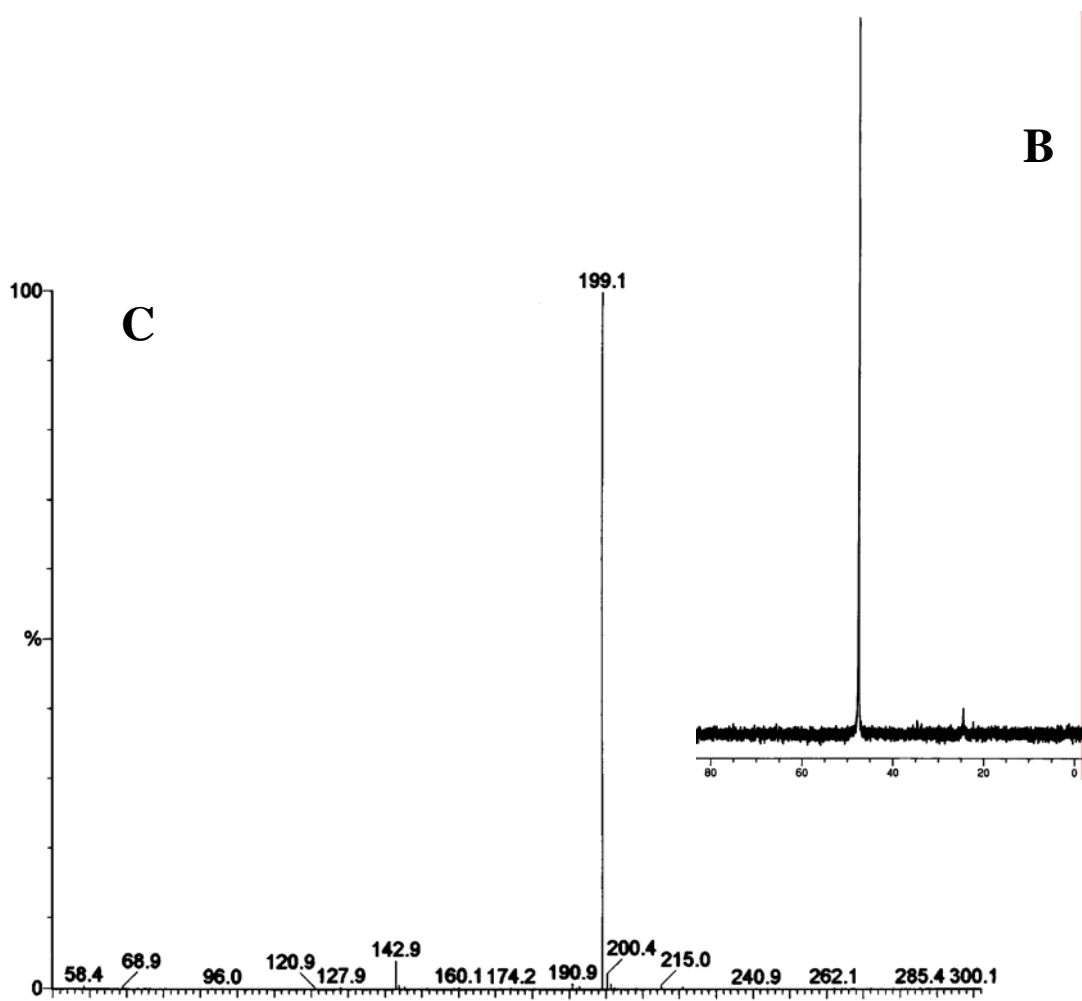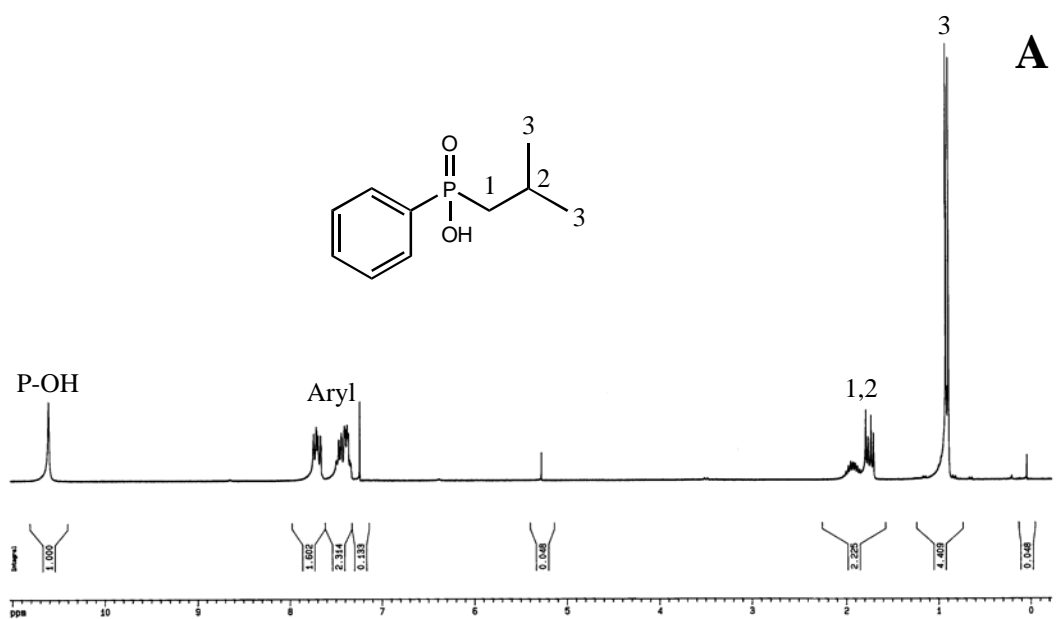
Figure B2: ^{1}H NMR spectrum (**A**) ^{31}P NMR spectrum (**B**) and mass spectrum (**C**) of compound PPA4.
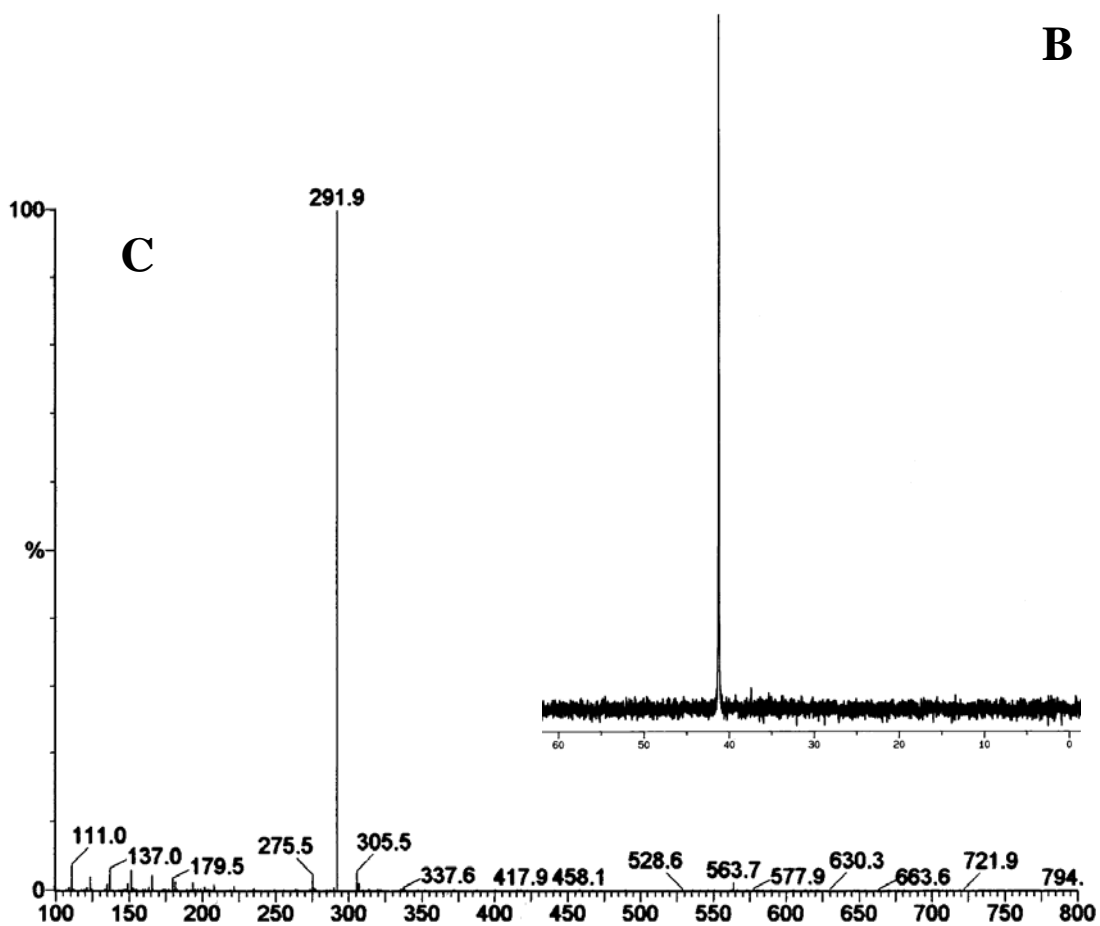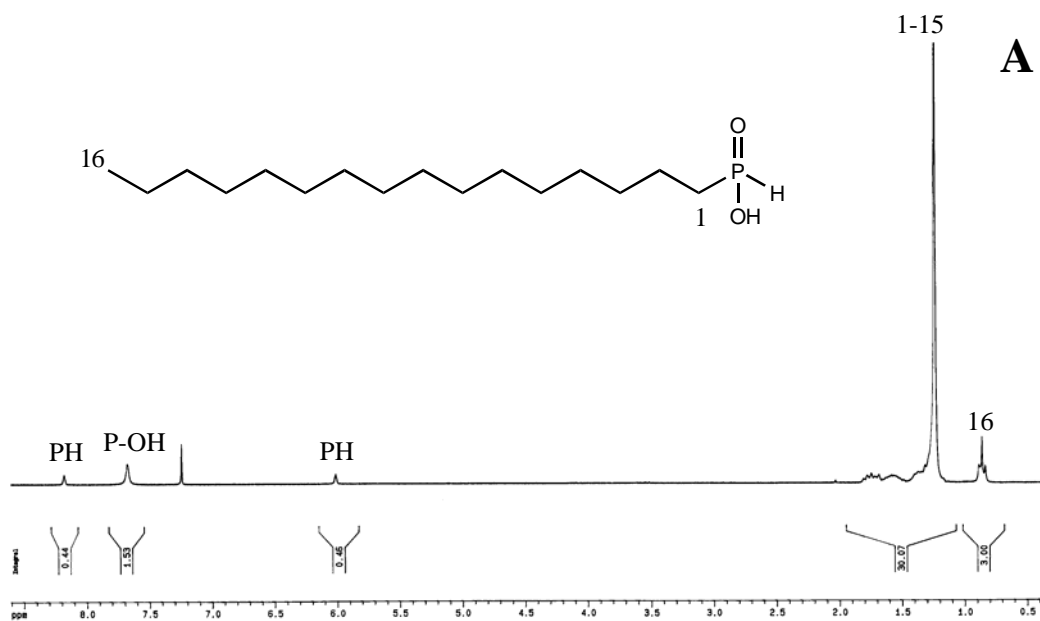
Figure B3: ^{1}H NMR spectrum (**A**) ^{31}P NMR spectrum (**B**) and mass spectrum (**C**) of compound APA2.
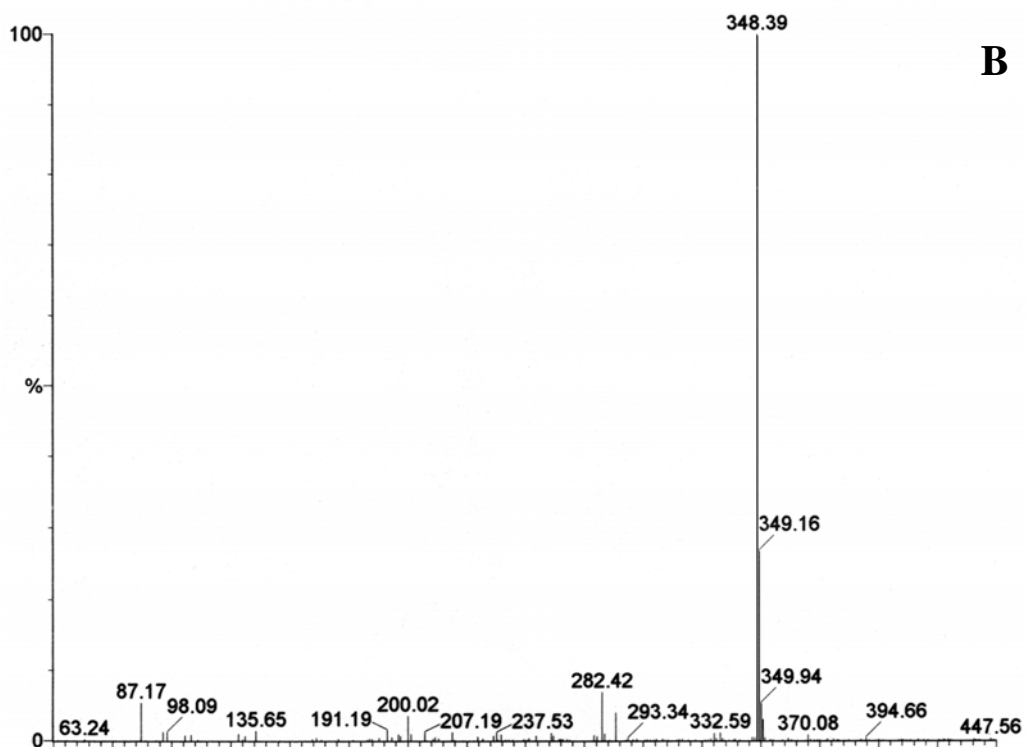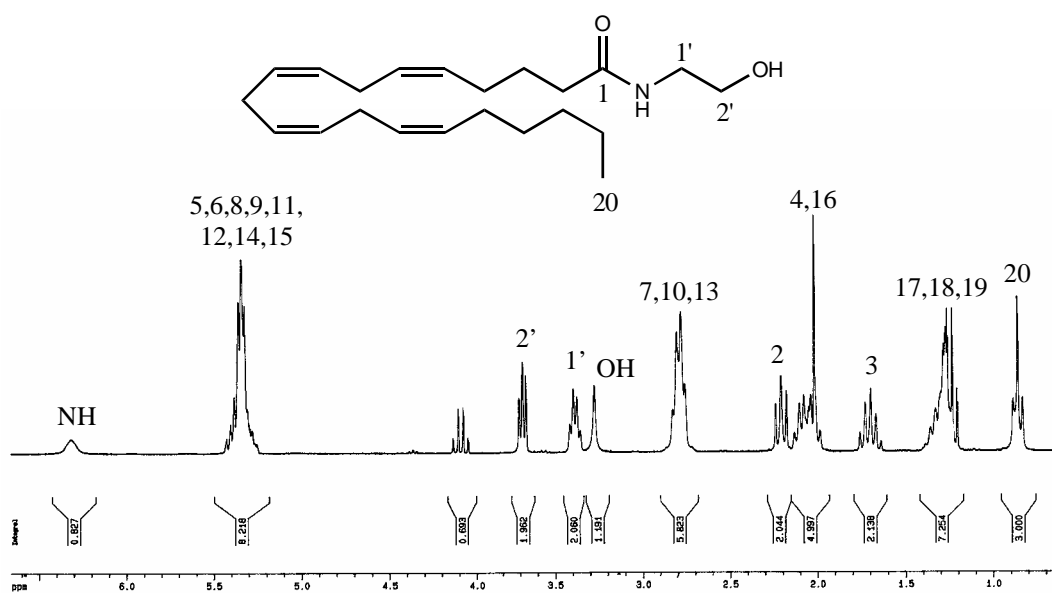
Figure B4: ^{1}H NMR spectrum (**A**) and mass spectrum (**B**) of synthetic
anandamide.

Bibliography

Abadji, V., Lin, S.Y., Taha, G., Griffin, G., Stevenson, L.A., Pertwee, R.G., & Makriyannis, A. (1994) (R)-Methanandamide: A Chiral Novel Anandamide Possessing Higher Potency and Metabolic Stability. *J.Med.Chem.,* **37**, 1889-1893.

Bailey, J., Bell, E.T., & Bell, J.E. (1982) Regulation of Bovine Glutamate Dehydrogenase - The Effects of pH and ADP. *J.Biol.Chem.,* **257**, 5579-5583.

Baker, D., Pryce, G., Croxford, J.L., Brown, P., Pertwee, R.G., Huffman, J.W., & Layward, L. (2000) Cannabinoids Control Spasticity and Tremor in a Multiple Sclerosis Model. *Nature,* **404**, 84-87.

Bartlett, P.A. & Kezer, W.B. (1984) Phosphinic Acid Dipeptide Analogs: Potent, Slow-Binding Inhibitors of Aspartic Peptidases. *J.Am.Chem.Soc.,* **106**, 4282-4283.

Bartlett, P.A., Hanson, J.E., & Giannousis, P.P. (1990) Potent Inhibition of Pepsin and Penicillopepsin by Phosphorus-Containing Peptide Analogs. *J.Org.Chem.,* **55**, 6268-6274.

Bayewitch, M., Avidor-Reiss, T., Levy, R., Barg, J., Mechoulam, R., & Vogel, Z. (1995) The Peripheral Cannabinoid Receptor - Adenylate Cyclase Inhibition and G-Protein Coupling. *FEBS Lett.,* **375**, 143-147.

Bell, M.R., Dambra, T.E., Kumar, V., Eissenstat, M.A., Herrmann, J.L., Wetzel, J.R., Rosi, D., Philion, R.E., Daum, S.J., Hlasta, D.J., Kullnig, R.K., Ackerman, J.H., Haubrich, D.R., Luttinger, D.A., Baizman, E.R., Miller, M.S., & Ward, S.J. (1991) Antinociceptive (Aminoalkyl)Indoles. *J.Med.Chem.,* **34**, 1099-1110.

Beltramo, M., Stella, N., Calignano, A., Lin, S.Y., Makriyannis, A., & Piomelli, D. (1997) Functional Role of High-Affinity Anandamide Transport, as Revealed by Selective Inhibition. *Science,* **277**, 1094-1097.

Ben-Shabat, S., Fride, E., Sheskin, T., Tamiri, T., Rhee, M.H., Vogel, Z., Bisogno, T., De Petrocellis, L., Di Marzo, V., & Mechoulam, R. (1998) An Entourage Effect: Inactive Endogenous Fatty Acid Glycerol Esters Enhance 2-Arachidonoyl-Glycerol Cannabinoid Activity. *Eur.J.Pharmacol.,* **353**, 23-31.

Berdyshev, E., Boichot, E., Corbel, M., Germain, N., & Lagente, V. (1998) Effects of Cannabinoid Receptor Ligands on LPS-Induced Pulmonary Inflammation in Mice. *Life Sci.,* **63**, L125-L129.

Berglund, B.A., Fleming, P.R., Rice, K.C., Shim, J.Y., Welsh, W.J., & Howlett, A.C. (2000) Development of a Novel Class of Monocyclic and Bicyclic Alkyl Amides that Exhibit CB1 and CB2 Cannabinoid Receptor Affinity and Receptor Activation. *Drug Des.Discov.,* **16**, 281-294.

Bergmeyer, H.U. & Beutler, H. (1985) in *Methods of Enzymatic Analysis, Volume 8* (Bergmeyer, H.U., Ed.) pp 454-462, Academic Press, New York.

Bisogno, T., Maurelli, S., Melck, D., De Petrocellis, L., & Di Marzo, V. (1997a) Biosynthesis, Uptake, and Degradation of Anandamide and Palmitoylethanolamide in Leukocytes. *J.Biol.Chem.,* **272**, 3315-3323.

Bisogno, T., Ventriglia, M., Milone, A., Mosca, M., Cimino, G., & Di Marzo, V. (1997b) Occurrence and Metabolism of Anandamide and Related Acyl-Ethanolamides in Ovaries of the Sea Urchin *Paracentrotus lividus. Biochim.Biophys.Acta-Lipids And Lipid Metabolism,* **1345**, 338-348.

Bisogno, T., Katayama, K., Melck, D., Ueda, N., De Petrocellis, L., Yamamoto, S., & Di Marzo, V. (1998) Biosynthesis and Degradation of Bioactive Fatty Acid Amides in Human Breast Cancer and Rat Pheochromocytoma cells - Implications for Cell Proliferation and Differentiation. *Eur.J.Biochem.,* **254**, 634-642.

Boger, D.L., Sato, H., Lerner, A.E., Austin, B.J., Patterson, J.E., Patricelli, M.P., & Cravatt, B.F. (1999) Trifluoromethyl Ketone Inhibitors of Fatty Acid Amide Hydrolase: A Probe of Structural and Conformational Features Contributing to Inhibition. *Bioorg.Med.Chem.Lett.,* **9**, 265-270.

Boger, D.L., Sato, H., Lerner, A.E., Hedrick, M.P., Fecik, R.A., Miyauchi, H., Wilkie, G.D., Austin, B.J., Patricelli, M.P., & Cravatt, B.F. (2000) Exceptionally Potent Inhibitors of Fatty Acid Amide Hydrolase: The Enzyme Responsible for Degradation of Endogenous Oleamide and Anandamide. *Proc.Natl.Acad.Sci. USA,* **97**, 5044-5049.

Bouaboula, M., Rinaldi, M., Carayon, P., Carillon, C., Delpech, B., Shire, D., Lefur, G., & Casellas, P. (1993) Cannabinoid Receptor Expression in Human Leukocytes. *Eur.J.Biochem.,* **214**, 173-180.

Bouaboula, M., Perrachon, S., Milligan, L., Canat, X., Rinaldi-Carmona, M., Portier, M., Barth, F., Calandra, B., Pecceu, F., Lupker, J., Maffrand, J.P., Lefur, G., & Casellas, P. (1997) A Selective Inverse Agonist for Central Cannabinoid Receptor Inhibits Mitogen-Activated Protein Kinase Activation Stimulated by Insulin or Insulin-like Growth Factor 1 - Evidence for a New Model of Receptor/Ligand Interactions. *J.Biol.Chem.,* **272**, 22330-22339.

Bouaboula, M., Desnoyer, N., Carayon, P., Combes, T., & Casellas, P. (1999) G_i Protein Modulation Induced by a Selective Inverse Agonist for the Peripheral Cannabinoid Receptor CB2: Implication for Intracellular Signalization Cross-Regulation. *Mol.Pharmacol.,* **55**, 473-480.

Boyd, E.A., Corless, M., James, K., & Regan, A.C. (1990) A Versatile Route to Substituted Phosphinic Acids. *Tetrahedron Lett.,* **31**, 2933-2936.

Boyd, E.A., Regan, A.C., & James, K. (1994) Synthesis of Alkyl Phosphinic Acids from Silyl Phosphonites and Alkyl Halides. *Tetrahedron Lett.,* **35**, 4223-4226.

Boyd, E.A., Boyd, M.E.K., & Loh, V.M. (1996) Facile Synthesis of Functionalised Phenylphosphinic Acid Derivatives. *Tetrahedron Lett.,* **37**, 1651-1654.

Bradford, M.M. (1976) A Rapid and Sensitive Method for the Quantitation of Microgram Quantities of Protein Utilizing the Principle of Protein-Dye Binding. *Anal.Biochem.,* **72**, 248-254.

Bruns, R.F. (1981) Adenosine Antagonism by Purines, Pteridines and Benzopteridines in Human Fibroblasts. *Biochem.Pharmacol.,* **30**, 325-333.

Bruns, R.F., Lawson-Wendling, K., & Pugsley, T.A. (1983) A Rapid Filtration Assay for Soluble Receptors Using Polyethylenimine-Treated Filters. *Anal.Biochem.,* **132**, 74-81.

Burkey, T.H., Quock, R.M., Consroe, P., Ehlert, F.J., Hosohata, Y., Roeske, W.R., & Yamamura, H.I. (1997) Relative Efficacies of Cannabinoid CB1 Receptor Agonists in the Mouse Brain. *Eur.J.Pharmacol.,* **336**, 295-298.

Calignano, A., LaRana, G., Beltramo, M., Makriyannis, A., & Piomelli, D. (1997) Potentiation of Anandamide Hypotension by the Transport Inhibitor, AM404. *Eur.J.Pharmacol.,* **337**, R1-R2.

Calignano, A., LaRana, G., Giuffrida, A., & Piomelli, D. (1998) Control of Pain Initiation by Endogenous Cannabinoids. *Nature,* **394**, 277-281.

Carta, G., Nava, F., & Gessa, G.L. (1998) Inhibition of Hippocampal Acetylcholine Release After Acute and Repeated Δ^9-Tetrahydrocannabinol in Rats. *Brain Res.,* **809**, 1-4.

Caulfield, M.P. & Brown, D.A. (1992) Cannabinoid Receptor Agonists Inhibit Ca Current in NG108-15 Neuroblastoma Cells *via* a Pertussis Toxin-Sensitive Mechanism. *Br.J.Pharmacol.,* **106**, 231-232.

Chakrabarti, A., Onaivi, E.S., & Chaudhuri, G. (1995) Cloning and Sequencing of a cDNA Encoding the Mouse Brain-Type Cannabinoid Receptor Protein. *DNA Sequence,* **5**, 385-388.

Chapman, V. (1999) The Cannabinoid CB1 Receptor Antagonist, SR141716A, Selectively Facilitates Nociceptive Responses of Dorsal Horn Neurones in the Rat. *Br.J.Pharmacol.,* **127**, 1765-1767.

Cheer, J.F., Cadogan, A.K., Marsden, C.A., Fone, K.C., & Kendall, D.A. (1999) Modification of 5-HT2 Receptor Mediated Behaviour in the Rat by Oleamide and the Role of Cannabinoid Receptors. *Neuropharmacology,* **38**, 533-541.

Cheng, Y. & Prusoff, W.H. (1973) Relationship Between the Inhibition Constant (K_I) and the Concentration of Inhibitor Which Causes 50 per cent Inhibition (I_{50}) of an Enzymatic Reaction. *Biochem.Pharmacol.,* **22**, 3099-3108.

Compton, D.R., Rice, K.C., De Costa, B.R., Razdan, R.K., Melvin, L.S., Johnson, M.R., & Martin, B.R. (1993) Cannabinoid Structure-Activity Relationships:

Correlation of Receptor Binding and *in vivo* Activities. *J.Pharmacol.Exp.Ther.,* **265**, 218-226.

Condie, R., Herring, A., Koh, W.S., Lee, M., & Kaminski, N.E. (1996) Cannabinoid Inhibition of Adenylate Cyclase-Mediated Signal Transduction and Interleukin 2 (IL-2) Expression in the Murine T-Cell Line, EL4.IL-2. *J.Biol.Chem.,* **271**, 13175-13183.

Corchero, J., Avila, M.A., Fuentes, J.A., & Manzanares, J. (1997) Δ^9-Tetrahydrocannabinol Increases Prodynorphin and Proenkephalin Gene Expression in the Spinal Cord of the Rat. *Life Sci.,* **61**, L39-L43.

Cravatt, B.F., Prosperogarcia, O., Siuzdak, G., Gilula, N.B., Henriksen, S.J., Boger, D.L., & Lerner, R.A. (1995) Chemical Characterization of a Family of Brain Lipids that Induce Sleep. *Science,* **268**, 1506-1509.

Cravatt, B.F., Giang, D.K., Mayfield, S.P., Boger, D.L., Lerner, R.A., & Gilula, N.B. (1996) Molecular Characterization of an Enzyme that Degrades Neuromodulatory Fatty-Acid Amides. *Nature,* **384**, 83-87.

Croci, T., Manara, L., Aureggi, G., Guagnini, F., Rinaldi-Carmona, M., Maffrand, J.P., Lefur, G., Mukenge, S., & Ferla, G. (1998) *In Vitro* Functional Evidence of Neuronal Cannabinoid CB_1 Receptors in Human Ileum. *Br.J.Pharmacol.,* **125**, 1393-1395.

Dajani, E.Z., Larsen, K.R., Taylor, J., Dajani, N.E., Shahwan, T.G., Neeleman, S.D., Taylor, M.S., Dayton, M.T., & Mir, G.N. (1999) 1',1'-Dimethylheptyl-Delta-8-tetrahydrocannabinol-11-oic Acid: A Novel, Orally Effective Cannabinoid with Analgesic and Anti-inflammatory Properties. *J.Pharmacol.Exp.Ther.,* **291**, 31-38.

D'Ambra, T.E., Estep, K.G., Bell, M.R., Eissenstat, M.A., Josef, K.A., Ward, S.J., Haycock, D.A., Baizman, E.R., Casiano, F.M., Beglin, N.C., Chippari, S.M., Grego, J.D., Kullnig, R.K., & Daley, G.T. (1992) Conformationally Restrained Analogs of Pravadoline: Nanomolar Potent, Enantioselective, (Aminoalkyl)Indole Agonists of the Cannabinoid Receptor. *J.Med.Chem.,* **35**, 124-135.

DeBlasi, A., O'Reilly, K., & Motulsky, H.J. (1989) Calculating Receptor Number from Binding Experiments using Same Compound as Radioligand and Competitor. *Trends Pharmacol.Sci.,* **10**, 227-229.

De Petrocellis, L., Melck, D., Ueda, N., Maurelli, S., Kurahashi, Y., Yamamoto, S., Marino, G., & Di Marzo, V. (1997) Novel Inhibitors of Brain, Neuronal, and Basophilic Anandamide Amidohydrolase. *Biochem.Biophys.Res.Comm.,* **231**, 82-88.

De Petrocellis, L., Melck, D., Palmisano, A., Bisogno, T., Laezza, C., Bifulco, M., & Di Marzo, V. (1998) The Endogenous Cannabinoid Anandamide Inhibits Human Breast Cancer Cell Proliferation. *Proc.Natl.Acad.Sci. USA,* **95**, 8375-8380.

Desarnaud, F., Cadas, H., & Piomelli, D. (1995) Anandamide Amidohydrolase Activity in Rat Brain Microsomes - Identification and Partial Characterization. *J.Biol.Chem.,* **270**, 6030-6035.

Deutsch, D.G. & Chin, S.A. (1993) Enzymatic Synthesis and Degradation of Anandamide, a Cannabinoid Receptor Agonist. *Biochem.Pharmacol.,* **46**, 791-796.

Deutsch, D.G., Goligorsky, M.S., Schmid, P.C., Krebsbach, R.J., Schmid, H.H.O., Das, S.K., Dey, S.K., Arreaza, G., Thorup, C., Stefano, G., & Moore, L.C. (1997a) Production and Physiological Actions of Anandamide in the Vasculature of the Rat Kidney. *J.Clin.Invest.,* **100**, 1538-1546.

Deutsch, D.G., Lin, S., Hill, W.A.G., Morse, K.L., Salehani, D., Arreaza, G., Omeir, R.L., & Makriyannis, A. (1997b) Fatty Acid Sulfonyl Fluorides Inhibit Anandamide Metabolism and Bind to the Cannabinoid Receptor. *Biochem.Biophys.Res.Comm.,* **231**, 217-221.

Deutsch, D.G., Omeir, R., Arreaza, G., Salehani, D., Prestwich, G.D., Huang, Z., & Howlett, A. (1997c) Methyl Arachidonyl Fluorophosphonate: A Potent Irreversible Inhibitor of Anandamide Amidase. *Biochem.Pharmacol.,* **53**, 255-260.

Devane, W.A., Dysarz, F.A., Johnson, M.R., Melvin, L.S., & Howlett, A.C. (1988) Determination and Characterization of a Cannabinoid Receptor in Rat Brain. *Mol.Pharmacol.,* **34**, 605-613.

Devane, W.A., Hanus, L., Breuer, A., Pertwee, R.G., Stevenson, L.A., Griffin, G., Gibson, D., Mandelbaum, A., Etinger, A., & Mechoulam, R. (1992a) Isolation and Structure of a Brain Constituent that Binds to the Cannabinoid Receptor. *Science,* **258**, 1946-1949.

Devane, W.A., Breuer, A., Sheskin, T., Jarbe, T.U.C., Eisen, M.S., & Mechoulam, R. (1992b) A Novel Probe for the Cannabinoid Receptor. *J.Med.Chem.,* **35**, 2065-2069.

Di Marzo, V., Fontana, A., Cadas, H., Schinelli, S., Cimino, G., Schwartz, J.C., & Piomelli, D. (1994) Formation and Inactivation of Endogenous Cannabinoid Anandamide in Central Neurons. *Nature,* **372**, 686-691.

Di Marzo, V., Bisogno, T., Sugiura, T., Melck, D., & De Petrocellis, L. (1998) The Novel Endogenous Cannabinoid 2-Arachidonoylglycerol is Inactivated by Neuronal- and Basophil-Like Cells: Connections with Anandamide. *Biochem.J.,* **331**, 15-19.

Di Marzo, V. & Deutsch, D.G. (1998) Biochemistry of the Endogenous Ligands of Cannabinoid Receptors. *Neurobiology Of Disease,* **5**, 386-404.

Drake, D.J., Jensen, R.S., Busch-Petersen, J., Kawakami, J.K., Fernandez-Garcia, M.C., Fan, P.S., Makriyannis, A., & Tius, M.A. (1998) Classical/Nonclassical Hybrid Cannabinoids: Southern Aliphatic Chain-Functionalized C-6β Methyl, Ethyl, and Propyl Analogues. *J.Med.Chem.,* **41**, 3596-3608.

Egertova, M., Giang, D.K., Cravatt, B.F., & Elphick, M.R. (1998) A New Perspective on Cannabinoid Signalling: Complementary Localization of Fatty Acid Amide Hydrolase and the CB1 Receptor in Rat Brain. *Proc.R.Soc.Lond.B,* **265**, 2081-2085.

Elphick, M.R. (1998) An Invertebrate G-Protein Coupled Receptor is a Chimeric Cannabinoid/Melanocortin Receptor. *Brain Res.,* **780**, 170-173.

Emrich, H.M., Leweke, F.M., & Schneider, U. (1997) Towards a Cannabinoid Hypothesis of Schizophrenia: Cognitive Impairments Due to Dysregulation of the Endogenous Cannabinoid System. *Pharmacol.Biochem.Behav.,* **56**, 803-807.

Facci, L., Dal Toso, R., Romanello, S., Buriani, A., Skaper, S.D., & Leon, A. (1995) Mast Cells Express a Peripheral Cannabinoid Receptor with Differential Sensitivity to Anandamide and Palmitoylethanolamide. *Proc.Natl.Acad.Sci. USA,* **92**, 3376-3380.

Fahien, L.A., Teller, J.K., Macdonald, M.J., & Fahien, C.M. (1990) Regulation of Glutamate Dehydrogenase by Mg^{2+} and Magnification of Leucine Activation by Mg^{2+}. *Mol.Pharmacol.,* **37**, 943-949.

Felder, C.C., Joyce, K.E., Briley, E.M., Mansouri, J., Mackie, K., Blond, O., Lai, Y., Ma, A.L., & Mitchell, R.L. (1995) Comparison of the Pharmacology and Signal Transduction of the Human Cannabinoid CB1 and CB2 Receptors. *Mol.Pharmacol.,* **48**, 443-450.

Felder, C.C., Nielsen, A., Briley, E.M., Palkovits, M., Priller, J., Axelrod, J., Nguyen, D.N., Richardson, J.M., Riggin, R.M., Koppel, G.A., Paul, S.M., & Becker, G.W. (1996) Isolation and Measurement of the Endogenous Cannabinoid Receptor Agonist, Anandamide, in Brain and Peripheral Tissues of Human and Rat. *FEBS Lett.,* **393**, 231-235.

Felder, C.C., Joyce, K.E., Briley, E.M., Glass, M., Mackie, K.P., Fahey, K.J., Cullinan, G.J., Hunden, D.C., Johnson, D.W., Chaney, M.O., Koppel, G.A., & Brownstein, M. (1998) LY320135, a Novel Cannabinoid CB1 Receptor Antagonist, Unmasks Coupling of the CB1 Receptor to Stimulation of cAMP Accumulation. *J.Pharmacol.Exp.Ther.,* **284**, 291-297.

Fowler, C.J., Stenstrom, A., & Tiger, G. (1997a) Ibuprofen Inhibits the Metabolism of the Endogenous Cannabimimetic Agent Anandamide. *Pharmacol.Toxicol.,* **80**, 103-107.

Fowler, C.J., Tiger, G., & Stenstrom, A. (1997b) Ibuprofen Inhibits Rat Brain Deamidation of Anandamide at Pharmacologically Relevant Concentrations.

Mode of Inhibition and Structure-Activity Relationship. *J.Pharmacol.Exp.Ther.,* **283** , 729-734.

Galiègue, S., Mary, S., Marchand, J., Dussossoy, D., Carrière, D., Carayon, P., Bouaboula, M., Shire, D., Lefur, G., & Casellas, P. (1995) Expression of Central and Peripheral Cannabinoid Receptors in Human Immune Tissues and Leukocyte Sub-populations. *Eur.J.Biochem.,* **232**, 54-61.

Gallant, M., Dufresne, C., Gareau, Y., Guay, D., Leblanc, Y., Prasit, P., Rochette, C., Sawyer, N., Slipetz, D.M., Tremblay, N., Metters, K.M., & Labelle, M. (1996) New Class of Potent Ligands for the Human Peripheral Cannabinoid Receptor. *Bioorg.Med.Chem.Lett.,* **6**, 2263-2268.

Gallily, R., Yamin, A., Waksmann, Y., Ovadia, H., Weidenfeld, J., Bar-Joseph, A., Biegon, A., Mechoulam, R., & Shohami, E. (1997) Protection Against Septic Shock and Suppression of Tumor Necrosis Factor α and Nitric Oxide Production by Dexanabinol (HU-211), a Nonpsychotropic Cannabinoid. *J.Pharmacol.Exp.Ther.,* **283**, 918-924.

Galve-Roperh, I., Sánchez, C., Cortés, M.L., del Pulgar, T.G., Izquierdo, M., & Guzmán, M. (2000) Anti-tumoral Action of Cannabinoids: Involvement of Sustained Ceramide Accumulation and Extracellular Signal-Regulated Kinase Activation. *Nature Medicine,* **6** , 313-319.

Gaoni, Y. & Mechoulam, R. (1964) Isolation, Structure, and Partial Synthesis of an Active Constituent of Hashish. *J.Am.Chem.Soc.,* **86**, 1646-1647.

Gérard, C.M., Mollereau, C., Vassart, G., & Parmentier, M. (1991) Molecular Cloning of a Human Cannabinoid Receptor Which is Also Expressed inTestis. *Biochem.J.,* **279**, 129-134.

Giang, D.K. & Cravatt, B.F. (1997) Molecular Characterization of Human and Mouse Fatty Acid Amide Hydrolases. *Proc.Natl.Acad.Sci. USA,* **94**, 2238-2242.

Glass, M., Dragunow, M., & Faull, R.L.M. (1997) Cannabinoid Receptors in the Human Brain: A Detailed Anatomical and Quantitative Autoradiographic Study in the Fetal, Neonatal and Adult Human Brain. *Neuroscience,* **77**, 299-318.

Glass, M. & Felder, C.C. (1997) Concurrent Stimulation of Cannabinoid CB1 and Dopamine D2 Receptors Augments cAMP Accumulation in Striatal Neurons: Evidence for a G_s Linkage to the CB1 Receptor. *J.Neurosci.,* **17**, 5327-5333.

Goparaju, S.K., Kurahashi, Y., Suzuki, H., Ueda, N., & Yamamoto, S. (1999a) Anandamide Amidohydrolase of Porcine Brain: cDNA Cloning, Functional Expression and Site-Directed Mutagenesis. *Biochim.Biophys.Acta,* **1441**, 77-84.

Goparaju, S.K., Ueda, N., Taniguchi, K., & Yamamoto, S. (1999b) Enzymes of Porcine Brain Hydrolyzing 2-Arachidonoylglycerol, an Endogenous Ligand of Cannabinoid Receptors. *Biochem.Pharmacol.,* **57**, 417-423.

Griffin, G., Fernando, S.R., Ross, R.A., Mckay, N.G., Ashford, M.L.J., Shire, D., Huffman, J.W., Yu, S., Lainton, J.A.H., & Pertwee, R.G. (1997) Evidence for the Presence of CB2-Like Cannabinoid Receptors on Peripheral Nerve Terminals. *Eur.J.Pharmacol.,* **339**, 53-61.

Griffin, G., Atkinson, P.J., Showalter, V.M., Martin, B.R., & Abood, M.E. (1998) Evaluation of Cannabinoid Receptor Agonists and Antagonists Using the Guanosine-5'-(3-[^{35}S]thio)-triphosphate Binding Assay in Rat Cerebellar Membranes. *J.Pharmacol.Exp.Ther.,* **285**, 553-560.

Griffin, G., Tao, Q., & Abood, M.E. (2000) Cloning and Pharmacological Characterization of the Rat CB2 Cannabinoid Receptor. *J.Pharmacol.Exp.Ther.,* **292**, 886-894.

Hanus, L., Gopher, A., Almog, S., & Mechoulam, R. (1993) Two New Unsaturated Fatty-Acid Ethanolamides in Brain that Bind to the Cannabinoid Receptor. *J.Med.Chem.,* **36**, 3032-3034.

Hanus, L., Breuer, A., Tchilibon, S., Shiloah, S., Goldenberg, D., Horowitz, M., Pertwee, R.G., Ross, R.A., Mechoulam, R., & Fride, E. (1999) HU-308: A Specific Agonist for CB_2, a Peripheral Cannabinoid Receptor. *Proc.Natl.Acad.Sci. USA,* **96**, 14228-14233.

Harris, D., Kendall, D.A., & Randall, M.D. (1999) Characterization of Cannabinoid Receptors Coupled to Vasorelaxation by Endothelium-Derived Hyperpolarizing Factor. *Naunyn-Schmiedeberg's Arch.Pharmacol., 359*, 48-52.

Harris, J., Drew, L.J., & Chapman, V. (2000) Spinal Anandamide Inhibits Nociceptive Transmission *Via* Cannabinoid Receptor Activation *In Vivo. Neuroreport, 11*, 2817-2819.

Hillard, C.J. & Campbell, W.B. (1997) Biochemistry and Pharmacology of Arachidonylethanolamide, a Putative Endogenous Cannabinoid. *J.Lipid.Res., 38*, 2383-2398.

Hillard, C.J., Edgemond, W.S., Jarrahian, A., & Campbell, W.B. (1997) Accumulation of *N*-Arachidonoylethanolamine (Anandamide) into Cerebellar Granule Cells Occurs *Via* Facilitated Diffusion. *J.Neurochem., 69*, 631-638.

Hillard, C.J., Manna, S., Greenberg, M.J., DiCamelli, R., Ross, R.A., Stevenson, L.A., Murphy, V., Pertwee, R.G., & Campbell, W.B. (1999) Synthesis and Characterization of Potent and Selective Agonists of the Neuronal Cannabinoid Receptor (CB1). *J.Pharmacol.Exp.Ther., 289*, 1427-1433.

Howlett, A.C. (1984) Inhibition of Neuroblastoma Adenylate Cyclase by Cannabinoid and Nantradol Compounds. *Life Sci., 35*, 1803-1810.

Howlett, A.C. (1985) Cannabinoid Inhibition of Adenylate Cyclase - Biochemistry of the Response in Neuroblastoma Cell Membranes. *Mol.Pharmacol., 27*, 429-436.

Howlett, A.C., Qualy, J.M., & Khachatrian, L.L. (1986) Involvement of G_i in the Inhibition of Adenylate Cyclase by Cannabimimetic Drugs. *Mol.Pharmacol., 29*, 307-313.

Howlett, A.C., Bidaut-Russell, M., Devane, W.A., Melvin, L.S., Johnson, M.R., & Herkenham, M. (1990) The Cannabinoid Receptor - Biochemical, Anatomical and Behavioral Characterization. *Trends Neurosci., 13*, 420-423.

Huffman, J.W., Yu, S., Showalter, V., Abood, M.E., Wiley, J.L., Compton, D.R., Martin, B.R., Bramblett, R.D., & Reggio, P.H. (1996) Synthesis and Pharmacology of a Very Potent Cannabinoid Lacking a Phenolic Hydroxyl with High Affinity for the CB2 Receptor. *J.Med.Chem.,* **39**, 3875-3877.

Huidobro-Toro, J.P. & Harris, R.A. (1996) Brain Lipids that Induce Sleep are Novel Modulators of 5-Hydroxytryptamine Receptors. *Proc.Natl.Acad.Sci. USA,* **93**, 8078-8082.

Japan Tobacco Inc.: Disclosure of a New Family of CB2 Selective Cannabinoid Ligands (1997). WO9729079.

Járai, Z., Wagner, J.A., Varga, K., Lake, K.D., Compton, D.R., Martin, B.R., Zimmer, A.M., Bonner, T.I., Buckley, N.E., Mezey, E., Razdan, R.K., Zimmer, A., & Kunos, G. (1999) Cannabinoid-Induced Mesenteric Vasodilation through an Endothelial Site Distinct from CB1 or CB2 Receptors. *Proc.Natl.Acad.Sci. USA,* **96**, 14136-14141.

Jarho, P., Urtti, A., Jarvinen, K., Pate, D.W., & Jarvinen, T. (1996) Hydroxypropyl-β-cyclodextrin Increases Aqueous Solubility and Stability of Anandamide. *Life Sci.,* **58**, L181-L185.

Jbilo, O., Derocq, J.M., Segui, M., Lefur, G., & Casellas, P. (1999) Stimulation of Peripheral Cannabinoid Receptor CB2 Induces MCP-1 and IL-8 Gene Expression in Human Promyelocytic Cell Line HL60. *FEBS Lett.,* **448**, 273-277.

Jeon, Y.J., Yang, K.H., Pulaski, J.T., & Kaminski, N.E. (1996) Attenuation of Inducible Nitric Oxide Synthase Gene Expression by Δ^9-Tetrahydrocannabinol is Mediated Through the Inhibition of Nuclear Factor-κB/Rel Activation. *Mol.Pharmacol.,* **50**, 334-341.

Johnson, M.K., Smith, R.P., Morrison, D., Laszlo, G., & White, R.J. (2000) Large Lung Bullae in Marijuana Smokers. *Thorax,* **55**, 340-342.

Kamath, S.A., Kummerow, F.A., & Narayan, K.A. (1971) A Simple Procedure for the Isolation of Rat Liver Microsomes. *FEBS Lett.,* **17**, 90-92.

Katayama, K., Ueda, N., Kurahashi, Y., Suzuki, H., Yamamoto, S., & Kato, I. (1997) Distribution of Anandamide Amidohydrolase in Rat Tissues with Special Reference to Small Intestine. *Biochim.Biophys.Acta-Lipids And Lipid Metabolism,* **1347**, 212-218.

Kearn, C.S., Greenberg, M.J., DiCamelli, R., Kurzawa, K., & Hillard, C.J. (1999) Relationships Between Ligand Affinities for the Cerebellar Cannabinoid Receptor CB1 and the Induction of GDP/GTP Exchange. *J.Neurochem.,* **72**, 2379-2387.

Kendall, D. (2000) SR-141716A. *Current Opinion in CPNS Investigational Drugs,* **2**, 112-122.

Khanolkar, A.D., Abadji, V., Lin, S.Y., Hill, W.A.G., Taha, G., Abouzid, K., Meng, Z.X., Fau, P.S., & Makriyannis, A. (1996) Head Group Analogs of Arachidonylethanolamide, the Endogenous Cannabinoid Ligand. *J.Med.Chem.,* **39**, 4515-4519.

Kondo, S., Kondo, H., Nakane, S., Kodaka, T., Tokumura, A., Waku, K., & Sugiura, T. (1998) 2-Arachidonoylglycerol, an Endogenous Cannabinoid Receptor Agonist: Identification as One of the Major Species of Monoacylglycerols in Various Rat Tissues, and Evidence for its Generation Through Ca^{2+}-Dependent and -Independent Mechanisms. *FEBS Lett.,* **429**, 152-156.

Kurahashi, Y., Ueda, N., Suzuki, H., Suzuki, M., & Yamamoto, S. (1997) Reversible Hydrolysis and Synthesis of Anandamide Demonstrated by Recombinant Rat Fatty-Acid Amide Hydrolase. *Biochem.Biophys.Res.Comm.,* **237**, 512-515.

Lambert, D.M., Di Paolo, F.G., Sonveaux, P., Kanyonyo, M., Govaerts, S.J., Hermans, E., Bueb, J.L., Delzenne, N.M., & Tschirhart, E.J. (1999) Analogues and Homologues of *N*-Palmitoylethanolamide, a Putative Endogenous CB2 Cannabinoid, as Potential Ligands for the Cannabinoid Receptors. *Biochim.Biophys.Acta-Molecular And Cell Biology Of Lipids,* **1440**, 266-274.

Lan, R.X., Liu, Q., Fan, P.S., Lin, S.Y., Fernando, S.R., McCallion, D., Pertwee, R., & Makriyannis, A. (1999) Structure-Activity Relationships of Pyrazole Derivatives as Cannabinoid Receptor Antagonists. *J.Med.Chem.,* **42**, 769-776.

Lang, W.S., Qin, C., Hill, W.A.G., Lin, S.Y., Khanolkar, A.D., & Makriyannis, A. (1996) High-Performance Liquid Chromatographic Determination of Anandamide Amidase Activity in Rat Brain Microsomes. *Anal.Biochem.,* **238**, 40-45.

Lang, W.S., Qin, C., Lin, S.Y., Khanolkar, A.D., Goutopoulos, A., Fan, P.S., Abouzid, K., Meng, Z.X., Biegel, D., & Makriyannis, A. (1999) Substrate Specificity and Stereoselectivity of Rat Brain Microsomal Anandamide Amidohydrolase. *J.Med.Chem.,* **42**, 896-902.

Lees, G., Edwards, M.D., Hassoni, A.A., Ganellin, C.R., & Galanakis, D. (1998) Modulation of GABA$_A$ Receptors and Inhibitory Synaptic Currents by the Endogenous CNS Sleep Regulator *cis*-9,10-Octadecenoamide (cOA). *Br.J.Pharmacol.,* **124**, 873-882.

Leweke, F.M., Giuffrida, A., Wurster, U., Emrich, H.M., & Piomelli, D. (1999) Elevated Endogenous Cannabinoids in Schizophrenia. *Neuroreport,* **10**, 1665-1669.

Lichtman, A.H., Peart, J., Poklis, J.L., Bridgen, D.T., Razdan, R.K., Wilson, D.M., Poklis, A., Meng, Y., Byron, P.R., & Martin, B.R. (2000) Pharmacological Evaluation of Aerosolized Cannabinoids in Mice. *Eur.J.Pharmacol.,* **399**, 141-149.

Lin, S., Khanolkar, A.D., Fan, P., Goutopoulos, A., Qin, C., Papahadjis, D., & Makriyannis, A. (1998) Novel Analogues of Arachidonylethanolamide (Anandamide): Affinities for the CB1 and CB2 Cannabinoid Receptors and Metabolic Stability. *J.Med.Chem.,* **41**, 5353-5361.

López-Redondo, F., Lees, G.M., & Pertwee, R.G. (1997) Effects of Cannabinoid Receptor Ligands on Electrophysiological Properties of Myenteric Neurones of the Guinea-Pig Ileum. *Br.J.Pharmacol.,* **122**, 330-334.

Lynn, A.B. & Herkenham, M. (1994) Localization of Cannabinoid Receptors and Non-Saturable High-Density Cannabinoid Binding Sites in Peripheral Tissues of the Rat - Implications for Receptor-Mediated Immune Modulation by Cannabinoids. *J.Pharmacol.Exp.Ther.,* **268**, 1612-1623.

Maccarrone, M., van der Stelt, M., Rossi, A., Veldink, G.A., Vliegenthart, J.F.G., & Agrio, A.F. (1998) Anandamide Hydrolysis by Human Cells in Culture and Brain. *J.Biol.Chem.,* **273**, 32332-32339.

Maccarrone, M., Bari, M., & Agro, A.F. (1999) A Sensitive and Specific Radiochromatographic Assay of Fatty Acid Amide Hydrolase Activity. *Anal.Biochem.,* **267**, 314-318.

Mackie, K. & Hille, B. (1992) Cannabinoids Inhibit N-Type Calcium Channels in Neuroblastoma-Glioma Cells. *Proc.Natl.Acad.Sci. USA,* **89**, 3825-3829.

Mackie, K., Lai, Y., Westenbroek, R., & Mitchell, R. (1995) Cannabinoids Activate an Inwardly Rectifying Potassium Conductance and Inhibit Q-Type Calcium Currents in AtT20 Cells Transfected with Rat Brain Cannabinoid Receptor. *J.Neurosci.,* **15**, 6552-6561.

Manzanares, J., Corchero, J., Romero, J., Fernández-Ruiz, J.J., Ramos, J.A., & Fuentes, J.A. (1999) Pharmacological and Biochemical Interactions Between Opioids and Cannabinoids. *Trends Pharmacol.Sci.,* **20**, 287-294.

Martin, B.R., Beletskaya, I., Patrick, G., Jefferson, R., Winckler, R., Deutsch, D.G., Di Marzo, V., Dasse, O., Mahadevan, A., & Razdan, R.K. (2000) Cannabinoid Properties of Methylfluorophosphonate Analogs. *J.Pharmacol.Exp.Ther.,* **294**, 1209-1218.

Massi, P., Fuzio, D., Viganò, D., Sacerdote, P., & Parolaro, D. (2000) Relative Involvement of Cannabinoid CB1 and CB2 Receptors in the Δ^9-Tetrahydrocannabinol-Induced Inhibition of Natural Killer activity. *Eur.J.Pharmacol.,* **387**, 343-347.

Matsuda, L.A., Lolait, S.J., Brownstein, M.J., Young, A.C., & Bonner, T.I. (1990) Structure of a Cannabinoid Receptor and Functional Expression of the Cloned cDNA. *Nature,* **346**, 561-564.

Maurelli, S., Bisogno, T., De Petrocellis, L., Di Luccia, A., Marino, G., & Di Marzo, V. (1995) Two Novel Classes of Neuroactive Fatty Acid Amides are Substrates for Mouse Neuroblastoma 'Anandamide Amidohydrolase'. *FEBS Lett.,* **377**, 82-86.

Mazzari, S., Canella, R., Petrelli, L., Marcolongo, G., & Leon, A. (1996) *N*-(2-Hydroxyethyl)hexadecanamide is Orally Active in Reducing Edema Formation and Inflammatory Hyperalgesia by Down-Modulating Mast Cell Activation. *Eur.J.Pharmacol.,* **300**, 227-236.

Mechoulam, R., Feigenbaum, J.J., Lander, N., Segal, M., Jarbe, T.U.C., Hiltunen, A.J., & Consroe, P. (1988) Enantiomeric Cannabinoids - Stereospecificity of Psychotropic Activity. *Experientia,* **44**, 762-764.

Mechoulam, R., Ben-Shabat, S., Hanus, L., Ligumsky, M., Kaminski, N.E., Schatz, A.R., Gopher, A., Almog, S., Martin, B.R., Compton, D.R., Pertwee, R.G., Griffin, G., Bayewitch, M., Barg, J., & Vogel, Z. (1995) Identification of an Endogenous 2-Monoglyceride, Present in Canine Gut, that Binds to Cannabinoid Receptors. *Biochem.Pharmacol.,* **50**, 83-90.

Mechoulam, R., Fride, E., Ben-Shabat, S., Meiri, U., & Horowitz, M. (1998) Carbachol, an Acetylcholine Receptor Agonist, Enhances Production in Rat Aorta of 2-Arachidonoyl Glycerol, a Hypotensive Endocannabinoid. *Eur.J.Pharmacol.,* **362**, R1-R3.

Melck, D., Rueda, D., Galve-Roperh, I., De Petrocellis, L., Guzmán, M., & Di Marzo, V. (1999a) Involvement of the cAMP/Protein Kinase A Pathway and of Mitogen-Activated Protein Kinase in the Anti-proliferative Effects of Anandamide in Human Breast Cancer Cells. *FEBS Lett.,* **463**, 235-240.

Melck, D., Bisogno, T., De Petrocellis, L., Chuang, H., Julius, D., Bifulco, M., & Di Marzo, V. (1999b) Unsaturated Long-Chain *N* -Acyl-vanillyl-amides (N-

AVAMs): Vanilloid Receptor Ligands That Inhibit Anandamide-Facilitated Transport and Bind to CB1 Cannabinoid Receptors. *Biochem.Biophys.Res.Comm.,* **262**, 275-284.

Melvin, L.S., Johnson, M.R., Harbert, C.A., Milne, G.M., & Weissman, A. (1984) A Cannabinoid Derived Prototypical Analgesic. *J.Med.Chem.,* **27**, 67-71.

Molina-Holgado, F., Molina-Holgado, E., & Guaza, C. (1998) The Endogenous Cannabinoid Anandamide Potentiates Interleukin-6 Production by Astrocytes Infected with Theiler's Murine Encephalomyelitis Virus by a Receptor-Mediated Pathway. *FEBS Lett.,* **433**, 139-142.

Munro, S., Thomas, K.L., & Abushaar, M. (1993) Molecular Characterization of a Peripheral Receptor for Cannabinoids. *Nature,* **365**, 61-65.

Nagayama, T., Sinor, A.D., Simon, R.P., Chen, J., Graham, S.H., Jin, K., & Greenberg, D.A. (1999) Cannabinoids and Neuroprotection in Global and Focal Cerebral Ischemia and in Neuronal Cultures. *J.Neurosci.,* **19**, 2987-2995.

Natarajan, V., Schmid, P.C., Reddy, P.V., & Schmid, H.H.O. (1984) Catabolism of *N*-Acylethanolamine Phospholipids by Dog Brain Preparations. *J.Neurochem.,* **42**, 1613-1619.

Omeir, R.L., Chin, S., Hong, Y., Ahern, D.G., & Deutsch, D.G. (1995) Arachidonoyl ethanolamide-[1,2-^{14}C] As a Substrate for Anandamide Amidase. *Life Sci.,* **56**, 1999-2005.

Patricelli, M.P., Lashuel, H.A., Giang, D.K., Kelly, J.W., & Cravatt, B.F. (1998) Comparative Characterization of a Wild Type and Transmembrane Domain-Deleted Fatty Acid Amide Hydrolase: Identification of the Transmembrane Domain as a Site for Oligomerization. *Biochem.,* **37**, 15177-15187.

Patricelli, M.P. & Cravatt, B.F. (1999) Fatty Acid Amide Hydrolase Competitively Degrades Bioactive Amides and Esters through a Nonconventional Catalytic Mechanism. *Biochem.,* **38**, 14125-14130.

Patricelli, M.P., Lovato, M.A., & Cravatt, B.F. (1999) Chemical and Mutagenic Investigations of Fatty Acid Amide Hydrolase: Evidence for a Family of Serine Hydrolases with Distinct Catalytic Properties. *Biochem.,* **38**, 9804-9812.

Patterson, J.E., Ollmann, I.R., Cravatt, B.F., Boger, D.L., Wong, C.H., & Lerner, R.A. (1996) Inhibition of Oleamide Hydrolase Catalyzed Hydrolysis of the Endogenous Sleep-Inducing Lipid *cis*-9-Octadecenamide. *J.Am.Chem.Soc.,* **118**, 5938-5945.

Pertwee, R.G., Fernando, S.R., Griffin, G., Abadji, V., & Makriyannis, A. (1995a) Effect of Phenylmethylsulfonyl Fluoride on the Potency of Anandamide as an Inhibitor of Electrically Evoked Contractions in Two Isolated Tissue Preparations. *Eur.J.Pharmacol.,* **272**, 73-78.

Pertwee, R., Griffin, G., Fernando, S., Li, X.Y., Hill, A., & Makriyannis, A. (1995b) AM630, a Competitive Cannabinoid Receptor Antagonist. *Life Sci.,* **56**, 1949-1955.

Pertwee, R.G. & Fernando, S.R. (1996) Evidence for the Presence of Cannabinoid CB1 Receptors in Mouse Urinary Bladder. *Br.J.Pharmacol.,* **118**, 2053-2058.

Pertwee, R.G. (1999) Evidence for the Presence of CB1 Cannabinoid Receptors on Peripheral Neurones and for the Existence of Neuronal Non-CB1 Cannabinoid Receptors. *Life Sci.,* **65**, 597-605.

Piomelli, D., Beltramo, M., Giuffrida, A., & Stella, N. (1998) Endogenous Cannabinoid Signaling. *Neurobiology Of Disease,* **5**, 462-473.

Piomelli, D., Beltramo, M., Glasnapp, S., Lin, S.Y., Goutopoulos, A., Xie, X.Q., & Makriyannis, A. (1999) Structural Determinants for Recognition and Translocation by the Anandamide Transporter. *Proc.Natl.Acad.Sci. USA,* **96**, 5802-5807.

Plane, F., Holland, M., Waldron, G.J., Garland, C.J., & Boyle, J.P. (1997) Evidence that Anandamide and EDHF Act *Via* Different Mechanisms in Rat Isolated Mesenteric Arteries. *Br.J.Pharmacol.,* **121**, 1509-1511.

Portier, M., Rinaldi-Carmona, M., Pecceu, F., Combes, T., Poinot-Chazel, C., Calandra, B., Barth, F., Le Fur, G., & Casellas, P. (1999) SR 144528, an Antagonist for the Peripheral Cannabinoid Receptor that Behaves as an Inverse Agonist. *J.Pharmacol.Exp.Ther.,* **288**, 582-589.

Qin, C., Lin, S.Y., Lang, W.S., Goutopoulos, A., Pavlopoulos, S., Mauri, F., & Makriyannis, A. (1998) Determination of Anandamide Amidase Activity Using Ultraviolet-Active Amine Derivatives and Reverse-Phase High-Performance Liquid Chromatography. *Anal.Biochem.,* **261**, 8-15.

Rakhshan, F., Day, T.A., Blakely, R.D., & Barker, E.L. (2000) Carrier-Mediated Uptake of the Endogenous Cannabinoid Anandamide in RBL-2H3 Cells. *J.Pharmacol.Exp.Ther.,* **292**, 960-967.

Randall, M.D., Alexander, S.P.H., Bennett, T., Boyd, E.A., Fry, J.R., Gardiner, S.M., Kemp, P.A., McCulloch, A.I., & Kendall, D.A. (1996) An Endogenous Cannabinoid as an Endothelium-Derived Vasorelaxant. *Biochem.Biophys.Res.Comm.,* **229**, 114-120.

Randall, M.D. & Kendall, D.A. (1997) Involvement of a Cannabinoid in Endothelium-Derived Hyperpolarizing Factor-Mediated Coronary Vasorelaxation. *Eur.J.Pharmacol.,* **335**, 205-209.

Randall, M.D., McCulloch, A.I., & Kendall, D.A. (1997) Comparative Pharmacology of Endothelium-Derived Hyperpolarizing Factor and Anandamide in Rat Isolated Mesentery. *Eur.J.Pharmacol.,* **333**, 191-197.

Rice, W., Shannon, J.M., Burton, F., & Fiedeldey, D. (1997) Expression of a Brain-Type Cannabinoid Receptor (CB1) in Alveolar Type II Cells in the Lung: Regulation by Hydrocortisone. *Eur.J.Pharmacol.,* **327**, 227-232.

Rinaldi-Carmona, M., Barth, F., Heaulme, M., Shire, D., Calandra, B., Congy, C., Martinez, S., Maruani, J., Neliat, G., Caput, D., Ferrara, P., Soubrie, P., Breliere, J.C., & Lefur, G. (1994) SR141716A, a Potent and Selective Antagonist of the Brain Cannabinoid Receptor. *FEBS Lett.,* **350**, 240-244.

Rinaldi-Carmona, M., Calandra, B., Shire, D., Bouaboula, M., Oustric, D., Barth, F., Casellas, P., Ferrara, P., & Lefur, G. (1996) Characterization of Two Cloned Human CB1 Cannabinoid Receptor Isoforms. *J.Pharmacol.Exp.Ther.,* **278**, 871-878.

Rinaldi-Carmona, M., Barth, F., Millan, J., Derocq, J.M., Casellas, P., Congy, C., Oustric, D., Sarran, M., Bouaboula, M., Calandra, B., Portier, M., Shire, D., Breliere, J.C., & Lefur, G. (1998) SR 144528, the First Potent and Selective Antagonist of the CB2 Cannabinoid Receptor. *J.Pharmacol.Exp.Ther.,* **284**, 644-650.

Ross, R.A., Brockie, H.C., Stevenson, L.A., Murphy, V.L., Templeton, F., Makriyannis, A., & Pertwee, R.G. (1999) Agonist-Inverse Agonist Characterization at CB1 and CB2 Cannabinoid Receptors of L759633, L759656 and AM630. *Br.J.Pharmacol.,* **126**, 665-672.

Ruiz, L., Miguel, A., & Díaz-Laviada, I. (1999) Δ^9-Tetrahydrocannabinol Induces Apoptosis in Human Prostate PC-3 Cells *via* a Receptor-Independent Mechanism. *FEBS Lett.,* **458**, 400-404.

Ryan, W.J., Banner, W.K., Wiley, J.L., Martin, B.R., Razdan, R.K., Thomas, B.F., Co, & Semus, S.F. (1997) Potent Anandamide Analogs: The Effect of Changing the Length and Branching of the End Pentyl Chain. *J.Med.Chem.,* **40**, 3617-3625.

Schatz, A.R., Lee, M., Condie, R.B., Pulaski, J.T., & Kaminski, N.E. (1997) Cannabinoid Receptors CB1 and CB2: A Characterization of Expression and Adenylate Cyclase Modulation Within the Immune System. *Toxicol.App.Pharmacol.,* **142**, 278-287.

Shire, D., Calandra, B., Rinaldi-Carmona, M., Oustric, D., Pessègue, B., Bonnin-Cabanne, O., Le Fur, G., Caput, D., & Ferrara, P. (1996) Molecular Cloning, Expression and Function of the Murine CB2 Peripheral Cannabinoid Receptor. *Biochim.Biophys.Acta,* **1307**, 132-136.

Schlicker, E., Timm, J., & Gothert, M. (1996) Cannabinoid Receptor-Mediated Inhibition of Dopamine Release in the Retina. *Naunyn-Schmiedeberg's Arch.Pharmacol.,* **354**, 791-795.

Schmid, P.C., Zuzarte-Augustin, M.L., & Schmid, H.H.O. (1985) Properties of Rat Liver *N*-Acylethanolamine Amidohydrolase. *J.Biol.Chem.,* **260**, 4145-4149.

Schmid, P.C., Paria, B.C., Krebsbach, R.J., Schmid, H.H.O., & Dey, S.K. (1997) Changes in Anandamide Levels in Mouse Uterus are Associated with Uterine Receptivity for Embryo Implantation. *Proc.Natl.Acad.Sci. USA,* **94**, 4188-4192.

Seltzman, H.H., Fleming, D.N., Thomas, B.F., Gilliam, A.F., McCallion, D.S., Pertwee, R.G., Compton, D.R., & Martin, B.R. (1997) Synthesis and Pharmacological Comparison of Dimethylheptyl and Pentyl Analogs of Anandamide. *J.Med.Chem.,* **40**, 3626-3634.

Sepe, N., De Petrocellis, L., Montanaro, F., Cimino, G., & Di Marzo, V. (1998) Bioactive Long Chain *N*-Acylethanolamines in Five Species of Edible Bivalve Molluscs - Possible Implications for Mollusc Physiology and Seafood Industry. *Biochim.Biophys.Acta-Lipids And Lipid Metabolism,* **1389**, 101-111.

Shen, M.X., Piser, T.M., Seybold, V.S., & Thayer, S.A. (1996) Cannabinoid Receptor Agonists Inhibit Glutamatergic Synaptic Transmission in Rat Hippocampal Cultures. *J.Neurosci.,* **16**, 4322-4334.

Sheskin, T., Hanus, L., Slager, J., Vogel, Z., & Mechoulam, R. (1997) Structural Requirements for Binding of Anandamide-Type Compounds to the Brain Cannabinoid Receptor. *J.Med.Chem.,* **40**, 659-667.

Shire, D., Carillon, C., Kaghad, M., Calandra, B., Rinaldi-Carmona, M., Lefur, G., Caput, D., & Ferrara, P. (1995) An Amino-Terminal Variant of the Central Cannabinoid Receptor Cesulting from Alternative Splicing. *J.Biol.Chem.,* **270**, 3726-3731.

Shire, D., Calandra, B., Rinaldi-Carmona, M., Oustric, D., Pessègue, B., Bonnin-Cabanne, O., Le Fur, G., Caput, D., & Ferrara, P. (1996) Molecular Cloning,

Expression and Function of the Murine CB2 Peripheral Cannabinoid Receptor. *Biochim.Biophys.Acta,* **1307**, 132-136.

Showalter, V.M., Compton, D.R., Martin, B.R., & Abood, M.E. (1996) Evaluation of Binding in aTransfected Cell Line Expressing a Peripheral Cannabinoid Receptor (CB2): Identification of Cannabinoid Receptor Subtype Selective Ligands. *J.Pharmacol.Exp.Ther.,* **278**, 989-999.

Skaper, S.D., Buriani, A., Dal Toso, R., Petrelli, L., Romanello, S., Facci, L., & Leon, A. (1996) The ALIAmide Palmitoylethanolamide and Cannabinoids, but not Anandamide, are Protective in a Delayed Postglutamate Paradigm of Excitotoxic Death in Cerebellar Granule Neurons. *Proc.Natl.Acad.Sci. USA,* **93**, 3984-3989.

Smith, P.B., Compton, D.R., Welch, S.P., Razdan, R.K., Mechoulam, R., & Martin, B.R. (1994) The Pharmacological Activity of Anandamide, a Putative Endogenous Cannabinoid, in Mice. *J.Pharmacol.Exp.Ther.,* **270**, 219-227.

Soderstrom, K., Leid, M., Moore, F.L., & Murray, T.F. (2000) Behavioral, Pharmacological, and Molecular Characterization of an Amphibian Cannabinoid Receptor. *J.Neurochem.,* **75**, 413-423.

Song, C. & Howlett, A.C. (1995) Rat Brain Cannabinoid Receptors are N-Linked Glycosylated Proteins. *Life Sci.,* **56**, 1983-1989.

Song, Z.H. & Bonner, T.I. (1996) A Lysine Residue of the Cannabinoid Receptor is Critical for Receptor Recognition by Several Agonists but not WIN55212-2. *Mol.Pharmacol.,* **49**, 891-896.

Stefano, G.B., Salzet, B., & Salzet, M. (1997) Identification and Characterization of the Leech CNS Cannabinoid Receptor: Coupling to Nitric Oxide Release. *Brain Res.,* **753**, 219-224.

Stella, N., Schweitzer, P., & Piomelli, D. (1997) A Second Endogenous Cannabinoid that Modulates Long-Term Potentiation. *Nature,* **388**, 773-778.

Straiker, A., Stella, N., Piomelli, D., Mackie, K., Karten, H.J., & Maguire, C. (1999) Cannabinoid CB1 Receptors and Ligands in Vertebrate Retina: Localization and Function of an Endogenous Signaling System. *Proc.Natl.Acad.Sci. USA,* **96**, 14565-14570.

Strangman, N.M., Patrick, S.L., Hohmann, A.G., Tsou, K., & Walker, J.M. (1998) Evidence for a Role of Endogenous Cannabinoids in the Modulation of Acute and Tonic Pain Sensitivity. *Brain Res.,* **813**, 323-328.

Sugiura, T., Kondo, S., Sukagawa, A., Nakane, S., Shinoda, A., Itoh, K., Yamashita, A., & Waku, K. (1995) 2-Arachidonoylgylcerol - A Possible Endogenous Cannabinoid Receptor Ligand in Brain. *Biochem.Biophys.Res.Comm.,* **215**, 89-97.

Tao, Q., Mcallister, S.D., Andreassi, J., Nowell, K.W., Cabral, G.A., Hurst, D.P., Bachtel, K., Ekman, M.C., Reggio, P.H., & Abood, M.E. (1999) Role of a Conserved Lysine Residue in the Peripheral Cannabinoid Receptor (CB$_2$): Evidence for Subtype Specificity. *Mol.Pharmacol.,* **55**, 605-613.

Thomas, B.F., Adams, I.B., Mascarella, S.W., Martin, B.R., & Razdan, R.K. (1996) Structure-Activity Analysis of Anandamide Analogs: Relationship to a Cannabinoid Pharmacophore. *J.Med.Chem.,* **39**, 471-479.

Thumser, A.E.A., Voysey, J., & Wilton, D.C. (1997) A Fluorescence Displacement Assay for the Measurement of Arachidonoyl Ethanolamide (Anandamide) and Oleoyl Amide (Octadecenoamide) Hydrolysis. *Biochem.Pharmacol.,* **53**, 433-435.

Tiger, G., Stenström, A., & Fowler, C.J. (2000) Pharmacological Properties of Rat Brain Fatty Acid Amidohydrolase in Different Subcellular Fractions Using Palmitoylethanolamide as Substrate. *Biochem.Pharmacol.,* **59**, 647-653.

Traynor, J.R. & Nahorski, S.R. (1995) Modulation by μ-Opioid Agonists of Guanosine-5'-*O*-(3-[35S]thio)triphosphate Binding to Membranes from Human Neuroblastoma SH-SY5Y Cells. *Mol.Pharmacol.,* **47**, 848-854.

Tsou, K., Nogueron, M.I., Muthian, S., Sañudo-Peña, M.C., Hillard, C.J., Deutsch, D.G., & Walker, J.M. (1998) Fatty Acid Amide Hydrolase is Located Preferentially in Large Neurons in the Rat Central Nervous System as Revealed by Immunohistochemistry. *Neurosci.Lett.,* **254**, 137-140.

Twitchell, W., Brown, S., & Mackie, K. (1997) Cannabinoids Inhibit N- and P/Q-Type Calcium Channels in Cultured Rat Hippocampal Neurons. *J. Neurophysiol.,* **78**, 43-50.

Ueda, N., Yamanaka, K., Terasawa, Y., & Yamamoto, S. (1999) An Acid Amidase Hydrolyzing Anandamide as an Endogenous Ligand for Cannabinoid Receptors. *FEBS Lett.,* **454**, 267-270.

van der Stelt, M., Paoletti, A.M., Maccarrone, M., Nieuwenhuizen, W.F., Bagetta, G., Veldink, G.A., Agro, A.F., & Vliegenthart, J.F.G. (1997) The Effect of Hydroxylation of Linoleoyl Amides on their Cannabinomimetic Properties. *FEBS Lett.,* **415**, 313-316.

Walker, J.M., Huang, S.M., Strangman, N.M., Tsou, K., & Sañudo-Peña, M.C. (1999) Pain Modulation by Release of the Endogenous Cannabinoid Anandamide. *Proc.Natl.Acad.Sci. USA,* **96**, 12198-12203.

Yamaguchi, F., Macrae, A.D., & Brenner, S. (1996) Molecular Cloning of Two Cannabinoid Type 1-like Receptor Genes from the Puffer Fish *Fugu rubripes. Genomics,* **35**, 603-605.

Zhu, W.G., Friedman, H., & Klein, T.W. (1998) Δ^9-Tetrahydrocannabinol Induces Apoptosis in Macrophages and Lymphocytes: Involvement of Bcl-2 and Caspase-1. *J.Pharmacol.Exp.Ther.,* **286**, 1103-1109.